

# **Constraining Quark Transversity through Collins Asymmetry Measurements in $p^\uparrow p$ Collisions at STAR**

**Robert Fersch**

**University of Kentucky**

*for the*  *STAR Collaboration*

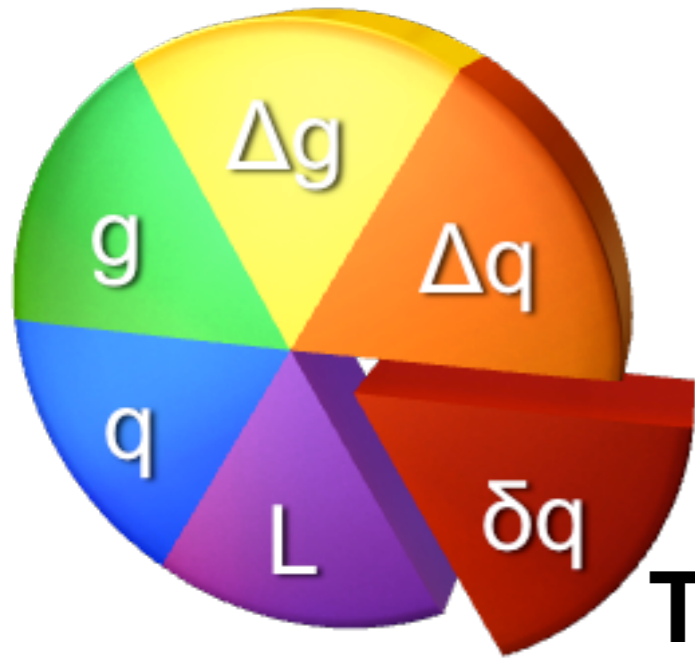
**Presentation for DIS2011 in  
Newport News, Virginia**

# Partonic Spin Distributions



*Parton Degrees  
of Freedom  
at Leading Twist*

# Partonic Spin Distributions



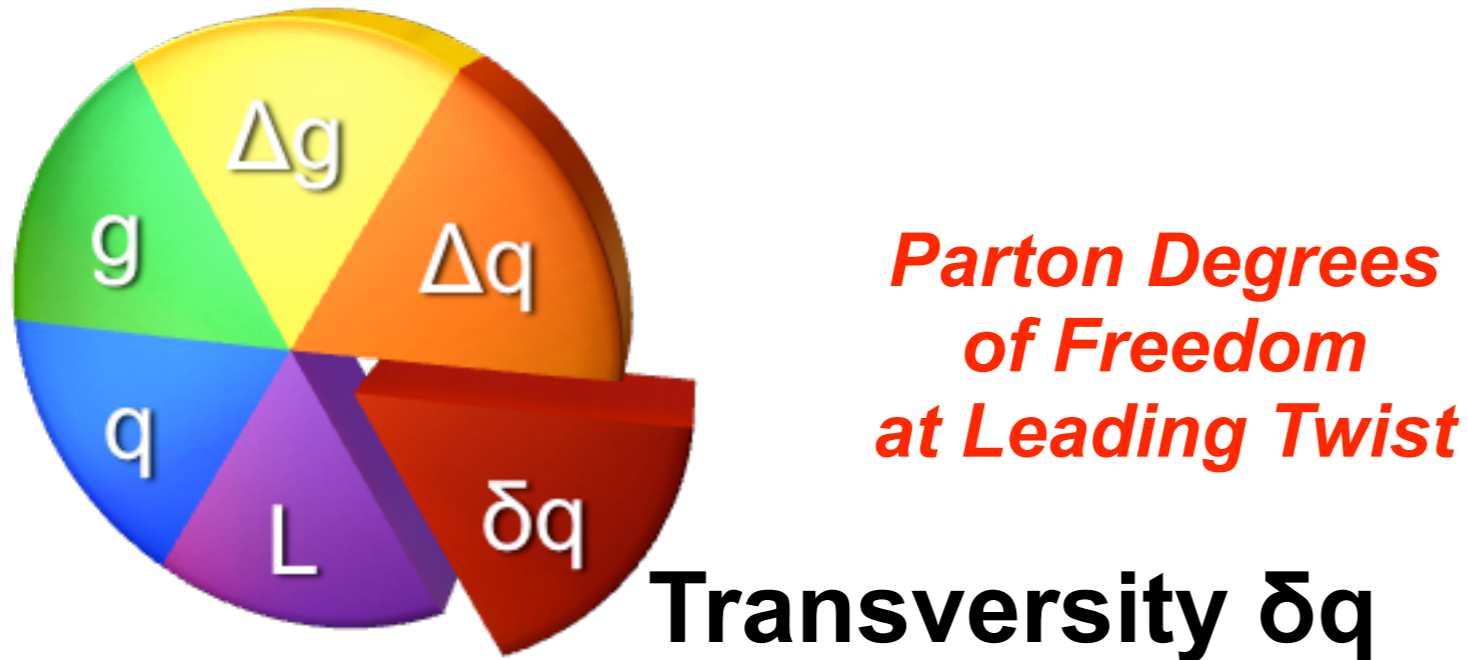
*Parton Degrees  
of Freedom  
at Leading Twist*

**Transversity  $\delta q$**

$\delta q$  part of a complete spin-density matrix rep. of the proton

$$\mathcal{F}(x, Q^2) = \frac{1}{2}q(x, Q^2)I \otimes I + \frac{1}{2}\Delta q(x, Q^2)\sigma_3 \otimes \sigma_3 + \frac{1}{2}\delta q(x, Q^2)(\sigma_+ \otimes \sigma_- + \sigma_- \otimes \sigma_+)$$

# Partonic Spin Distributions

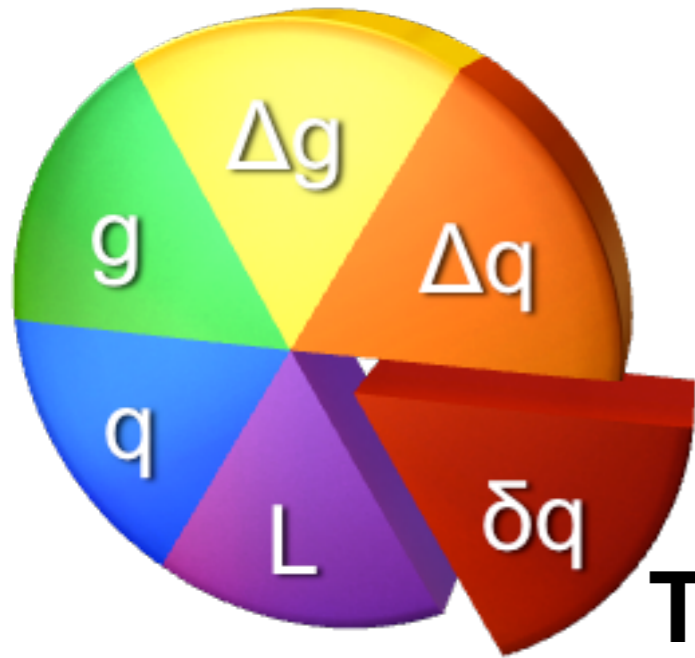


$\delta q$  part of a complete spin-density matrix rep. of the proton

$$\mathcal{F}(x, Q^2) = \frac{1}{2}q(x, Q^2)I \otimes I + \frac{1}{2}\Delta q(x, Q^2)\sigma_3 \otimes \sigma_3 + \frac{1}{2}\delta q(x, Q^2)(\sigma_+ \otimes \sigma_- + \sigma_- \otimes \sigma_+)$$

- $\delta q$  measurement requires transversely polarized beams/targets for precise statistics
- $\delta q$  is chiral odd  $\therefore$  requires chiral odd hadron fragmentation  $\Delta D^h_q \mid \delta q \otimes \Delta D^h_q$  is even
- $\delta q$  correlates left- and right-handed quarks ( $q_L \leftrightarrow q_R$ ), unlike helicity
- $\delta q \neq \Delta q$  due to relativistic effects

# Partonic Spin Distributions



*Parton Degrees  
of Freedom  
at Leading Twist*

**Transversity  $\delta q$**

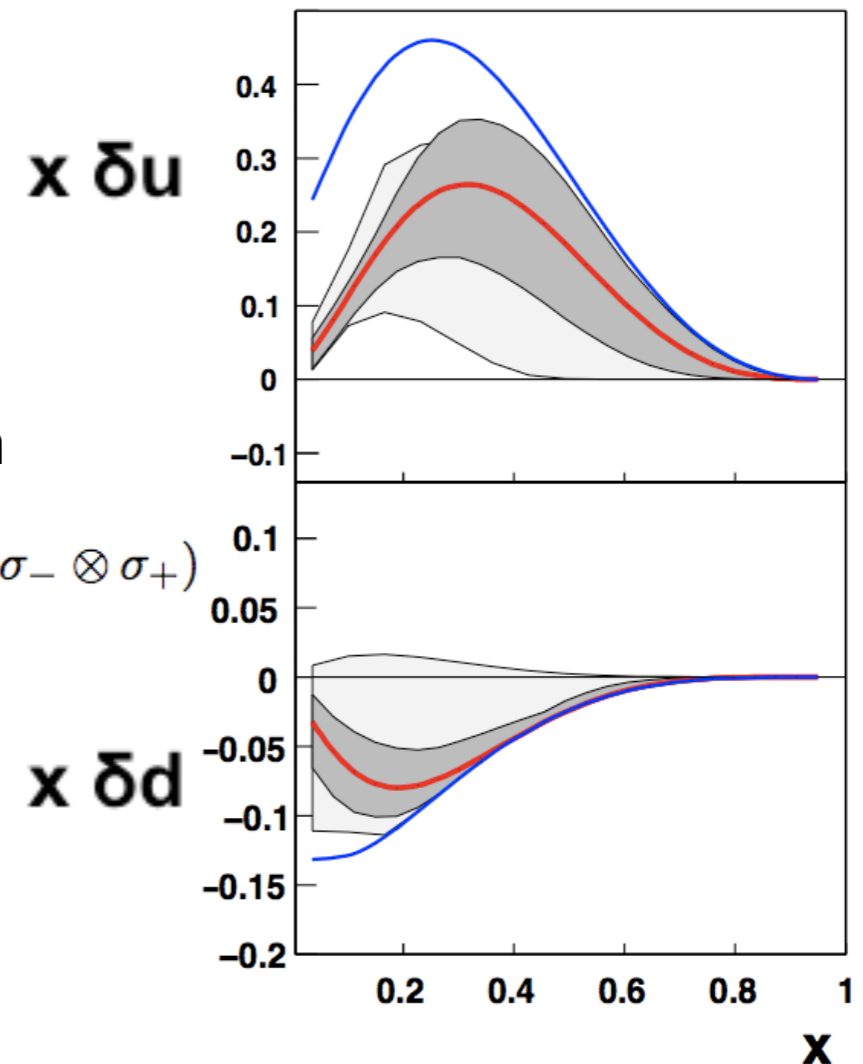
$\delta q$  part of a complete spin-density matrix rep. of the proton

$$\mathcal{F}(x, Q^2) = \frac{1}{2}q(x, Q^2)I \otimes I + \frac{1}{2}\Delta q(x, Q^2)\sigma_3 \otimes \sigma_3 + \frac{1}{2}\delta q(x, Q^2)(\sigma_+ \otimes \sigma_- + \sigma_- \otimes \sigma_+)$$

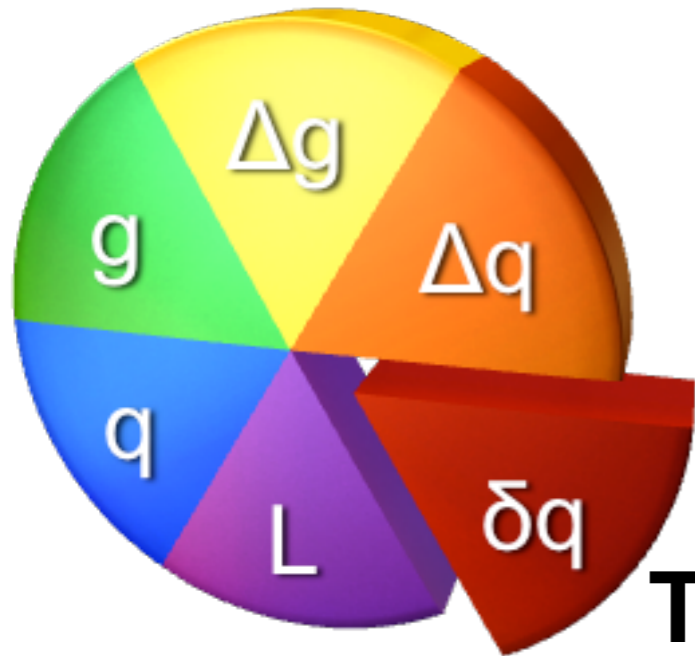
- $\delta q$  measurement requires transversely polarized beams/targets for precise statistics
- $\delta q$  is chiral odd  $\therefore$  requires chiral odd hadron fragmentation  $\Delta D^h_q \mid \delta q \otimes \Delta D^h_q$  is even
- $\delta q$  correlates left- and right-handed quarks ( $q_L \leftrightarrow q_R$ ), unlike helicity
- $\delta q \neq \Delta q$  due to relativistic effects

## Global Fit of Data:

Anselmino M et al. 2009 Nucl.Phys.Proc.Suppl. 191:98-107



# Partonic Spin Distributions



*Parton Degrees  
of Freedom  
at Leading Twist*

**Transversity  $\delta q$**

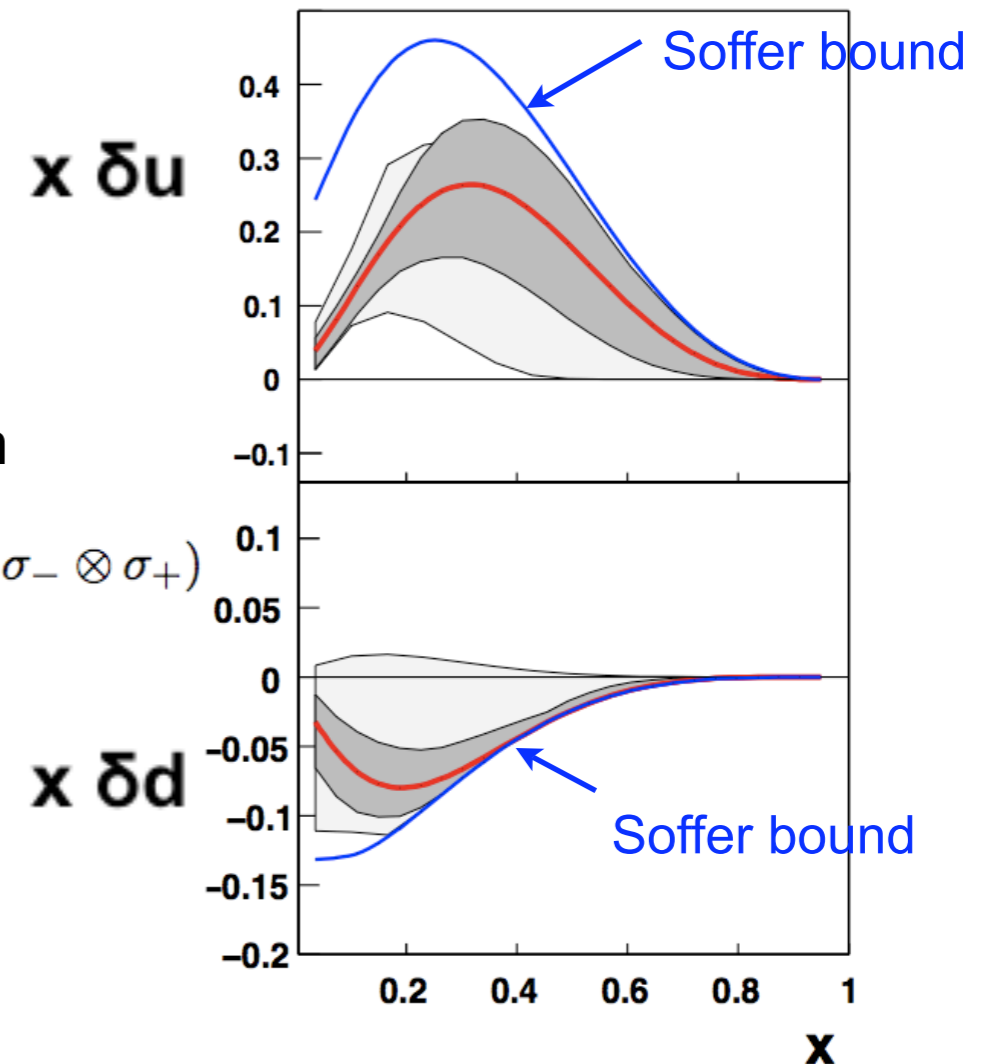
$\delta q$  part of a complete spin-density matrix rep. of the proton

$$\mathcal{F}(x, Q^2) = \frac{1}{2}q(x, Q^2)I \otimes I + \frac{1}{2}\Delta q(x, Q^2)\sigma_3 \otimes \sigma_3 + \frac{1}{2}\delta q(x, Q^2)(\sigma_+ \otimes \sigma_- + \sigma_- \otimes \sigma_+)$$

- $\delta q$  measurement requires transversely polarized beams/targets for precise statistics
- $\delta q$  is chiral odd  $\therefore$  requires chiral odd hadron fragmentation  $\Delta D^h_q$  |  $\delta q \otimes \Delta D^h_q$  is even
- $\delta q$  correlates left- and right-handed quarks ( $q_L \leftrightarrow q_R$ ), unlike helicity
- $\delta q \neq \Delta q$  due to relativistic effects

## Global Fit of Data:

Anselmino M et al. 2009 Nucl.Phys.Proc.Suppl. 191:98-107

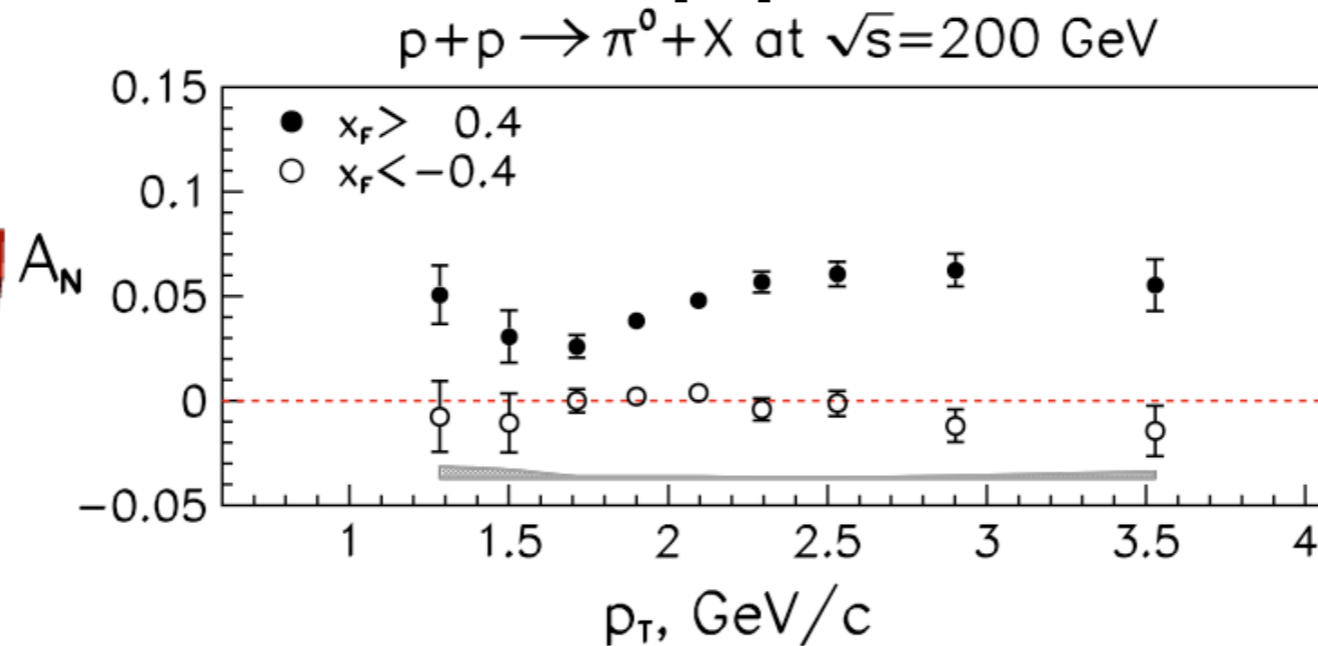


**Soffer bound:**

$$|\delta q(x, Q^2)| \leq \frac{1}{2}[q(x, Q^2) + \Delta q(x, Q^2)]$$

# Experimental Access to Transversity

## Measurement of left-right $\pi$ asymmetry $A_N$ in $p^\uparrow p \rightarrow \pi X$ reactions



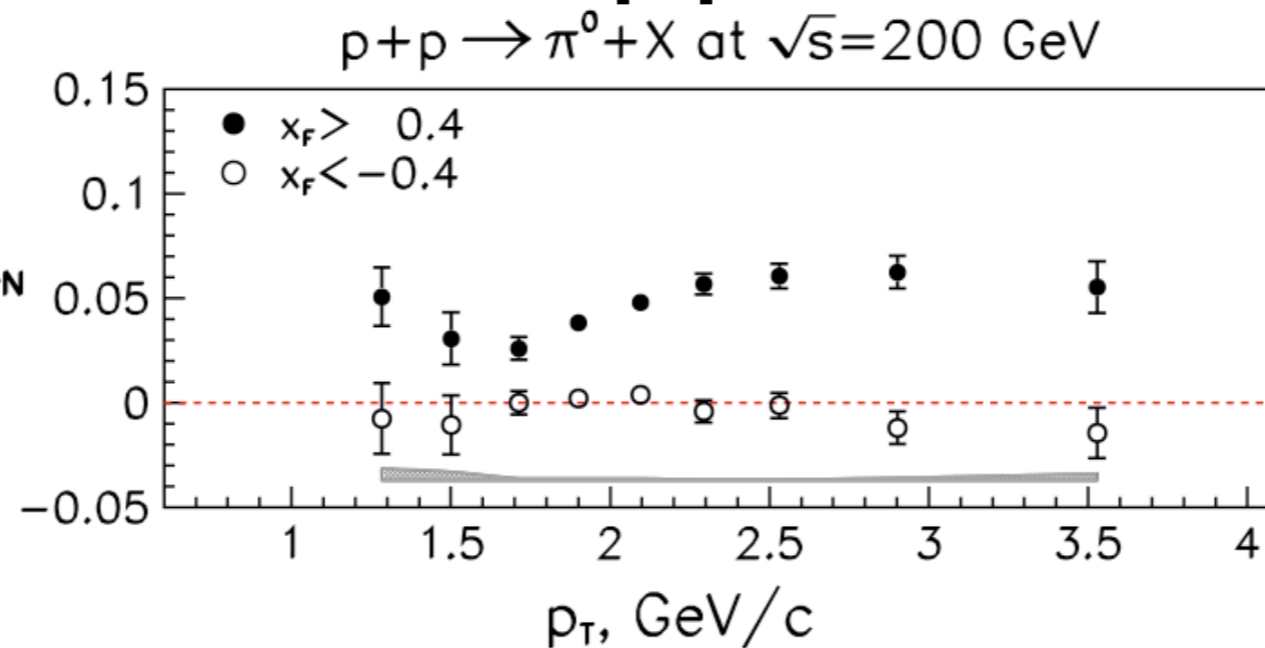
STAR Publication:  
PRL **101**, 222001  
(2008)

# Experimental Access to Transversity

## Measurement of left-right $\pi$ asymmetry $A_N$ in $p^\uparrow p \rightarrow \pi X$ reactions



Combined in  $A_N$  due to Collins-Sivers mixing



STAR Publication:  
PRL **101**, 222001  
(2008)

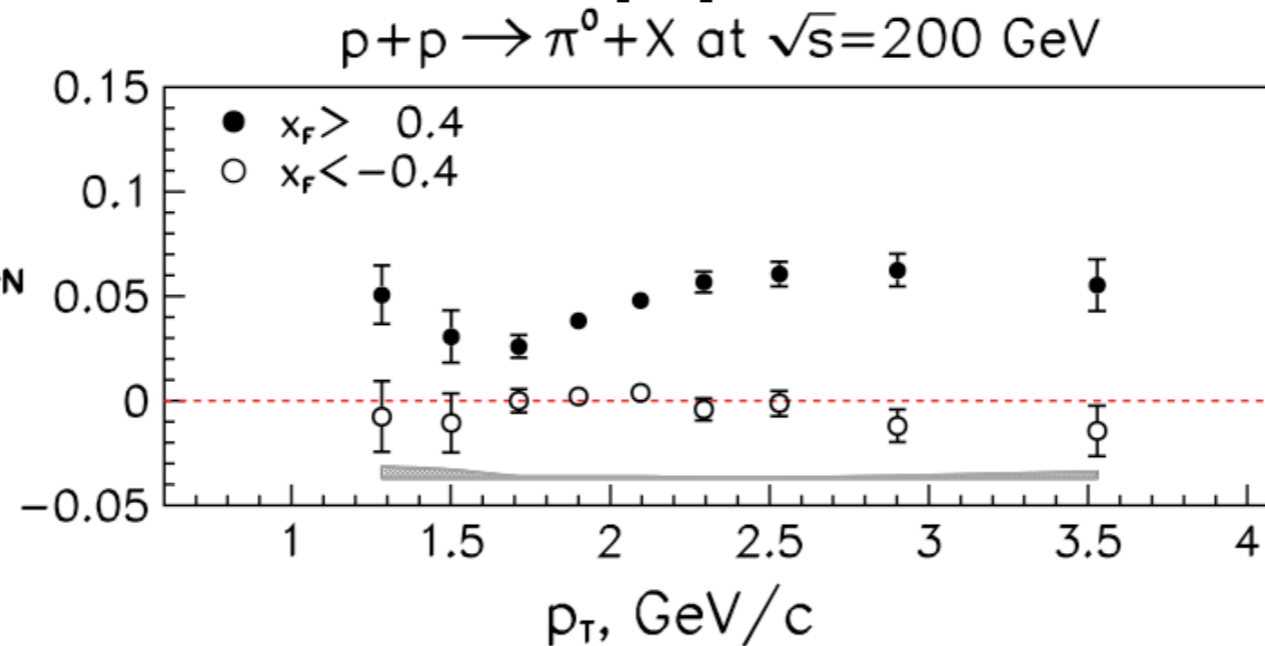
**TMD (Transverse Momentum Dependence)**  
implied by high  $x_F$  results

# Experimental Access to Transversity

## Measurement of left-right $\pi$ asymmetry $A_N$ in $p^\uparrow p \rightarrow \pi X$ reactions

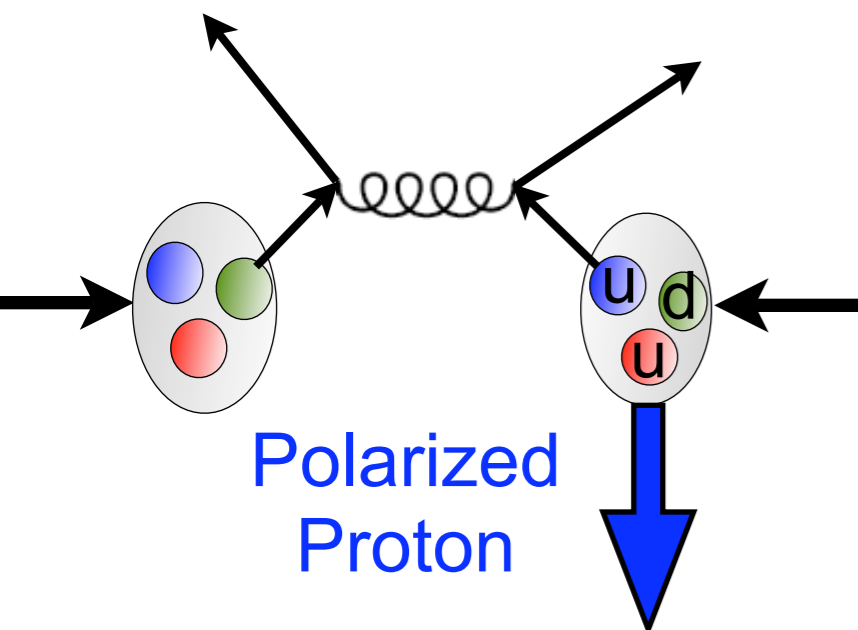


Combined in  $A_N$  due to Collins-Sivers mixing



STAR Publication:  
PRL **101**, 222001  
(2008)

**TMD (Transverse Momentum Dependence)**  
implied by high  $x_F$  results

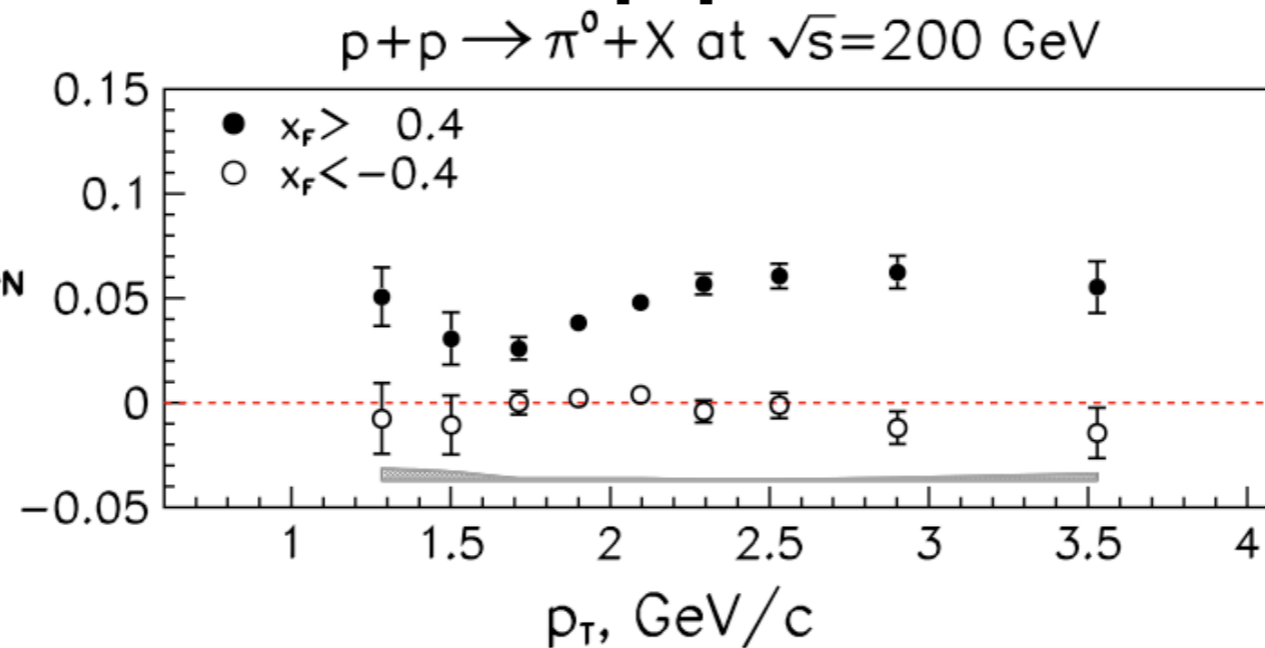


# Experimental Access to Transversity

## Measurement of left-right $\pi$ asymmetry $A_N$ in $p^\uparrow p \rightarrow \pi X$ reactions

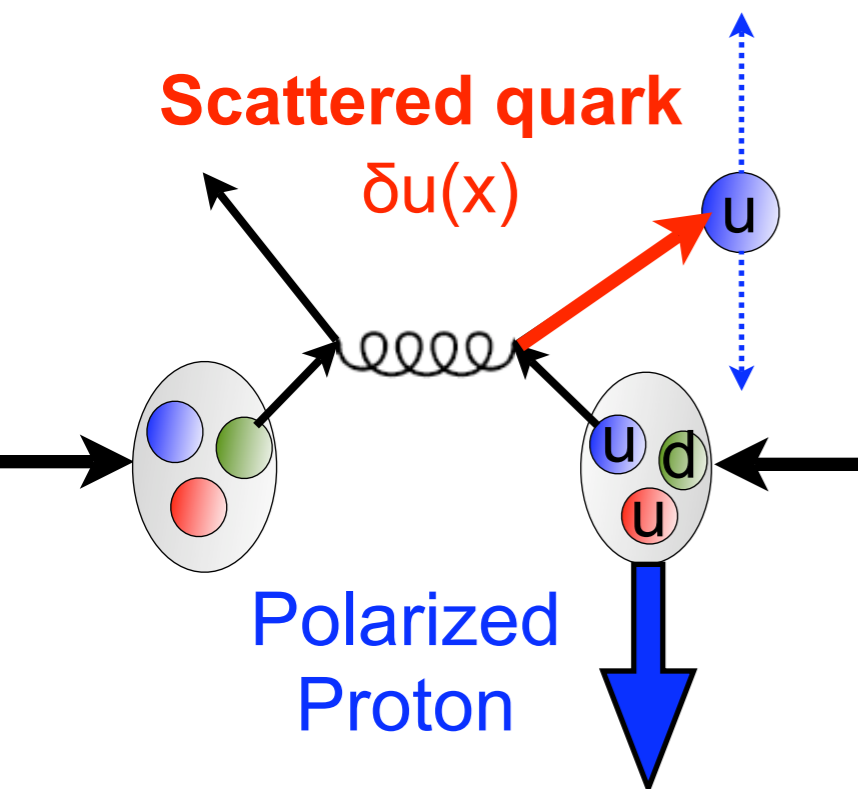


Combined in  $A_N$  due to Collins-Sivers mixing



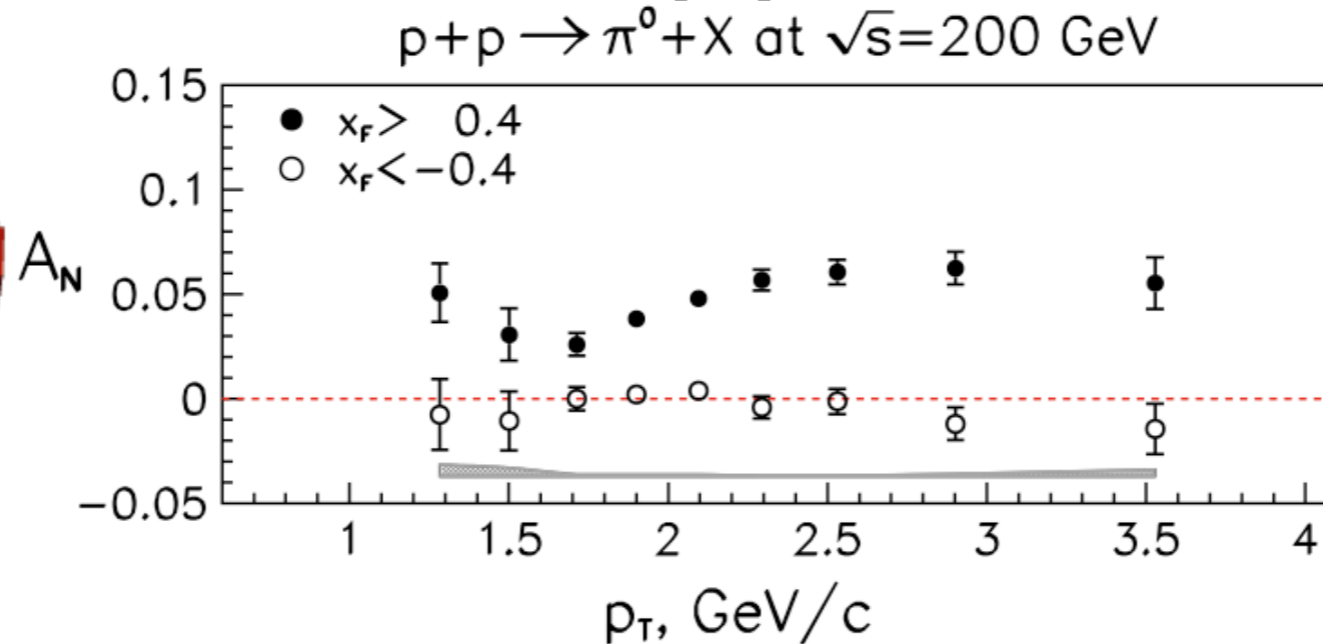
STAR Publication:  
PRL **101**, 222001  
(2008)

**TMD (Transverse Momentum Dependence)**  
implied by high  $x_F$  results



# Experimental Access to Transversity

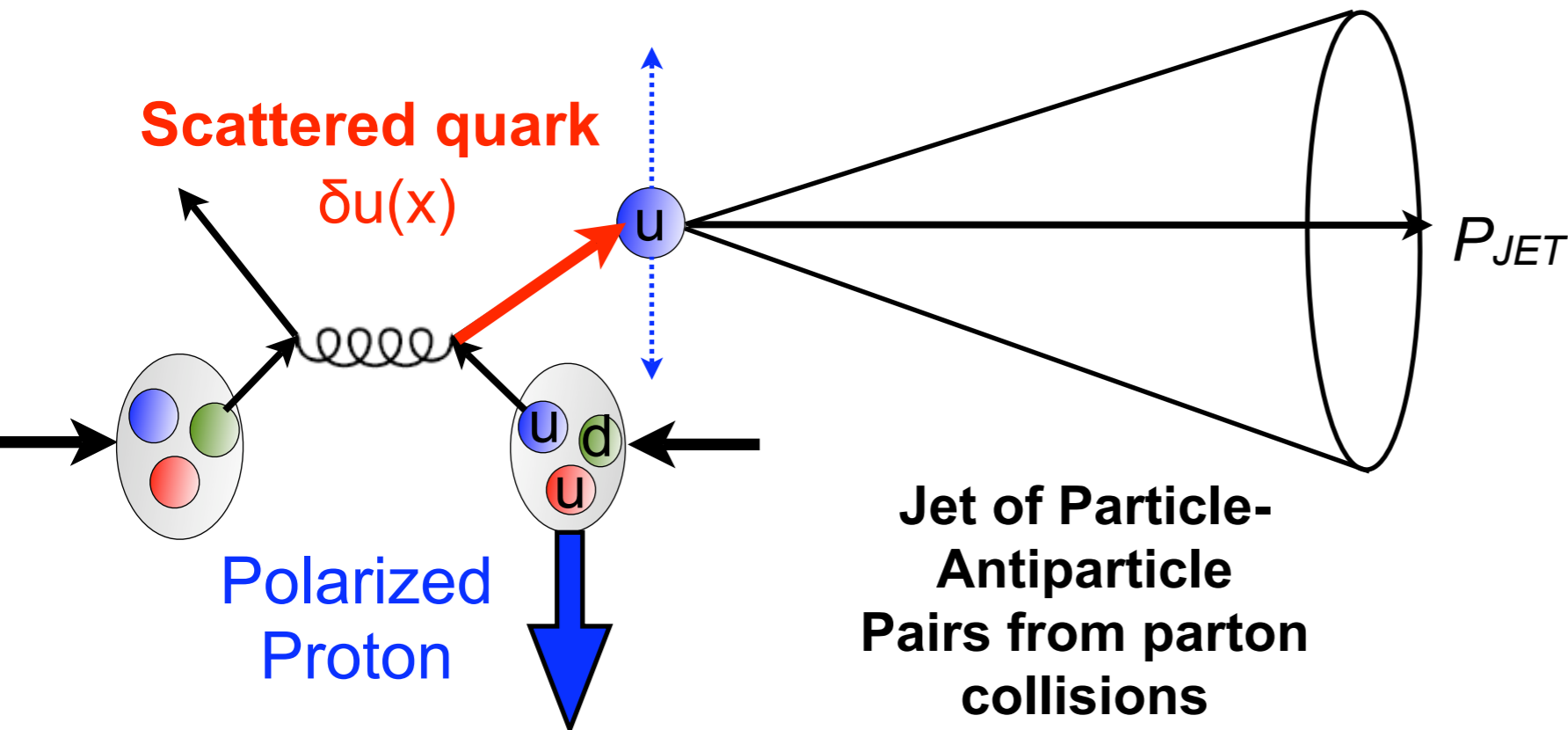
Measurement of left-right  $\pi$  asymmetry  $A_N$   
in  $p^\uparrow p \rightarrow \pi X$  reactions



STAR Publication:  
PRL **101**, 222001  
(2008)

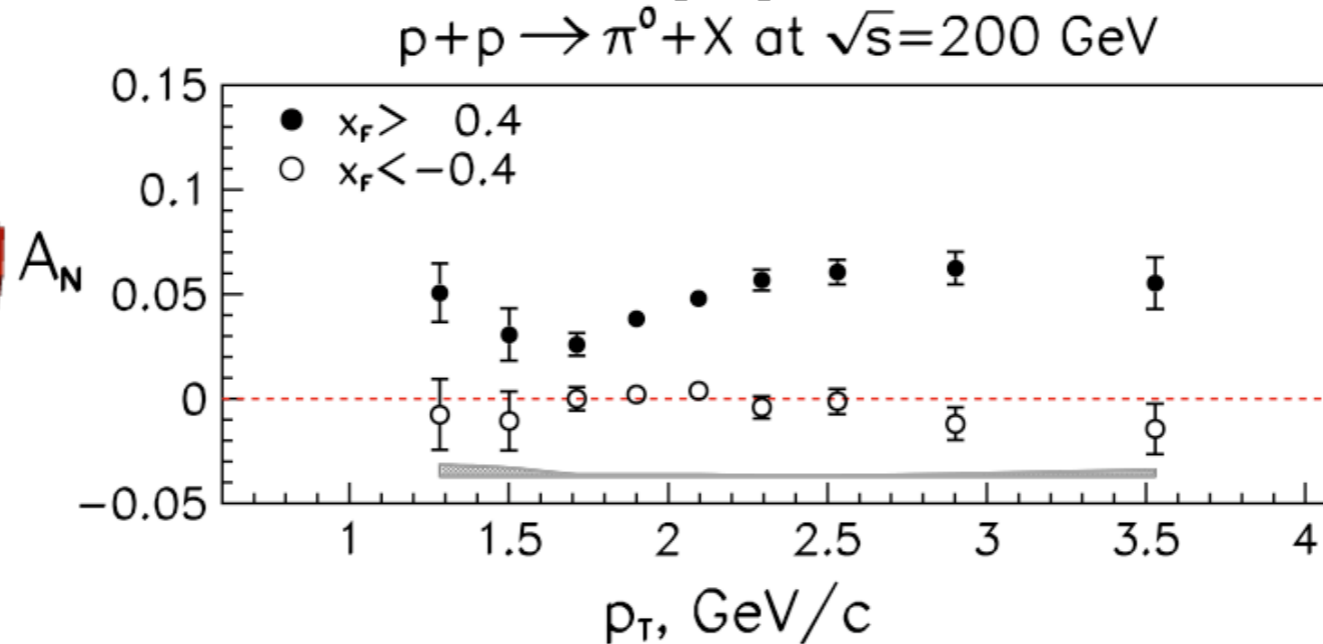
**TMD (Transverse  
Momentum  
Dependence)**  
implied by high  $x_F$   
results

Combined in  $A_N$  due to  
Collins-Sivers mixing



# Experimental Access to Transversity

Measurement of left-right  $\pi$  asymmetry  $A_N$   
in  $p^\uparrow p \rightarrow \pi X$  reactions



STAR Publication:  
PRL **101**, 222001  
(2008)

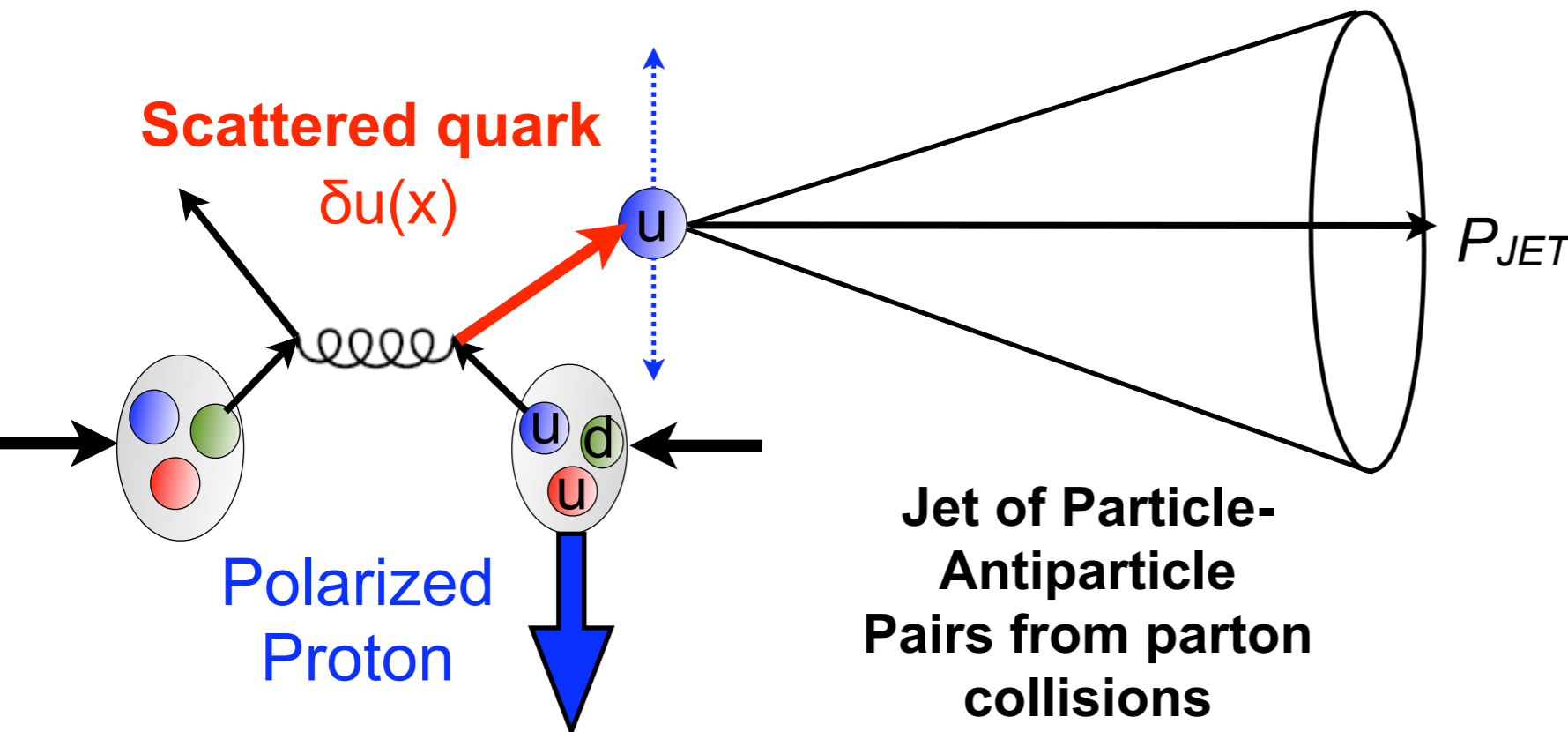
**TMD (Transverse  
Momentum  
Dependence)**  
implied by high  $x_F$   
results

Combined in  $A_N$  due to  
Collins-Sivers mixing

## Sivers Effect:

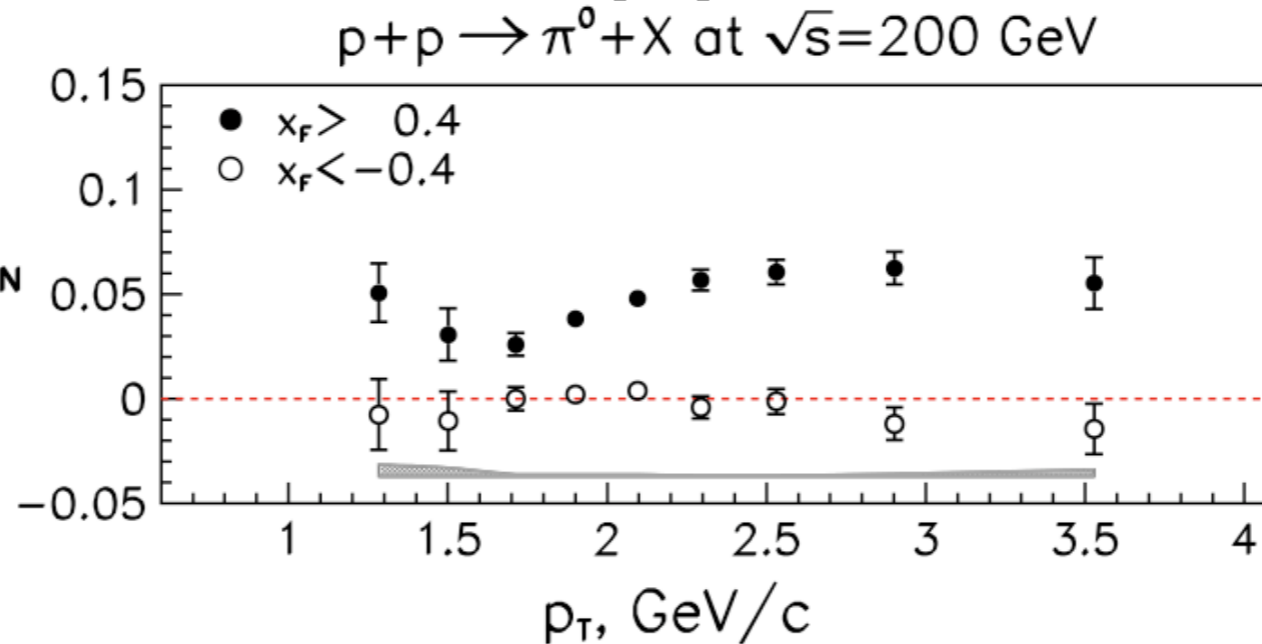
initial state effect (asymmetry  
in dijet opening angle  
distributions; L-dependent)

e.g. STAR Publication:  
PRL **99**, 142003 (2007)



# Experimental Access to Transversity

Measurement of left-right  $\pi$  asymmetry  $A_N$   
in  $p^\uparrow p \rightarrow \pi X$  reactions



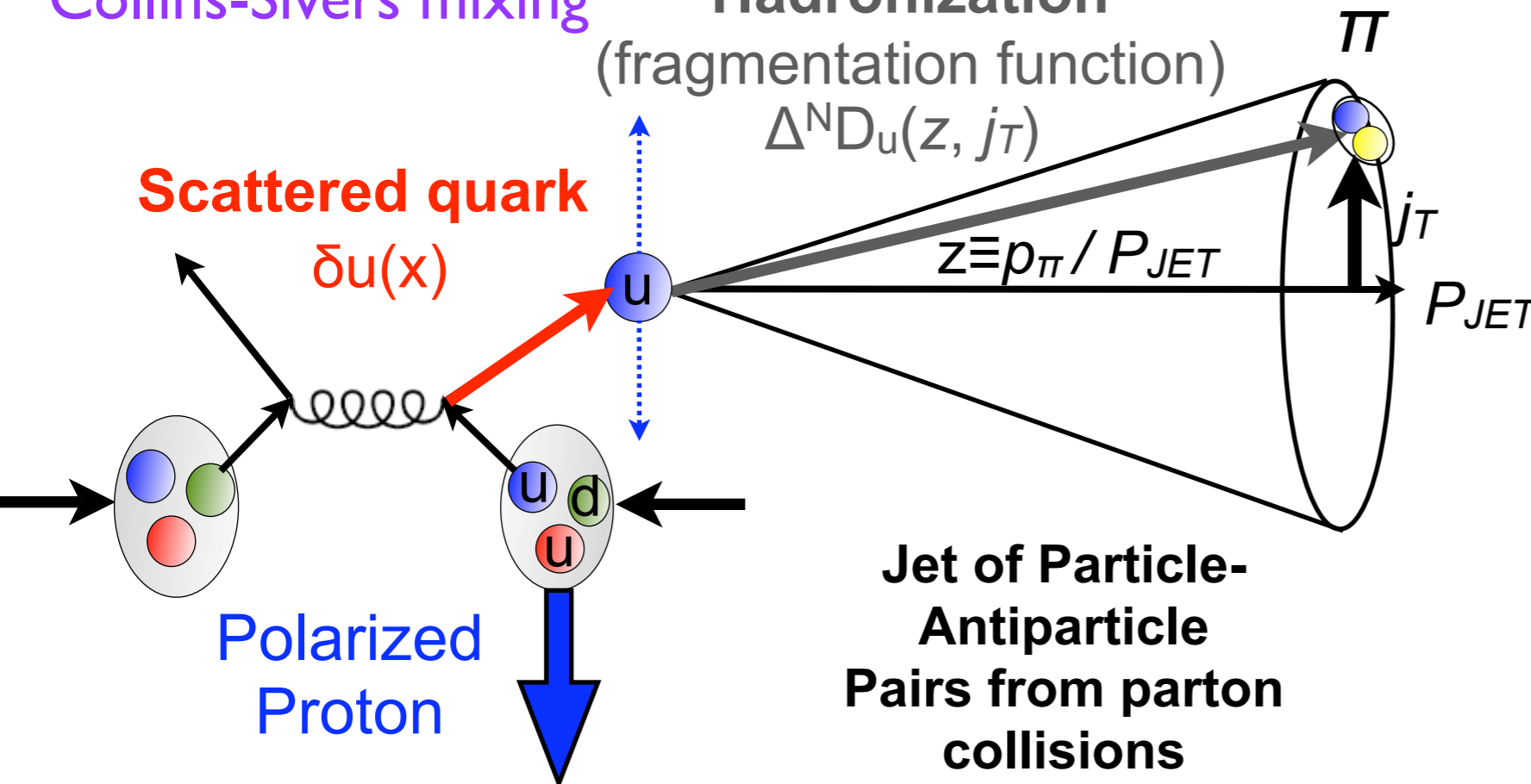
STAR Publication:  
PRL **101**, 222001  
(2008)

**TMD (Transverse Momentum Dependence)**  
implied by high  $x_F$  results

Combined in  $A_N$  due to  
Collins-Sivers mixing

**Hadronization**  
(fragmentation function)  
 $\Delta^N D_u(z, j_T)$

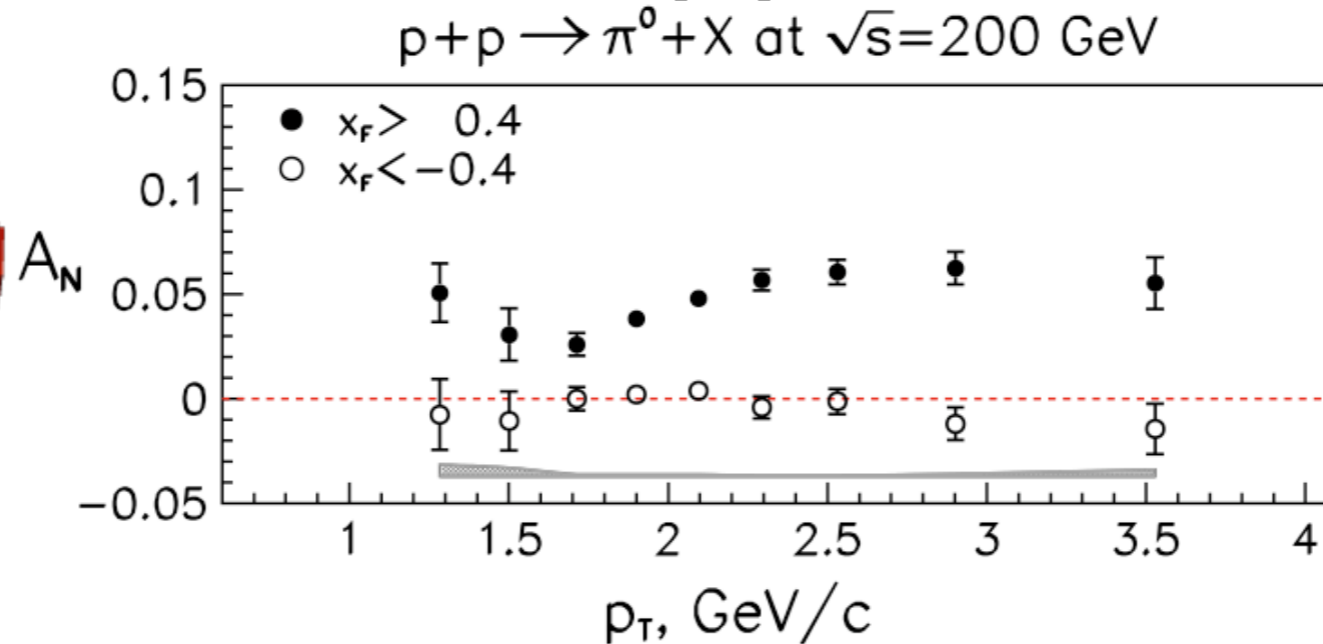
**Scattered quark**  
 $\delta u(x)$



**Sivers Effect:**  
initial state effect (asymmetry  
in dijet opening angle  
distributions; L-dependent)  
e.g. STAR Publication:  
PRL **99**, 142003 (2007)

# Experimental Access to Transversity

Measurement of left-right  $\pi$  asymmetry  $A_N$   
in  $p^\uparrow p \rightarrow \pi X$  reactions



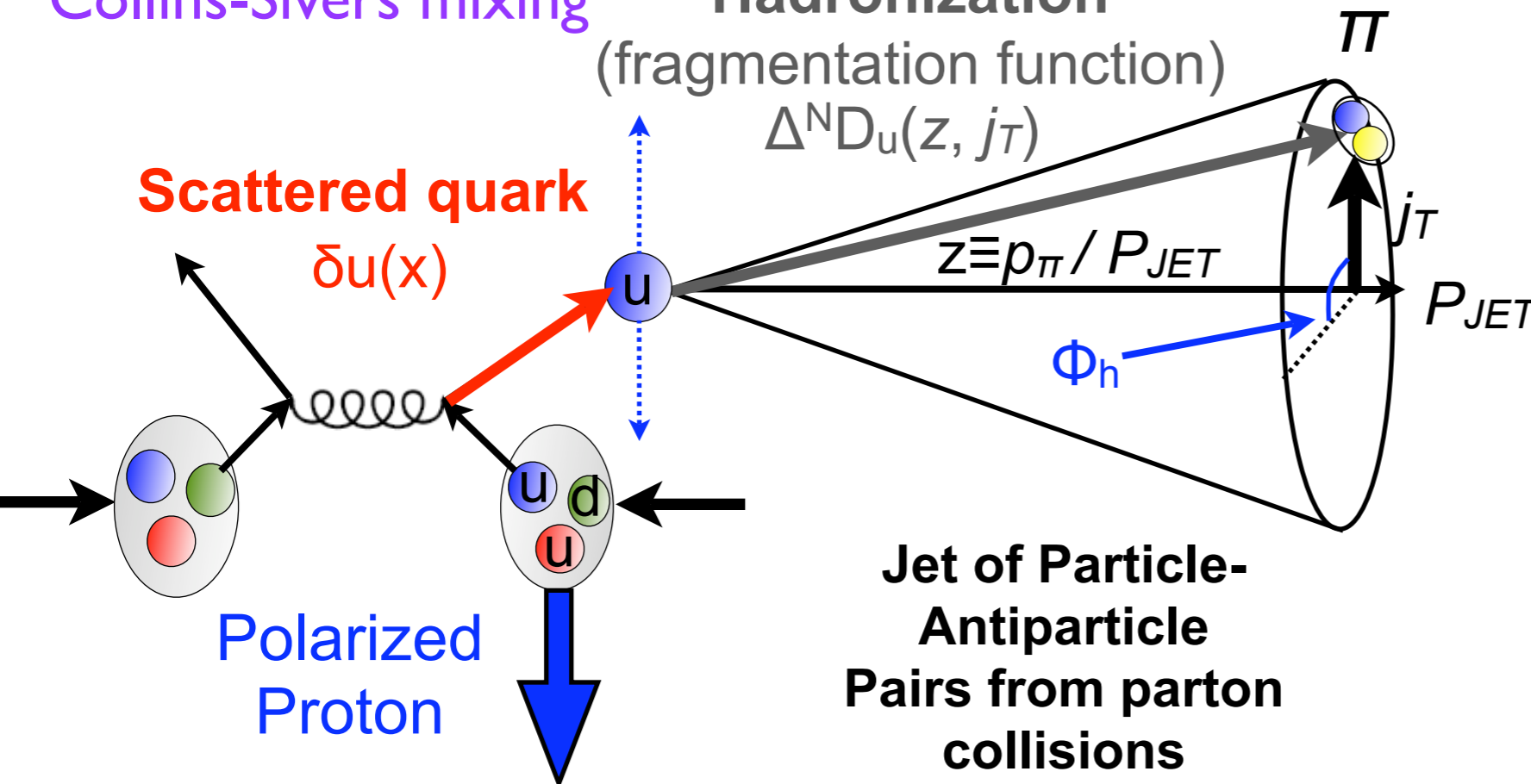
STAR Publication:  
PRL 101, 222001  
(2008)

**TMD (Transverse Momentum Dependence)**  
implied by high  $x_F$  results

Combined in  $A_N$  due to  
Collins-Sivers mixing

**Hadronization**  
(fragmentation function)  
 $\Delta^N D_u(z, j_T)$

**Scattered quark**  
 $\delta u(x)$



**Sivers Effect:**  
initial state effect (asymmetry  
in dijet opening angle  
distributions; **L-dependent**)  
e.g. STAR Publication:  
PRL 99, 142003 (2007)

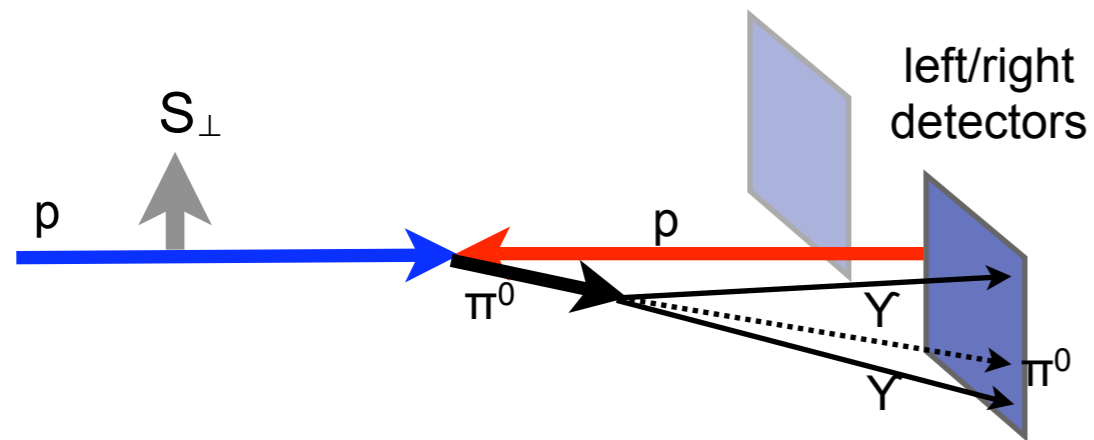
**Collins Effect:**  
final state effect (asymmetry  
in hadron fragmentation;  
 $\delta q$ -dependent)

# **Collins-Sivers Separation**

**Must move from inclusive  
pions to “jets”**

# Collins-Sivers Separation

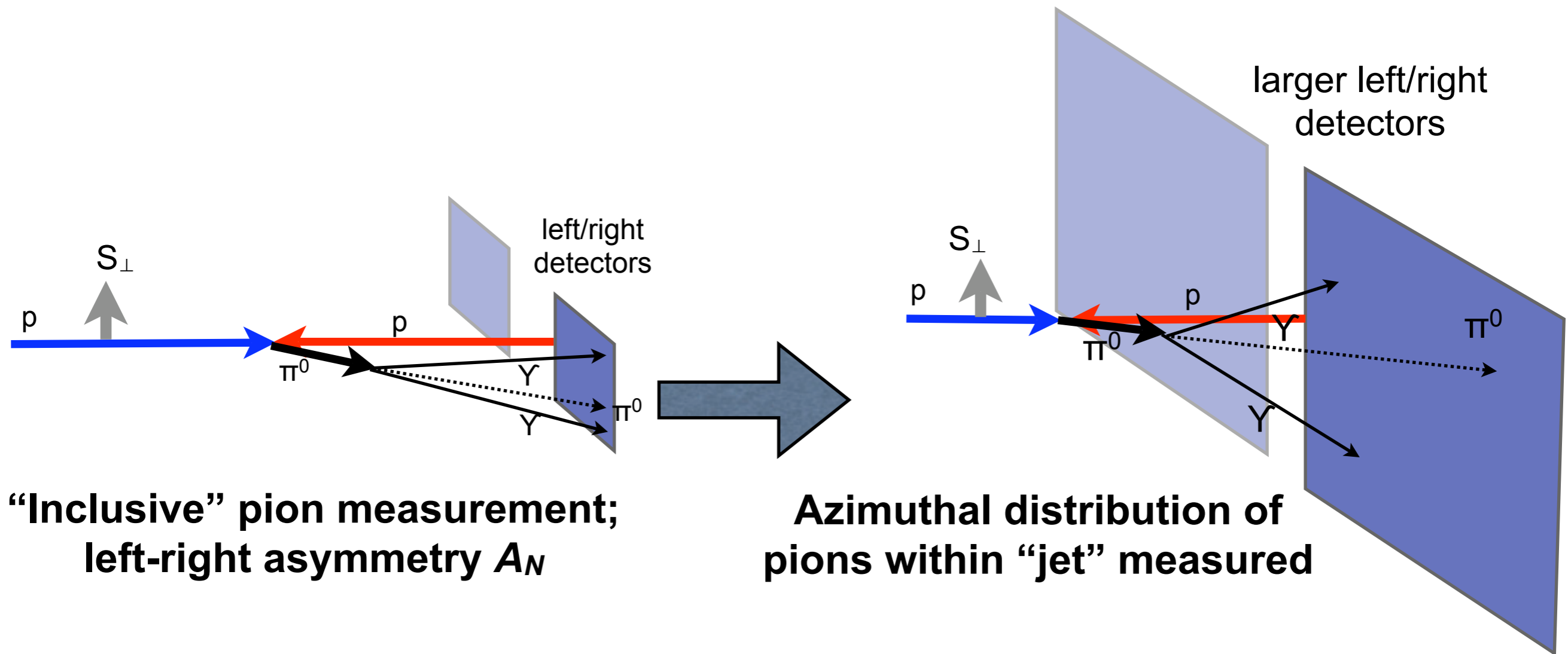
Must move from inclusive  
pions to “jets”



“Inclusive” pion measurement;  
left-right asymmetry  $A_N$

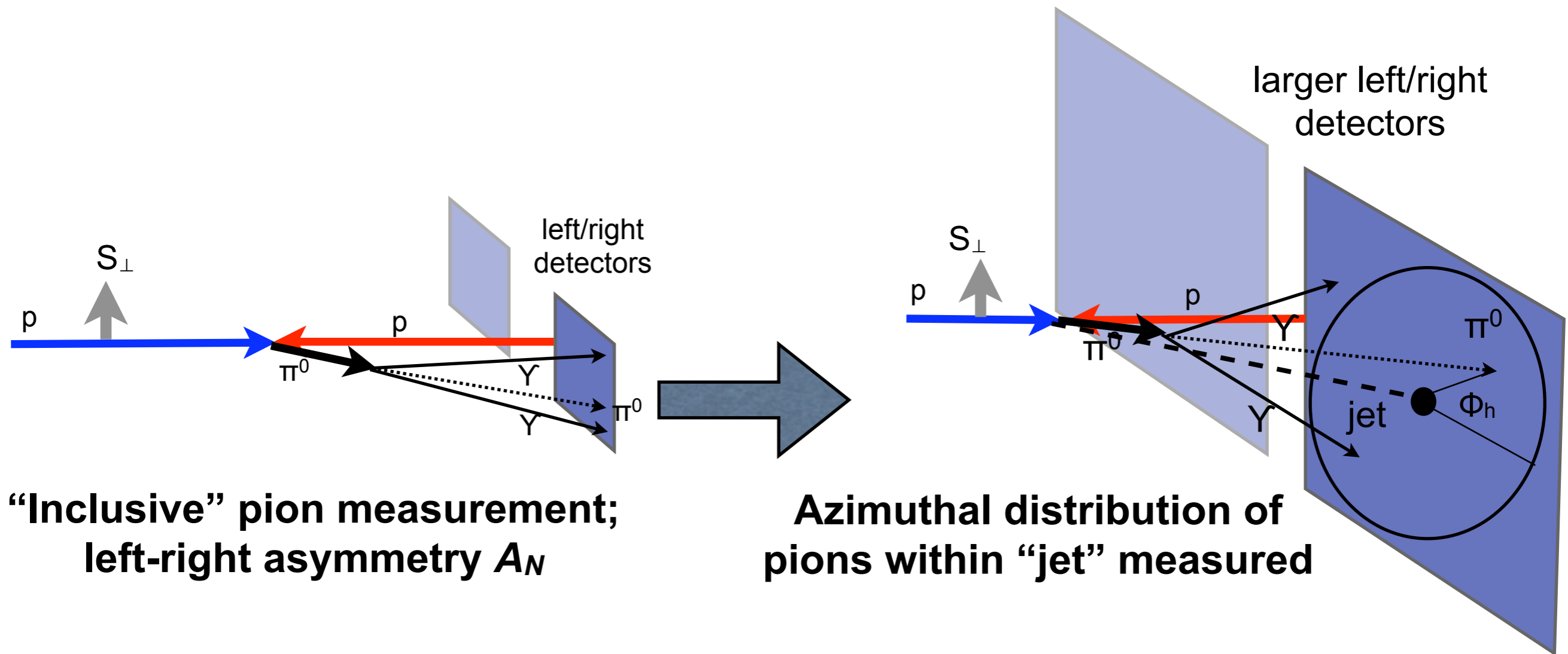
# Collins-Sivers Separation

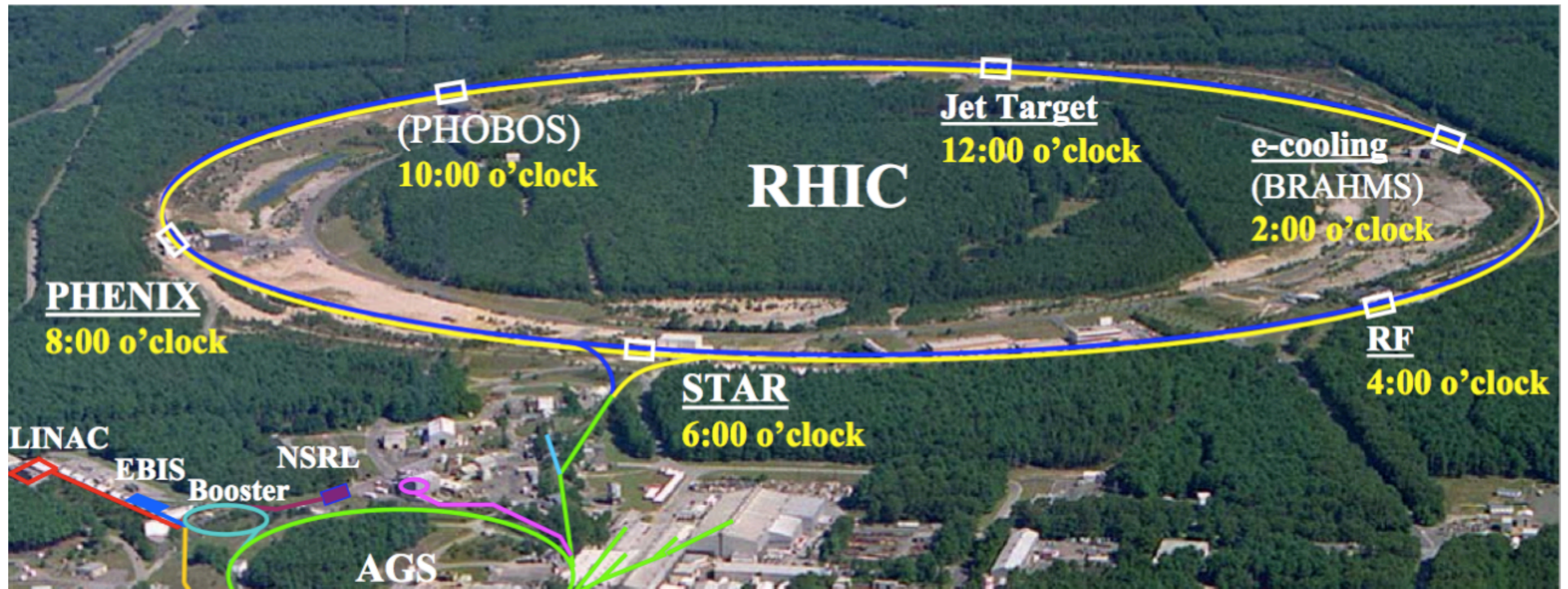
Must move from inclusive  
pions to “jets”

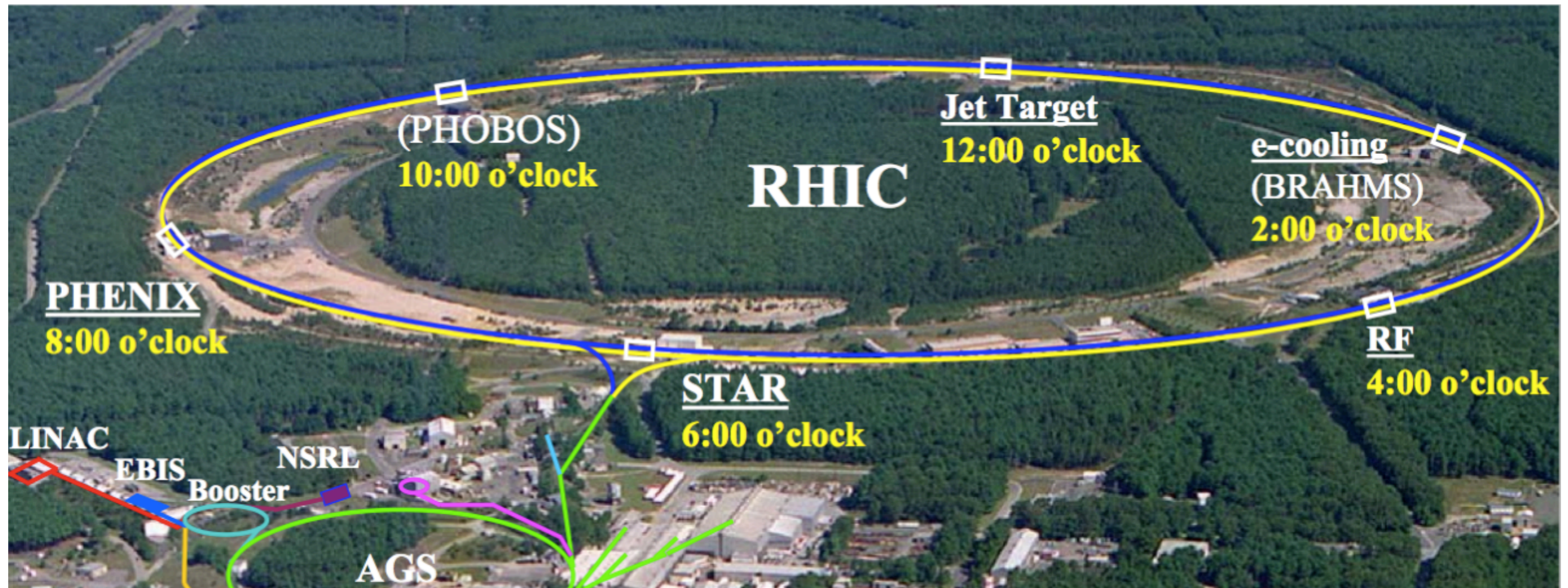


# Collins-Sivers Separation

Must move from inclusive  
pions to “jets”



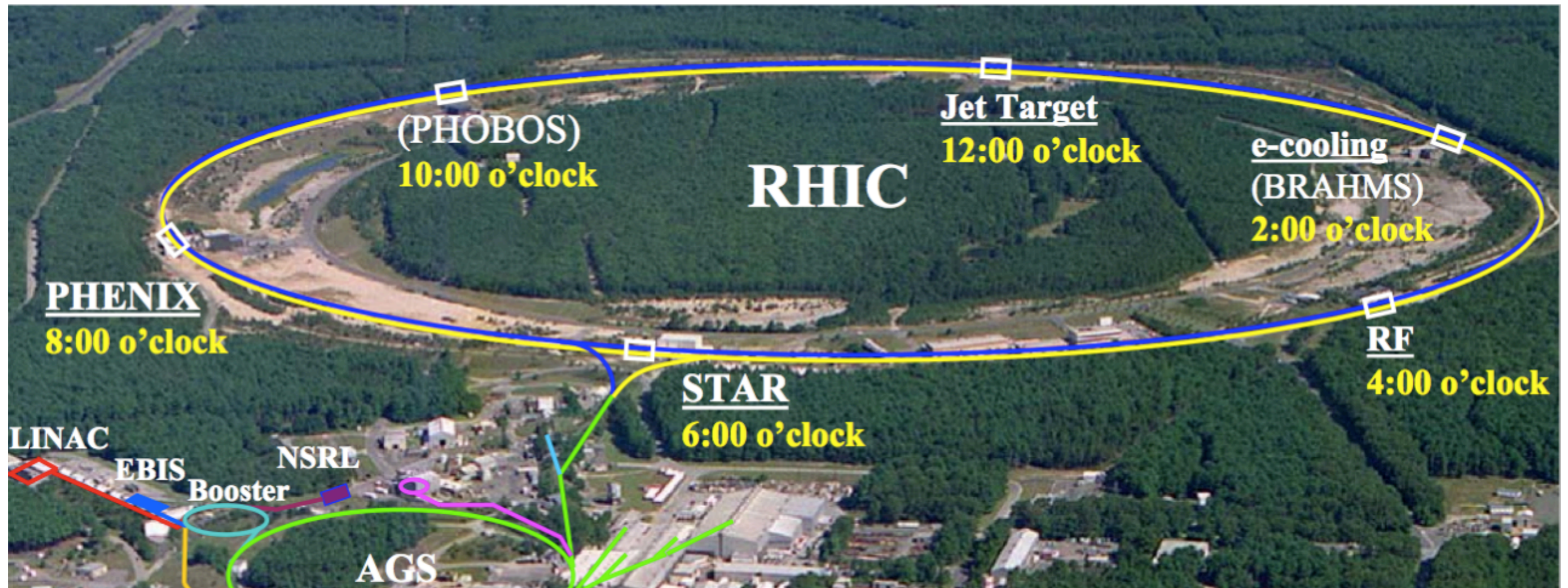




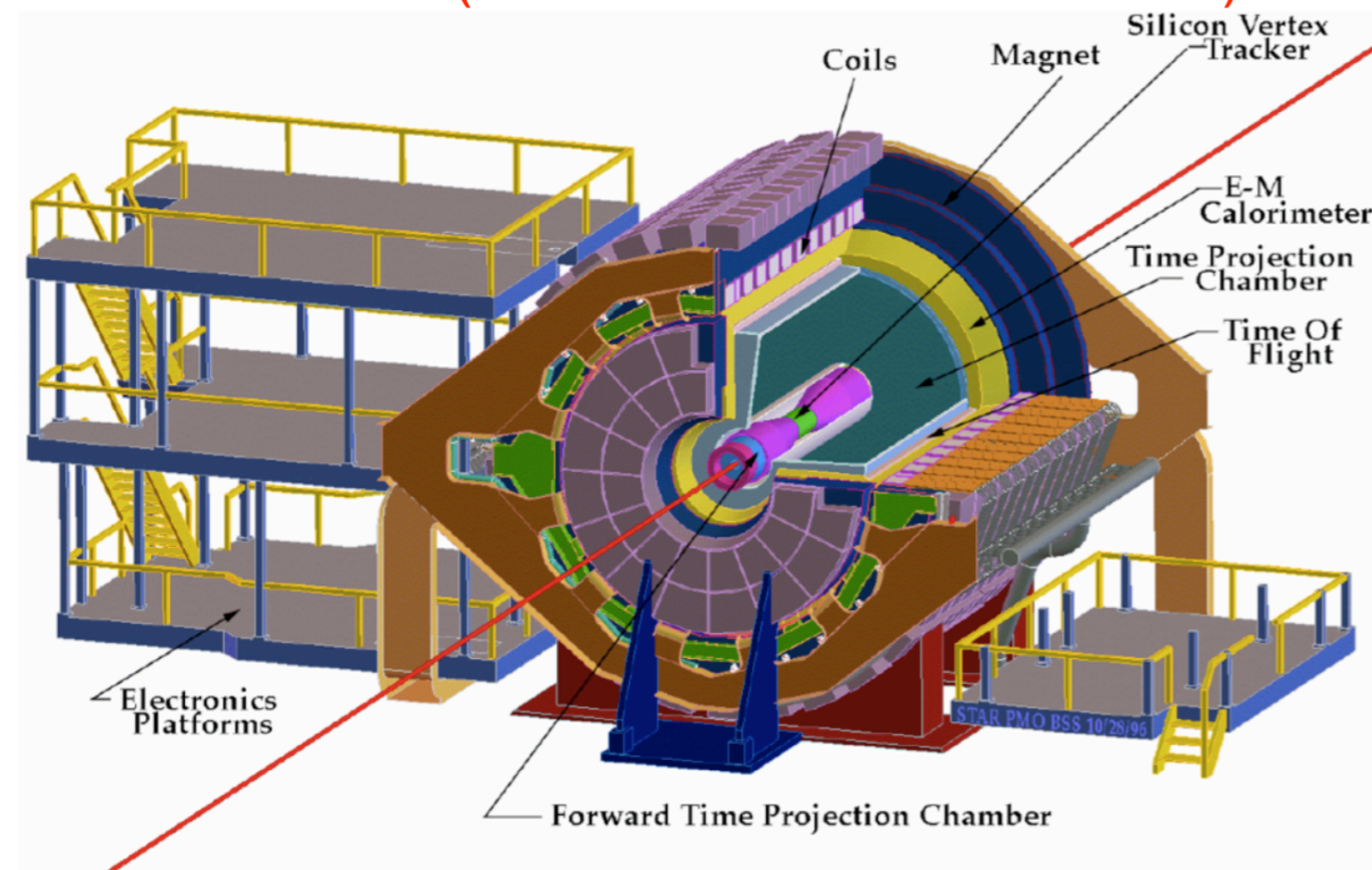
Proton-proton collisions up to  
 $\sqrt{s} = 500 \text{ GeV}$

Beam polarizations as high as  
 $\sim 60\%$  have been achieved (2006)

Beam luminosity  
 $\sim 10^{31} \text{ s}^{-1} \text{ cm}^{-2}$  (2006)



# STAR (Solenoidal Tracker at RHIC)



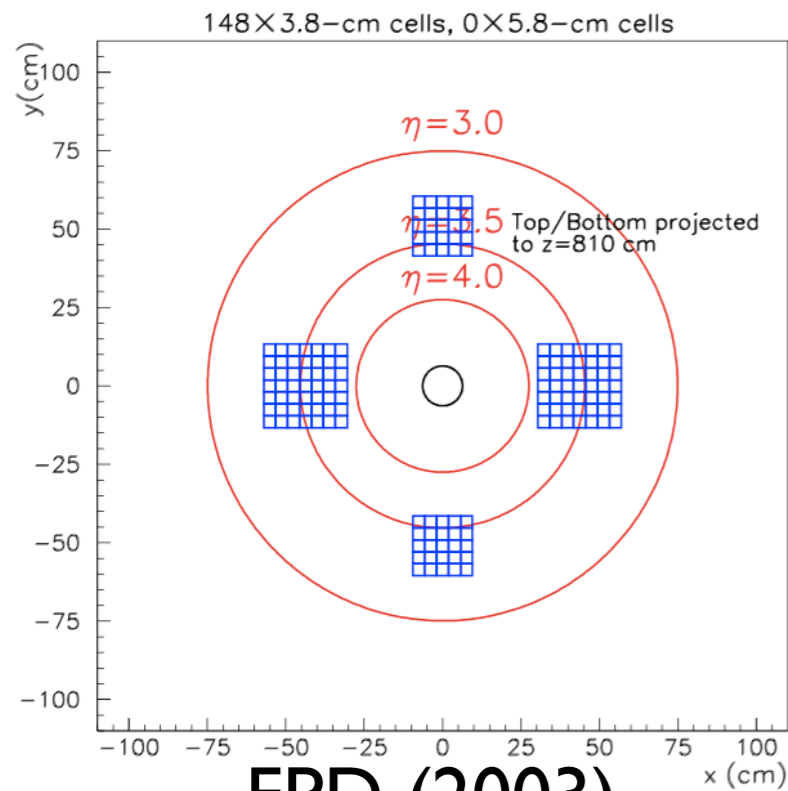
Proton-proton collisions up to  
 $\sqrt{s} = 500 \text{ GeV}$

Beam polarizations as high as  
 $\sim 60\%$  have been achieved (2006)

Beam luminosity  
 $\sim 10^{31} \text{ s}^{-1} \text{ cm}^{-2}$  (2006)

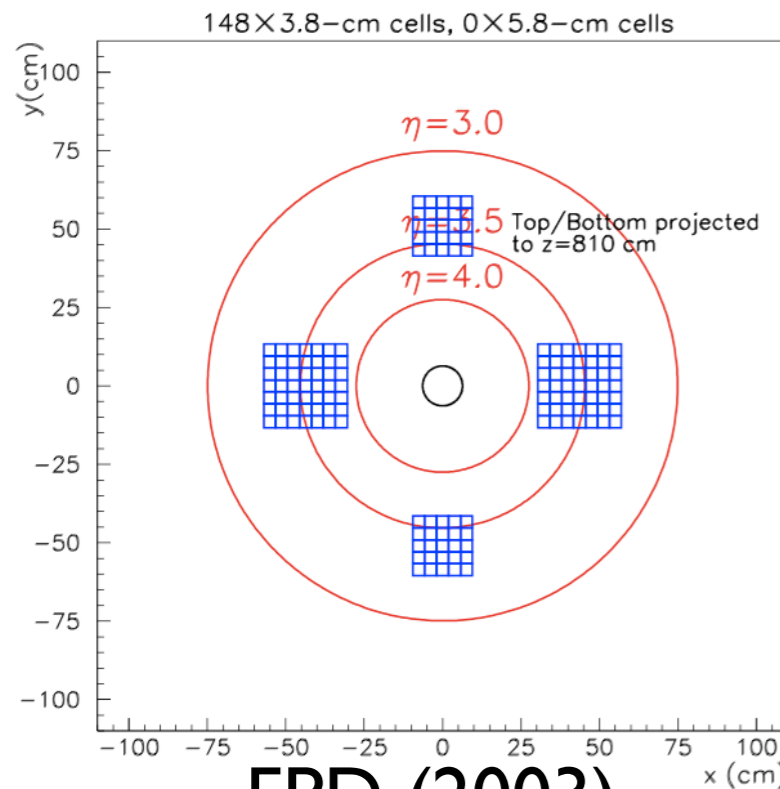
# Forward-Angle Detectors

# Forward-Angle Detectors

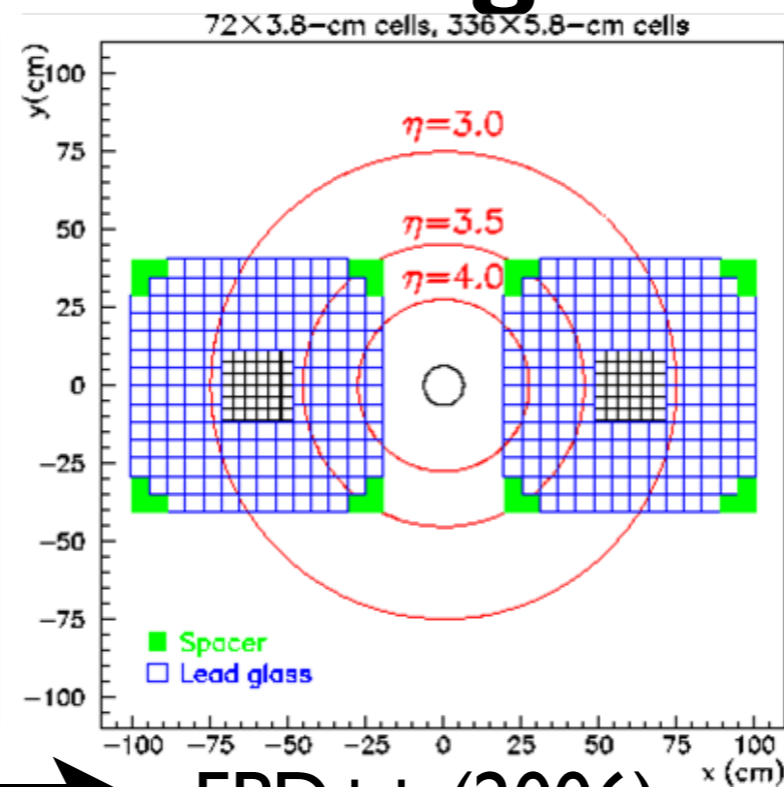


**FPD (2003)**  
(Forward Pion Detector)

# Forward-Angle Detectors

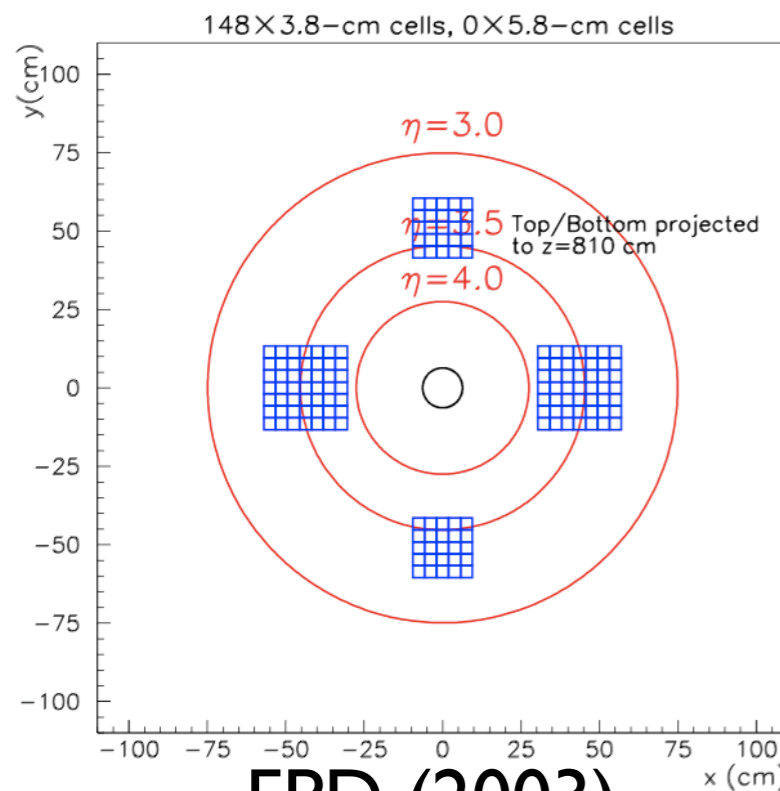


**FPD (2003)**  
(Forward Pion Detector)

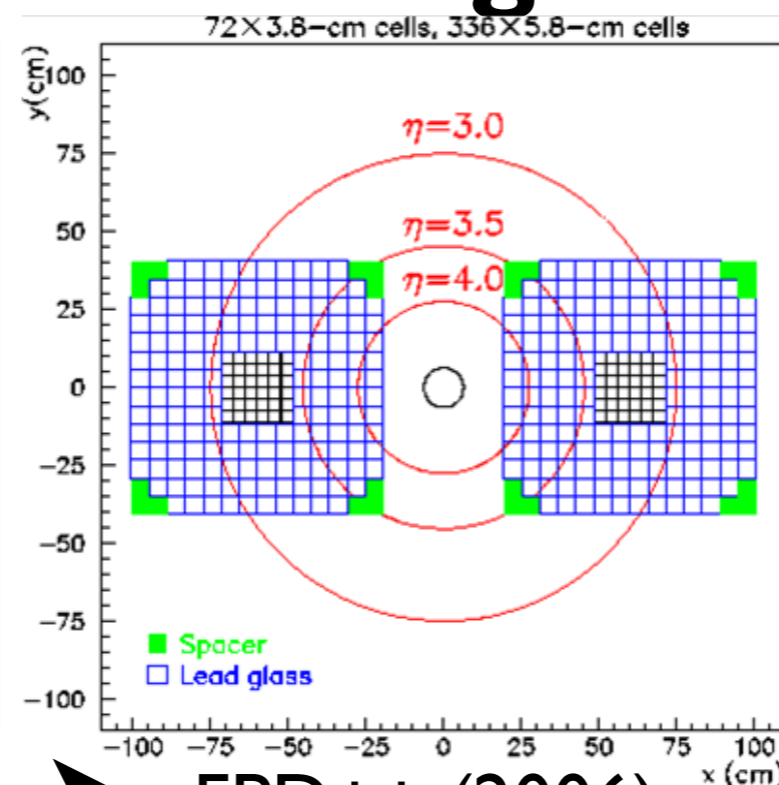


**FPD++ (2006)**

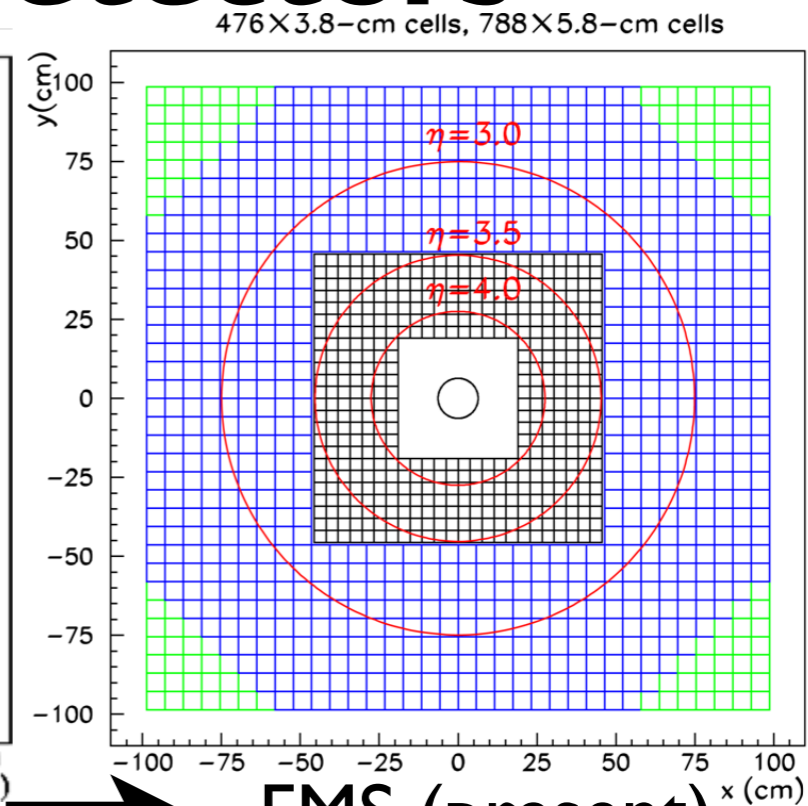
# Forward-Angle Detectors



**FPD (2003)**  
(Forward Pion Detector)

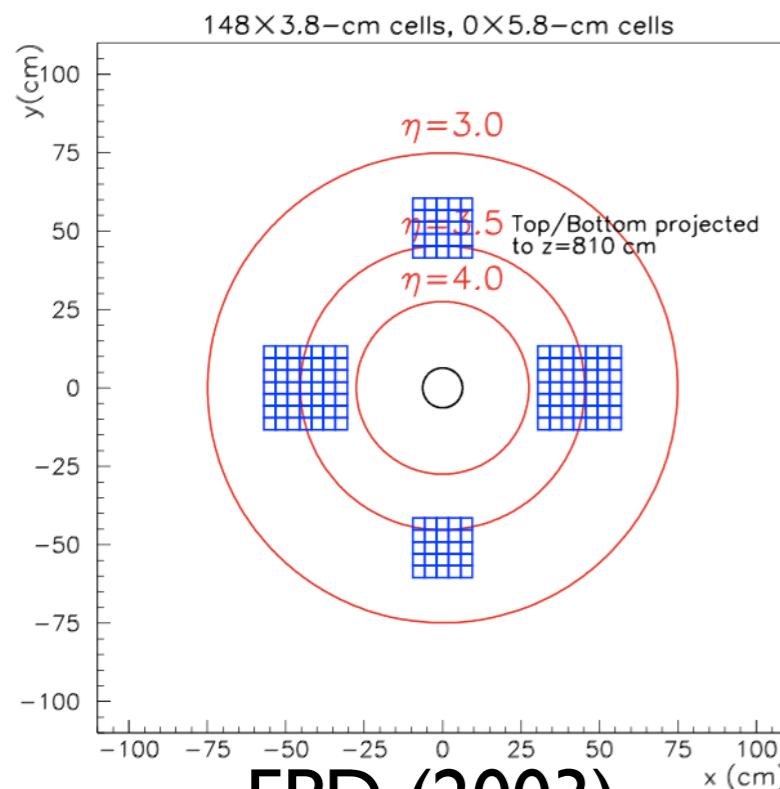


**FPD++ (2006)**

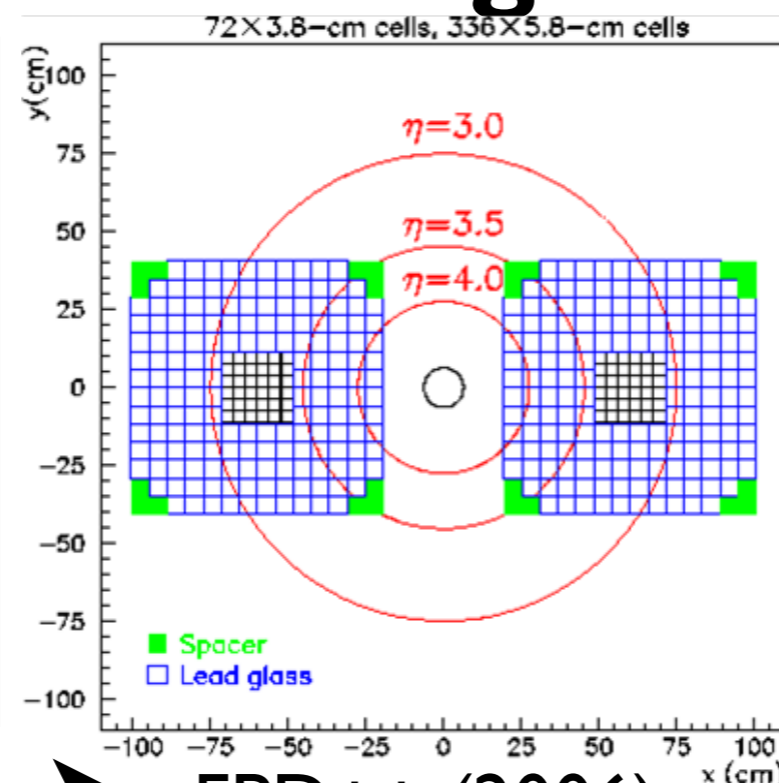


**FMS (present)**  
(Forward Meson Spectrometer)

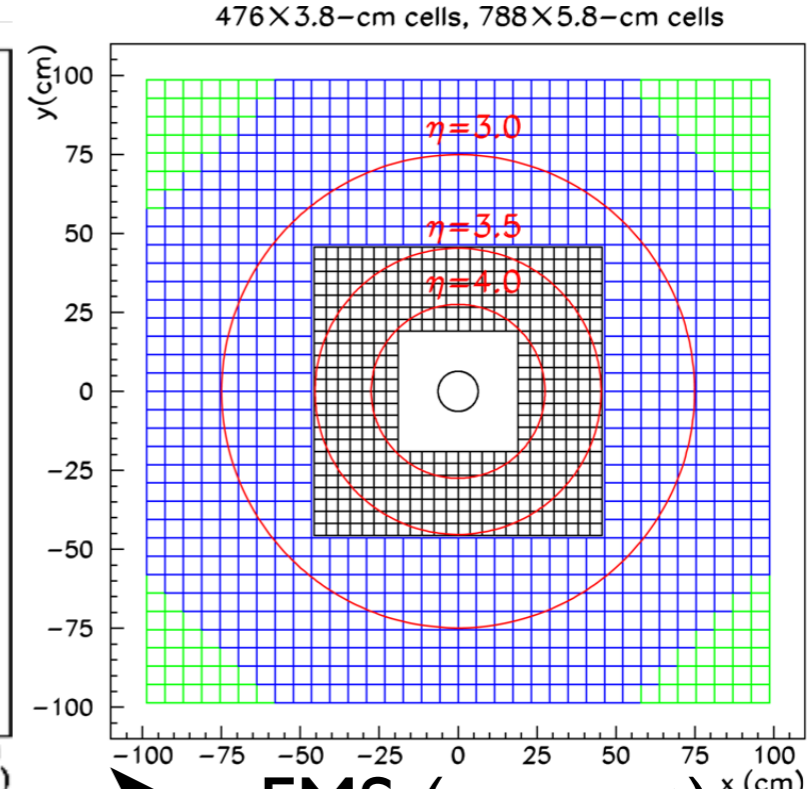
# Forward-Angle Detectors



**FPD (2003)**  
(Forward Pion Detector)

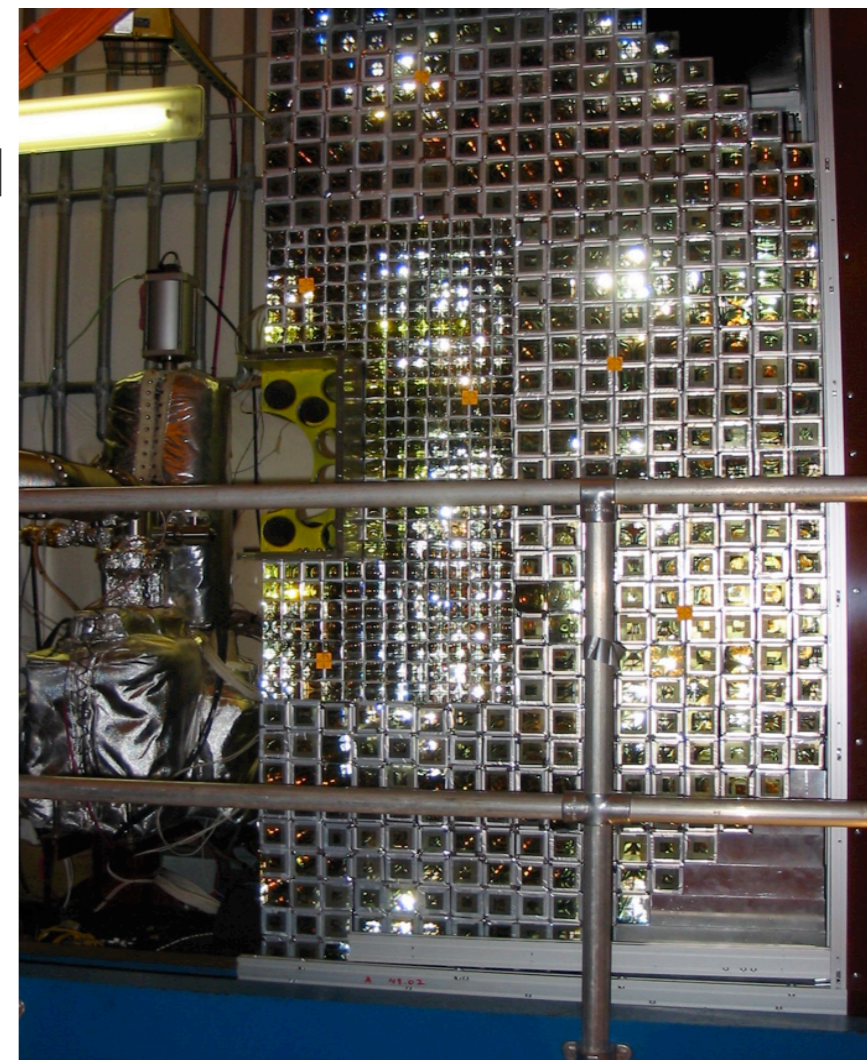


**FPD++ (2006)**

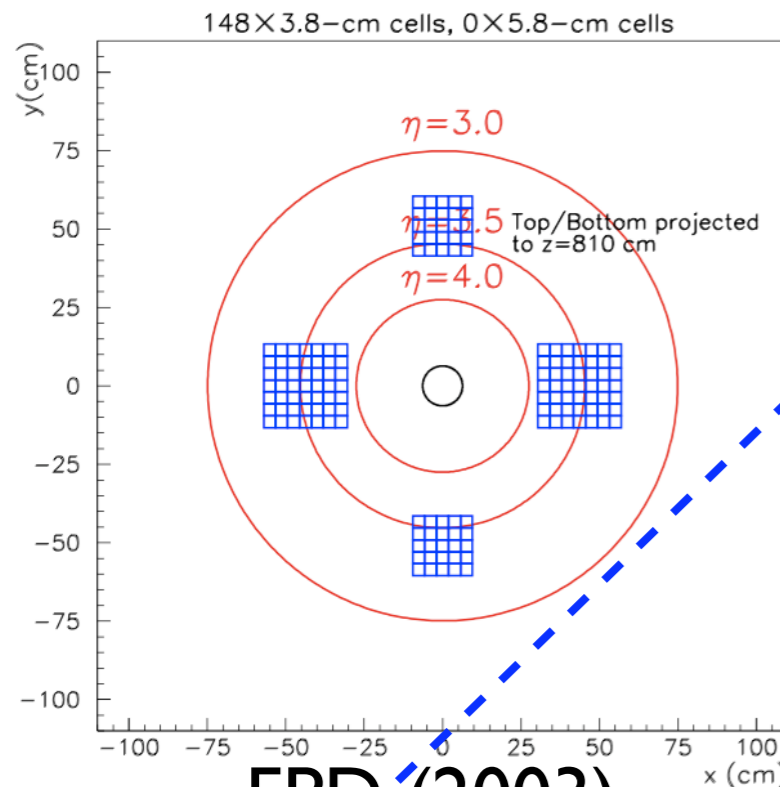


**FMS (present)**  
(Forward Meson Spectrometer)

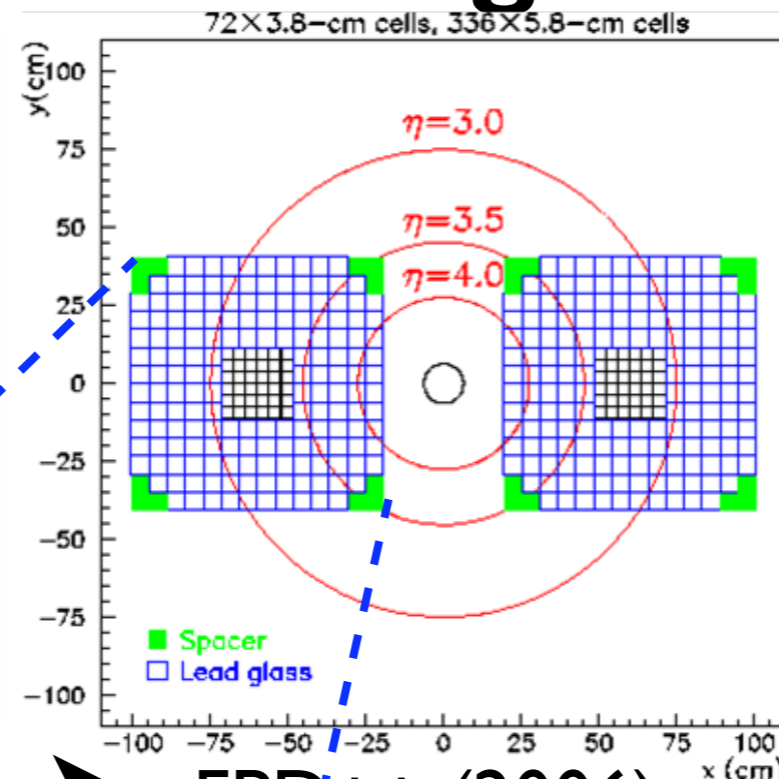
lead-glass/PMT  
detectors arranged  
in square cells



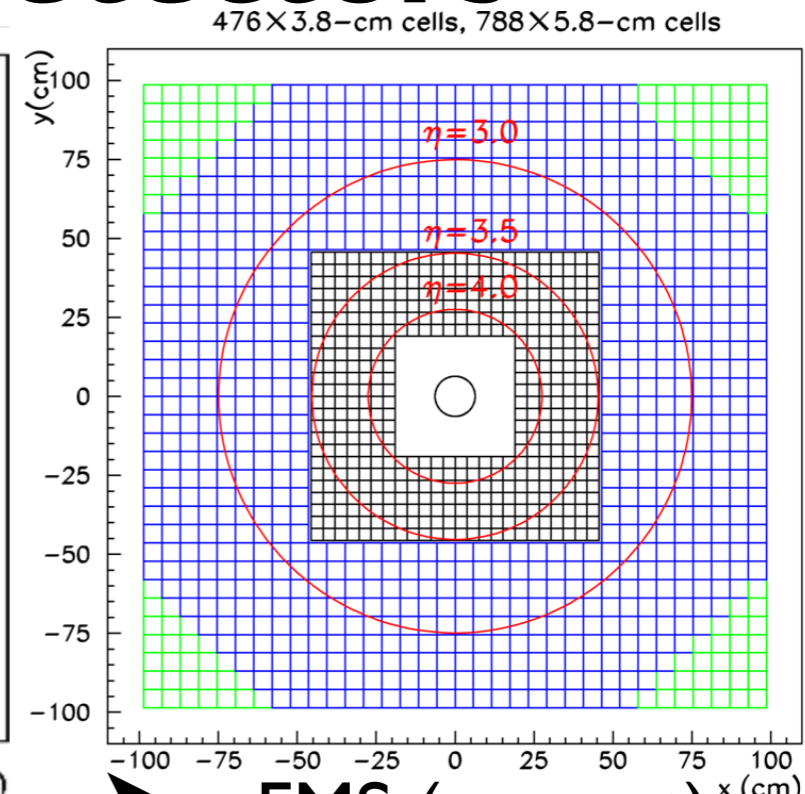
# Forward-Angle Detectors



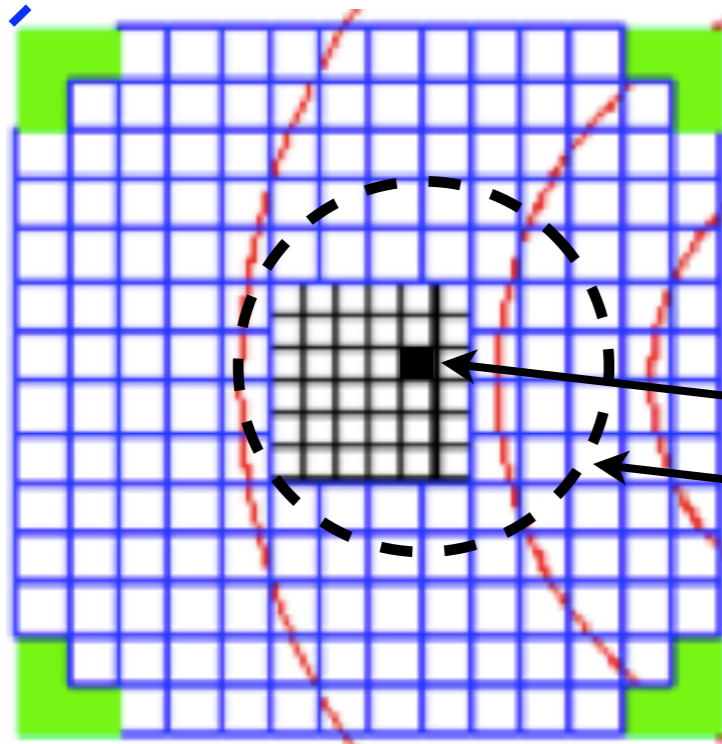
**FPD (2003)**  
(Forward Pion Detector)



**FPD++ (2006)**



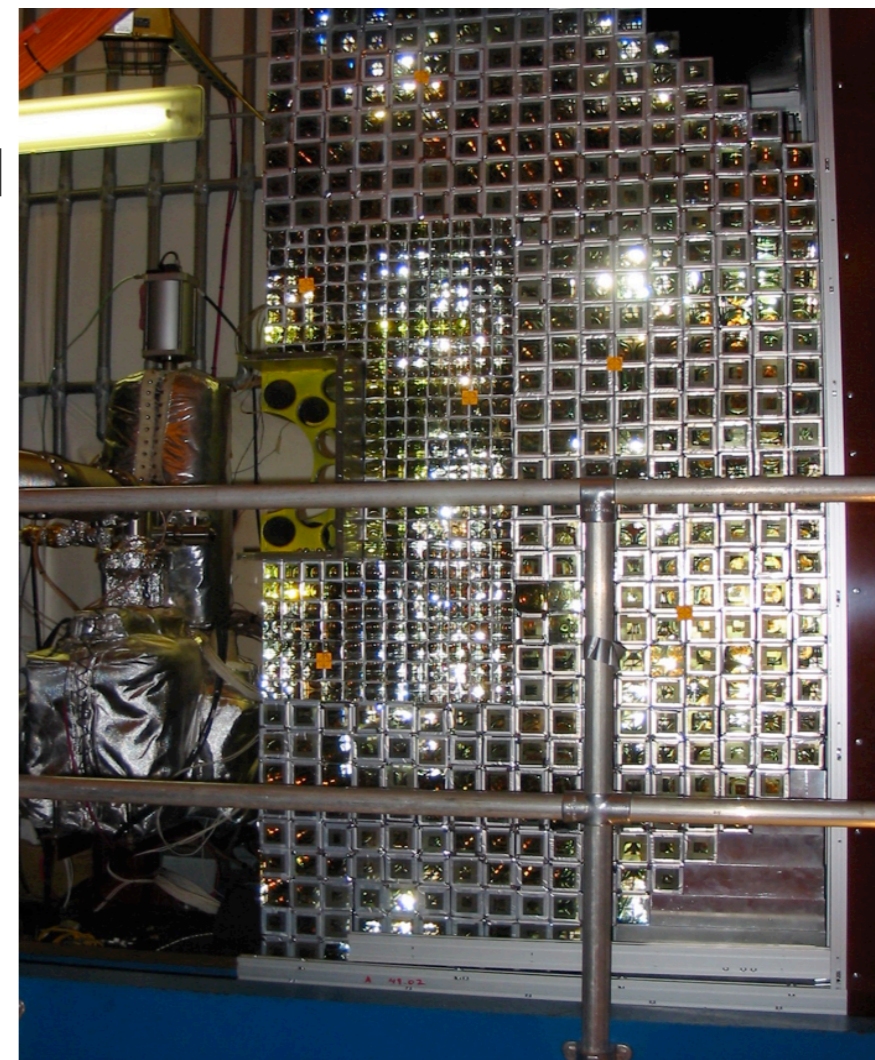
**FMS (present)**  
(Forward Meson Spectrometer)



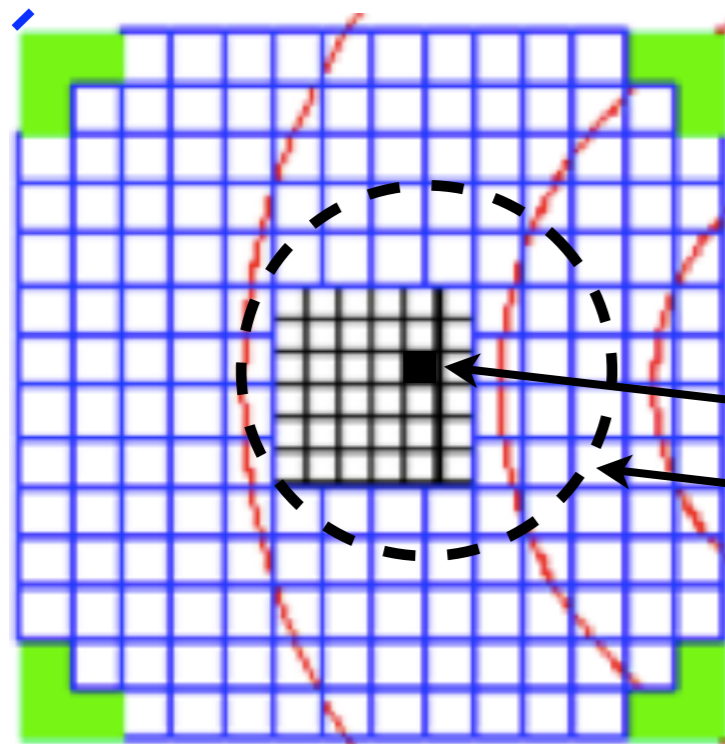
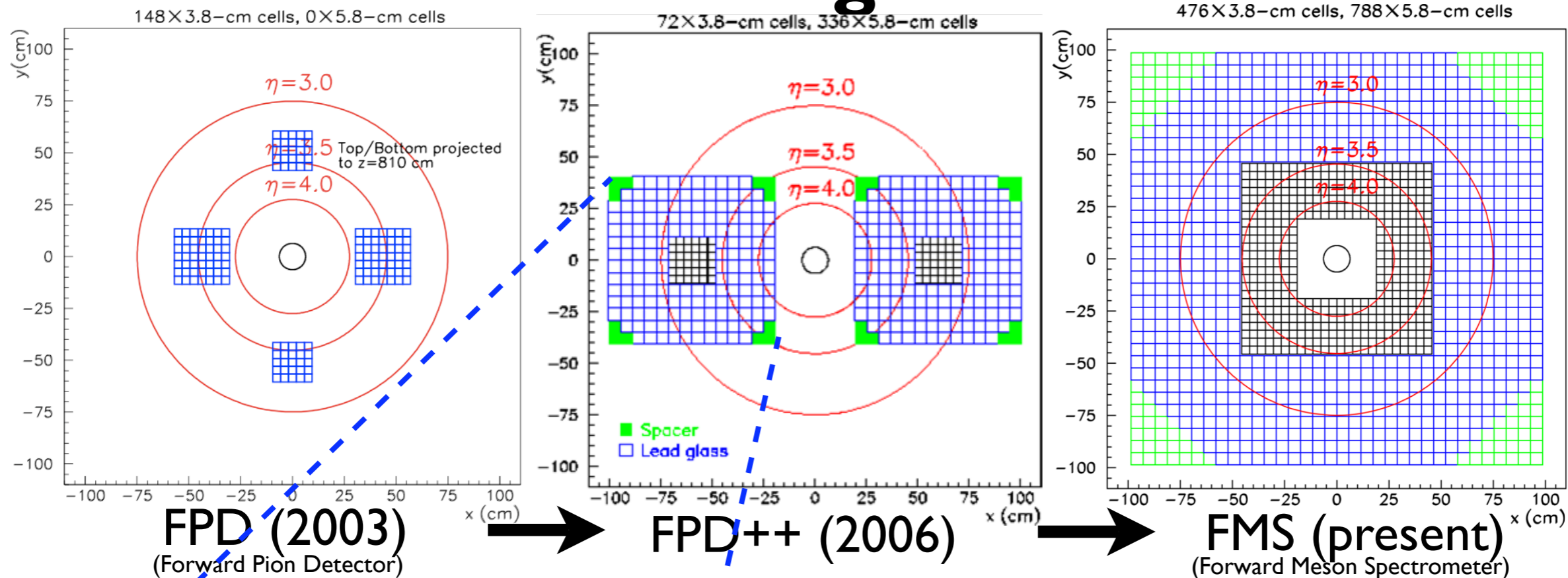
lead-glass/PMT  
detectors arranged  
in square cells

inner cell-module  
trigger ( $\pi^0$   $\gamma$ s)

Search area  
for deposited  
energy



# Forward-Angle Detectors



lead-glass/PMT detectors arranged in square cells

inner cell-module trigger ( $\pi^0$  Ys)

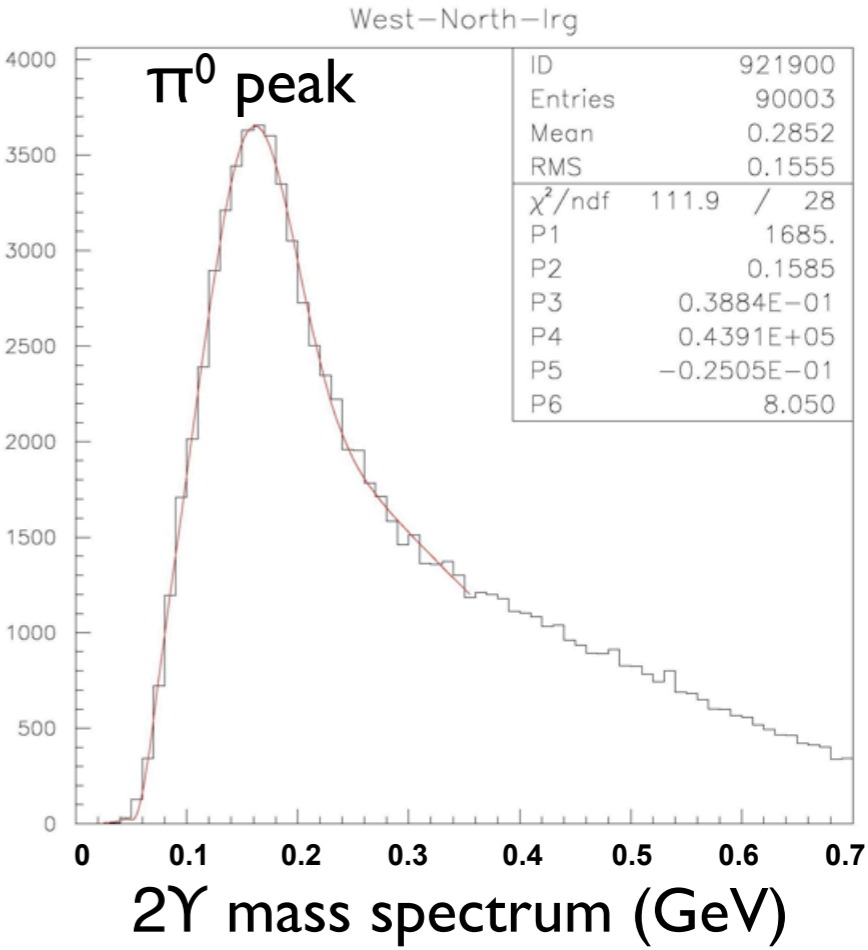
Search area for deposited energy

$\pi^0$  identification:  $|E_1 - E_2|/(E_1 + E_2) < 0.7$  (+ lead photon energy-dependent and rate-dependent corrections on reconstructed mass)

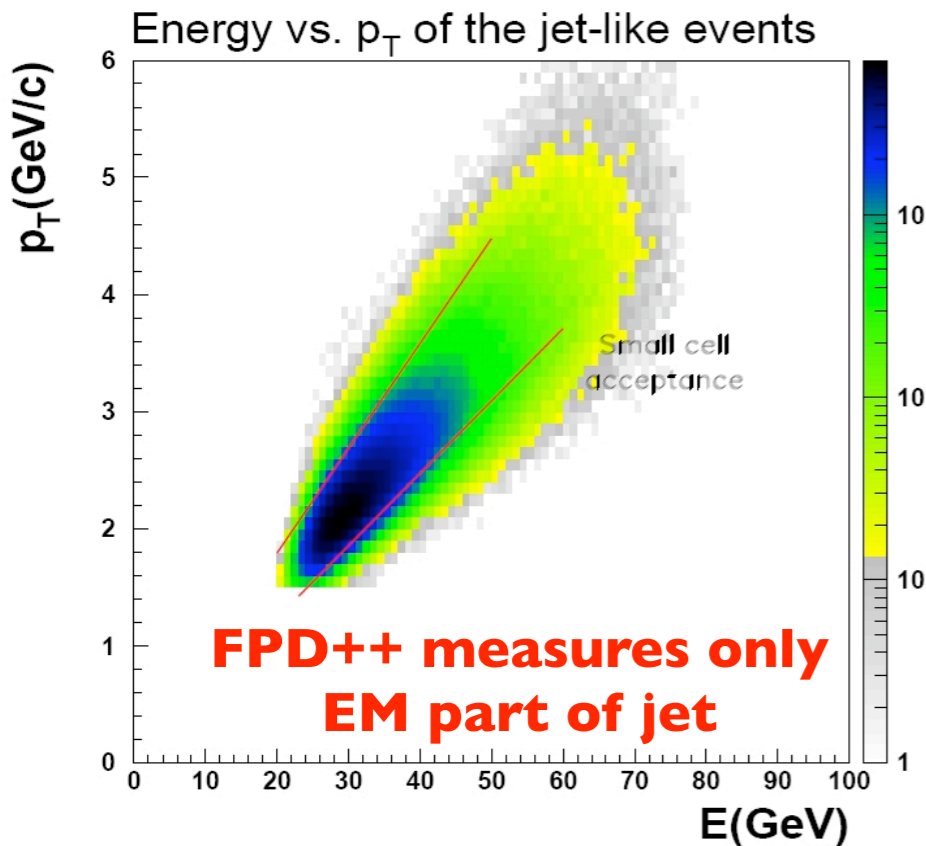
“jet-like” event: cluster of 10 (weighted) cells in live readout with  $p_T > 1.5$  GeV,  $x_F > 0.23$



# Analysis of $\pi^0$ data from the FPD++

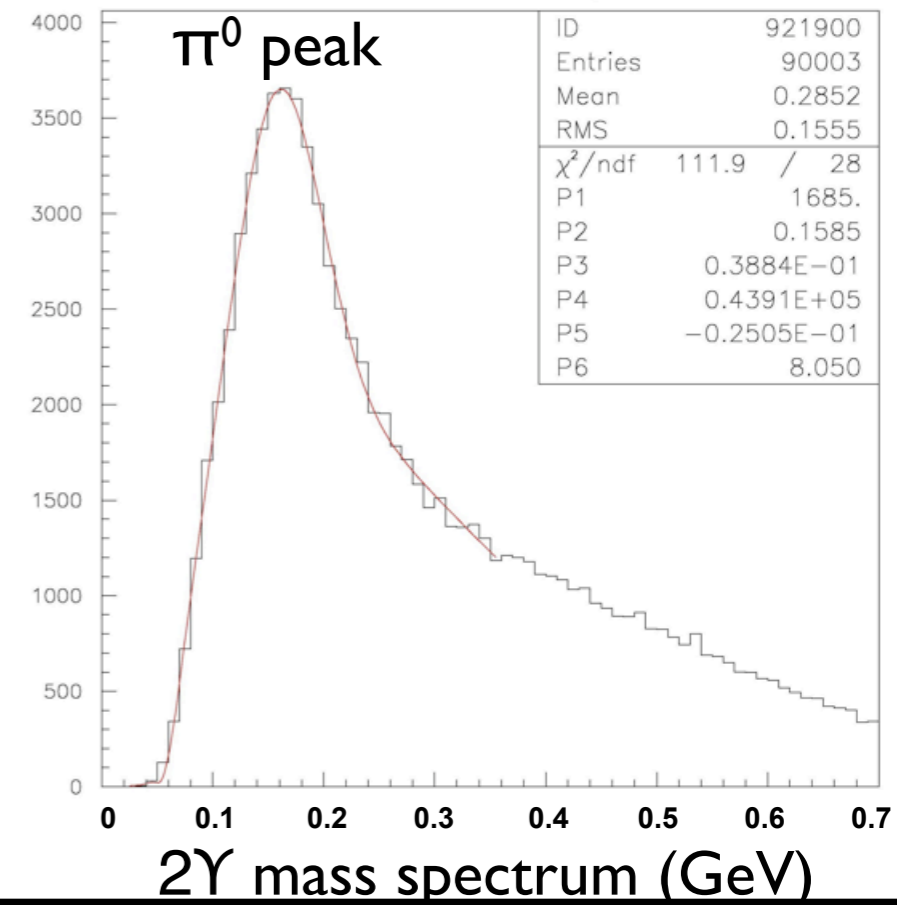


# Analysis of $\pi^0$ data from the FPD++

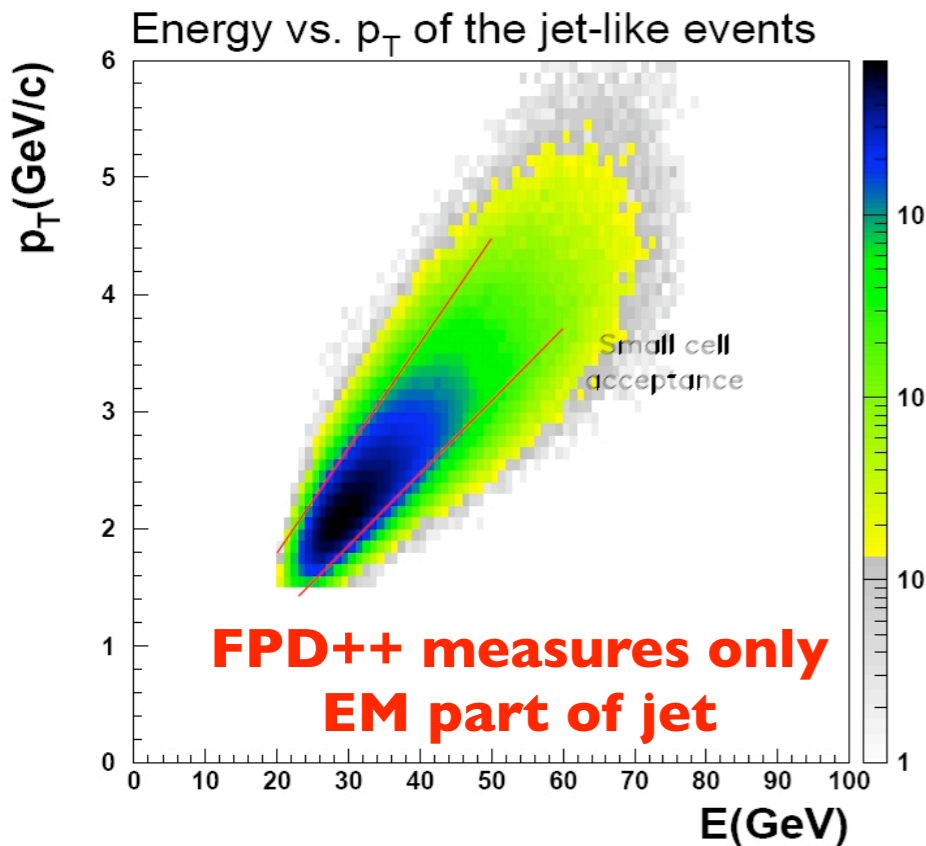


## Identification of “jet-like” events

- Require 4 cells with minimum energy 0.4 GeV
- Minimum weighted sum of cells
- Minimum cuts on total energy (20 GeV) and average  $p_T$  (1.5 GeV)
- Maximum cone size  $\Delta R \equiv \sqrt{(\Delta\eta^2 + \Delta\phi^2)} > 0.5$
- 2-large-cell fiducial cut around “jet”-axis

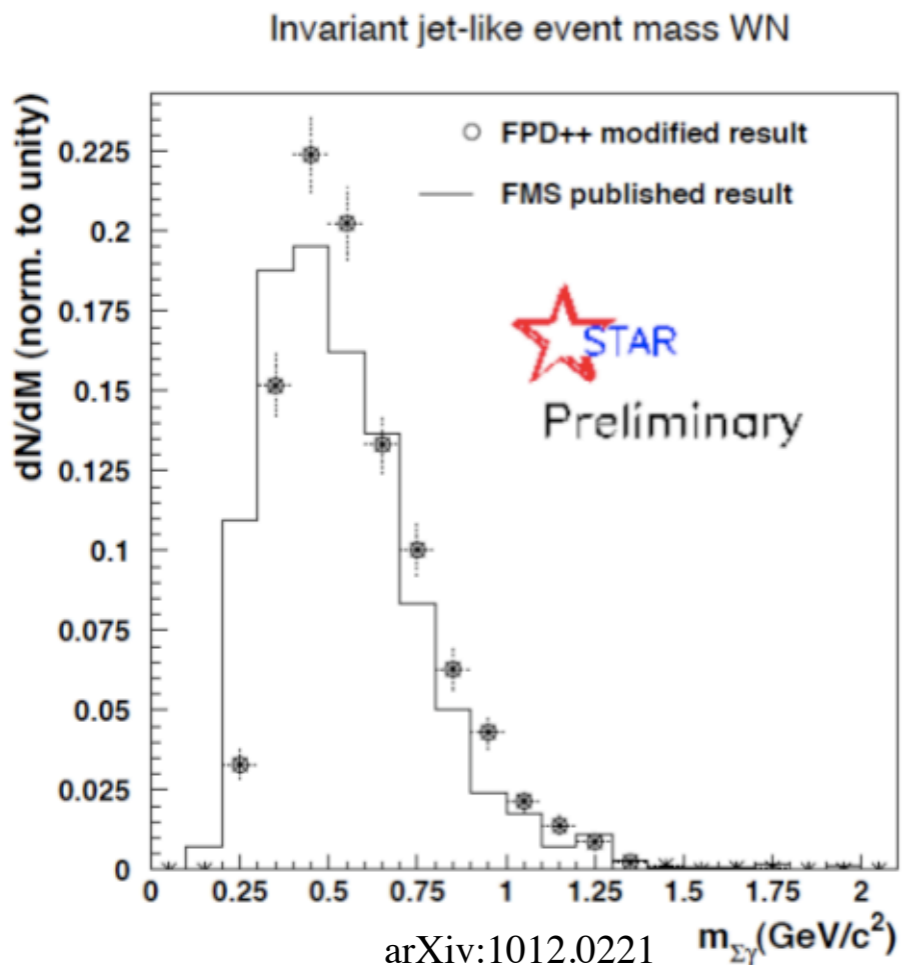
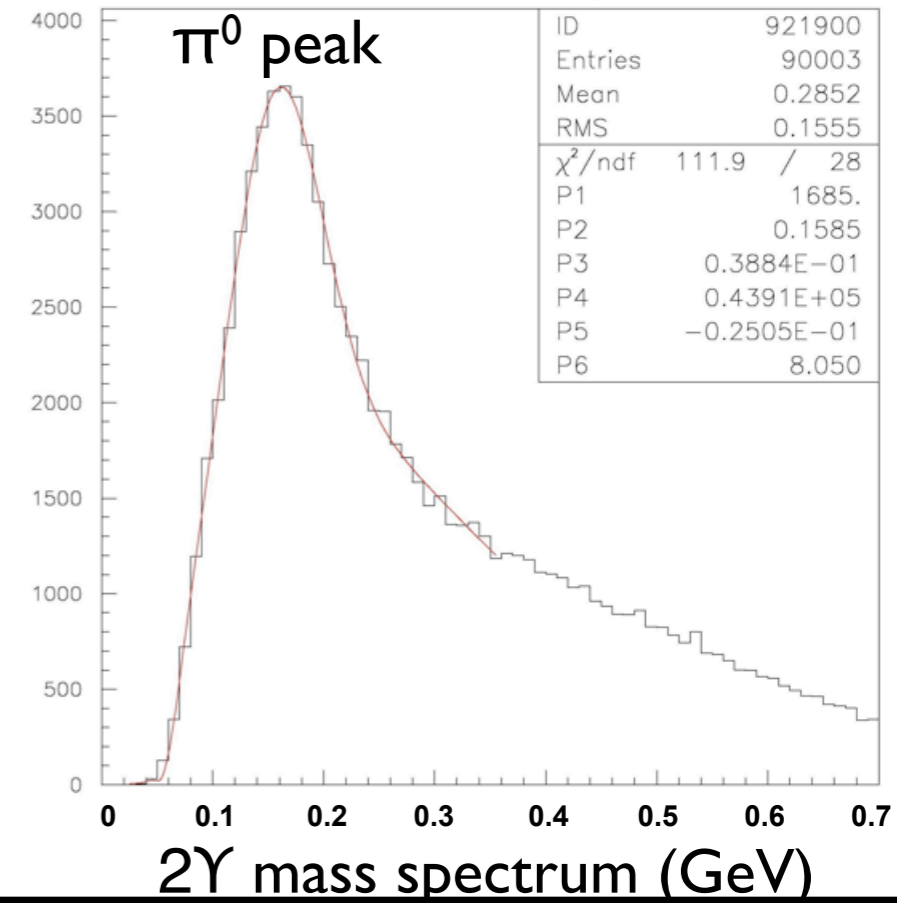


# Analysis of $\pi^0$ data from the FPD++



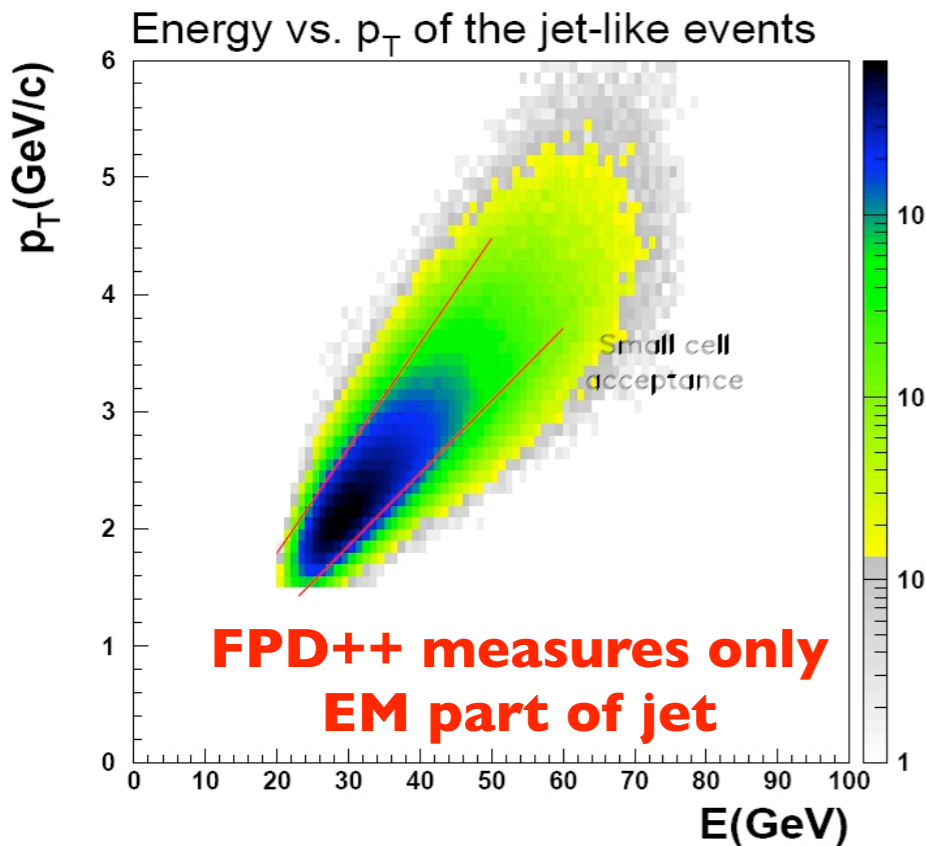
## Identification of “jet-like” events

- Require 4 cells with minimum energy 0.4 GeV
- Minimum weighted sum of cells
- Minimum cuts on total energy (20 GeV) and average  $p_T$  (1.5 GeV)
- Maximum cone size  $\Delta R \equiv \sqrt{(\Delta\eta^2 + \Delta\phi^2)} > 0.5$
- 2-large-cell fiducial cut around “jet”-axis



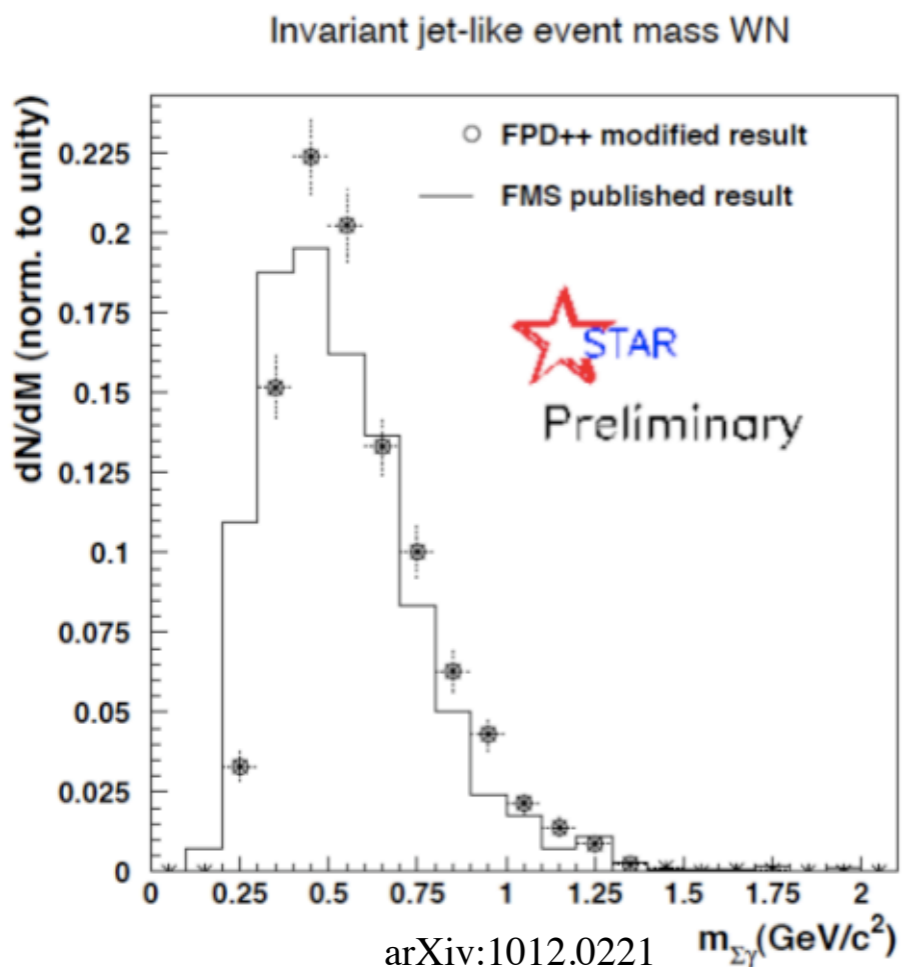
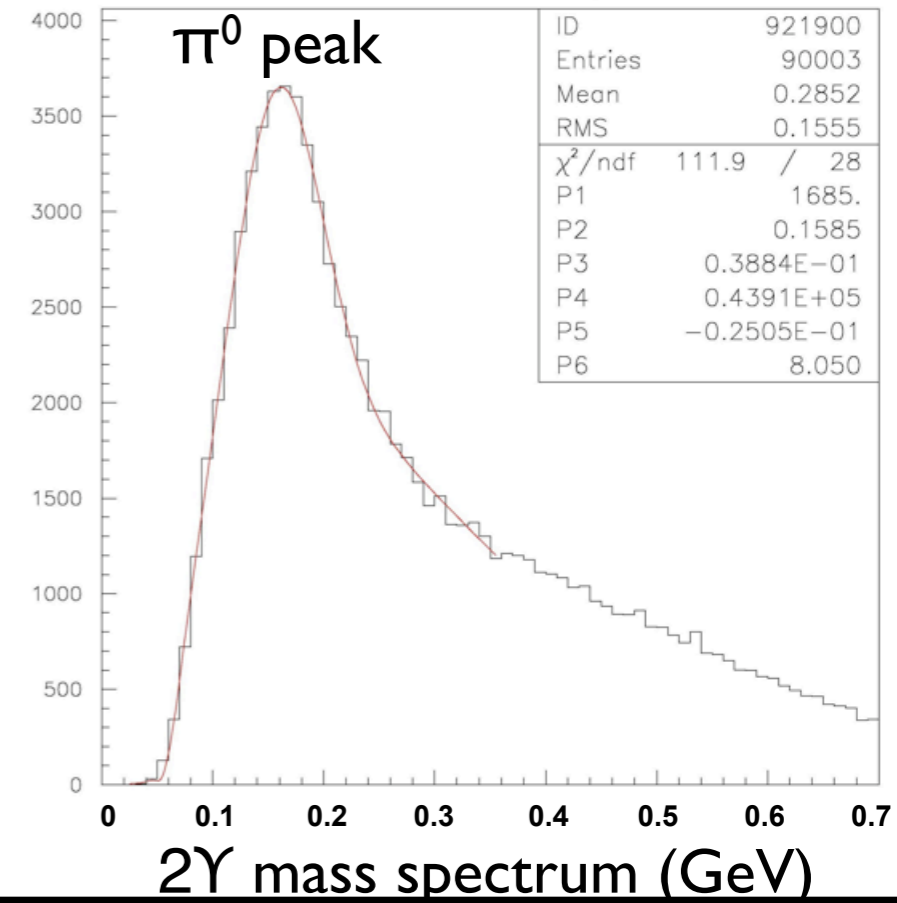
**Invariant mass spectrum comparison of “jet-like” events between FPD++, FMS (2008 run)**

# Analysis of $\pi^0$ data from the FPD++



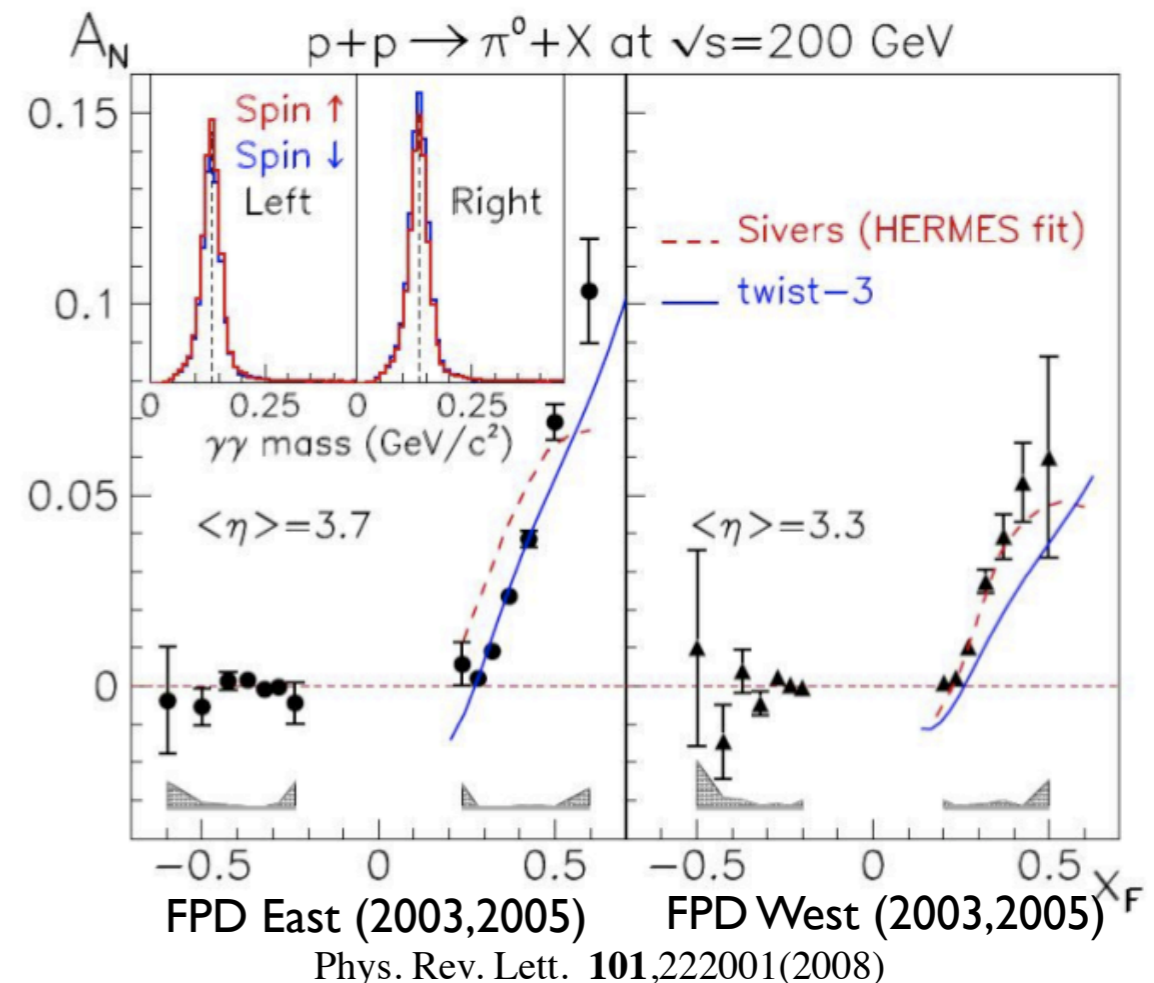
## Identification of “jet-like” events

- Require 4 cells with minimum energy 0.4 GeV
- Minimum weighted sum of cells
- Minimum cuts on total energy (20 GeV) and average  $p_T$  (1.5 GeV)
- Maximum cone size  $\Delta R \equiv \sqrt{(\Delta\eta^2 + \Delta\phi^2)} > 0.5$
- 2-large-cell fiducial cut around “jet”-axis

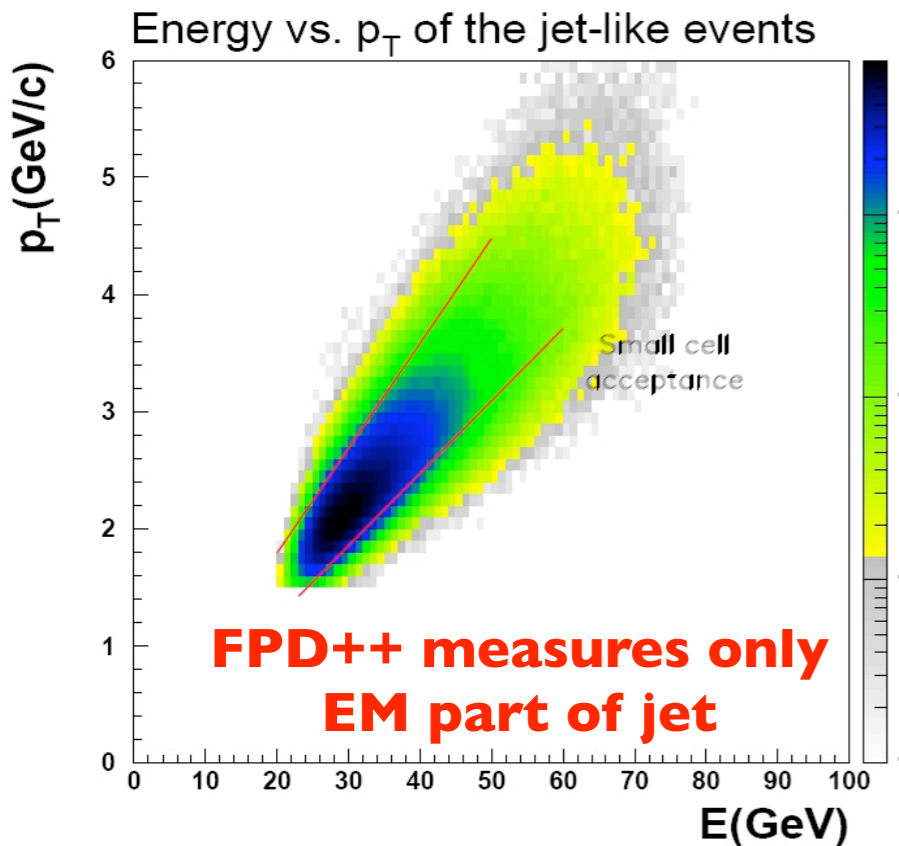


## Consistency check: inclusive $\pi^0 A_N$

Invariant mass spectrum comparison of “jet-like” events between FPD++, FMS (2008 run)

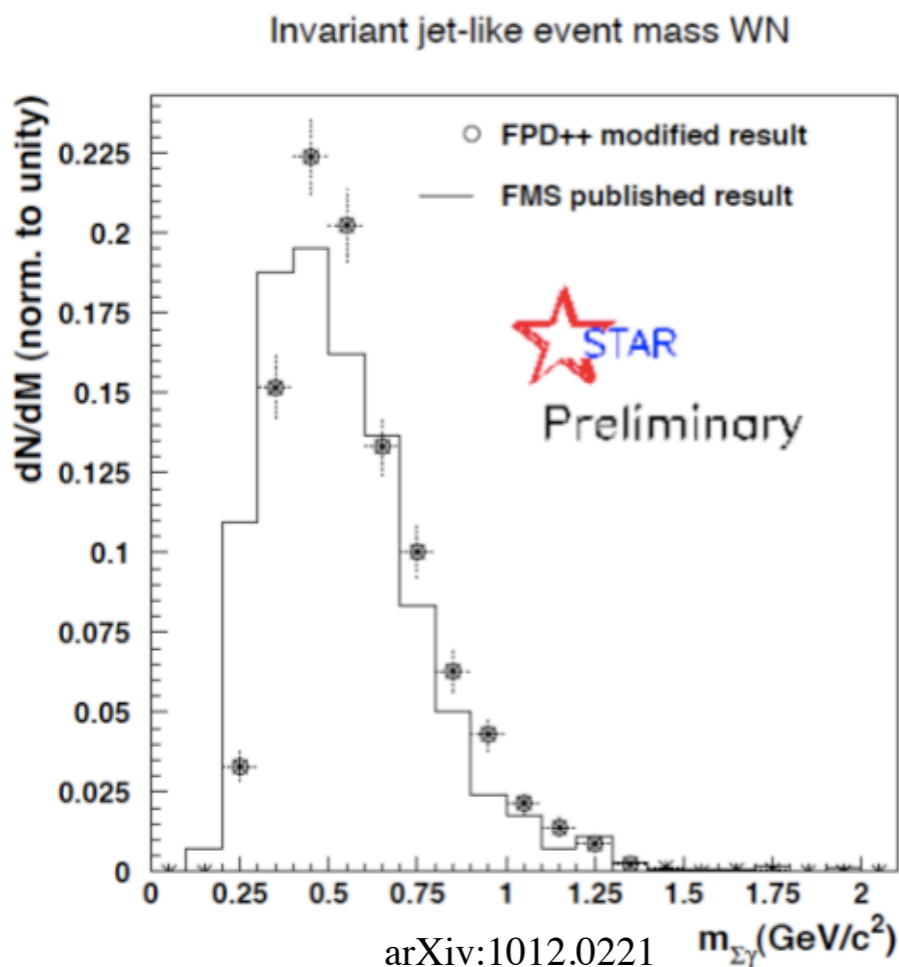
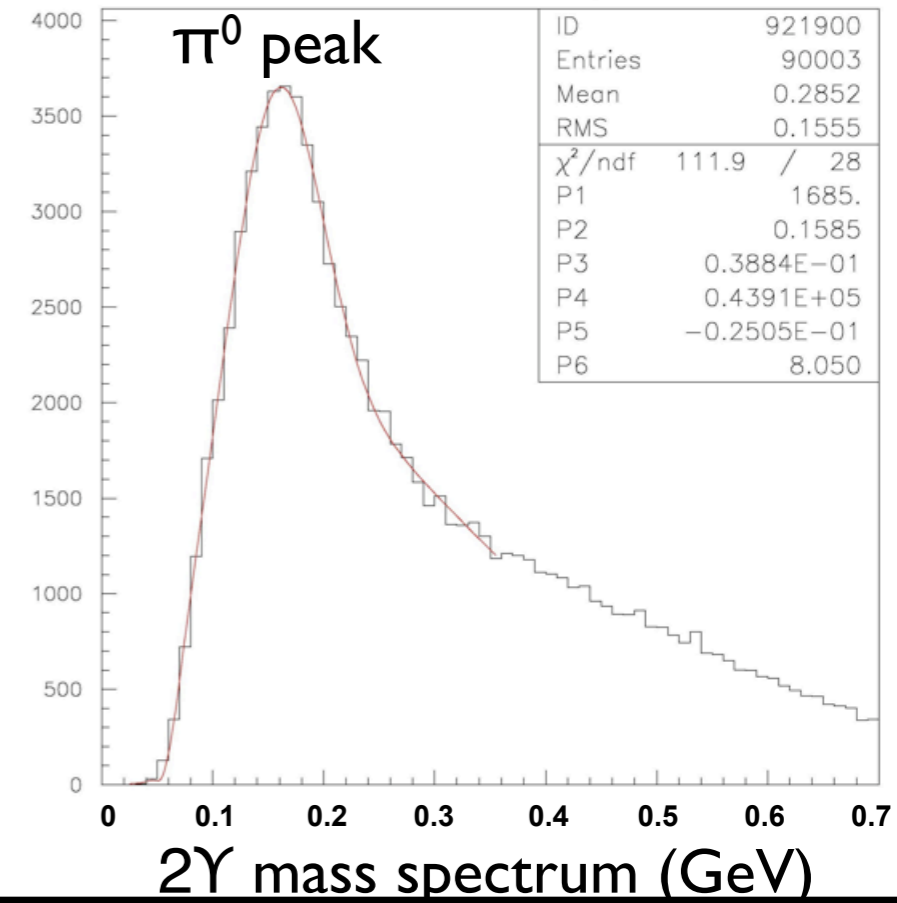


# Analysis of $\pi^0$ data from the FPD++



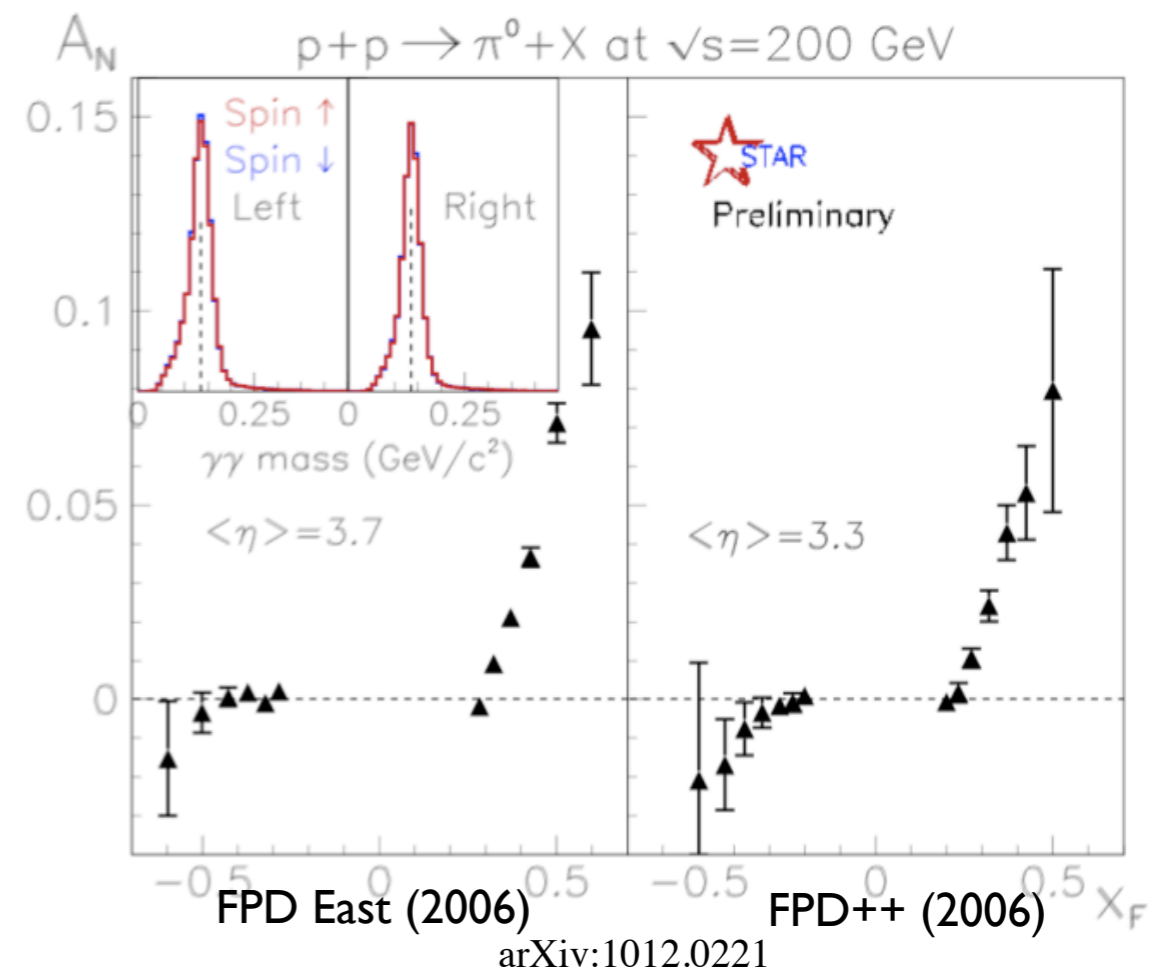
## Identification of “jet-like” events

- Require 4 cells with minimum energy 0.4 GeV
- Minimum weighted sum of cells
- Minimum cuts on total energy (20 GeV) and average  $p_T$  (1.5 GeV)
- Maximum cone size  $\Delta R \equiv \sqrt{(\Delta\eta^2 + \Delta\phi^2)} > 0.5$
- 2-large-cell fiducial cut around “jet”-axis

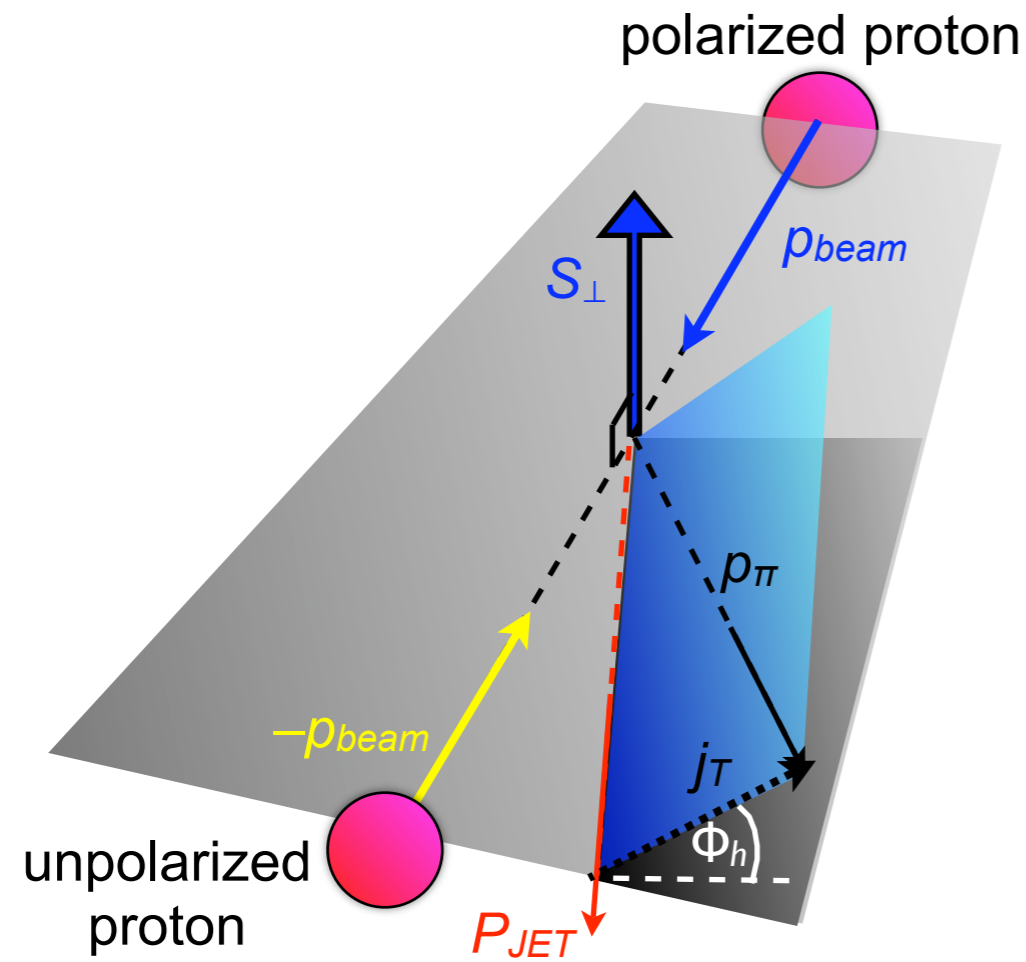


## Consistency check: inclusive $\pi^0 A_N$

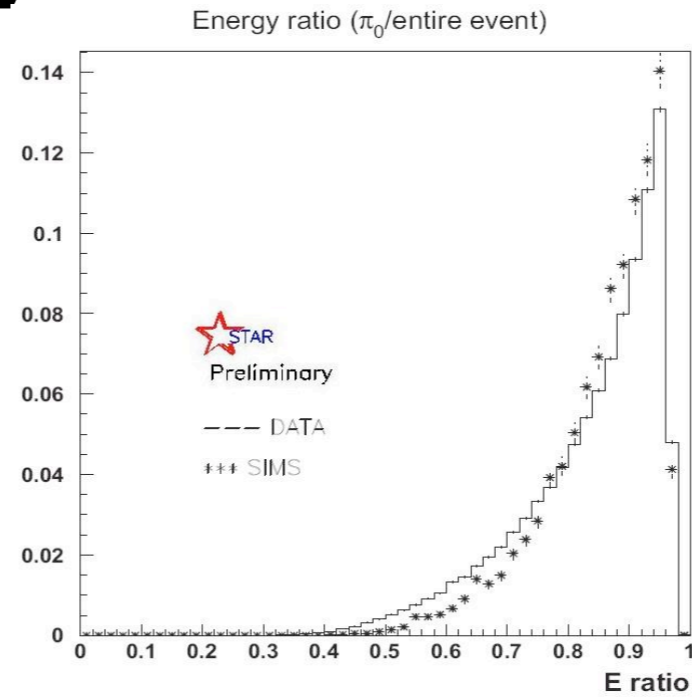
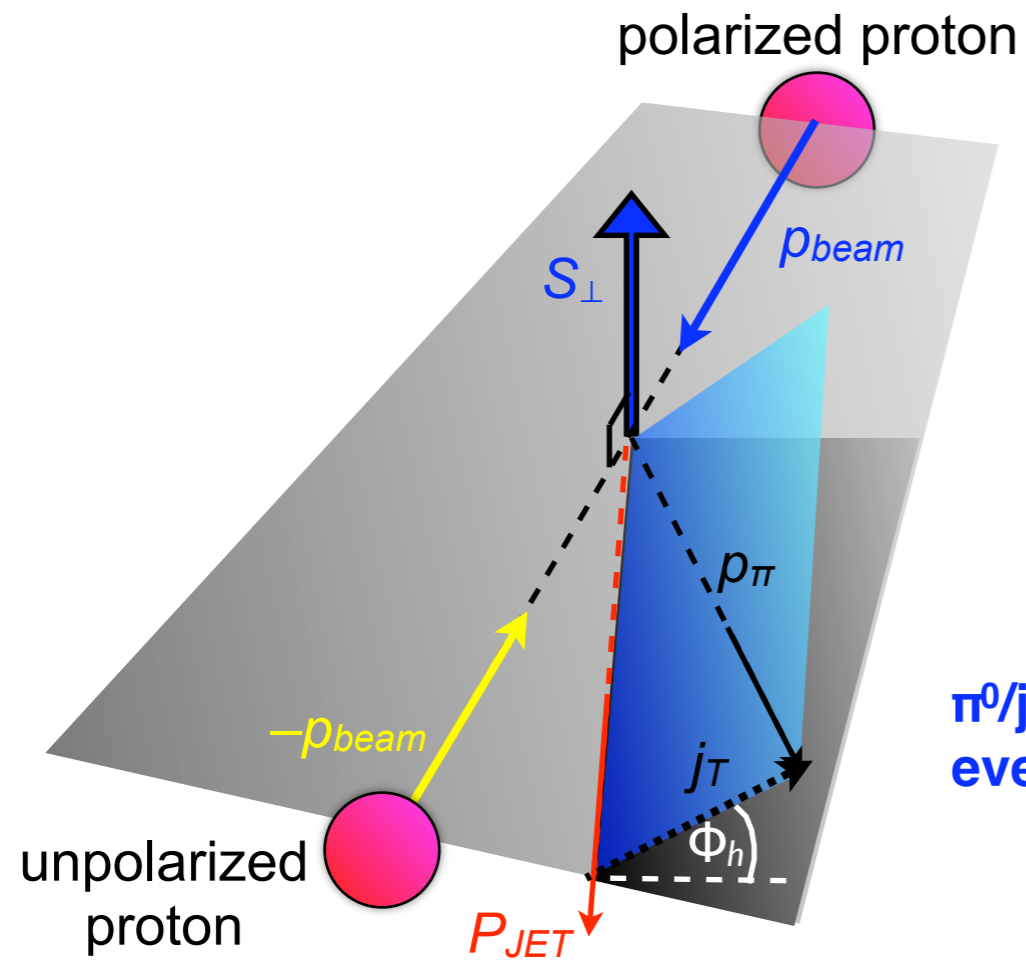
**Invariant mass spectrum comparison of “jet-like” events between FPD++, FMS (2008 run)**



# Collins Asymmetry Results from FPD++

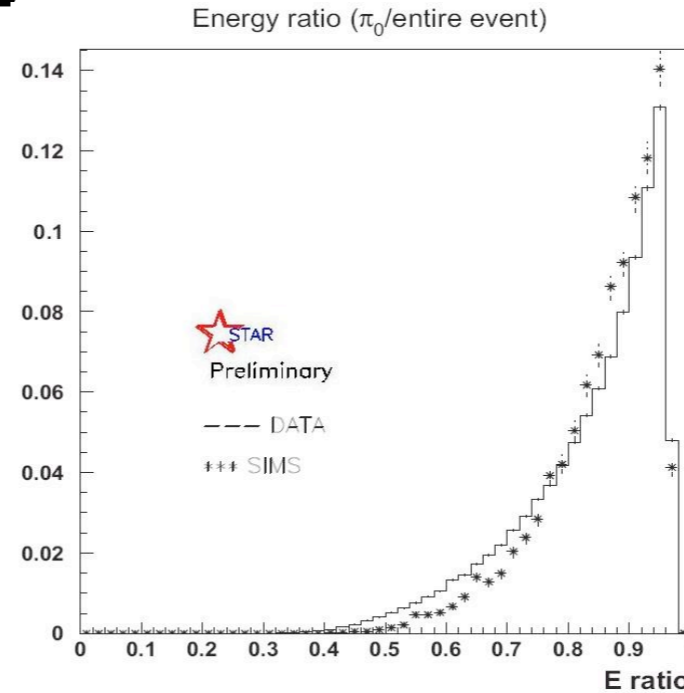
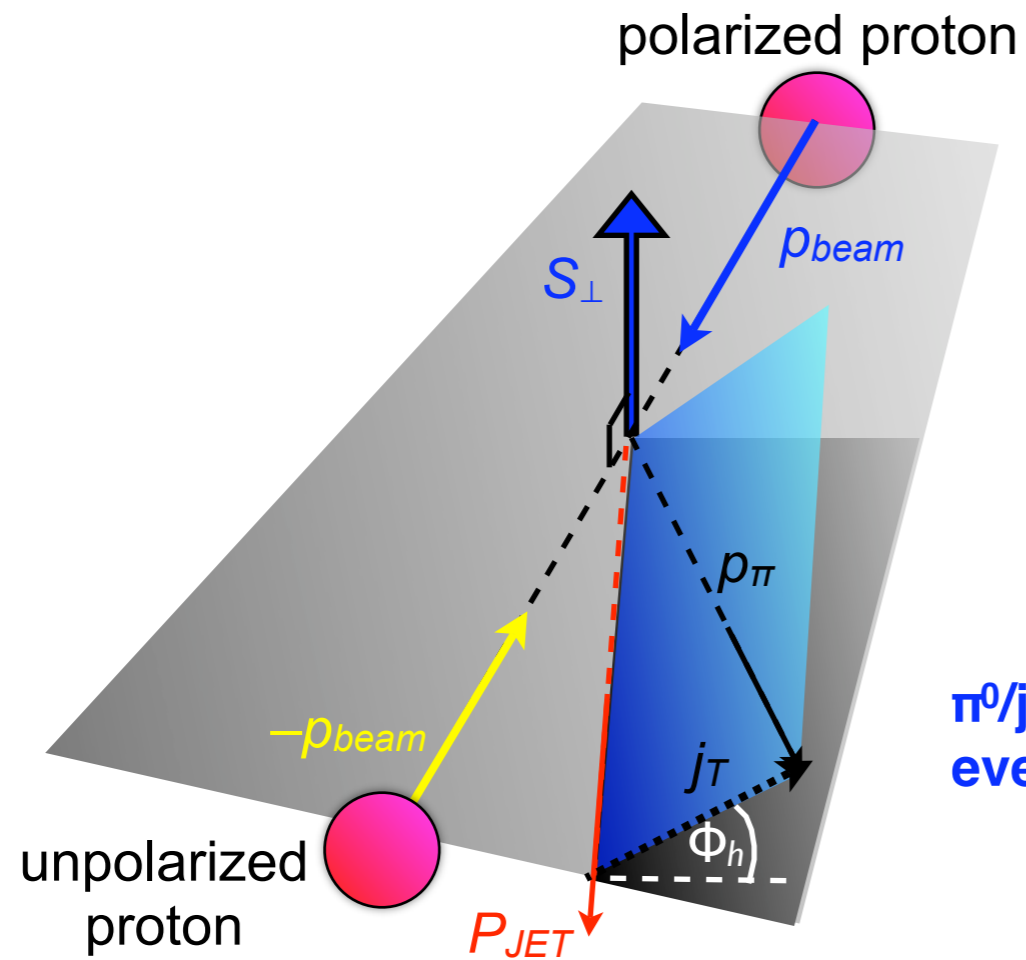


# Collins Asymmetry Results from FPD++



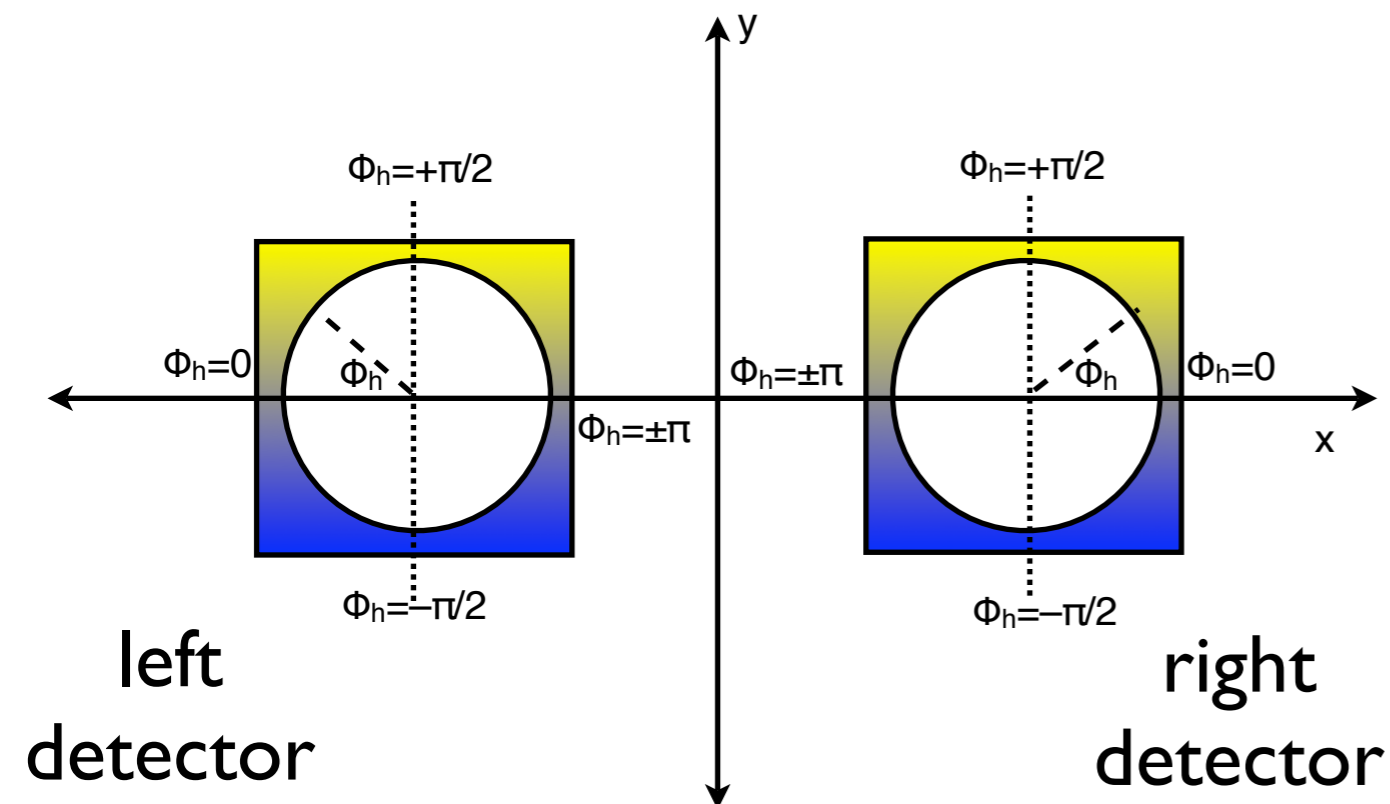
$\pi^0/\text{jet}$  energy ratios show  
events are very high- $z$  (avg.  $z > 0.8$ )

# Collins Asymmetry Results from FPD++

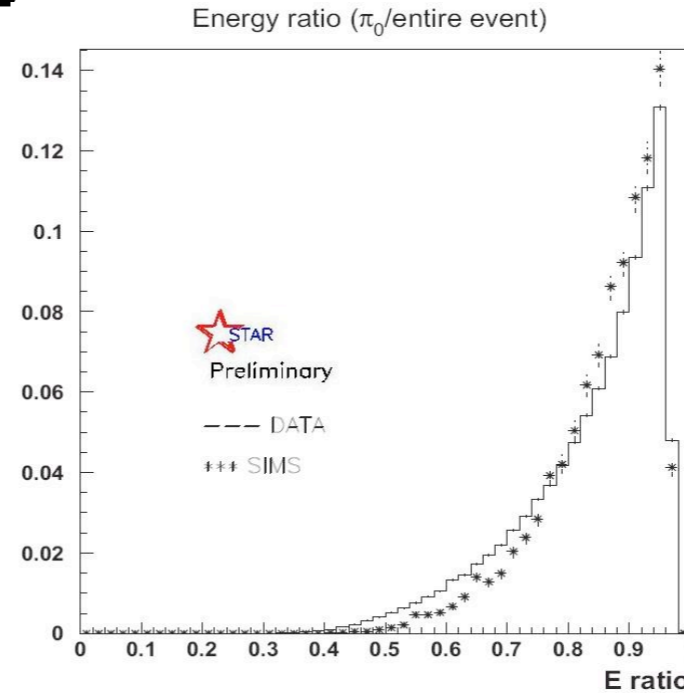
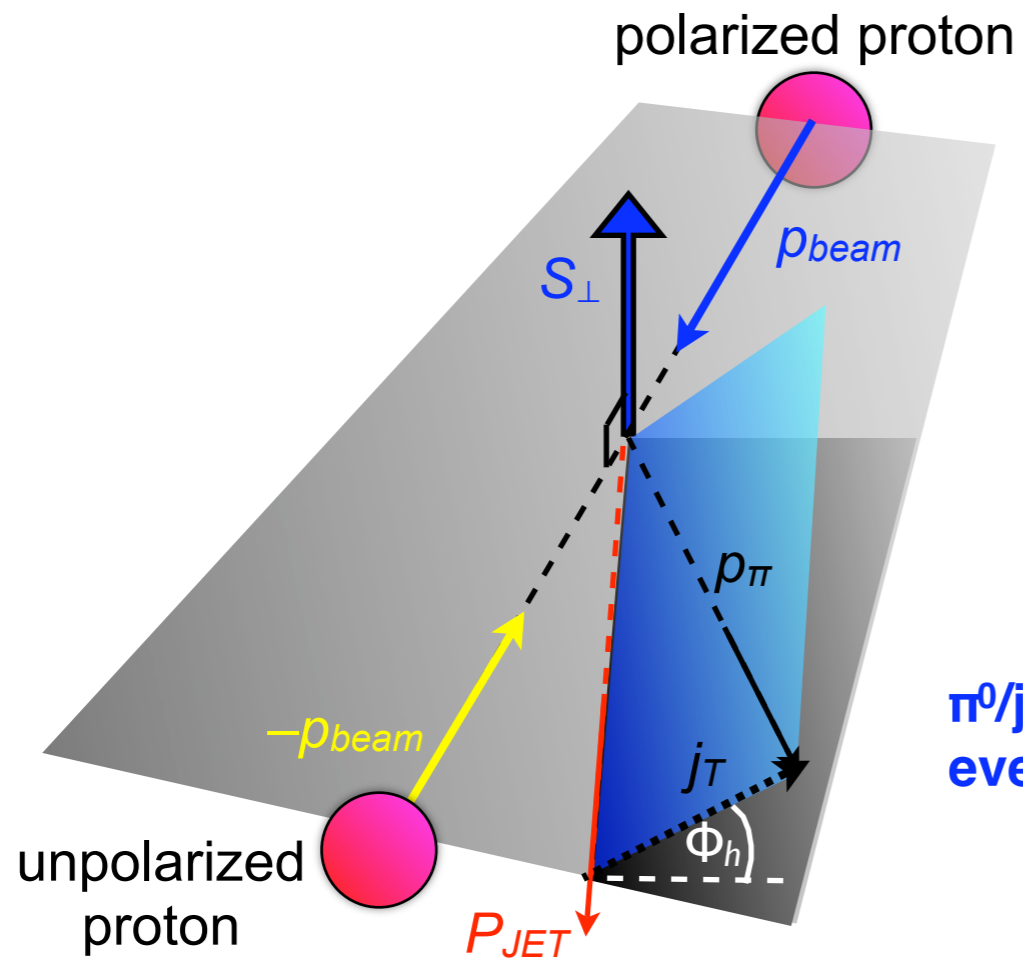


$\pi^0$ /jet energy ratios show events are very high- $z$  (avg.  $z > 0.8$ )

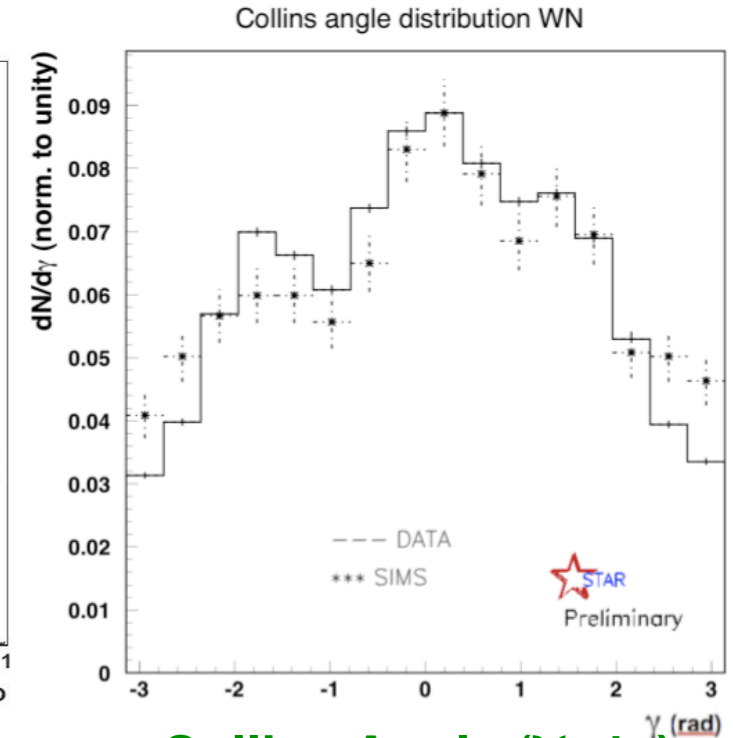
$\Phi_h$  in FPD++ C.S.



# Collins Asymmetry Results from FPD++

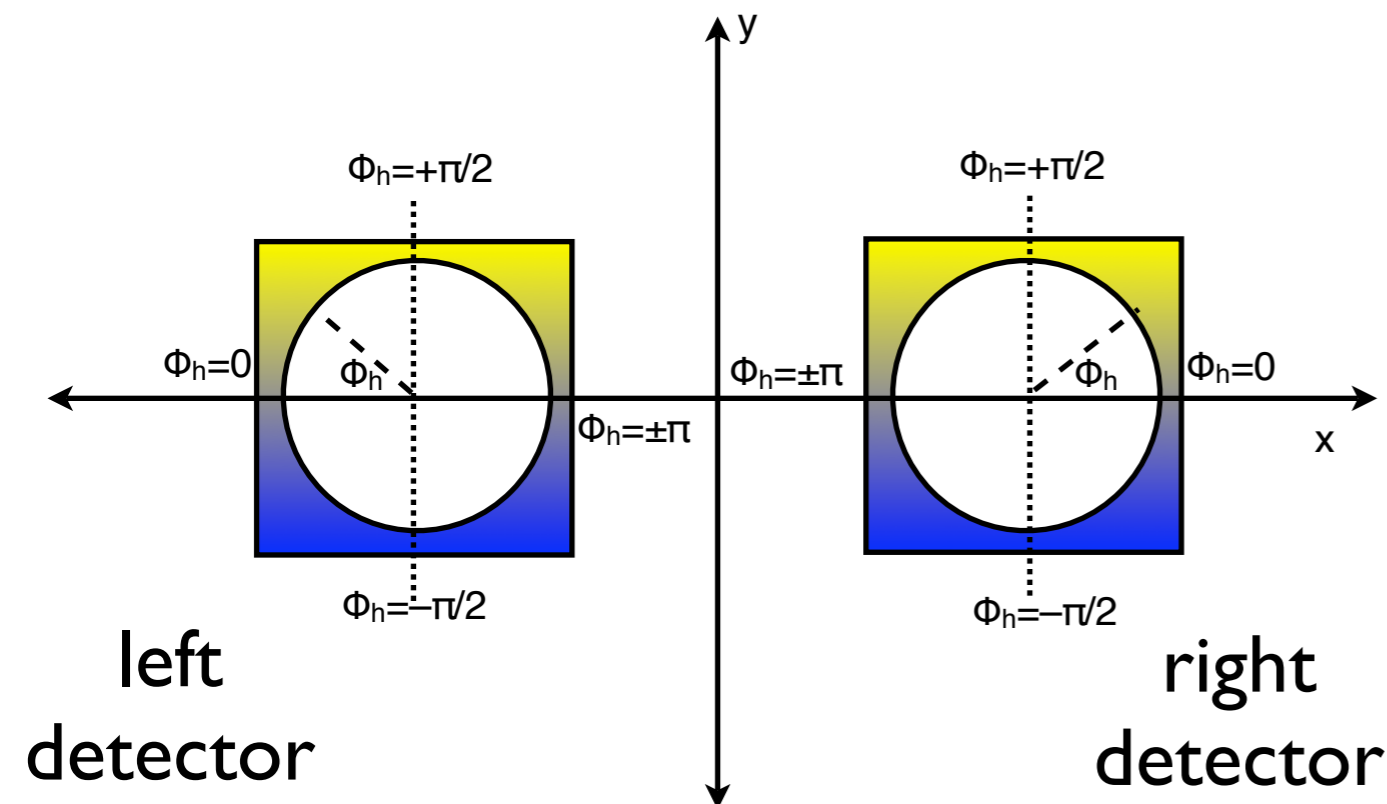


$\pi^0$ /jet energy ratios show events are very high- $z$  (avg.  $z > 0.8$ )

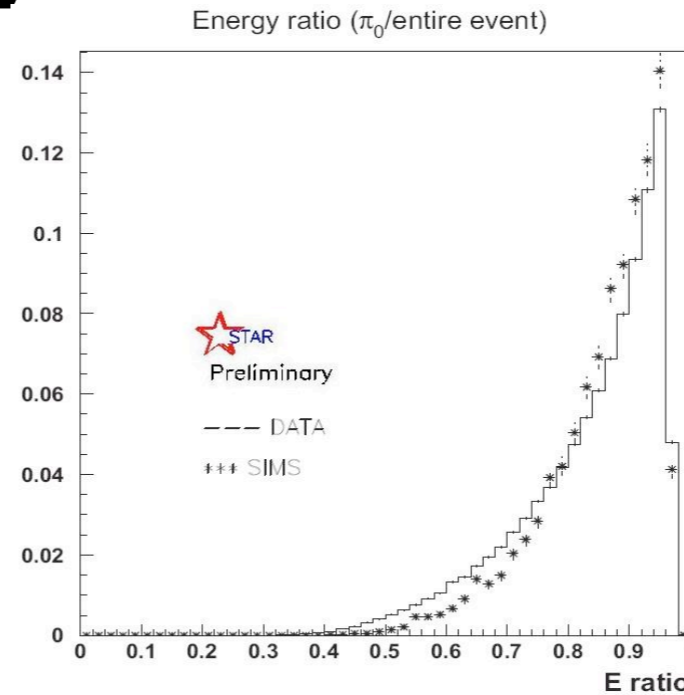
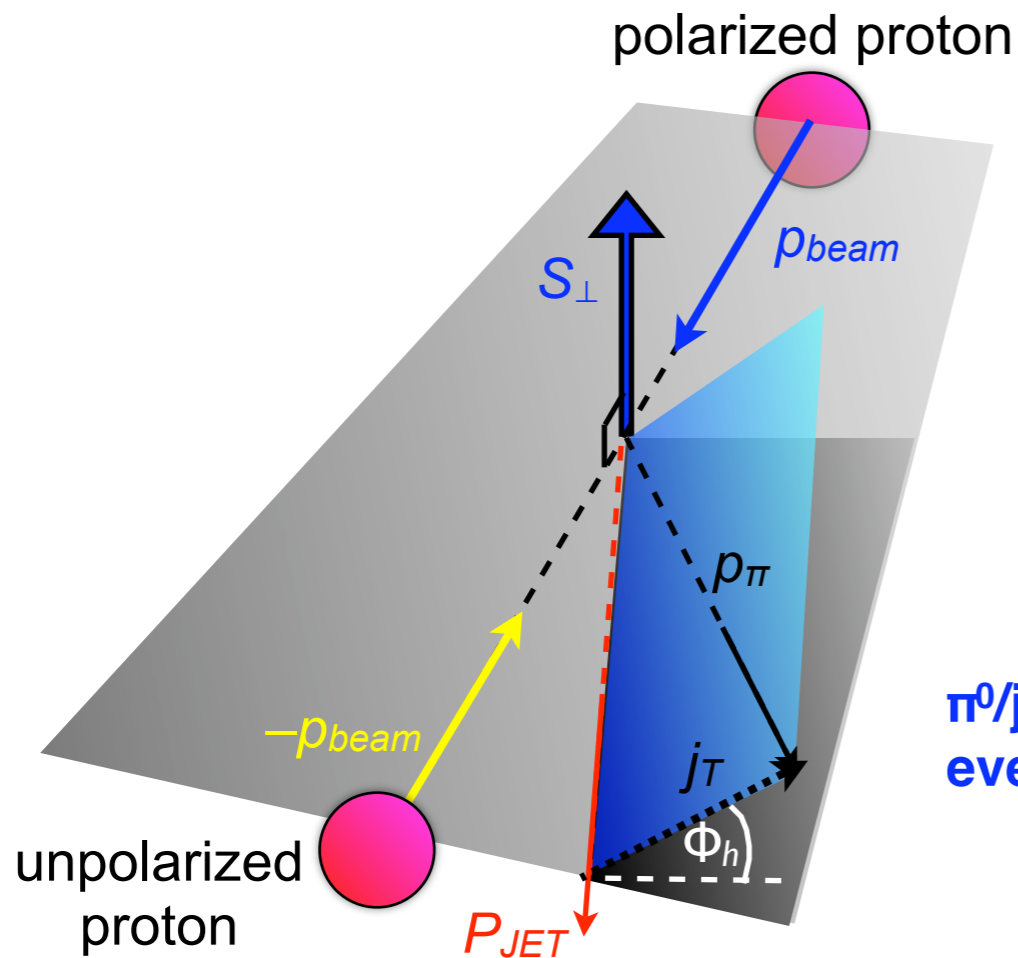


Collins Angle ( $\gamma \equiv \Phi_h$ ) distribution of data

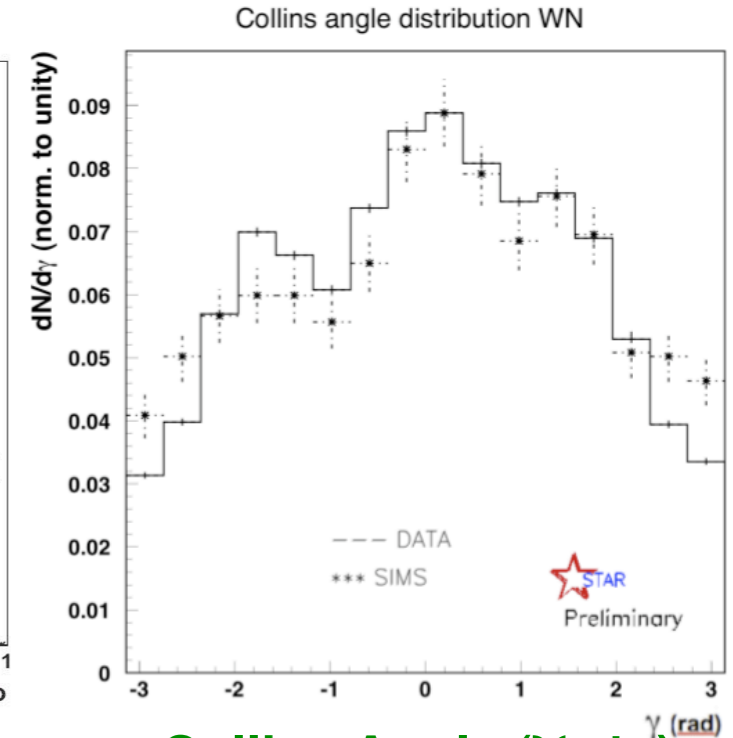
$\Phi_h$  in FPD++ C.S.



# Collins Asymmetry Results from FPD++



$\pi^0$ /jet energy ratios show events are very high- $z$  (avg.  $z > 0.8$ )

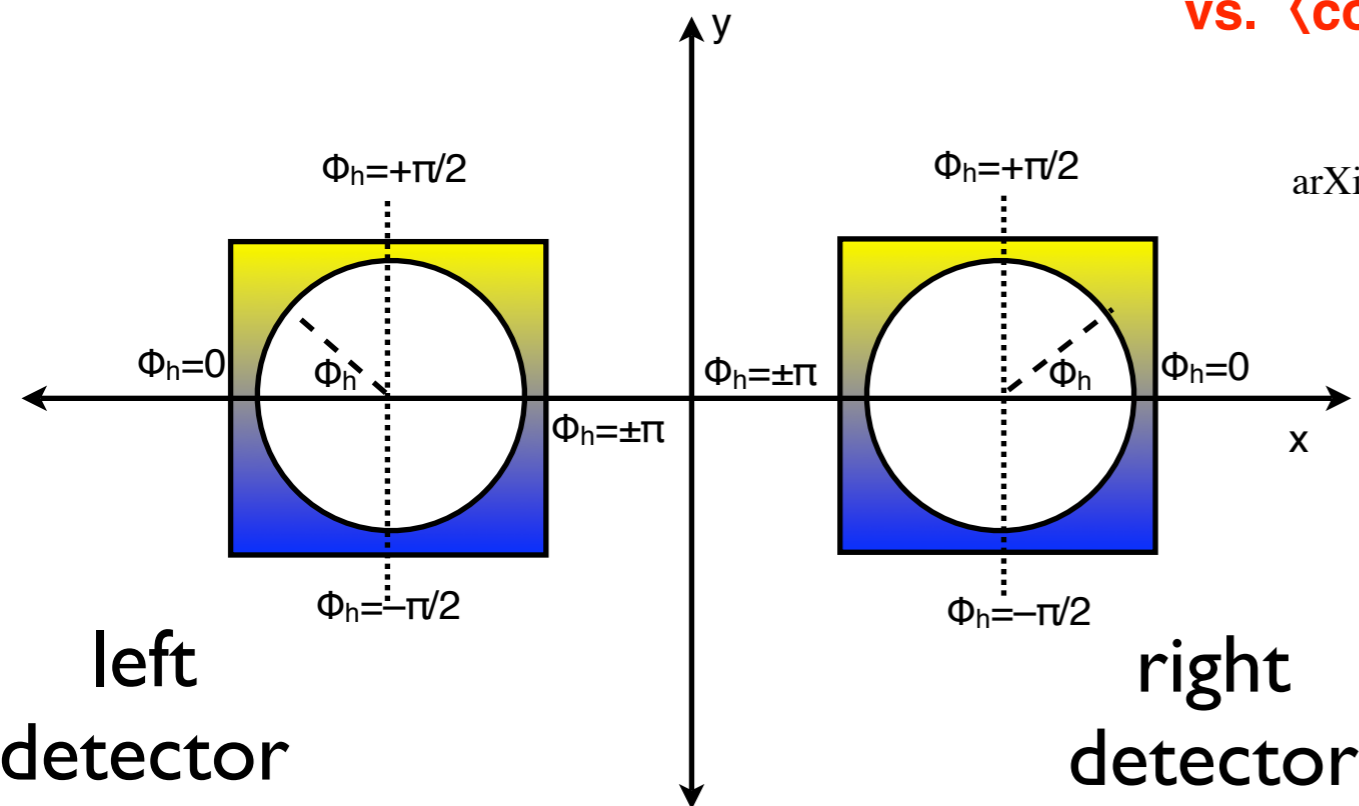
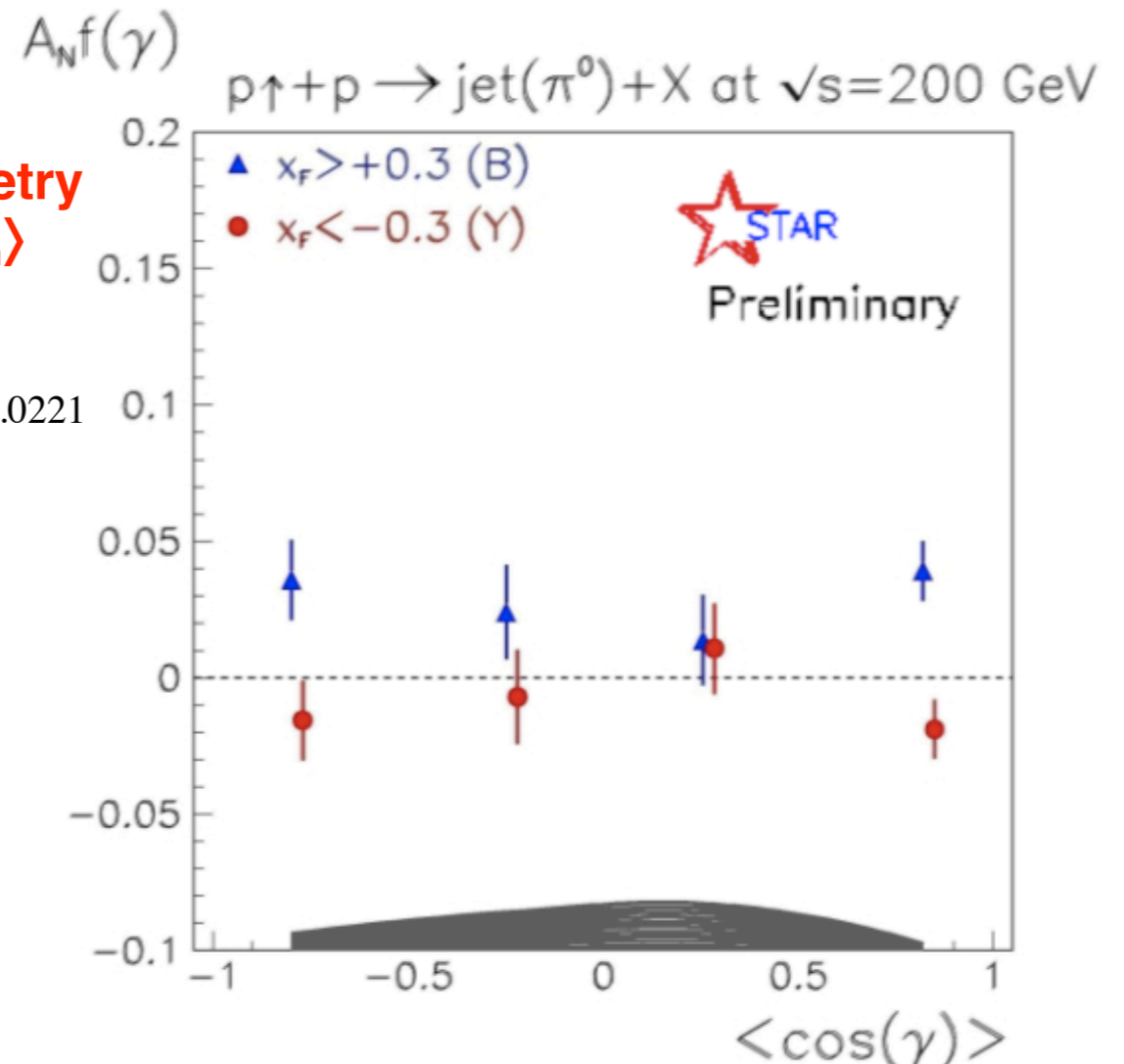


Collins Angle ( $\gamma \equiv \Phi_h$ ) distribution of data

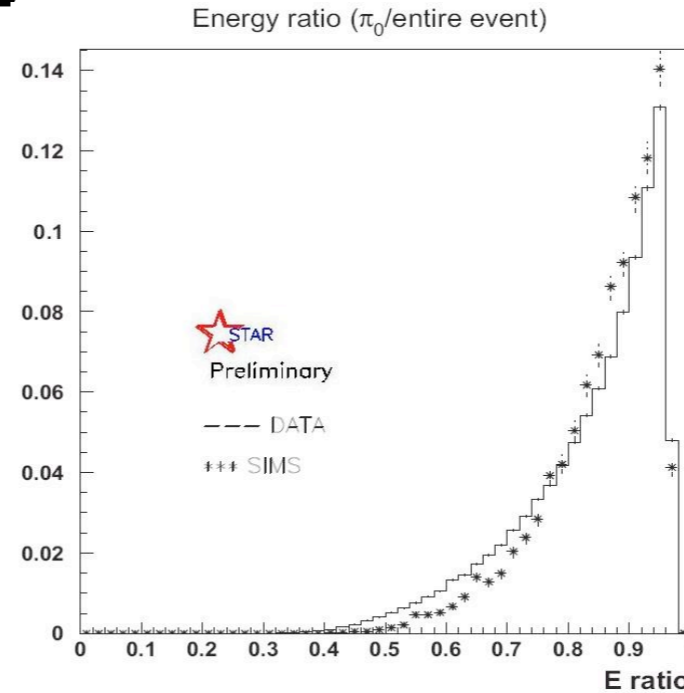
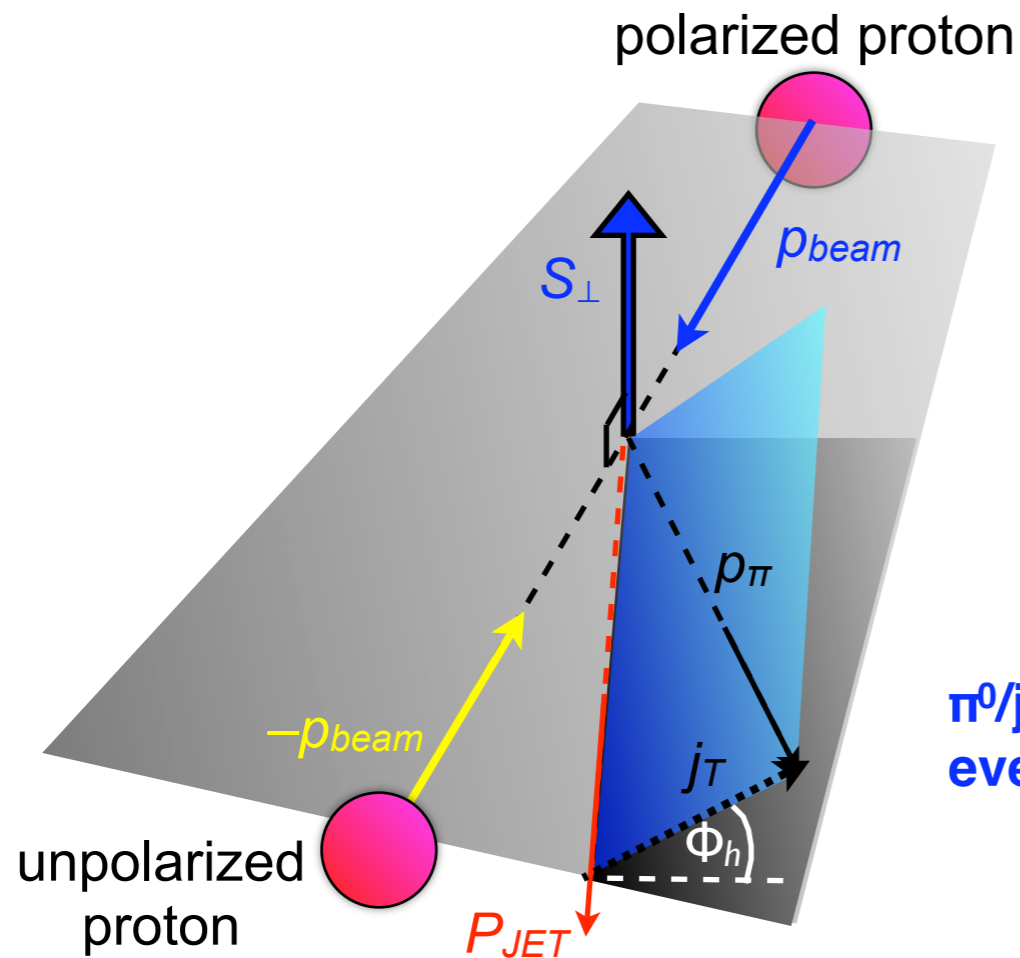
$\Phi_h$  in FPD++ C.S.

L-R  $\pi^0$  asymmetry vs.  $\langle \cos \Phi_h \rangle$

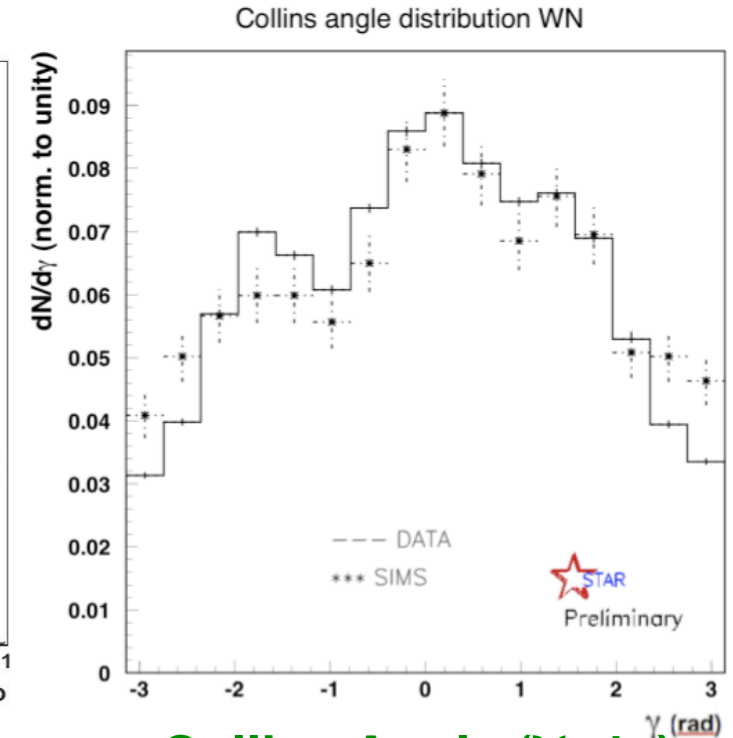
arXiv:1012.0221



# Collins Asymmetry Results from FPD++



$\pi^0$ /jet energy ratios show events are very high- $z$  (avg.  $z > 0.8$ )

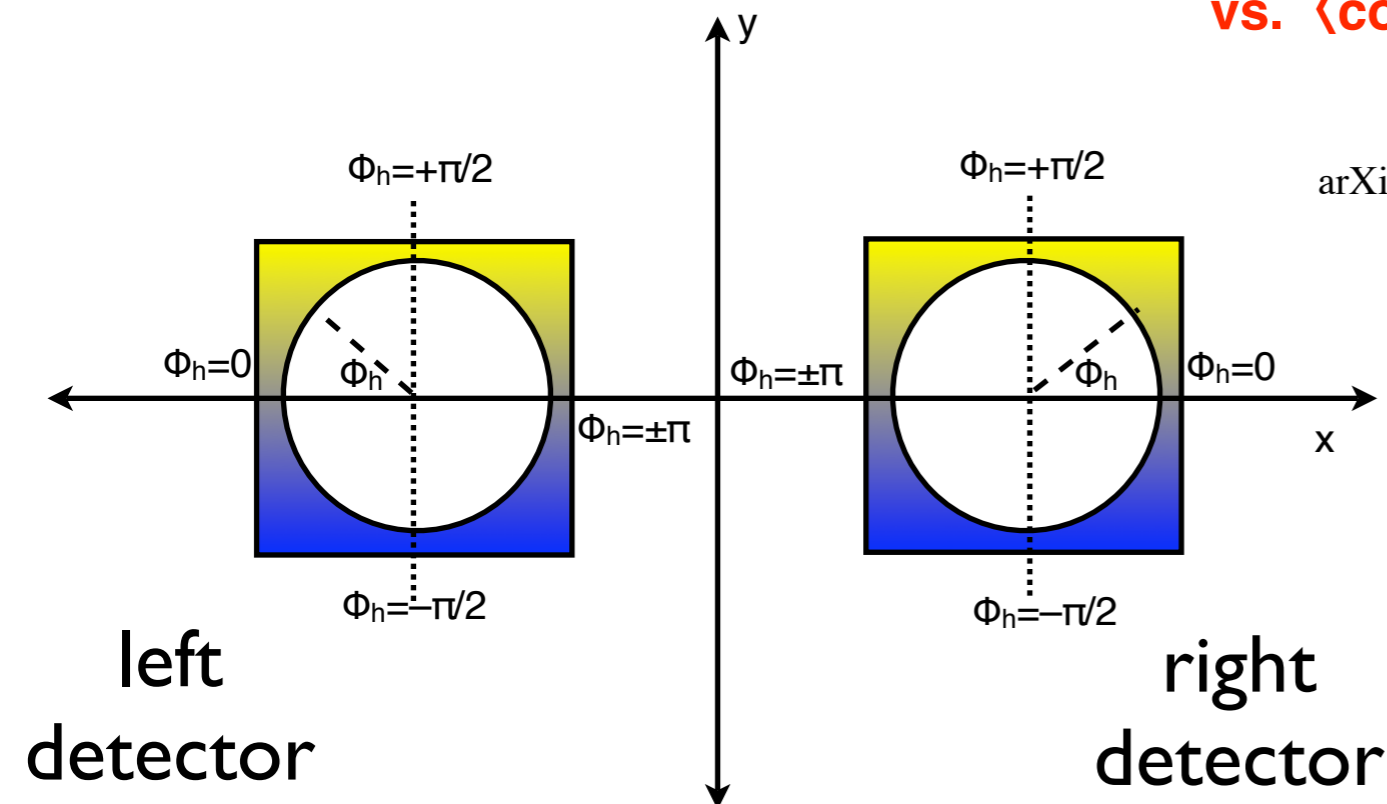
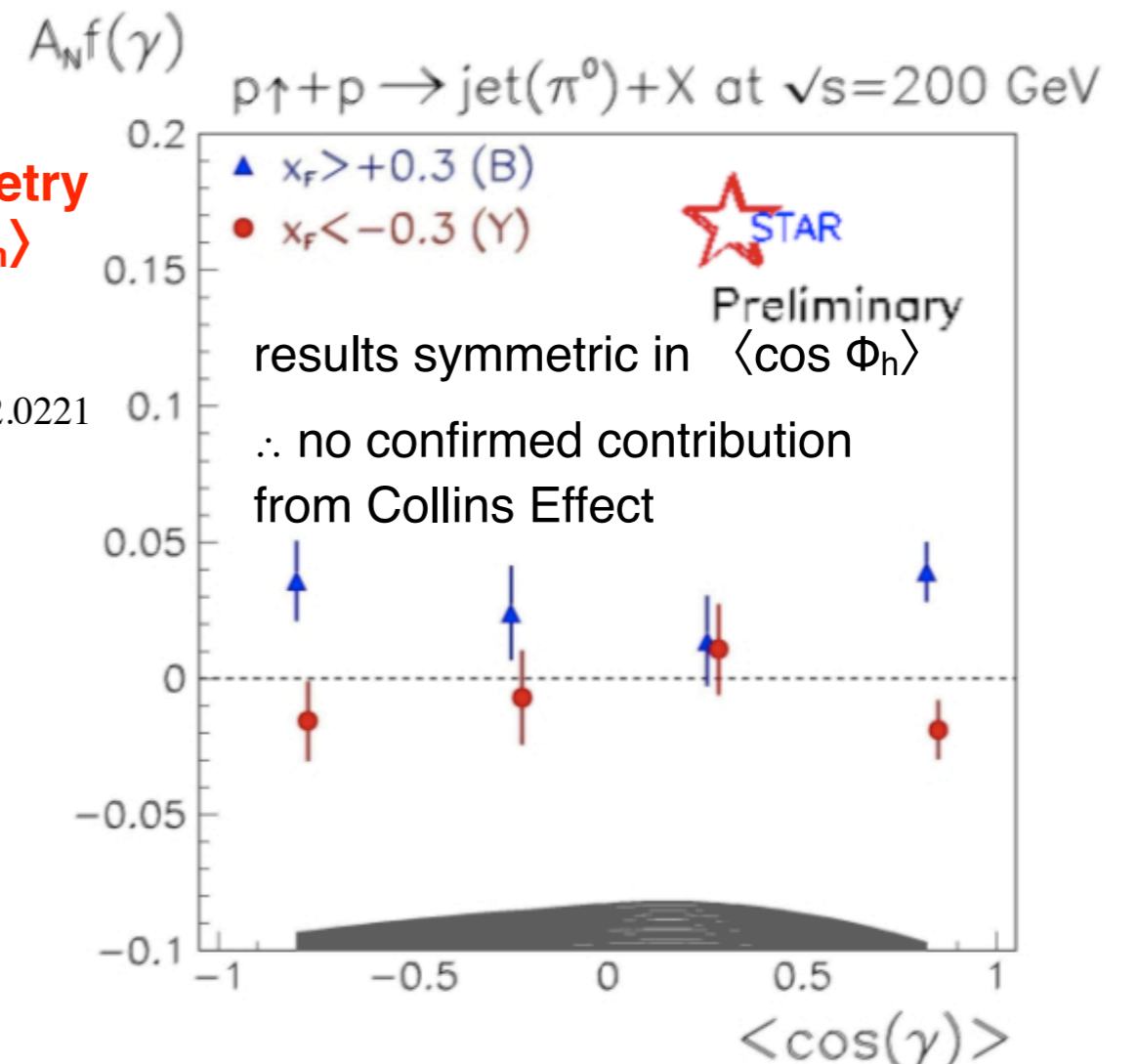


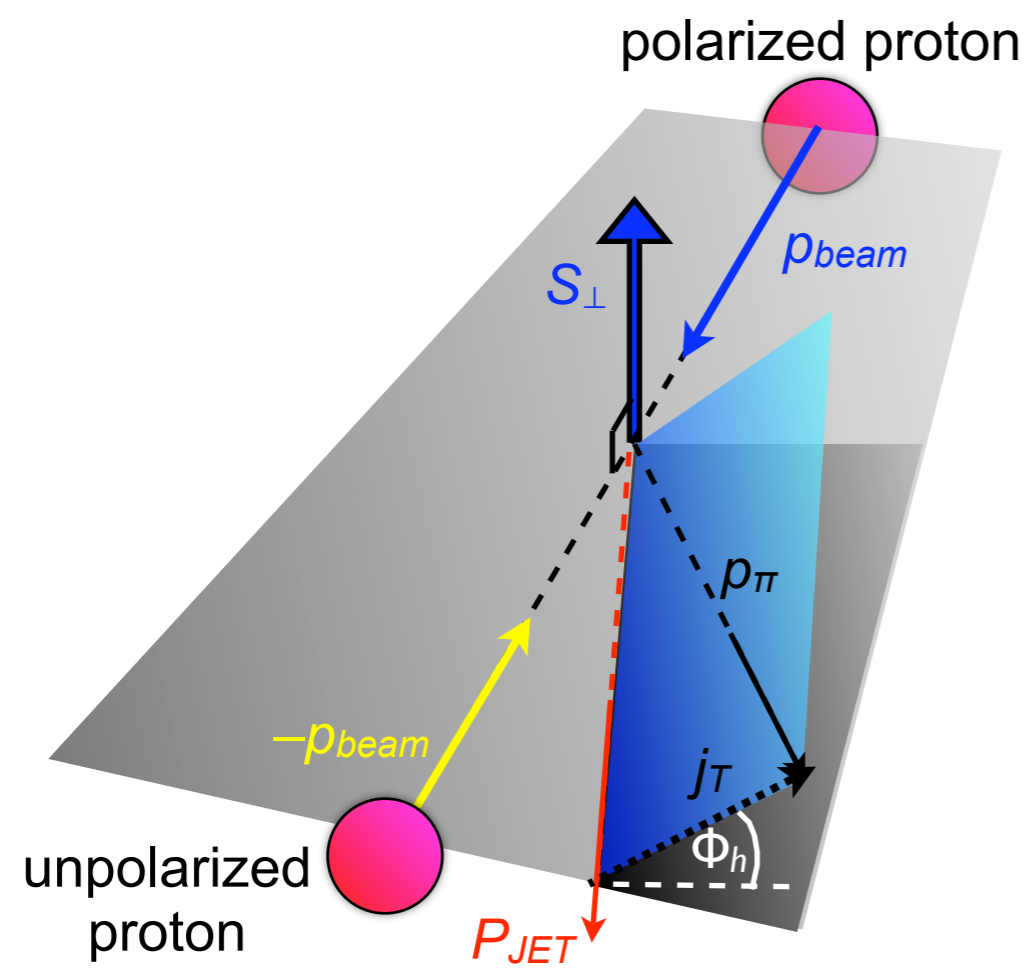
Collins Angle ( $\gamma \equiv \Phi_h$ ) distribution of data

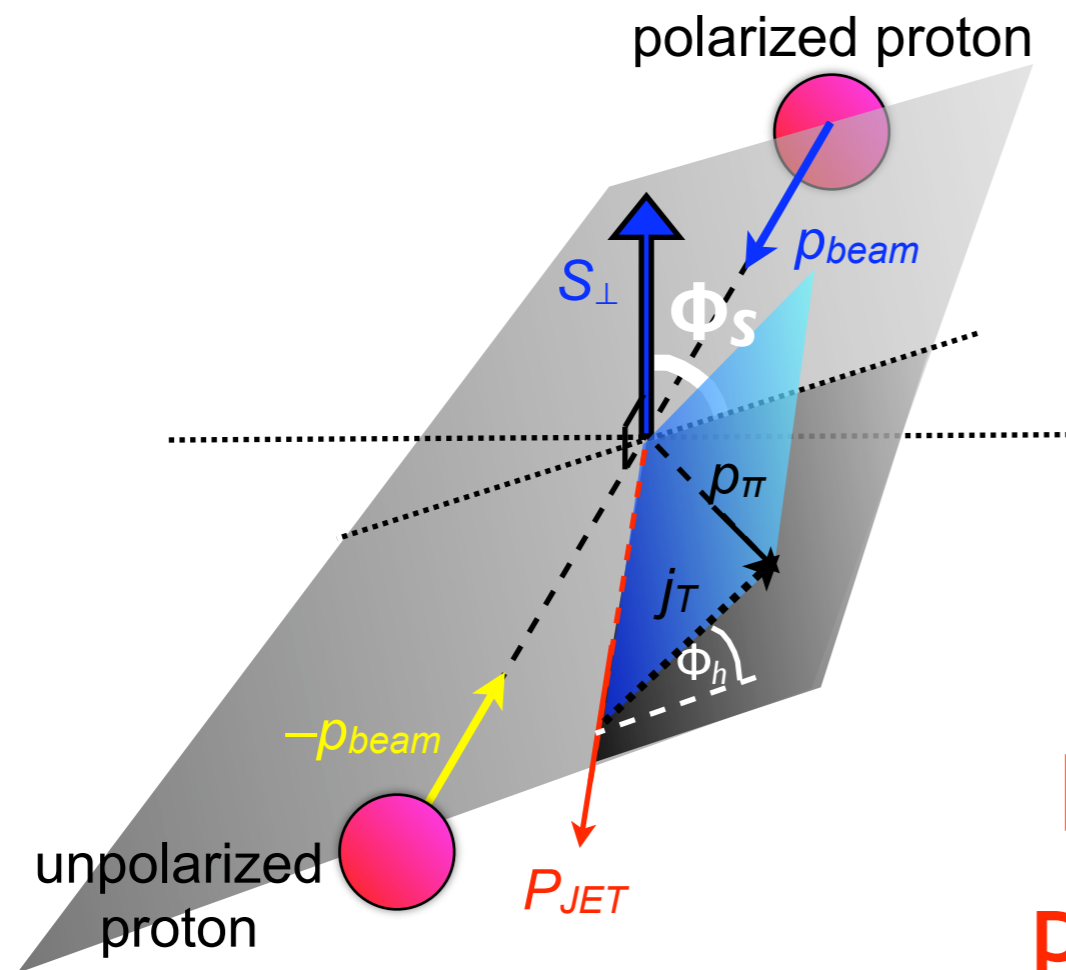
$\Phi_h$  in FPD++ C.S.

L-R  $\pi^0$  asymmetry vs.  $\langle \cos \Phi_h \rangle$

arXiv:1012.0221

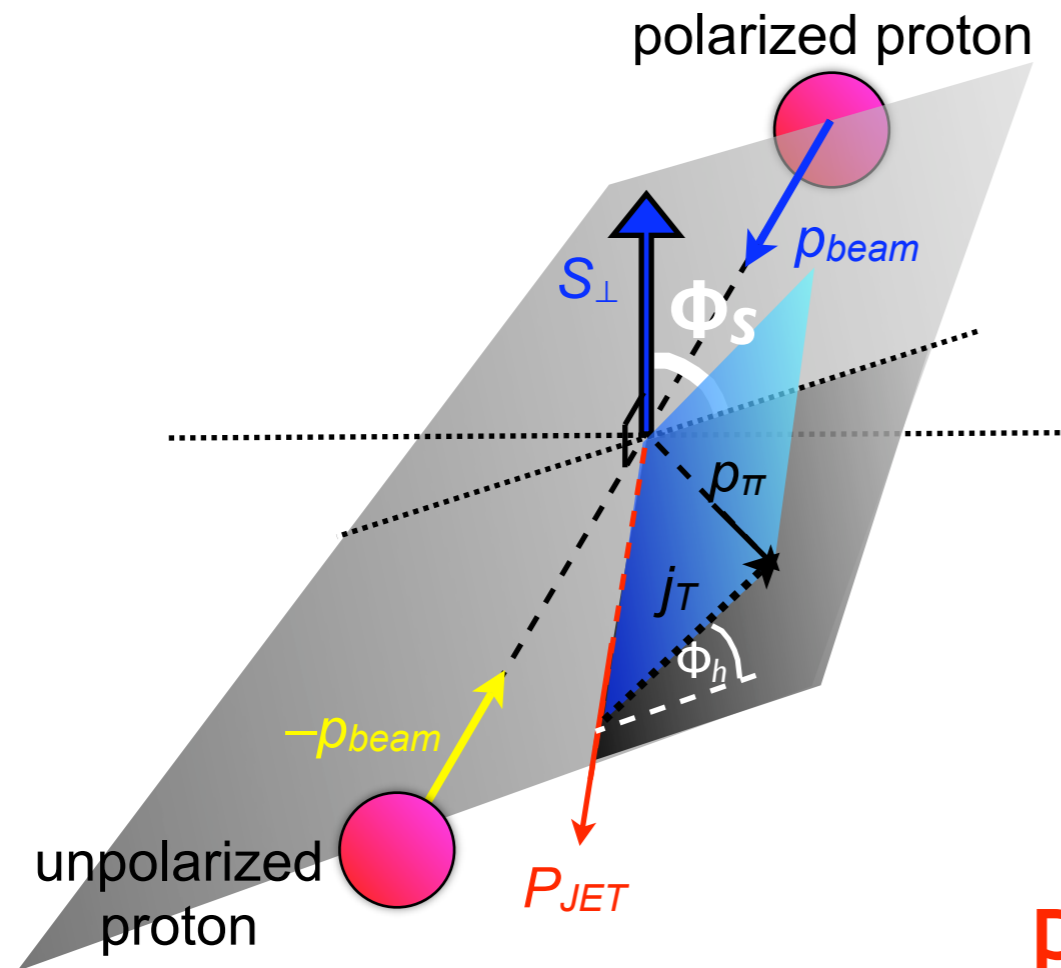






New angle  $\Phi_s$ : angle between polarization and jet **reaction plane**

# Collins Asymmetries at Mid-Rapidity

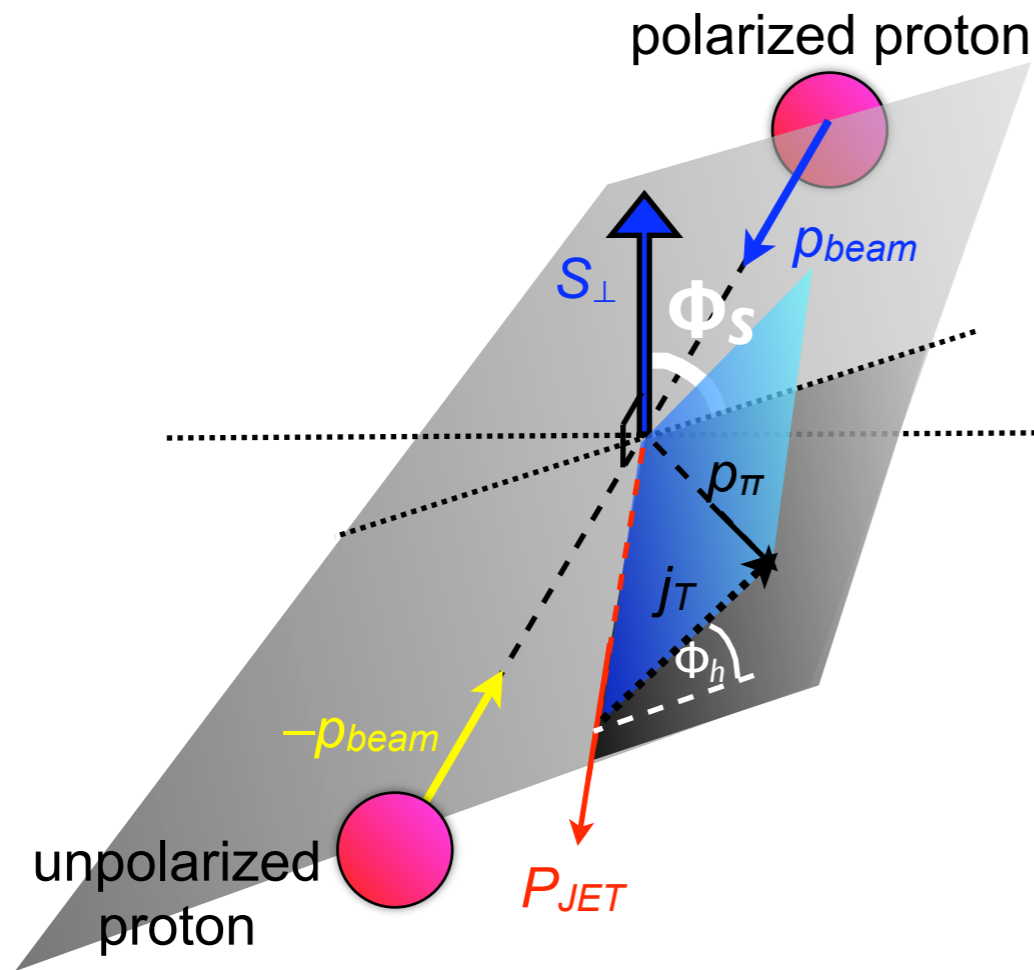


Generalization of principle to full  $\Phi, \eta$ -range of STAR

STAR accurately reconstructs charged  $\pi^{\pm}$  momenta and jets

New angle  $\Phi_s$ : angle between polarization and jet **reaction plane**

# Collins Asymmetries at Mid-Rapidity



Generalization of principle to full  $\Phi, \eta$ -range of STAR

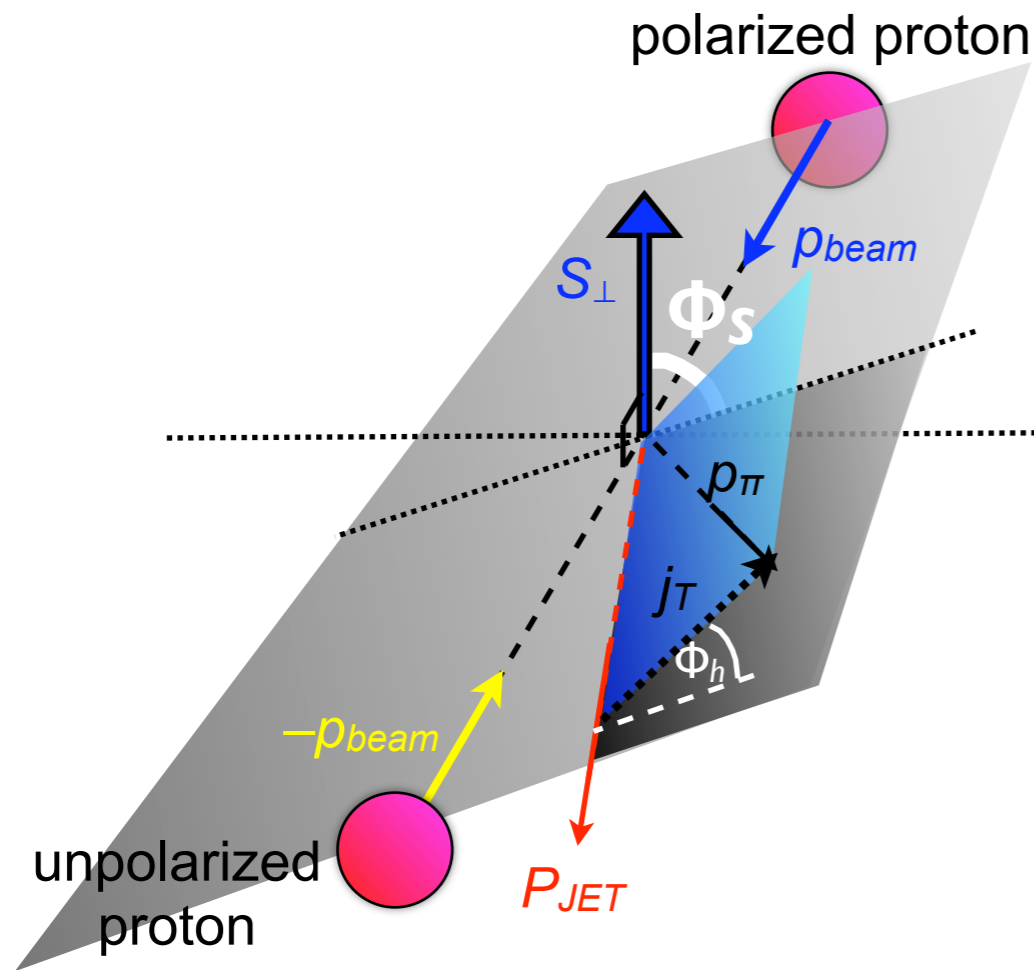
STAR accurately reconstructs charged  $\pi^{\pm}$  momenta and jets

New angle  $\Phi_S$ : angle between polarization and jet **reaction plane**

$$A = \langle \sin(\Phi_h - \Phi_S) \rangle$$

$$= \langle \sin\Phi_h \cos\Phi_S - \cos\Phi_h \sin\Phi_S \rangle$$

# Collins Asymmetries at Mid-Rapidity



Generalization of principle to full  $\Phi, \eta$ -range of STAR

STAR accurately reconstructs charged  $\pi^\pm$  momenta and jets

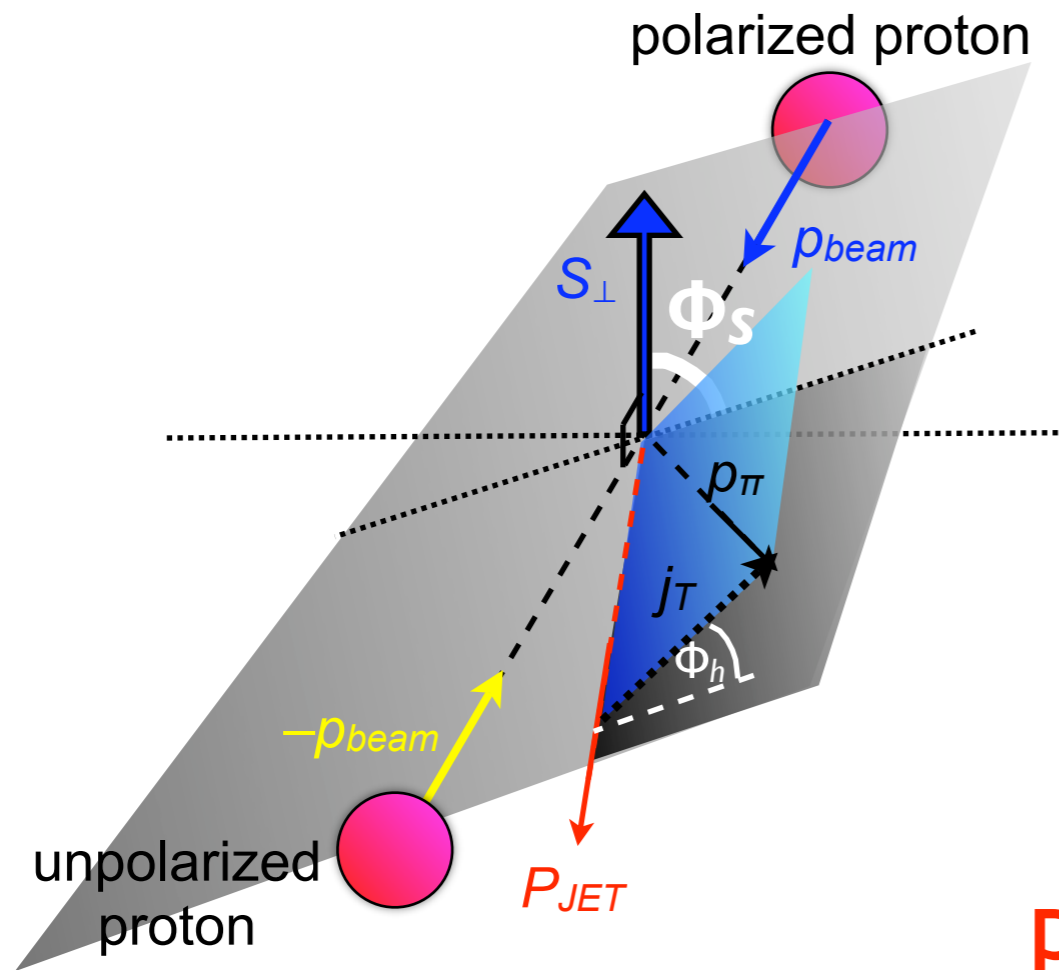
New angle  $\Phi_S$ : angle between polarization and jet **reaction plane**

$$A = \langle \sin(\Phi_h - \Phi_S) \rangle$$

$$= \langle \sin\Phi_h \cos\Phi_S - \cos\Phi_h \sin\Phi_S \rangle \xrightarrow{(\Phi_S \sim 90^\circ)} - \langle \cos\Phi_h \rangle$$

for forward L-R asymmetries

# Collins Asymmetries at Mid-Rapidity



Generalization of principle to full  $\Phi, \eta$ -range of STAR

STAR accurately reconstructs charged  $\pi^\pm$  momenta and jets

New angle  $\Phi_S$ : angle between polarization and jet **reaction plane**

$$A = \langle \sin(\Phi_h - \Phi_S) \rangle$$

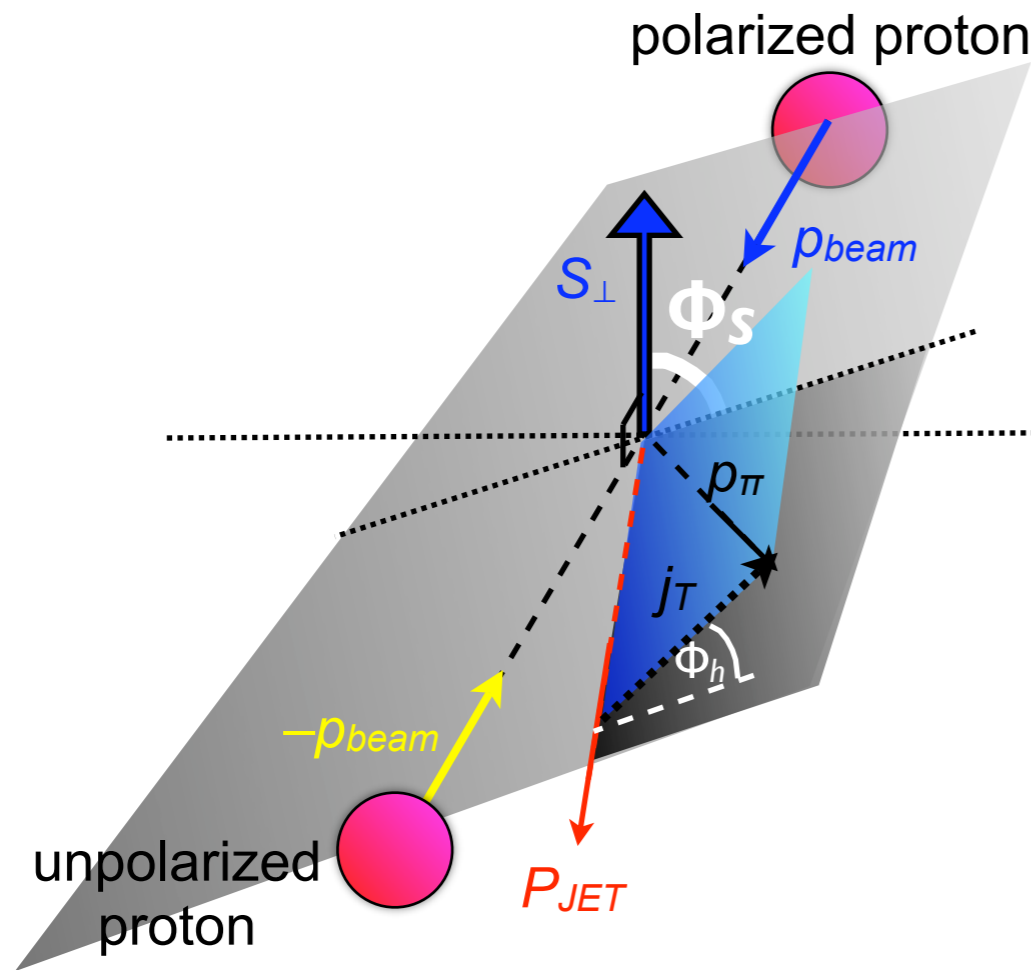
$$= \langle \sin\Phi_h \cos\Phi_S - \cos\Phi_h \sin\Phi_S \rangle \xrightarrow{(\Phi_S \sim 90^\circ)} - \langle \cos\Phi_h \rangle$$

for forward L-R asymmetries

(unpolarized contributions excluded here)

$$A \sim \sum_q \delta q(x) \otimes \Delta D_q(j_T, z) \otimes H^{\text{Collins}}$$

# Collins Asymmetries at Mid-Rapidity



Generalization of principle to full  $\Phi, \eta$ -range of STAR

STAR accurately reconstructs charged  $\pi^\pm$  momenta and jets

New angle  $\Phi_s$ : angle between polarization and jet **reaction plane**

$$A = \langle \sin(\Phi_h - \Phi_s) \rangle$$

$$= \langle \sin\Phi_h \cos\Phi_s - \cos\Phi_h \sin\Phi_s \rangle \xrightarrow{(\Phi_s \sim 90^\circ)} - \langle \cos\Phi_h \rangle$$

for forward L-R asymmetries

(unpolarized contributions excluded here)

$$A \sim \sum_q \delta q(x) \otimes \Delta D_q(j_T, z) \otimes H^{\text{Collins}}$$

azimuthal asymmetry within jet

transversity

Collins fragmentation

calculable function of  $\hat{s}, \hat{t}, \hat{u}$

# Collins Asymmetries at Mid-Rapidity

Potential insight  
into  $\delta q$   
if  $\Delta D_q$  known

$$A \sim \sum_q \delta q(x) \otimes \Delta D_q(j_T, z) \otimes H^{\text{Collins}}$$

azimuthal asymmetry within jet

(unpolarized contributions excluded here)

transversity

Collins fragmentation

calculable function of  $\hat{s}, \hat{t}, \hat{u}$

# Collins Asymmetries at Mid-Rapidity

Potential insight  
into  $\delta q$   
if  $\Delta D_q$  known

Extraction of Collins  
fragmentation function from  
fit to SIDIS data (HERMES,  
COMPASS) and Belle  
Collab.  $e^+e^-$  data (KEK)  
(Anselmino, *et al.*, 2008)

$$A \sim \sum_q \delta q(x) \otimes \Delta D_q(j_T, z) \otimes H^{\text{Collins}}$$

azimuthal asymmetry within jet

$\delta q(x)$  transversity

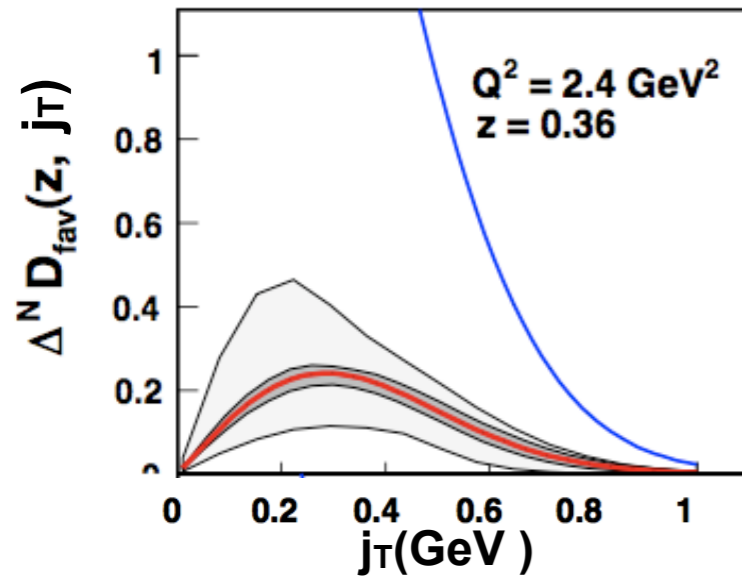
$\Delta D_q(j_T, z)$  Collins fragmentation

$H^{\text{Collins}}$  calculable function of  $\hat{s}, \hat{t}, \hat{u}$

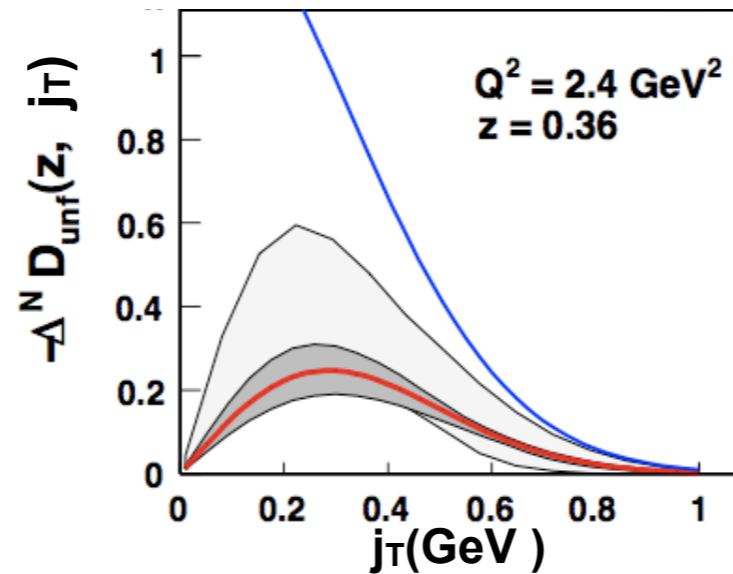
(unpolarized contributions excluded here)

# Collins Asymmetries at Mid-Rapidity

isospin-favored (u for  $\pi^+$ , d for  $\pi^-$ )  
Collins fragmentation function



isospin-unfavored (d for  $\pi^+$ , u for  $\pi^-$ )  
Collins fragmentation function



**Potential insight  
into  $\delta q$   
if  $\Delta D_q$  known**

Extraction of Collins fragmentation function from fit to SIDIS data (HERMES, COMPASS) and Belle Collab.  $e^+e^-$  data (KEK) (Anselmino, *et al.*, 2008)

(unpolarized contributions excluded here)

$$A \sim \sum_q \delta q(x) \otimes \Delta D_q(j_T, z) \otimes H^{\text{Collins}}$$

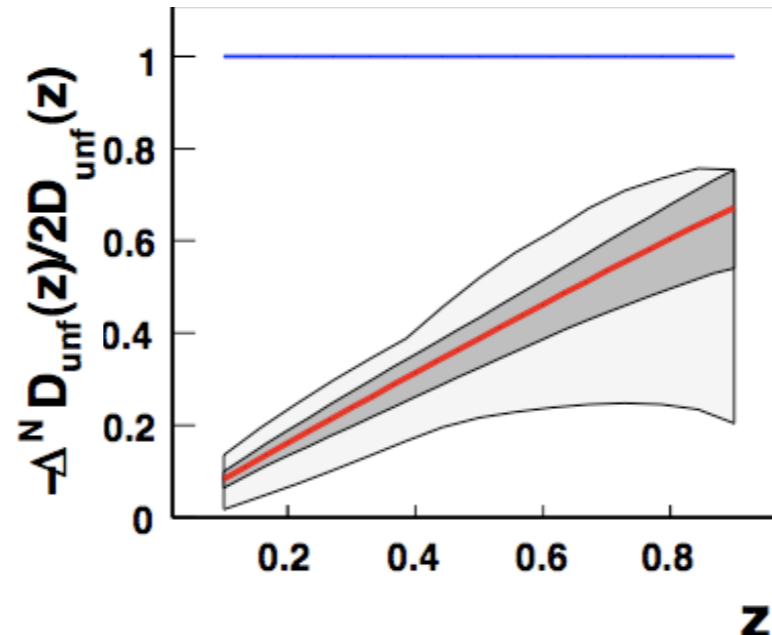
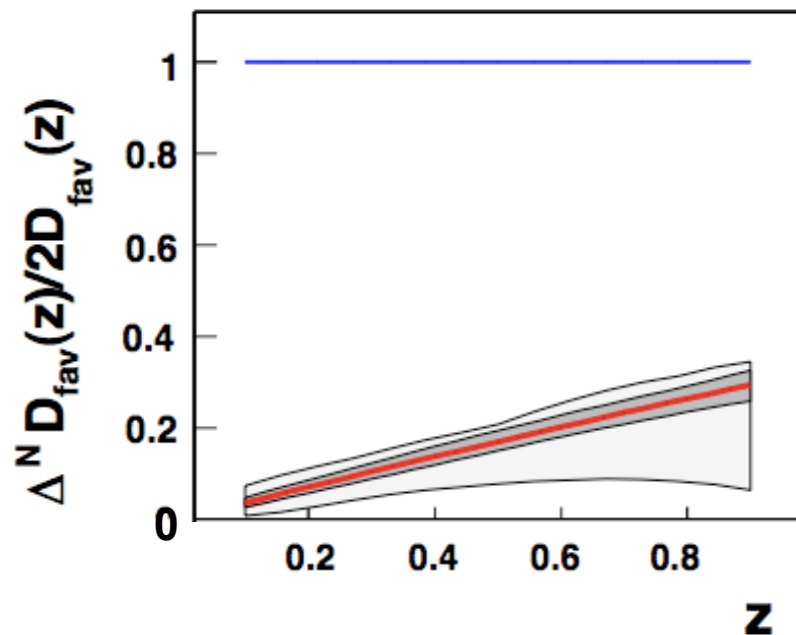
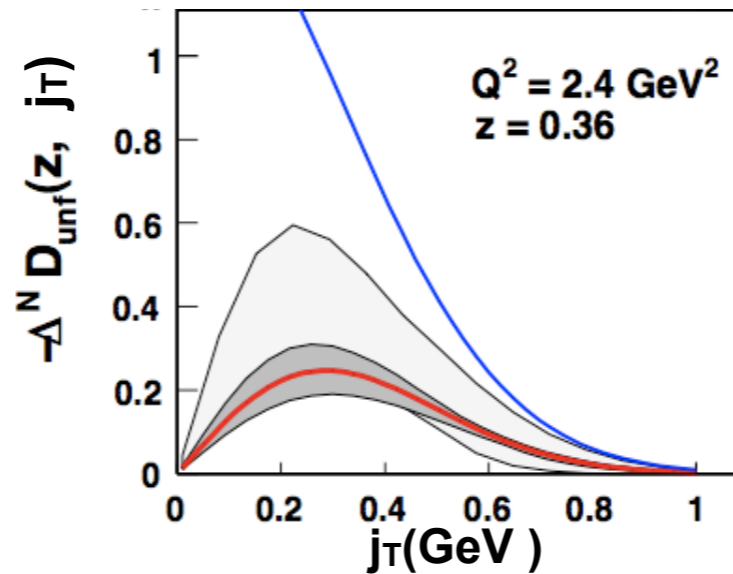
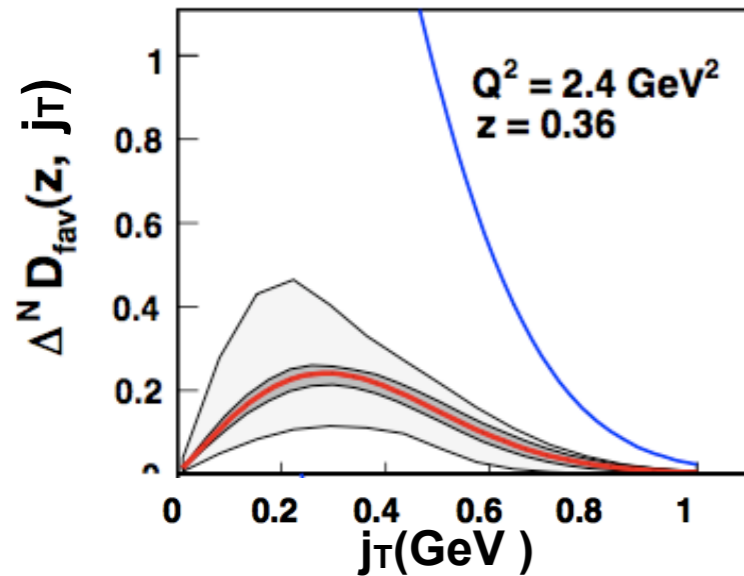
azimuthal asymmetry within jet      transversality      Collins fragmentation      calculable function of  $\hat{s}, \hat{t}, \hat{u}$

# Collins Asymmetries at Mid-Rapidity

isospin-favored (u for  $\pi^+$ , d for  $\pi^-$ )  
Collins fragmentation function

isospin-unfavored (d for  $\pi^+$ , u for  $\pi^-$ )  
Collins fragmentation function

Potential insight  
into  $\delta q$   
if  $\Delta D_q$  known



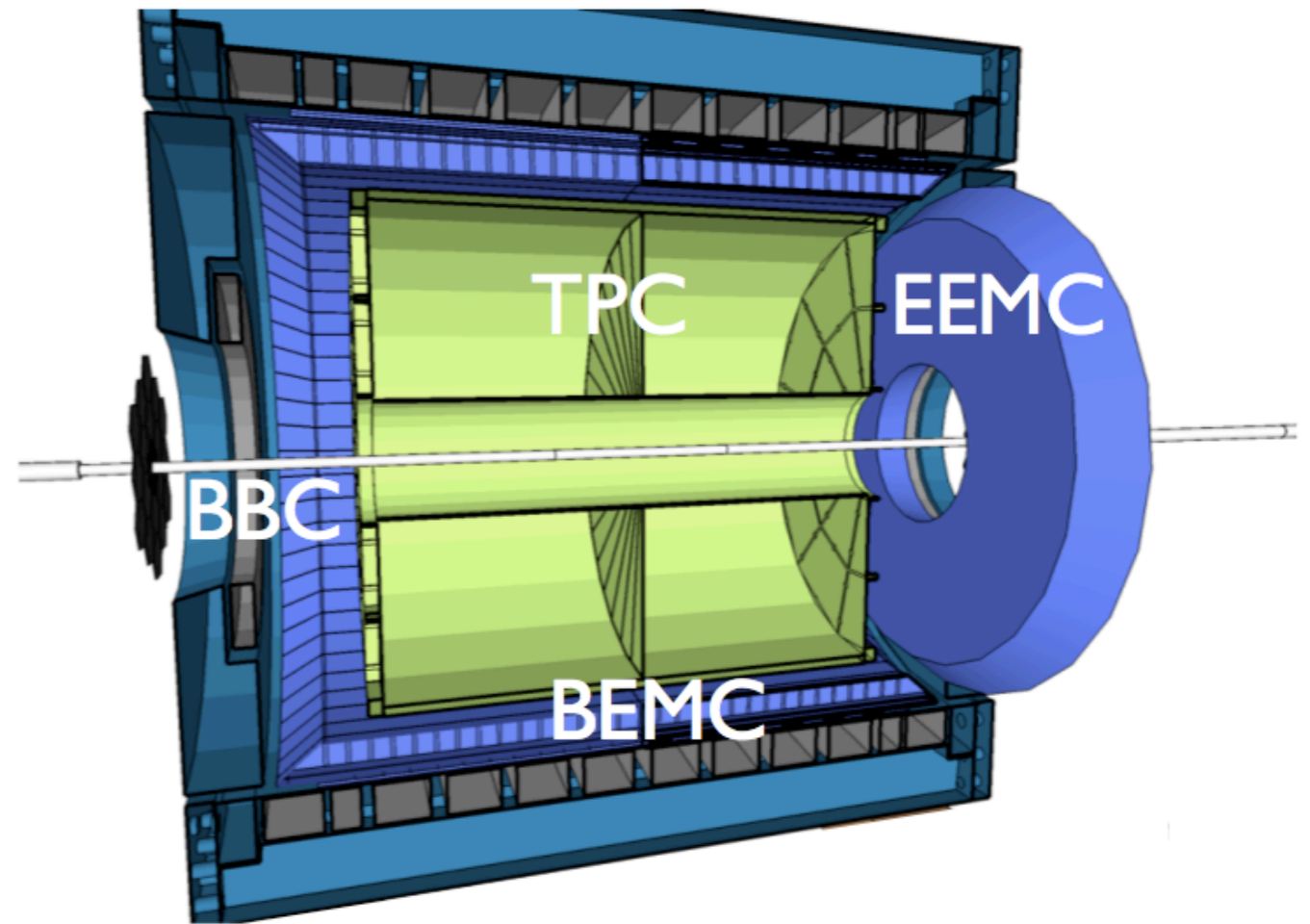
Extraction of Collins  
fragmentation function from  
fit to SIDIS data (HERMES,  
COMPASS) and Belle  
Collab.  $e^+e^-$  data (KEK)  
(Anselmino, *et al.*, 2008)

(unpolarized contributions excluded here)

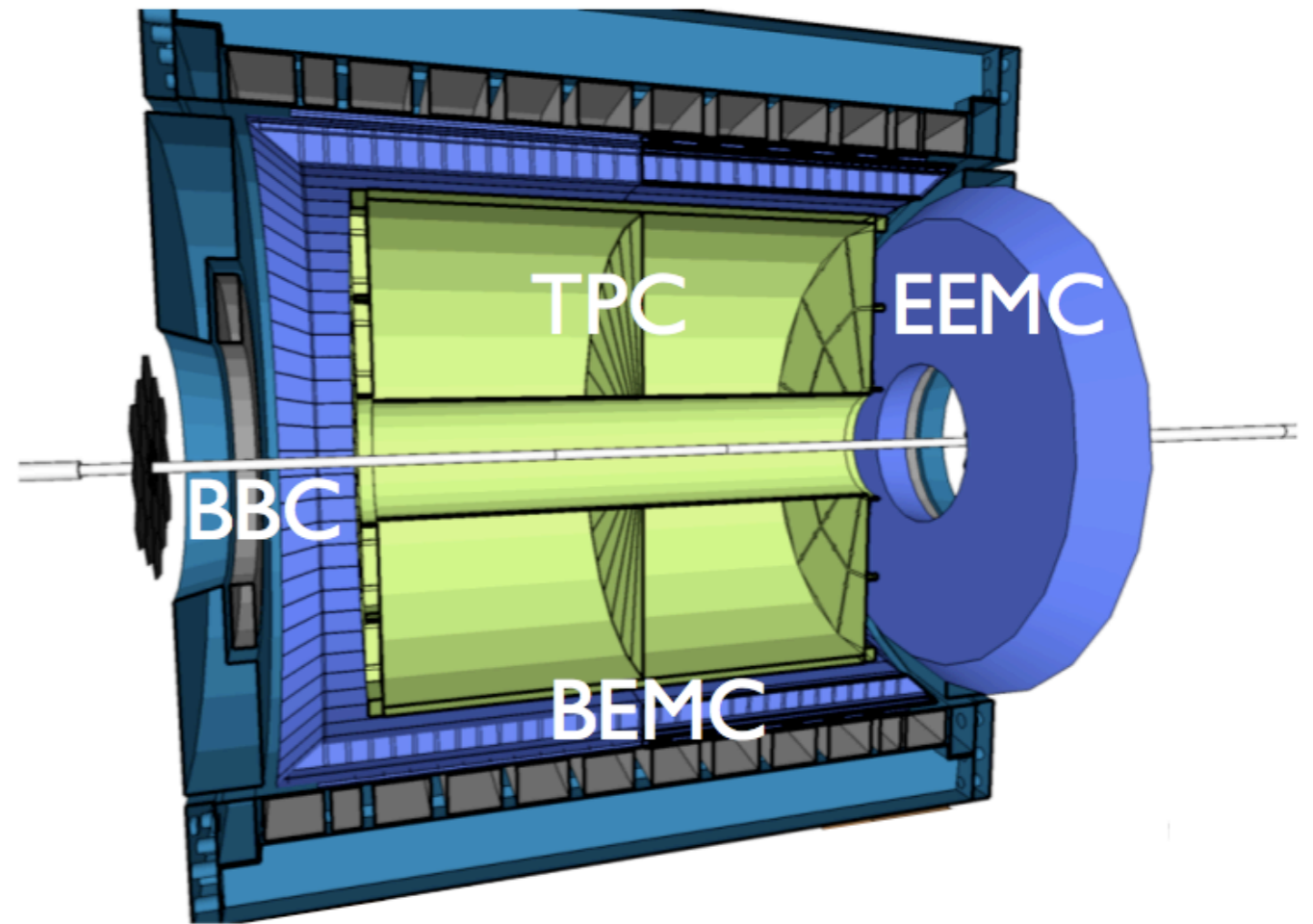
$$A \sim \sum_q \delta q(x) \otimes \Delta D_q(j_T, z) \otimes H^{\text{Collins}}$$

azimuthal asymmetry within jet      transversity      Collins fragmentation      calculable function of  $\hat{s}, \hat{t}, \hat{u}$

# Summary of Midrapidity STAR Components



# Summary of Midrapidity STAR Components



Beam Beam  
Counter (BBC)

relative polarization  
luminosities;  
minimum bias trigger

# Summary of Midrapidity STAR Components

Barrel Electromagnetic Calorimeter (BEMC)

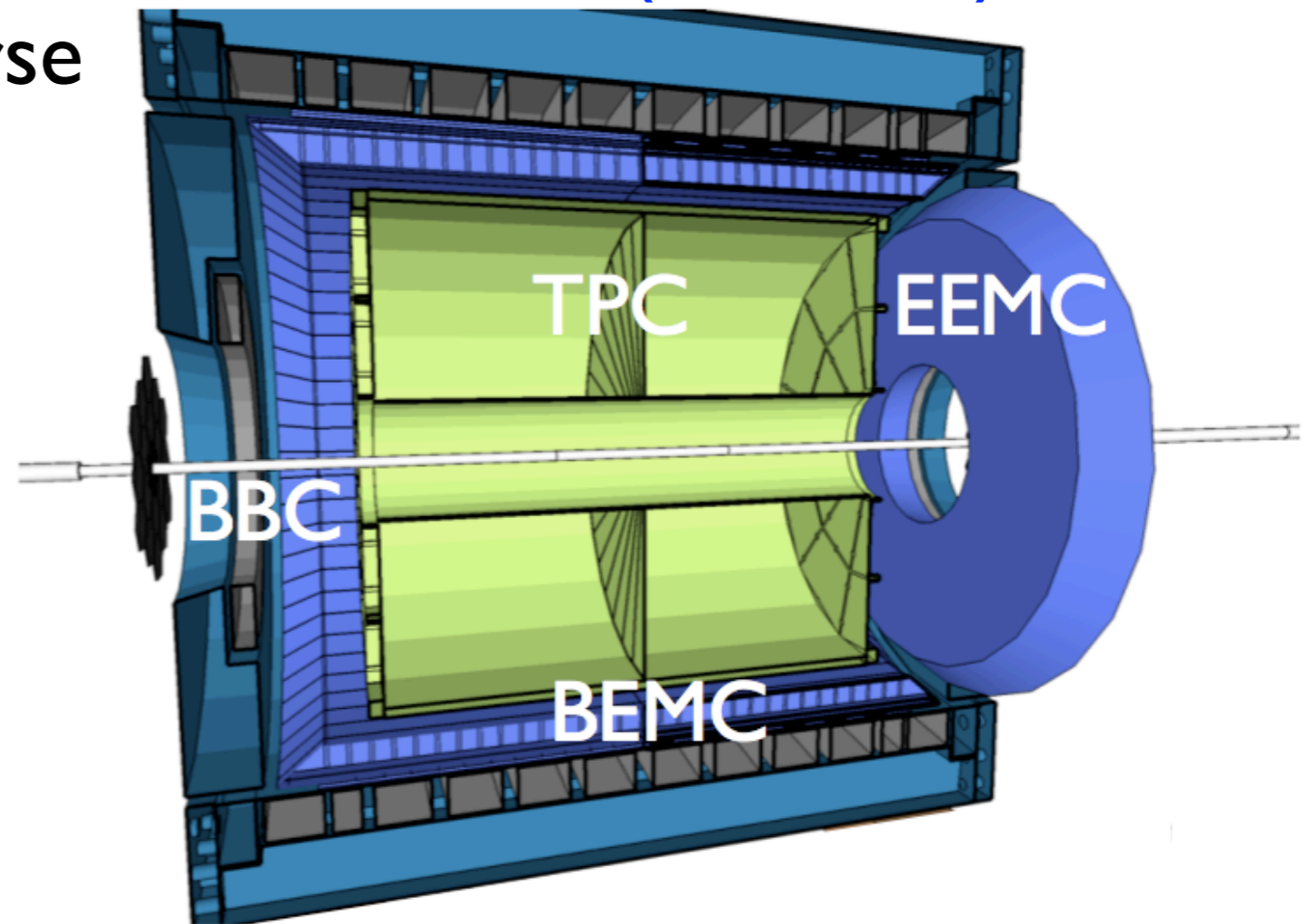
Endcap Electromagnetic Calorimeter (EEMC)

- Determines particle transverse energy

- Reconstruction of “jets” at mid-rapidity ( $-1 < \eta < 2$ )

Nucl. Instrum. Meth. A 499 (2003) 725–739

Nucl. Instrum. Meth. A 499 (2003) 740–750



Beam Beam  
Counter (BBC)

relative polarization  
luminosities;  
minimum bias trigger

# Summary of Midrapidity STAR Components

Barrel Electromagnetic Calorimeter (BEMC)

Endcap Electromagnetic Calorimeter (EEMC)

- Determines particle transverse energy

- Reconstruction of “jets” at mid-rapidity ( $-1 < \eta < 2$ )

Nucl. Instrum. Meth. A 499 (2003) 725–739

Nucl. Instrum. Meth. A 499 (2003) 740–750

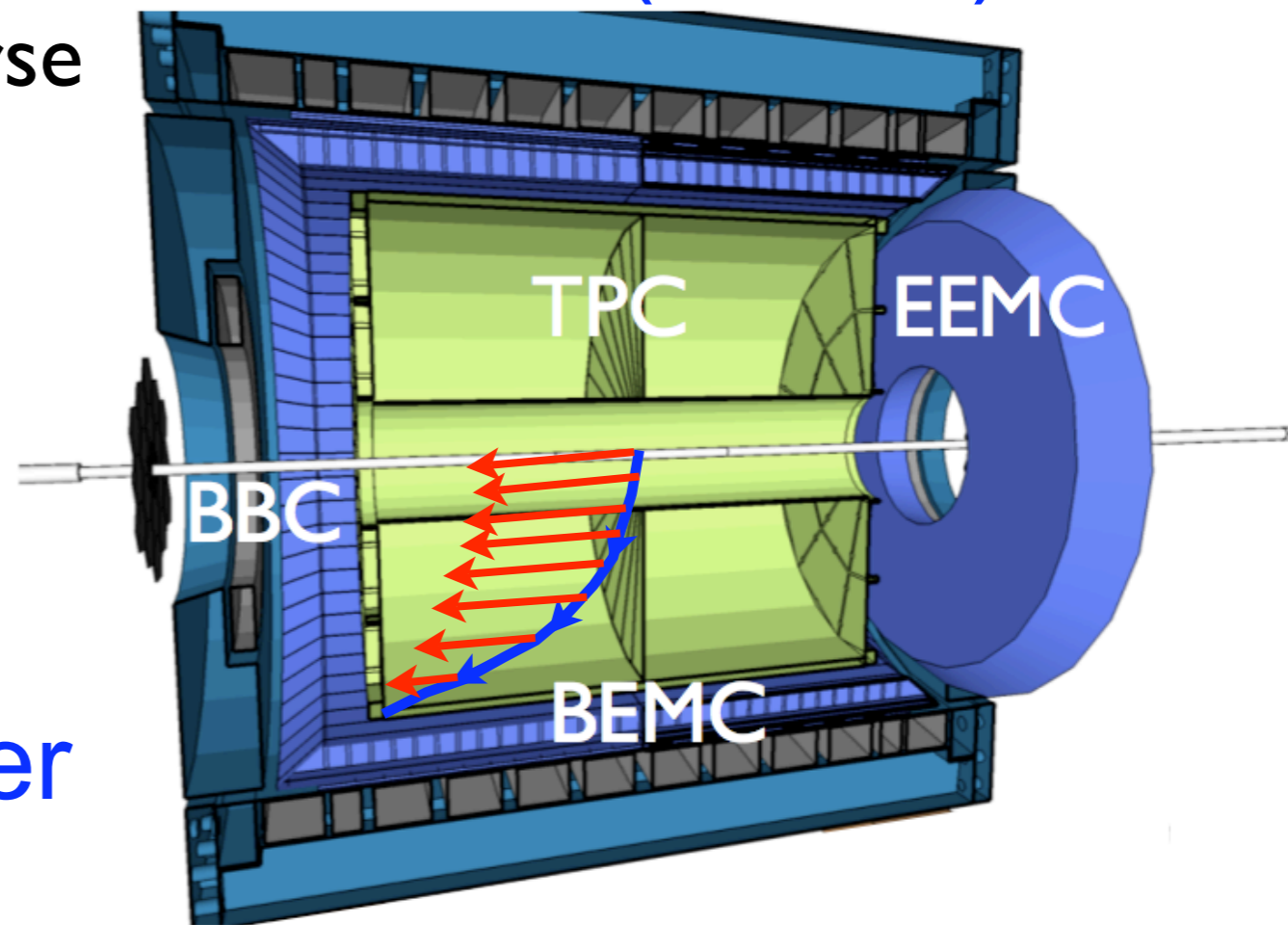
Time Projection Chamber (TPC)

- Particle track ionizes Ar/CH<sub>4</sub> gas

- HV induces ion drift to collection “pad”

- Pad location & drift time determine particle trajectory → momentum → PID

Nucl. Instrum. Meth. A 499 (2003) 659–678

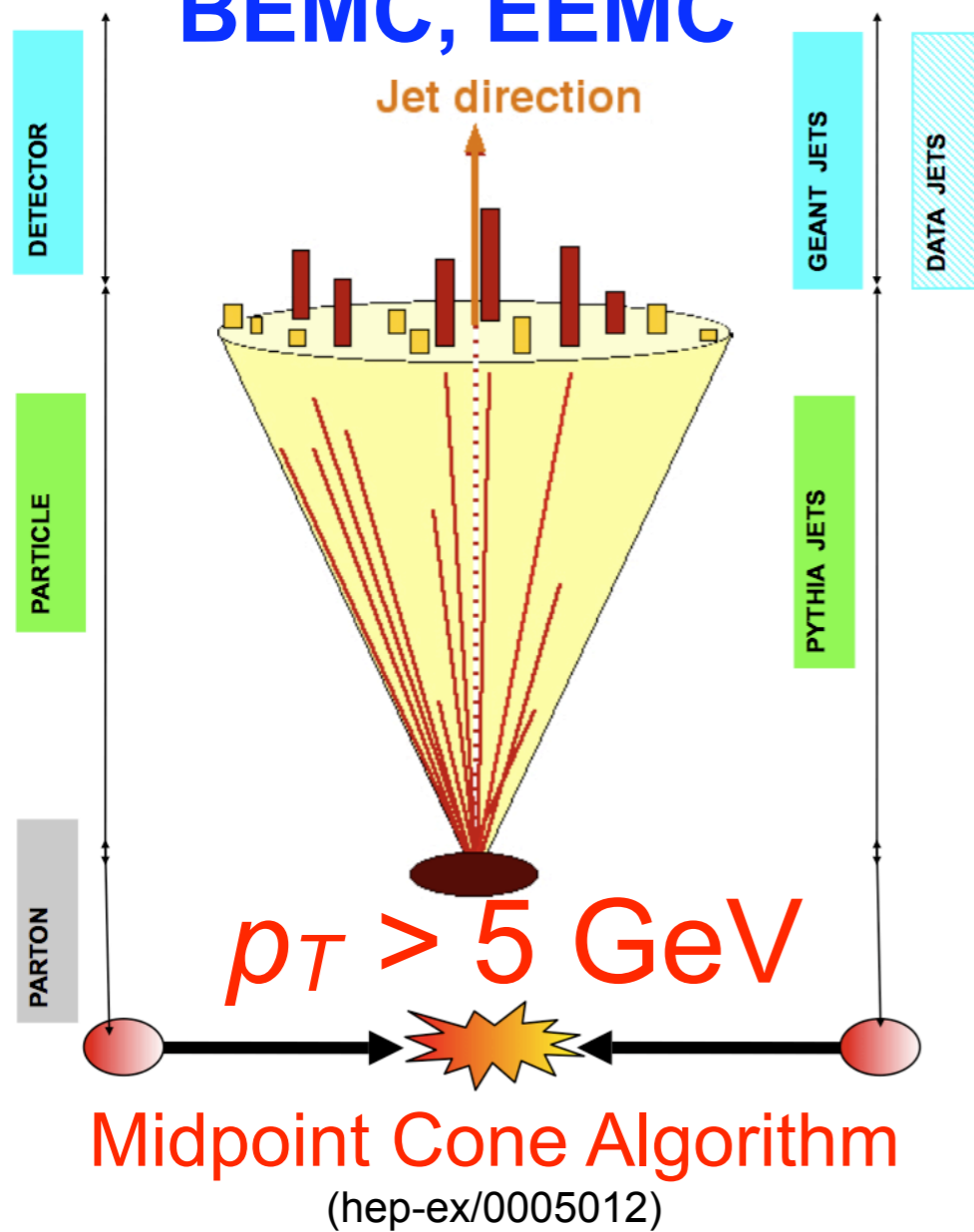


Beam Beam Counter (BBC)

relative polarization  
luminosities;  
minimum bias trigger

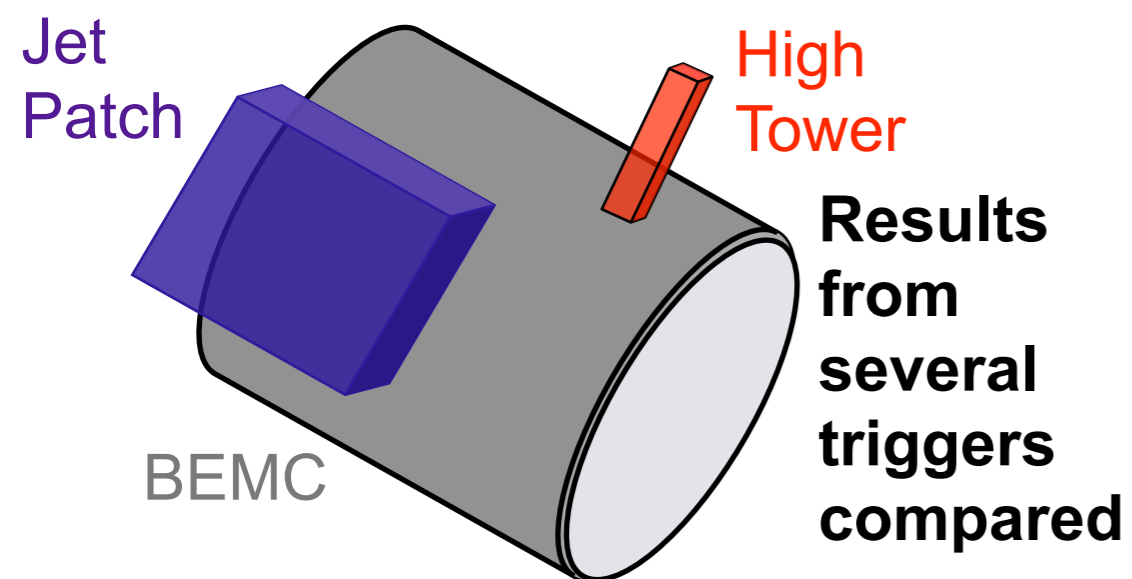
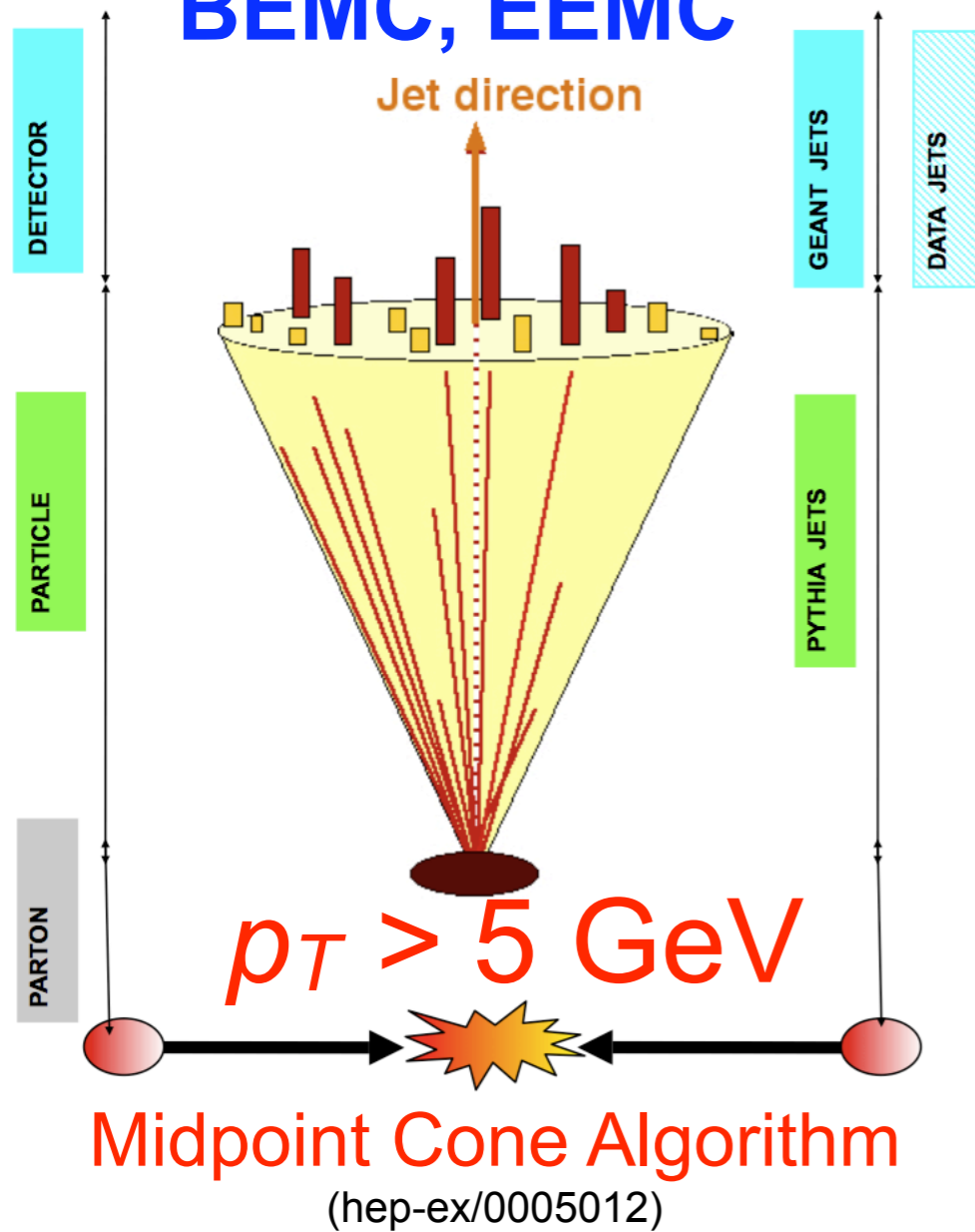
# Identification of Jets

BEMC, EEMC



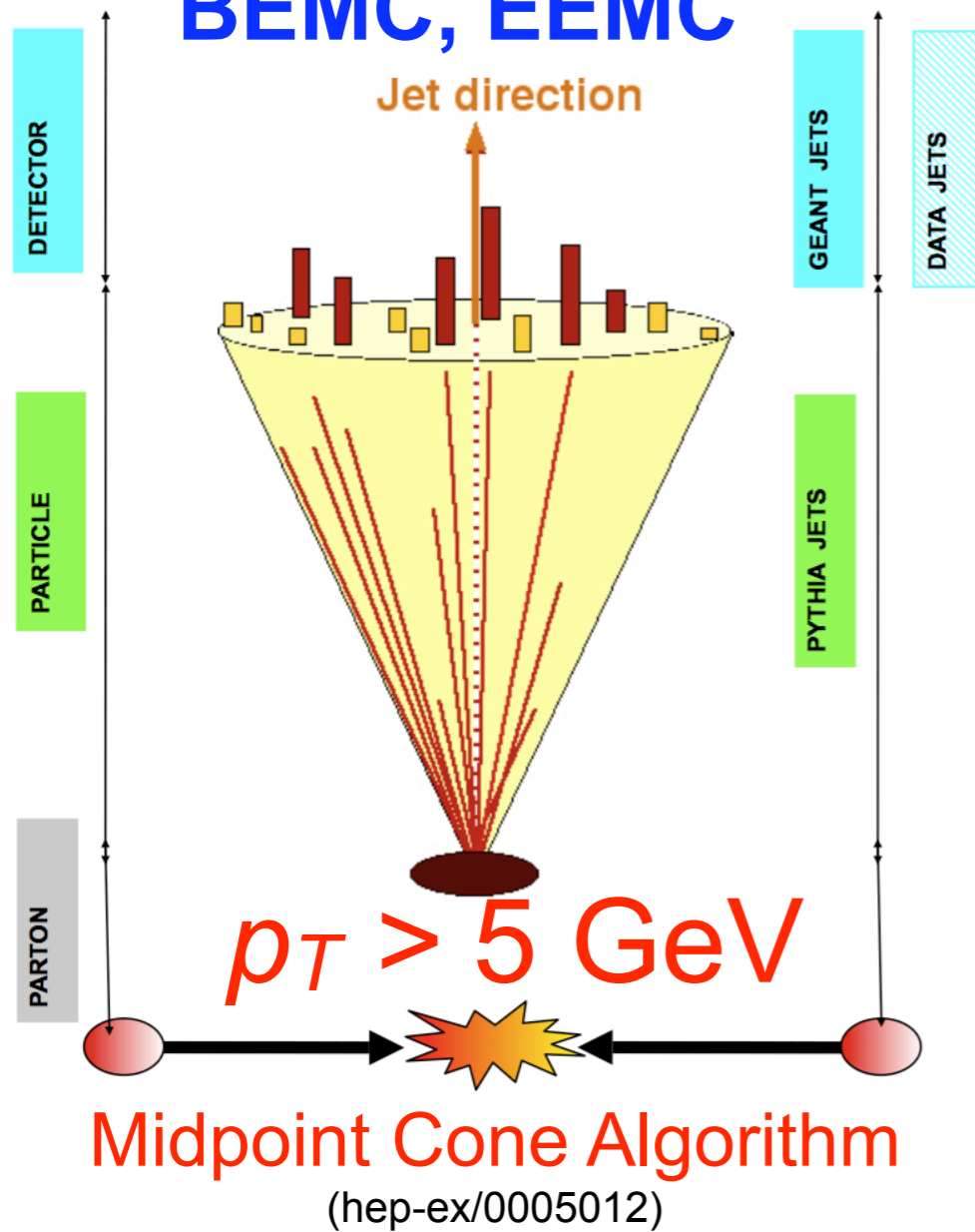
# Identification of Jets

**BEMC, EEMC**



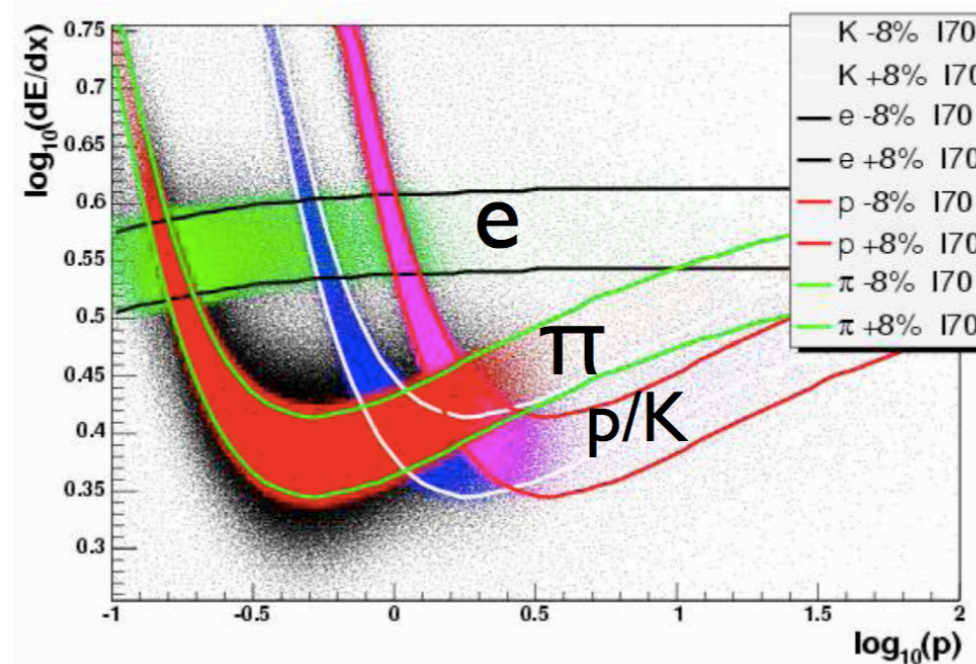
# Identification of Jets

**BEMC, EEMC**



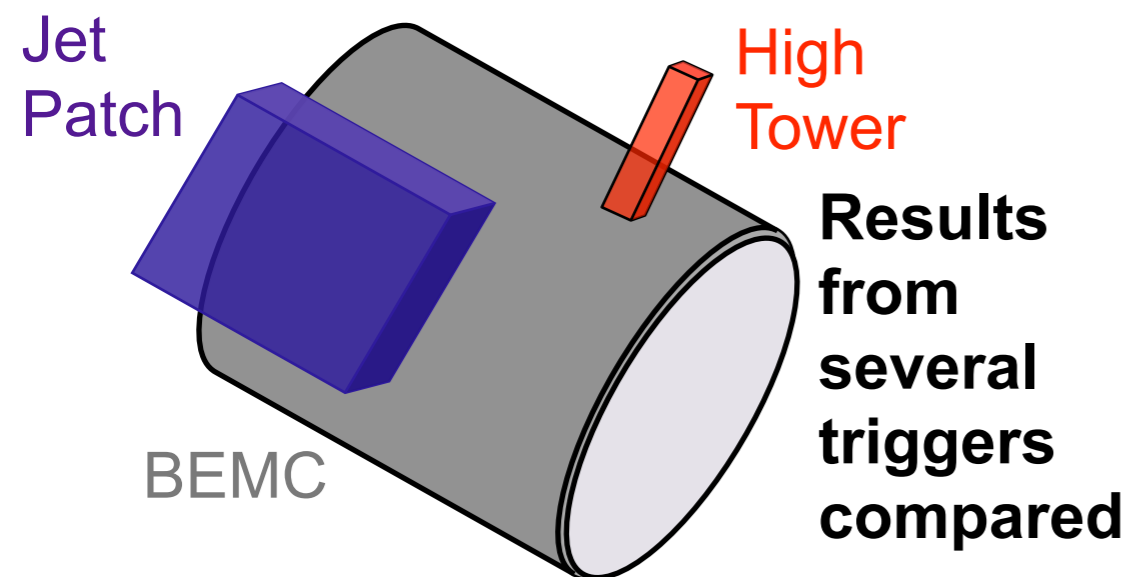
# Identification of Charged Pions

**TPC**



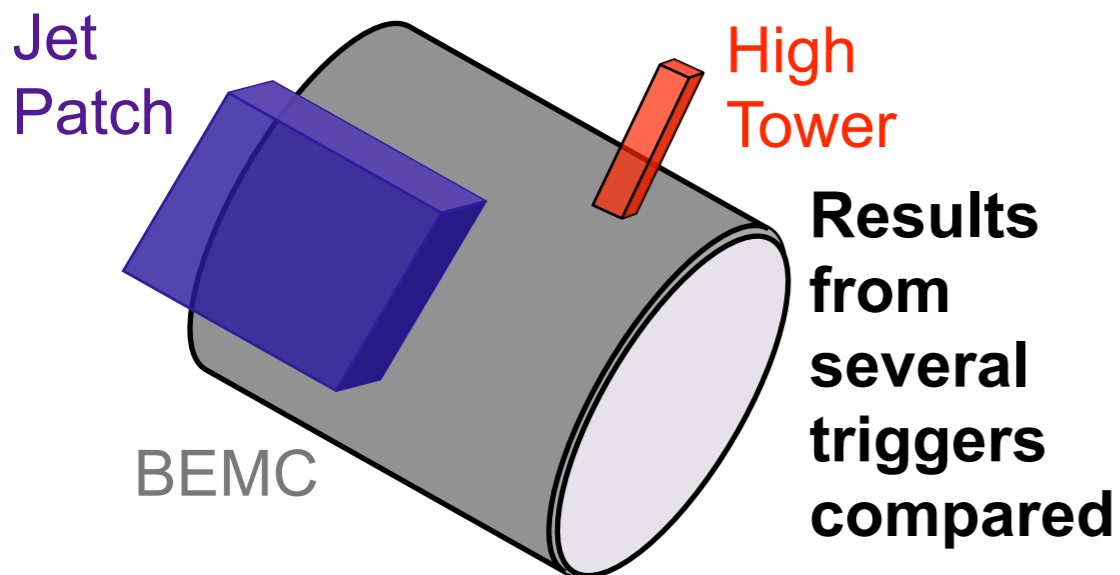
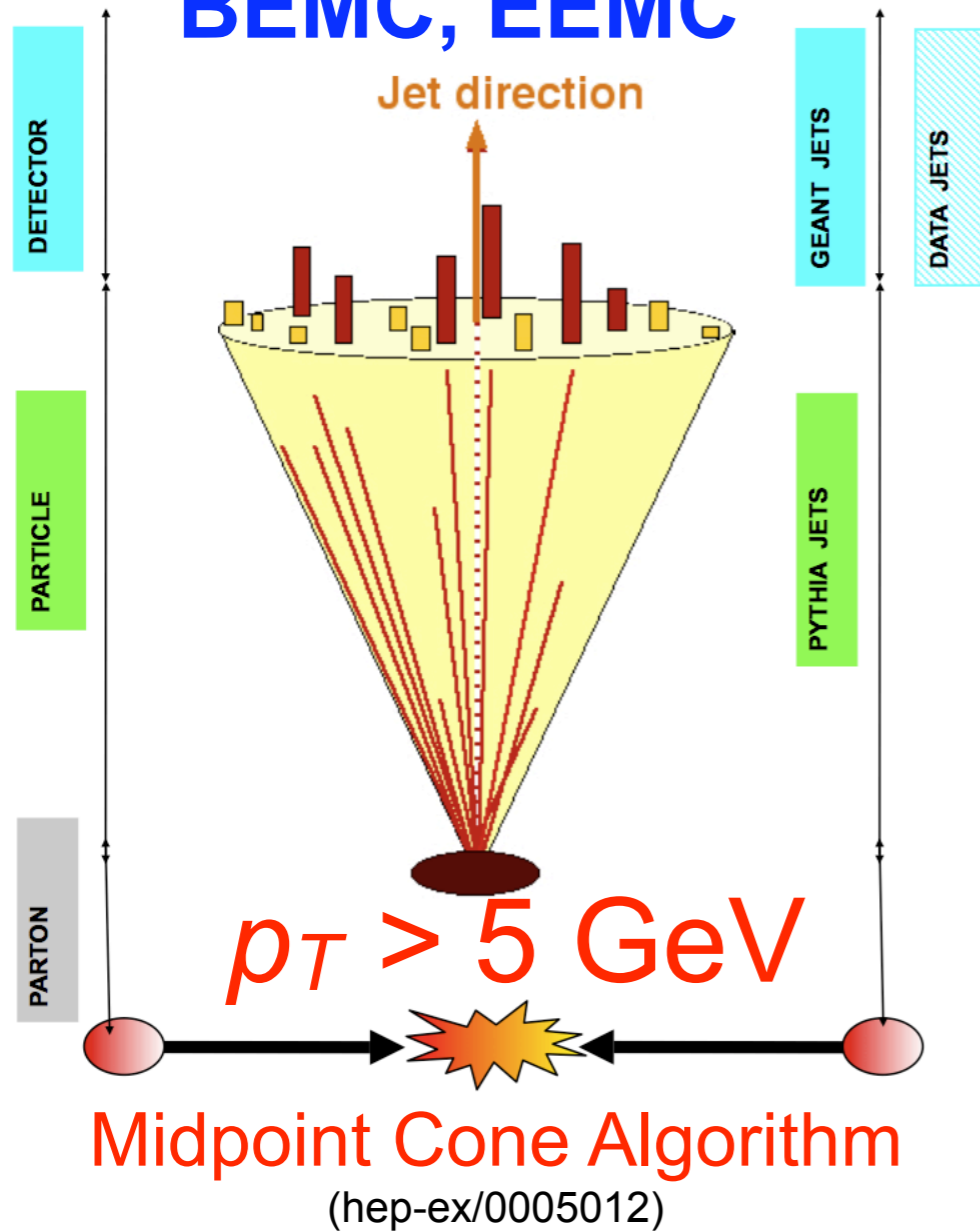
Nucl.Instrum.Meth.  
A558:419-429,2006

Bounds on dE/dx as function of momentum used to separate particles



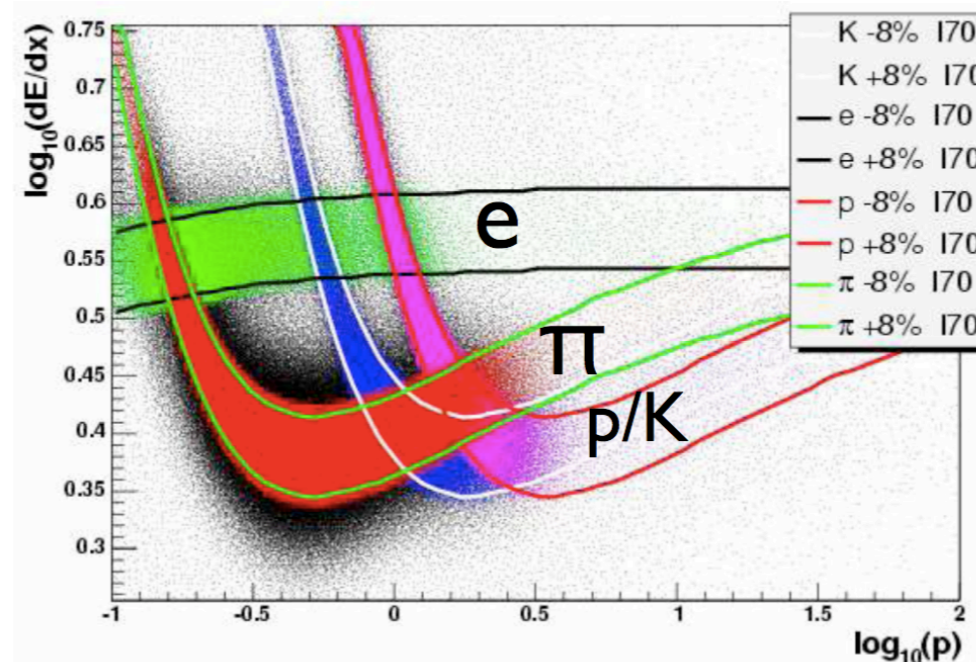
# Identification of Jets

**BEMC, EEMC**

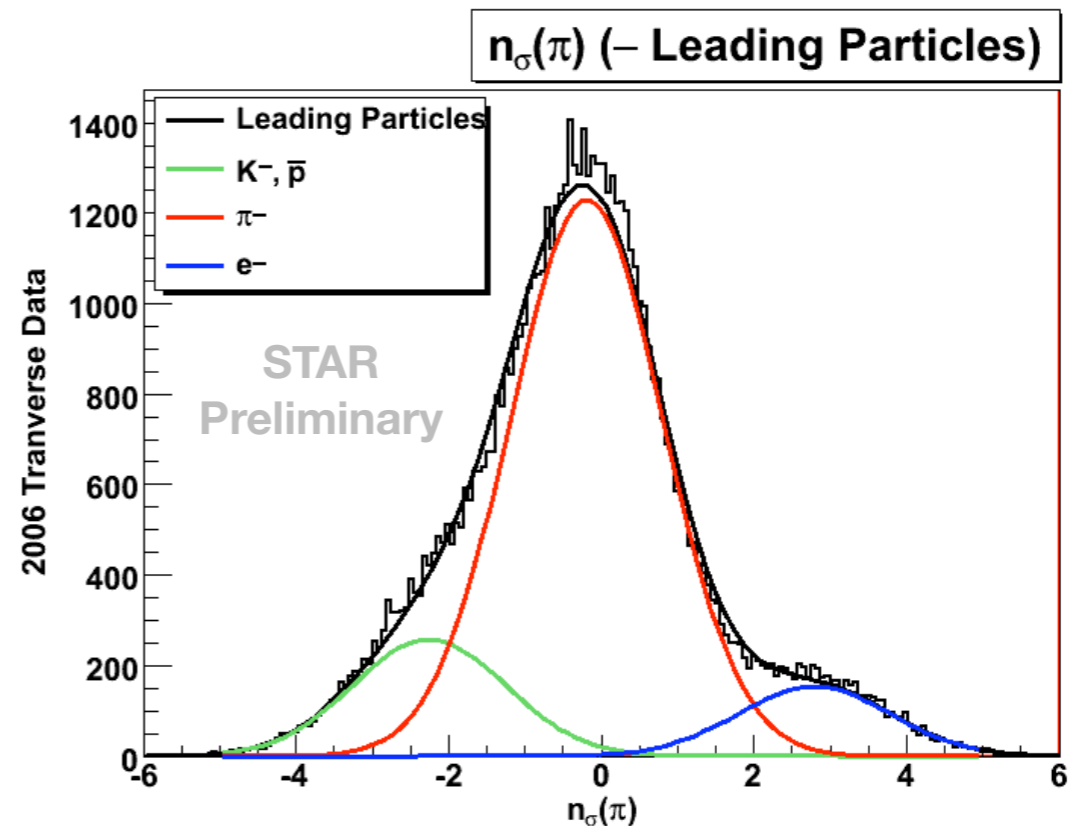


# Identification of Charged Pions

**TPC**



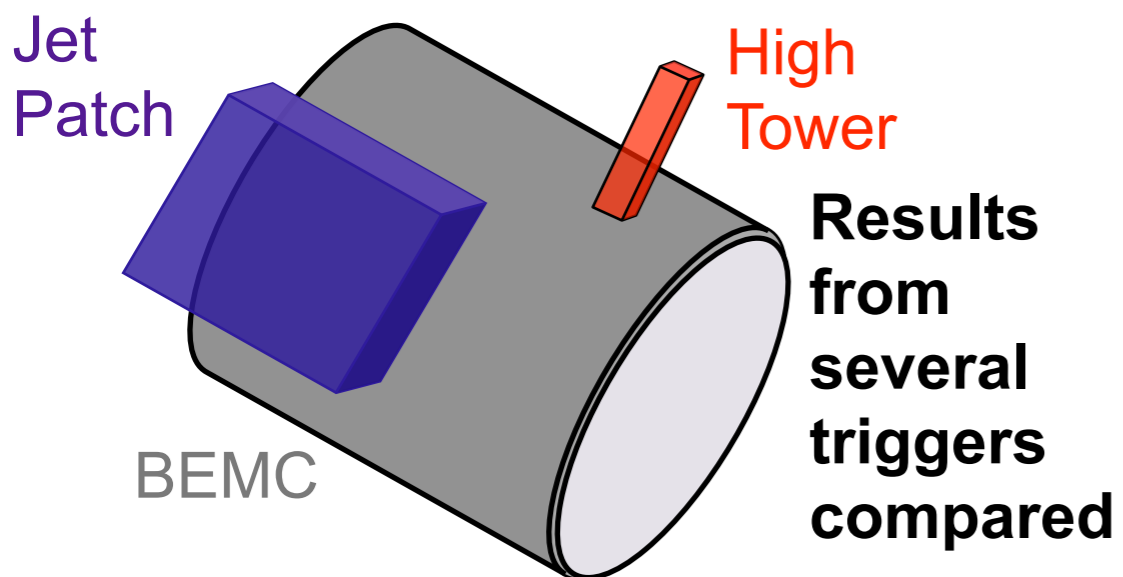
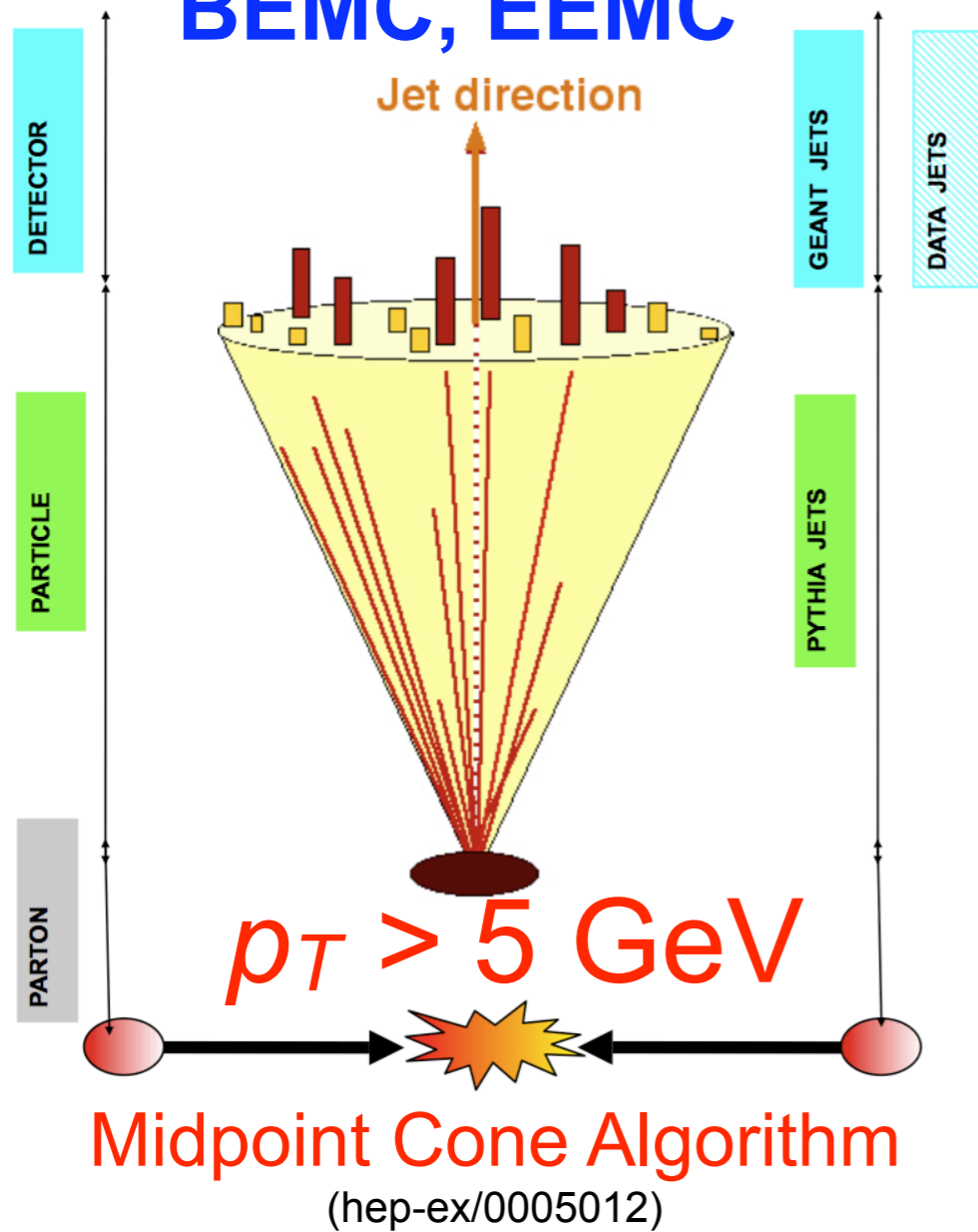
Bounds on dE/dx as function of momentum used to separate particles



Distributions can be used to estimate background contamination

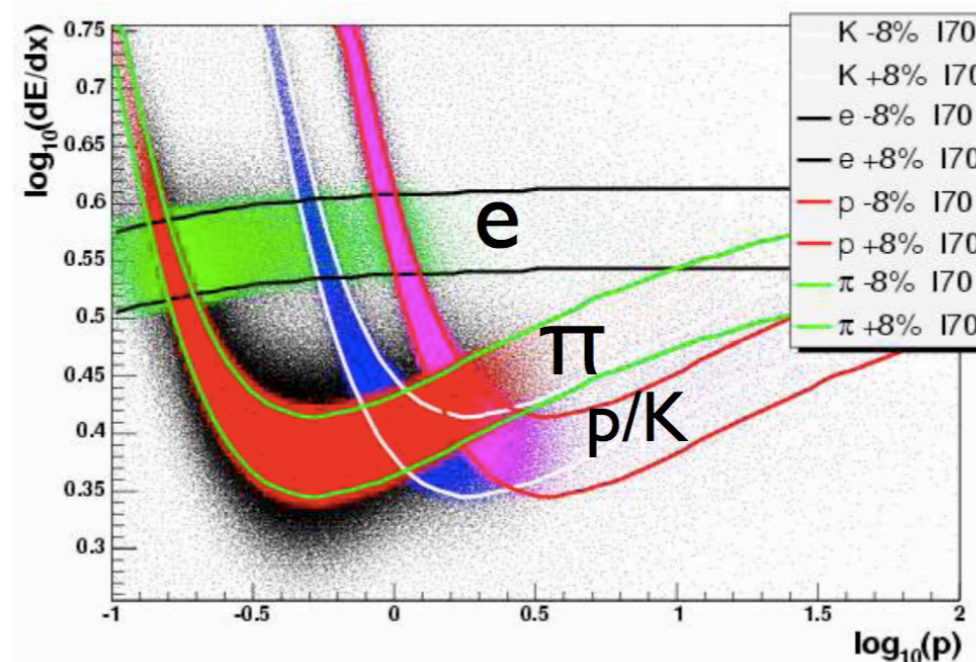
# Identification of Jets

**BEMC, EEMC**



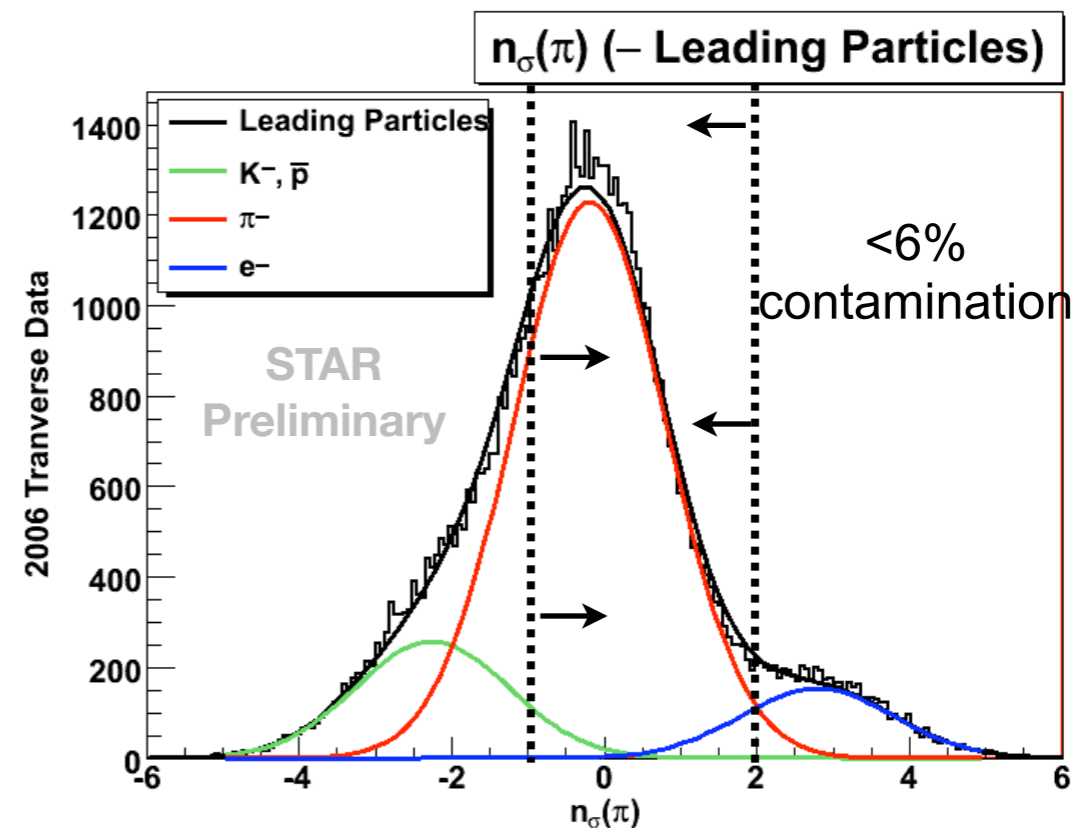
# Identification of Charged Pions

**TPC**



Nucl.Instrum.Meth.  
A558:419-429,2006

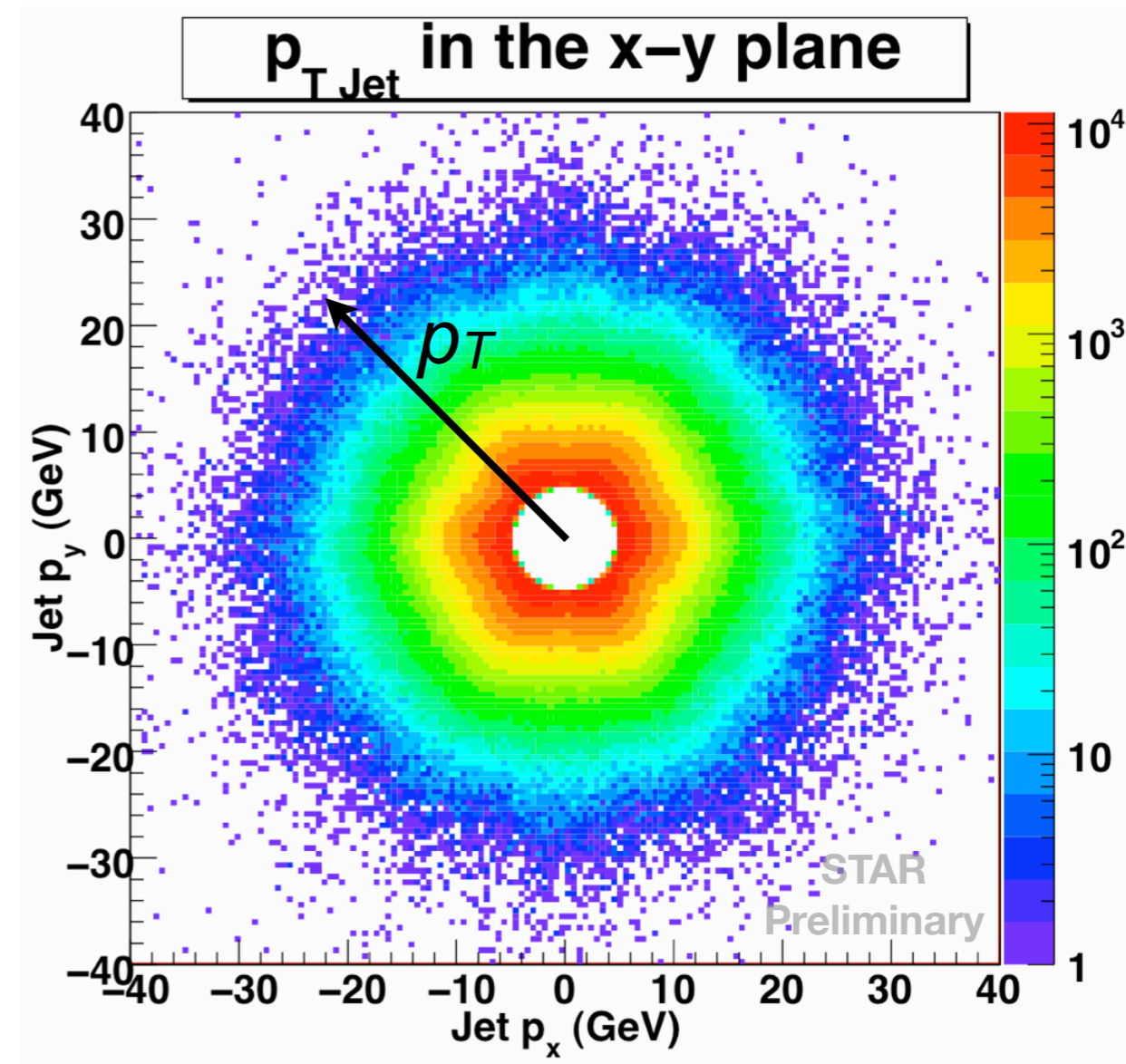
Bounds on  $dE/dx$  as function of momentum used to separate particles



Distributions can be used to estimate background contamination

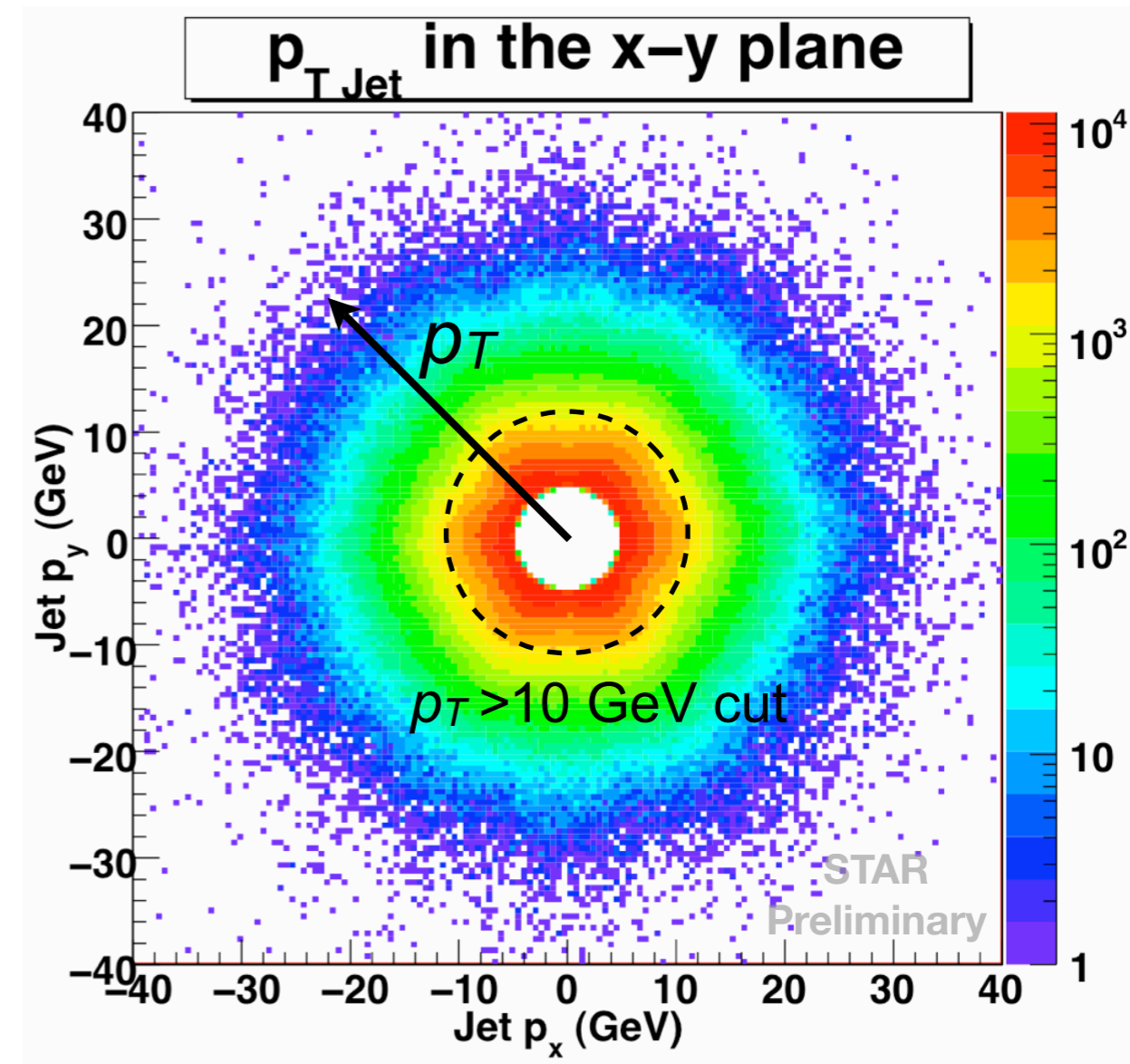
# Kinematic Coverage

Jets have full  
azimuthal ( $\Phi$ ) coverage



# Kinematic Coverage

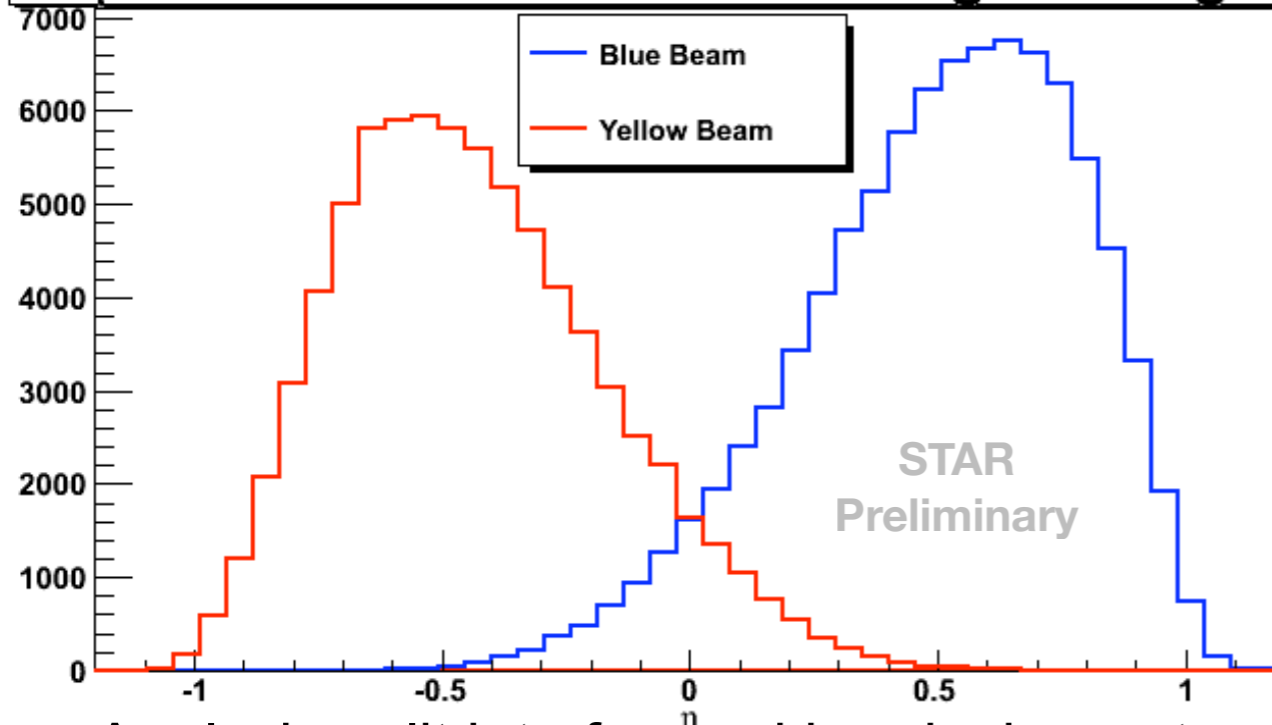
Jets have full  
azimuthal ( $\Phi$ ) coverage



10 GeV nominal  $p_T$  cut on jets  
is used as a tradeoff between statistics  
and gluon event contamination.

# Kinematic Coverage

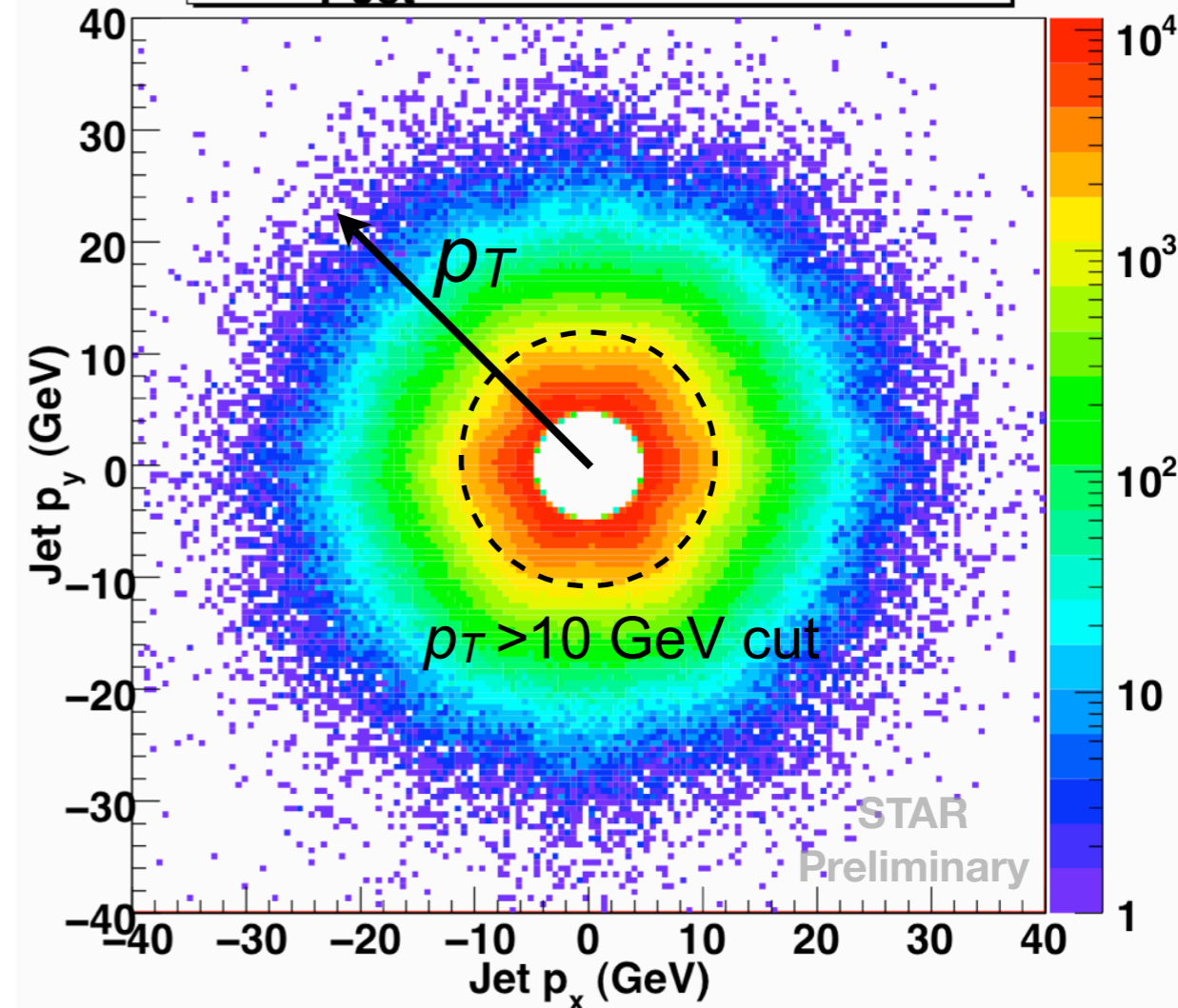
$\eta$  Distribution of Jets Containing Leading  $\pi^+$



Analysis split into forward hemispheres to maximize partonic spin transfer

Jets have full azimuthal ( $\Phi$ ) coverage

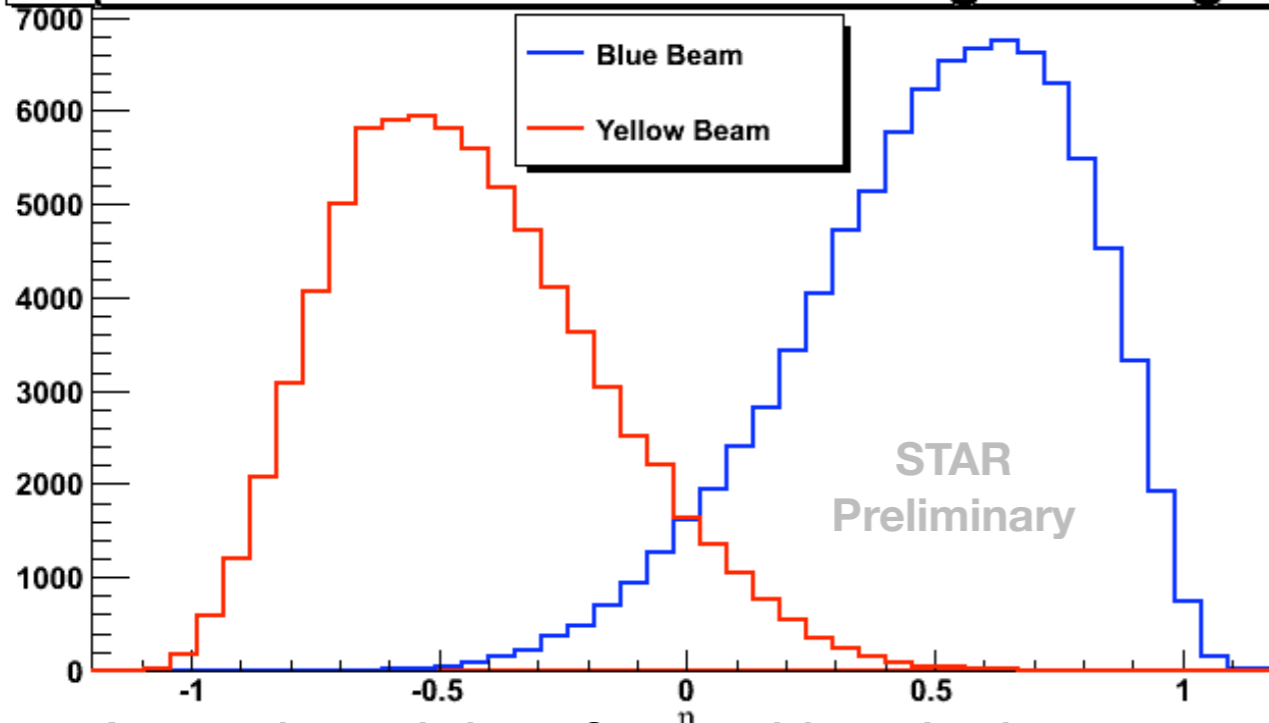
$p_{T \text{ Jet}}$  in the x-y plane



10 GeV nominal  $p_T$  cut on jets is used as a tradeoff between statistics and gluon event contamination.

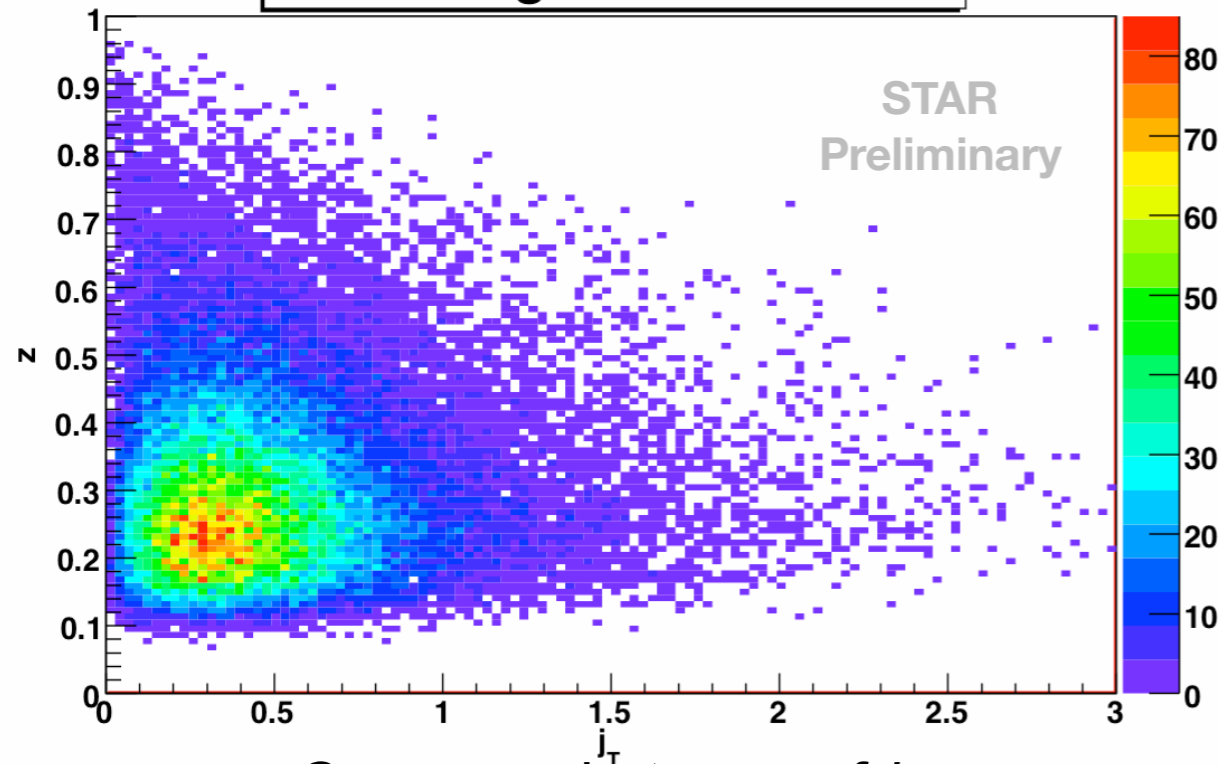
# Kinematic Coverage

$\eta$  Distribution of Jets Containing Leading  $\pi^+$



Analysis split into forward hemispheres to maximize partonic spin transfer

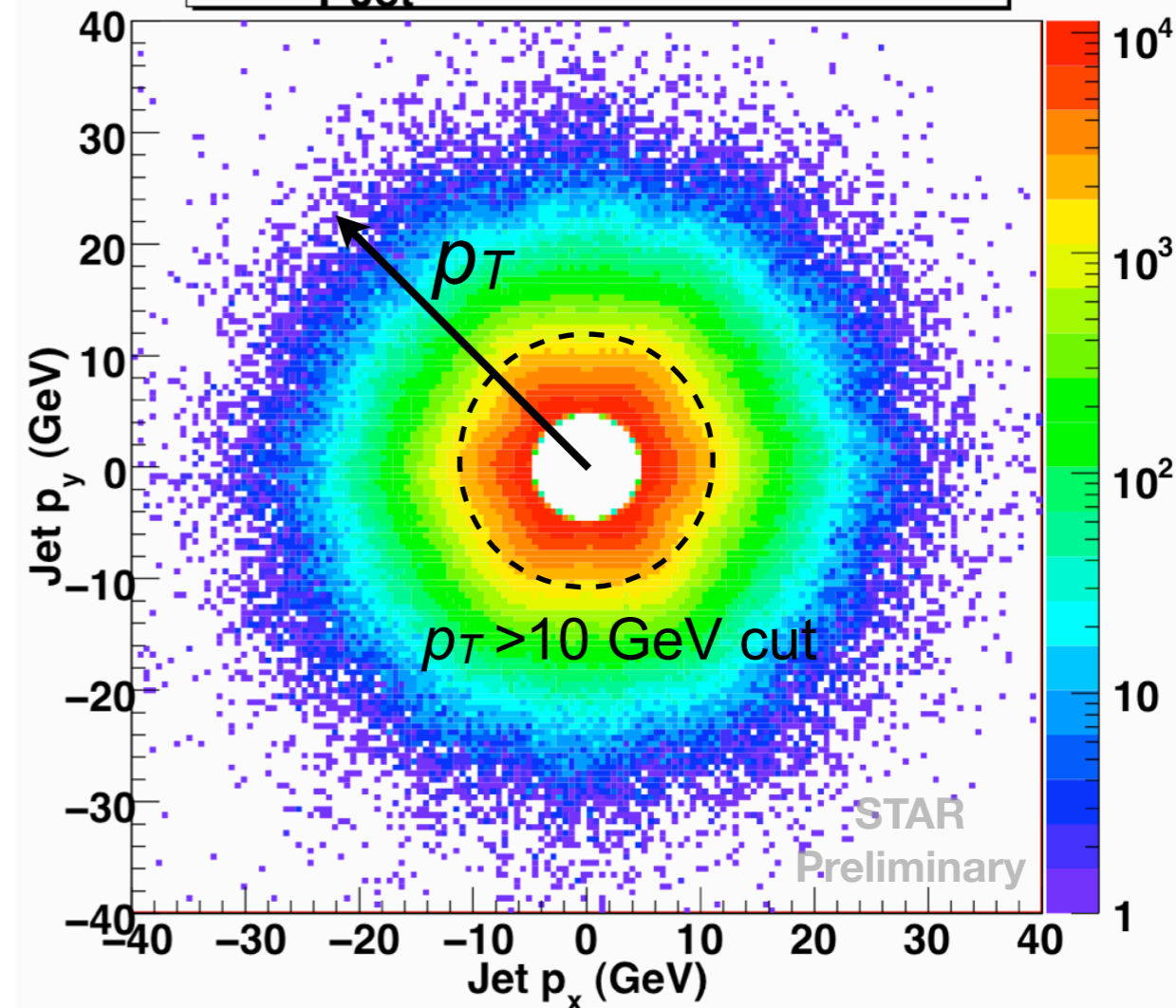
Leading  $\pi$  Kinematics



Coverage in terms of  $j_T, z$   
(kinematic degrees of freedom within jet)

Jets have full azimuthal ( $\Phi$ ) coverage

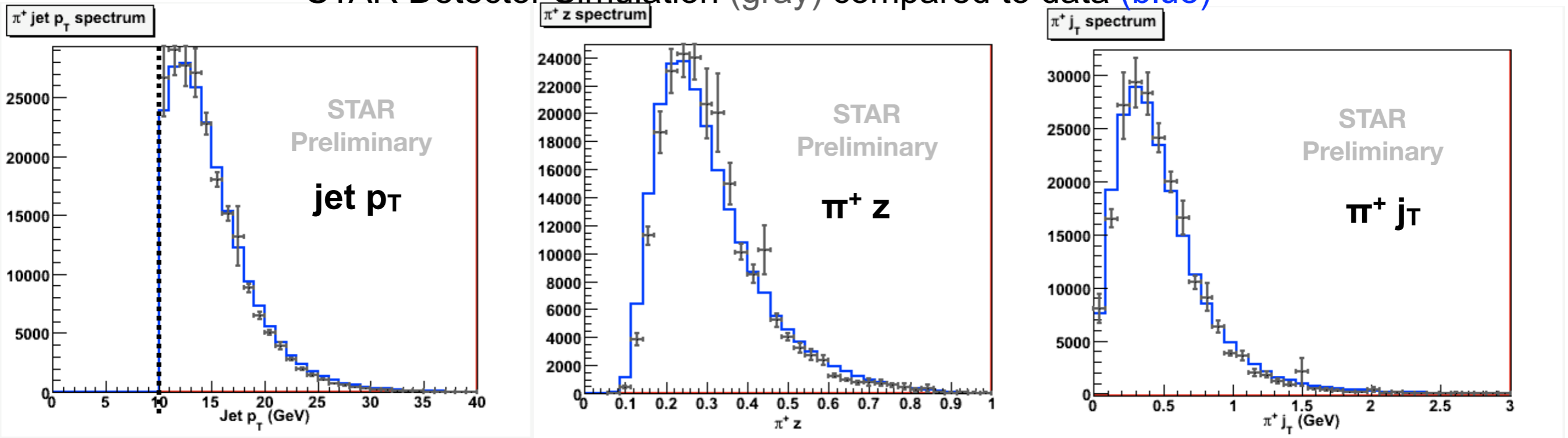
$p_{T \text{ Jet}}$  in the x-y plane



10 GeV nominal  $p_T$  cut on jets is used as a tradeoff between statistics and gluon event contamination.

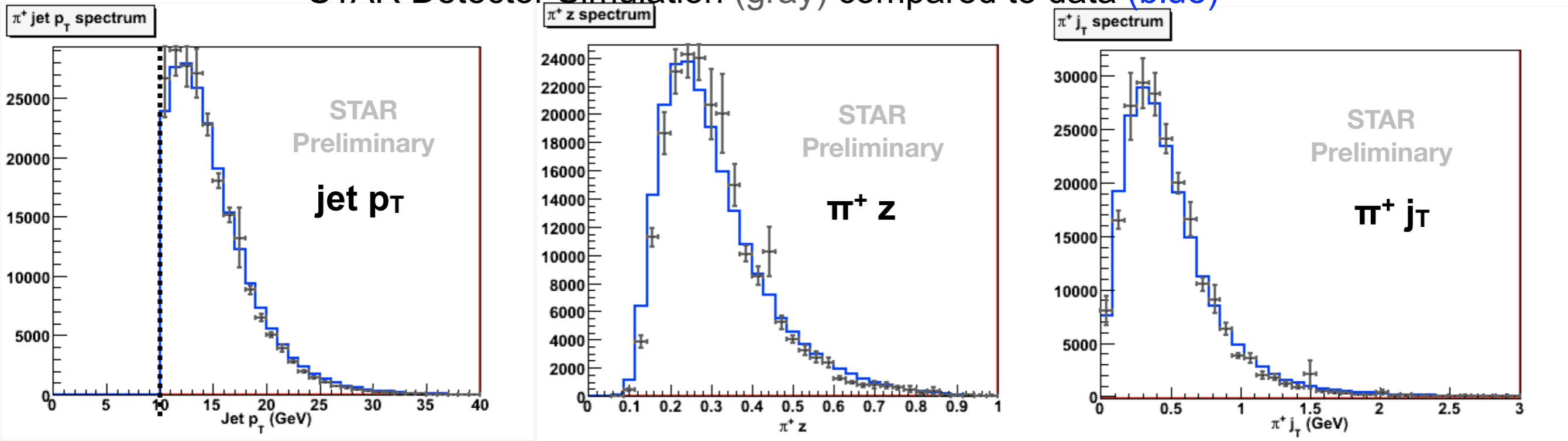
# Simulation Comparison

STAR Detector Simulation (gray) compared to data (blue)

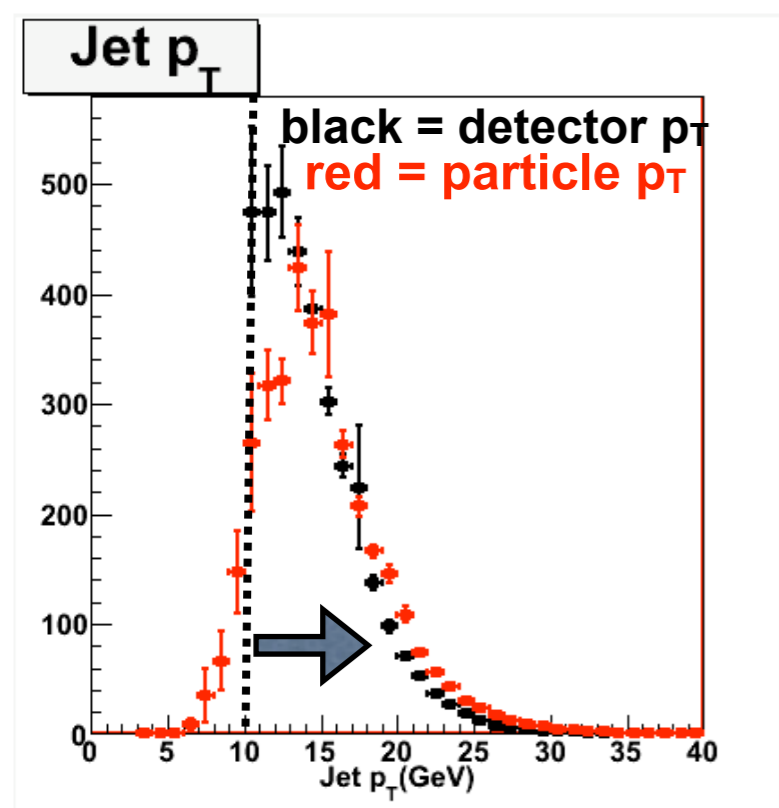


# Simulation Comparison

STAR Detector Simulation (gray) compared to data (blue)

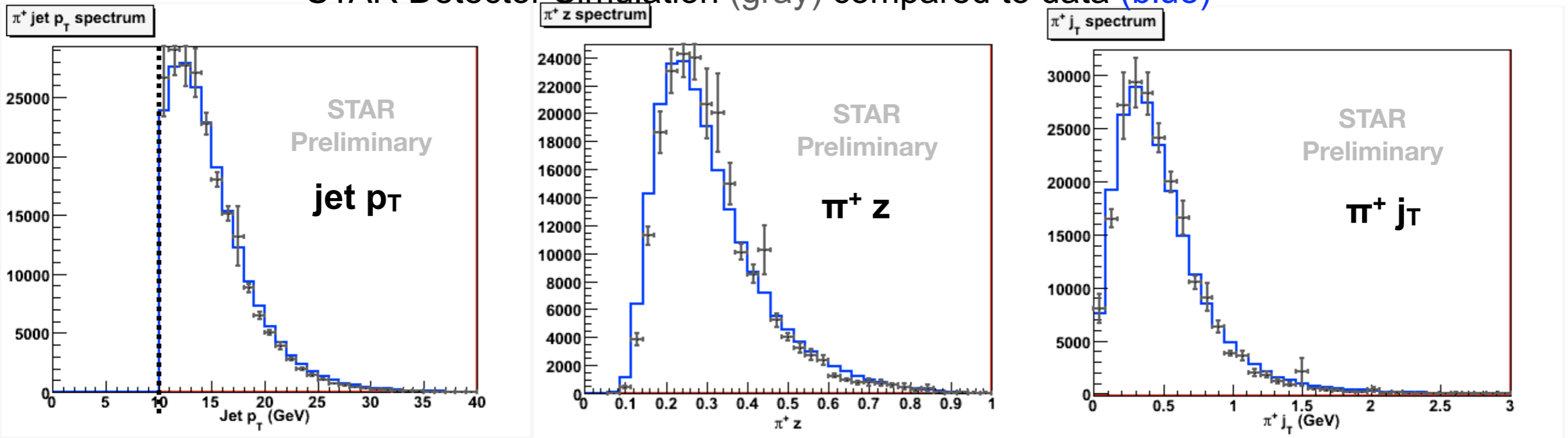


True jet  $p_T$  at particle level  
different than measured

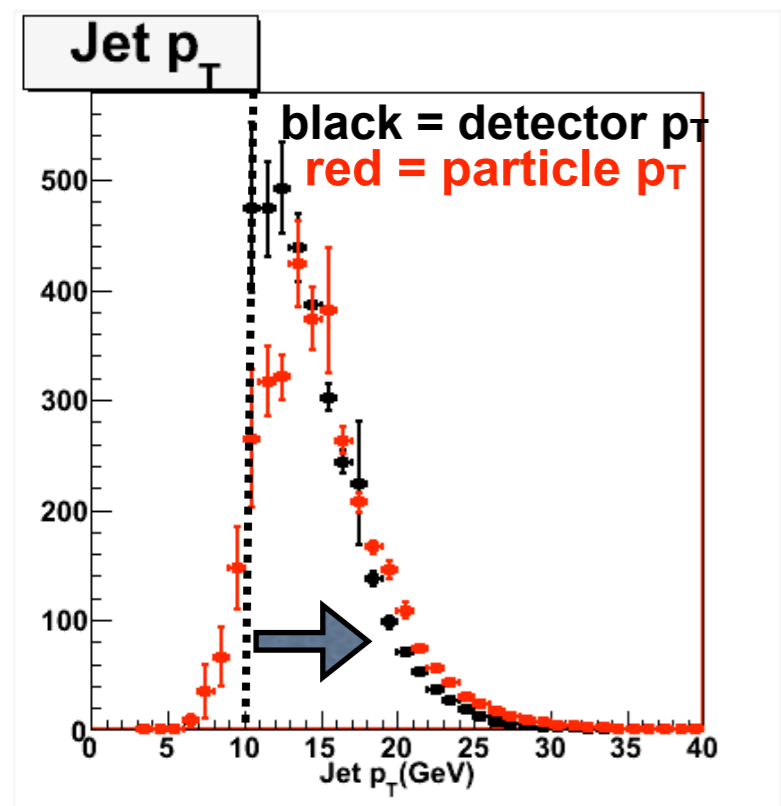


# Simulation Comparison

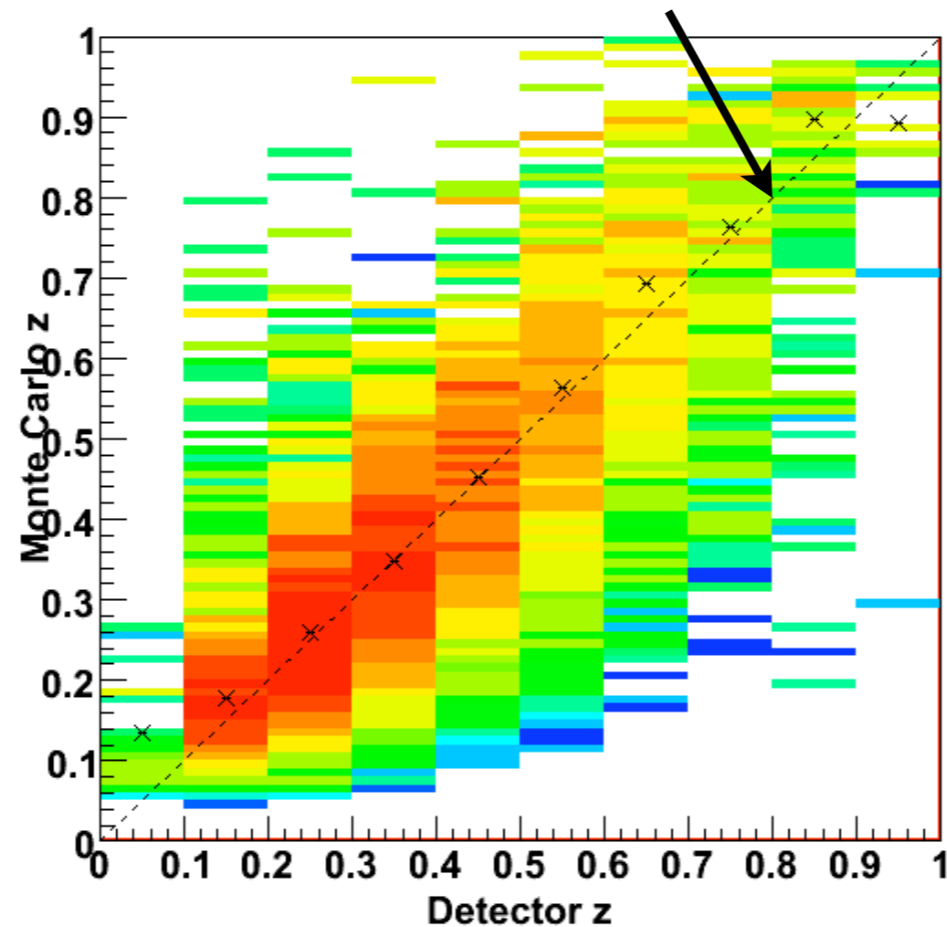
STAR Detector Simulation (gray) compared to data (blue)



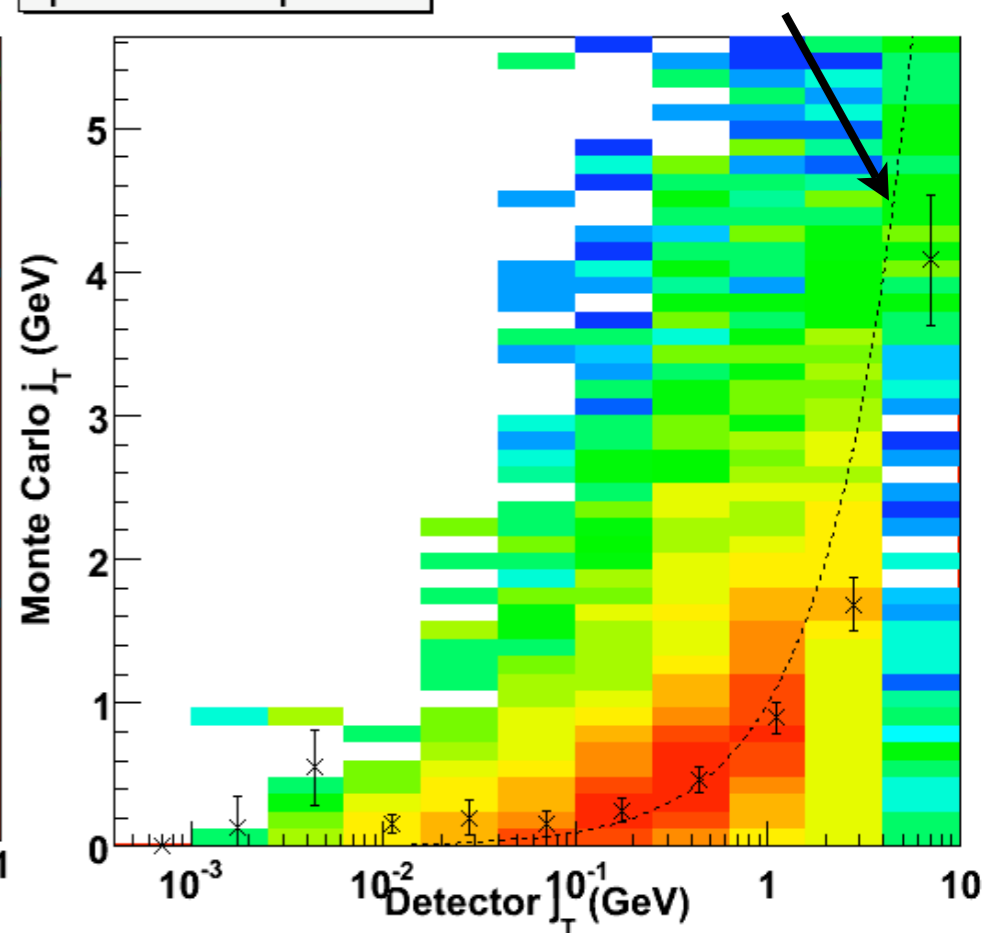
True jet  $p_T$  at particle level  
different than measured



$z$ [MC] vs.  $z$ [DET] 1:1 ratio line

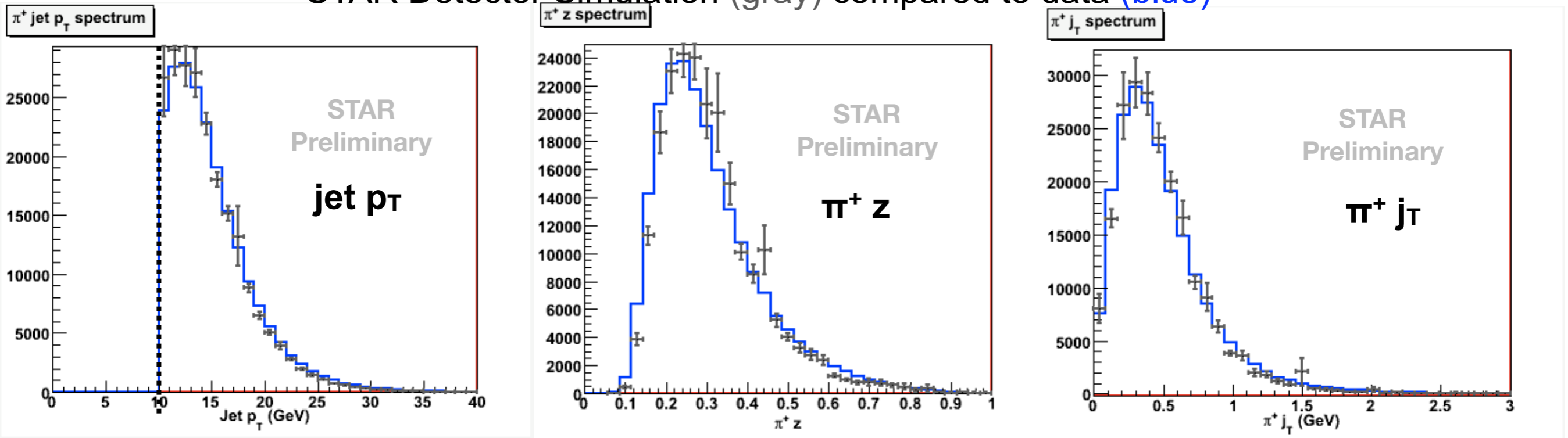


$j_T$ [MC] vs.  $j_T$ [DET] 1:1 ratio line

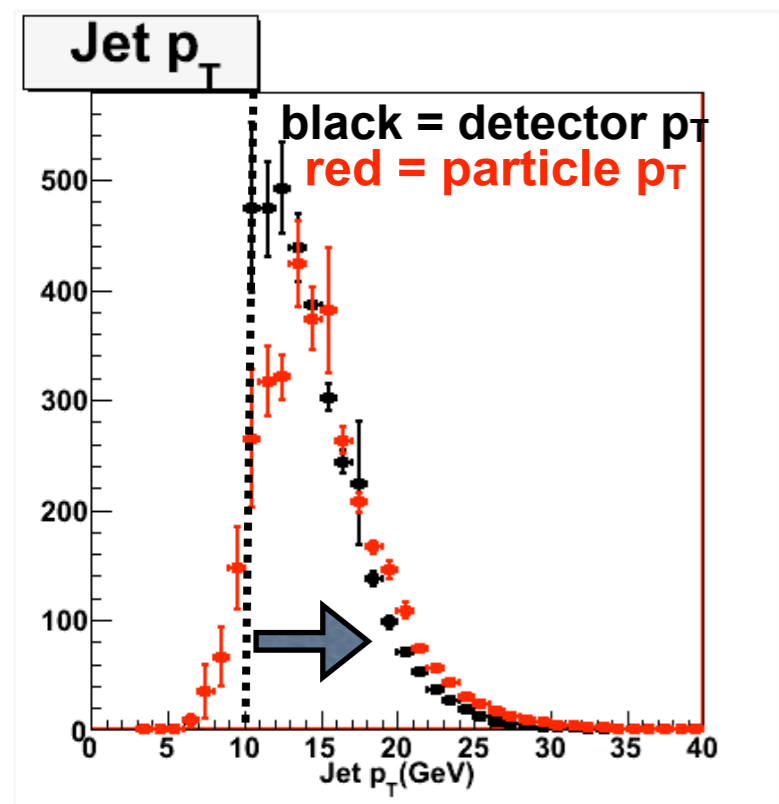


# Simulation Comparison

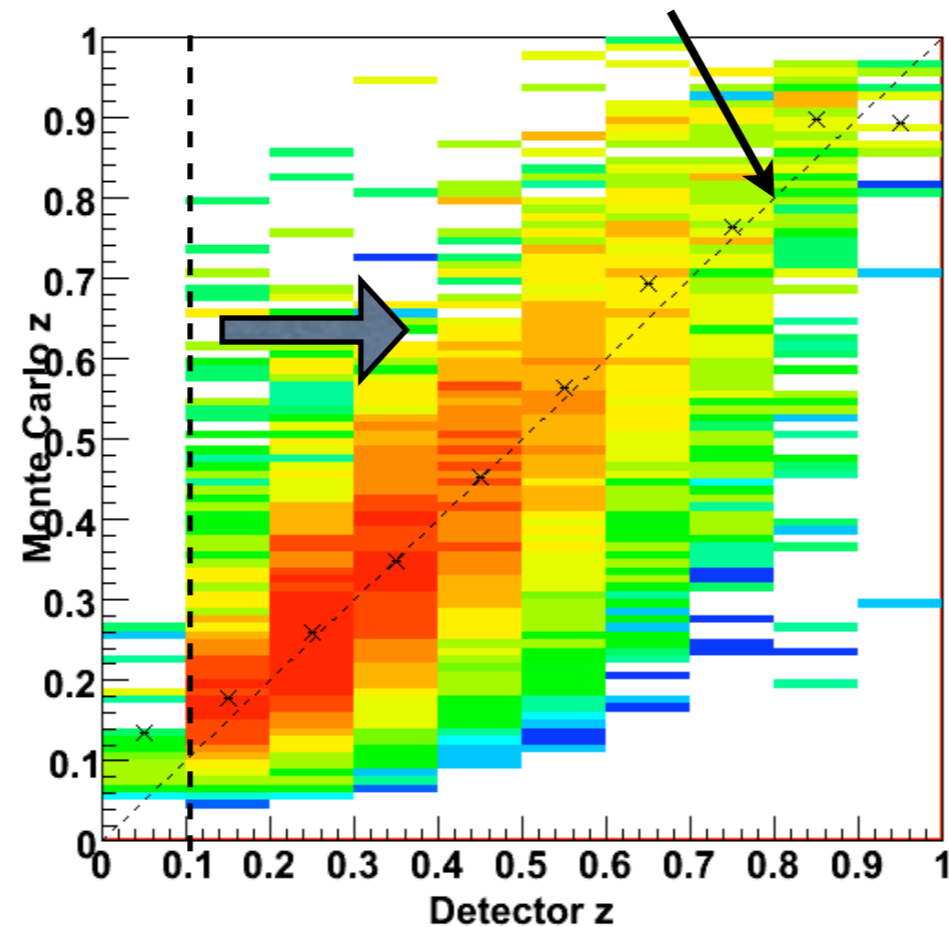
STAR Detector Simulation (gray) compared to data (blue)



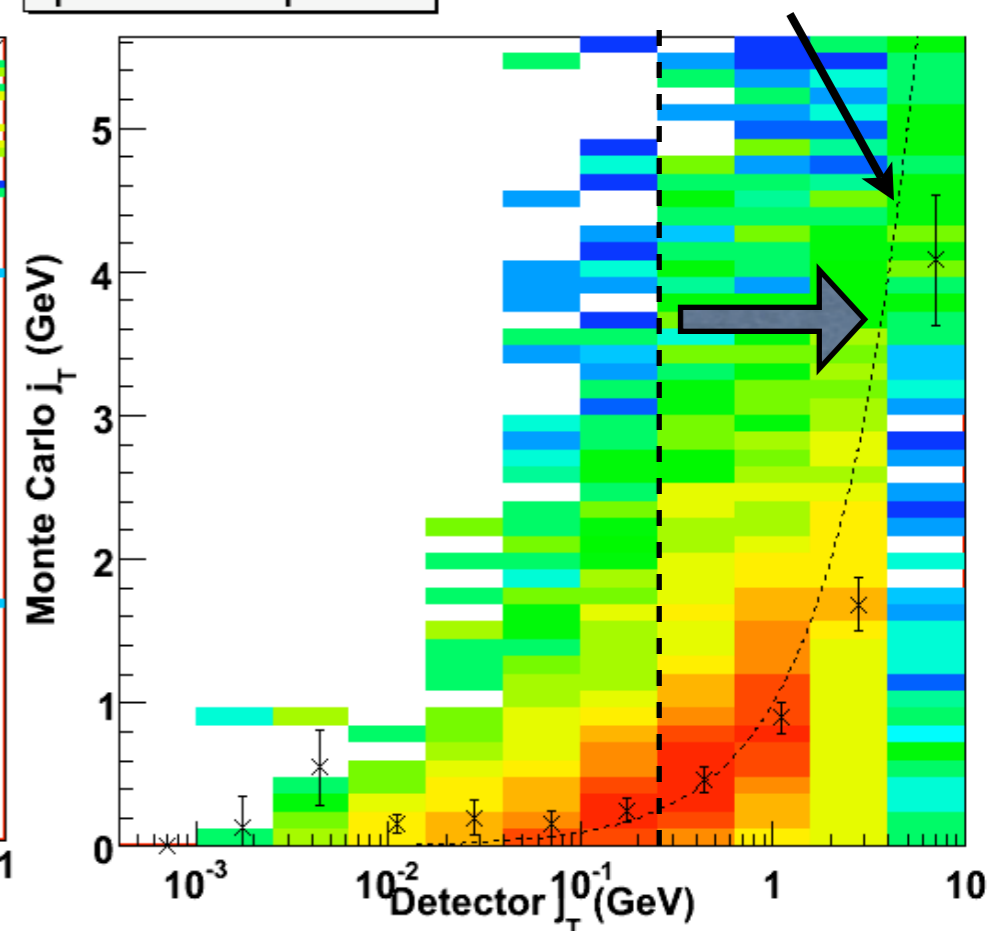
True jet  $p_T$  at particle level  
different than measured



$z$ [MC] vs.  $z$ [DET] 1:1 ratio line

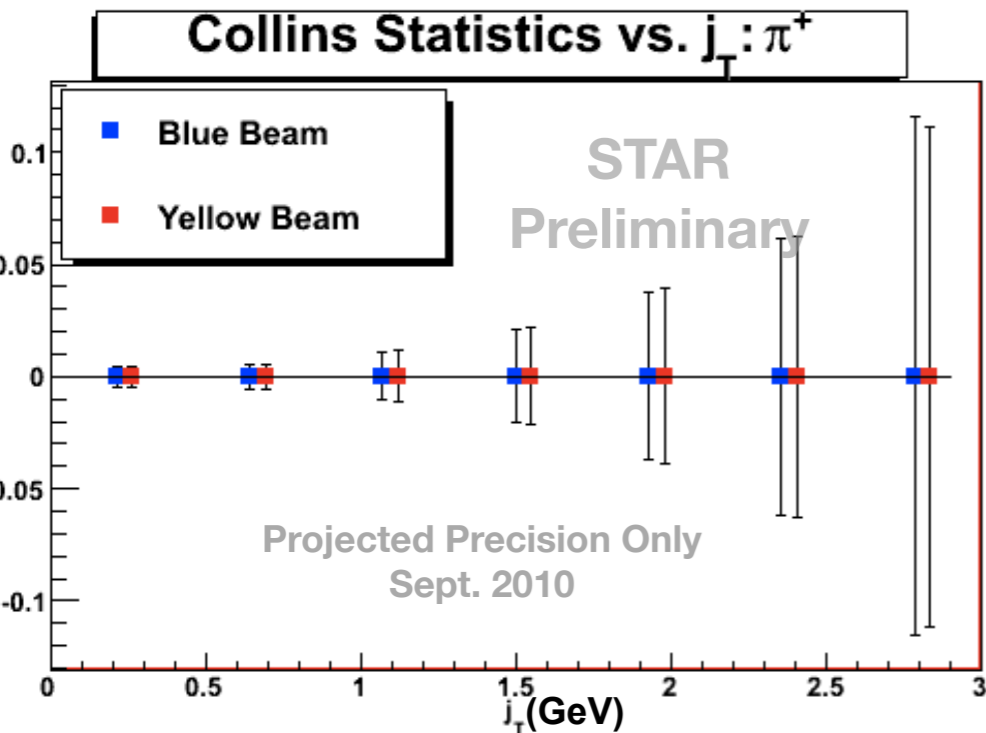
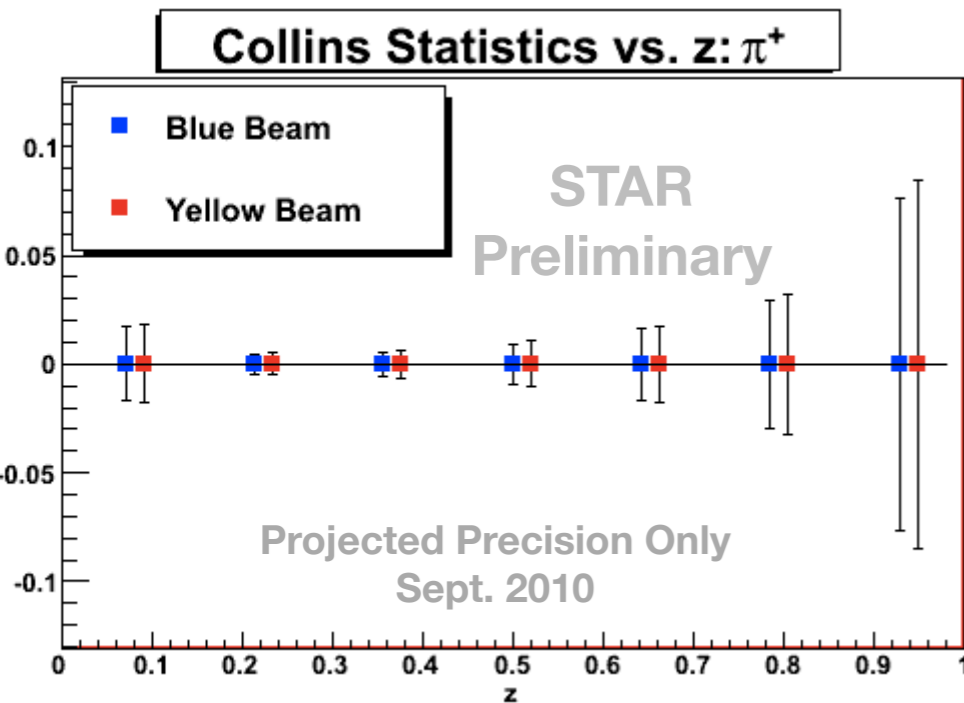


$j_T$ [MC] vs.  $j_T$ [DET] 1:1 ratio line



Limiting Factor in Systematic Error is resolution of  $\phi_h$ ; worst at low  $j_T$

# Conclusion

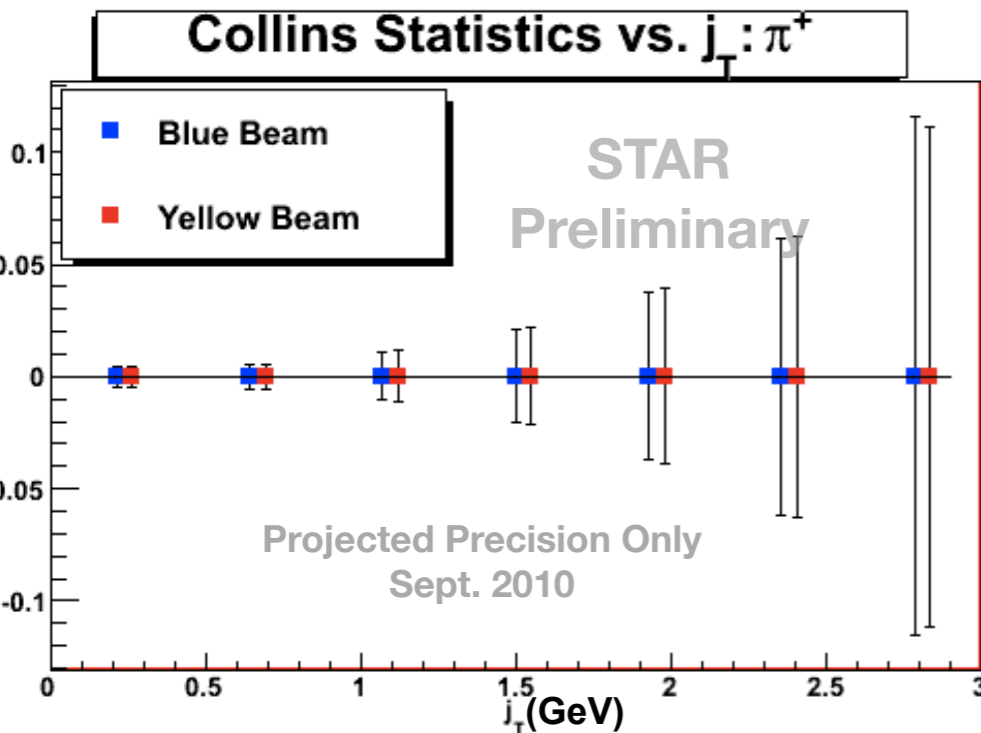
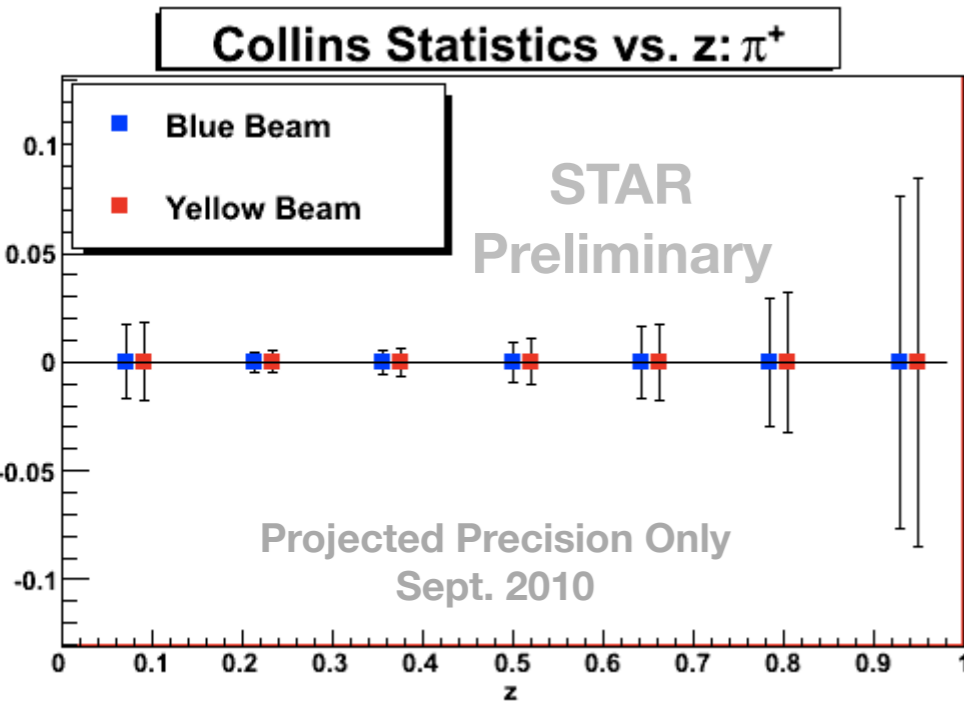


**Similar statistics  
available for  $\pi^-$**

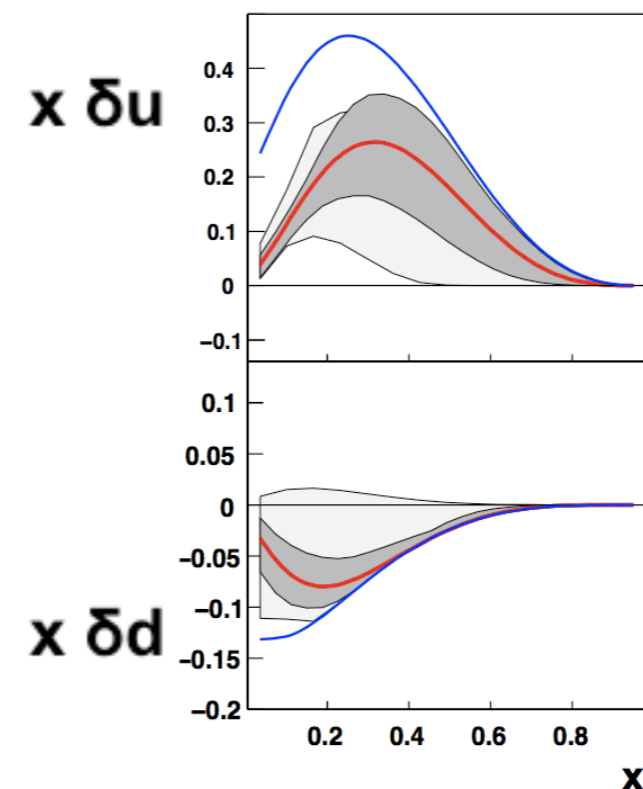
# Conclusion

## Review of Abstract

Valence quark transverse spin distributions ( $\delta u(x, Q^2)$  and  $\delta d(x, Q^2)$ ) in the proton are not well-constrained by experimental data due to the limited amount of transverse data available to separate Collins and Sivers effects. Data from the expanded Forward Pion Detector (FPD++) and the Forward Meson Spectrometer (FMS) at high pseudorapidity ( $2.0 < |\eta| < 4.0$ ), in the Solenoidal Tracker at RHIC (STAR), enable reconstruction of “jet-like events” and  $\pi^0$  mesons in polarized  $p \uparrow p \rightarrow \text{jet}(\pi^0) + X$  reactions. Measurement of the azimuthal distribution of  $\pi^0$  mesons in left-right scattering asymmetries allows separation of the Collins contribution from the analyzing power  $A_N$ . Extension of this concept to midrapidity ( $|\eta| < 1.0$ ) jets in STAR allows measurement of the Collins effect for  $\pi^\pm$ , as well. Progress toward the extraction of these azimuthally asymmetric distributions with respect to the jet momentum axis for  $\langle x \rangle \sim 0.2$  will be shown.



Similar statistics available for  $\pi^-$

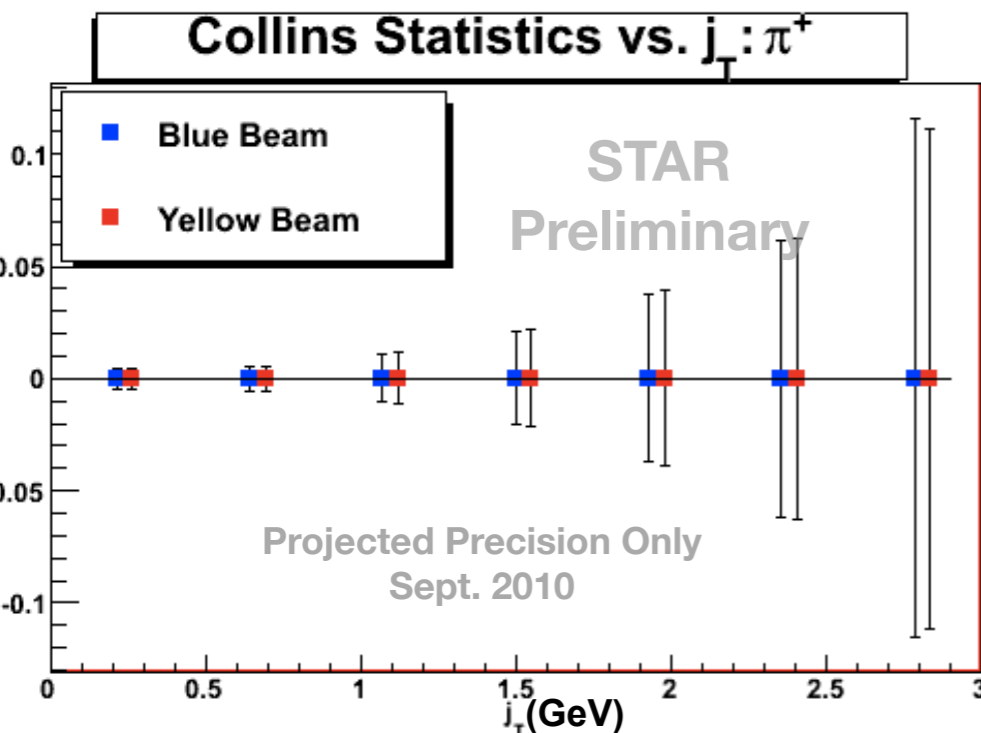
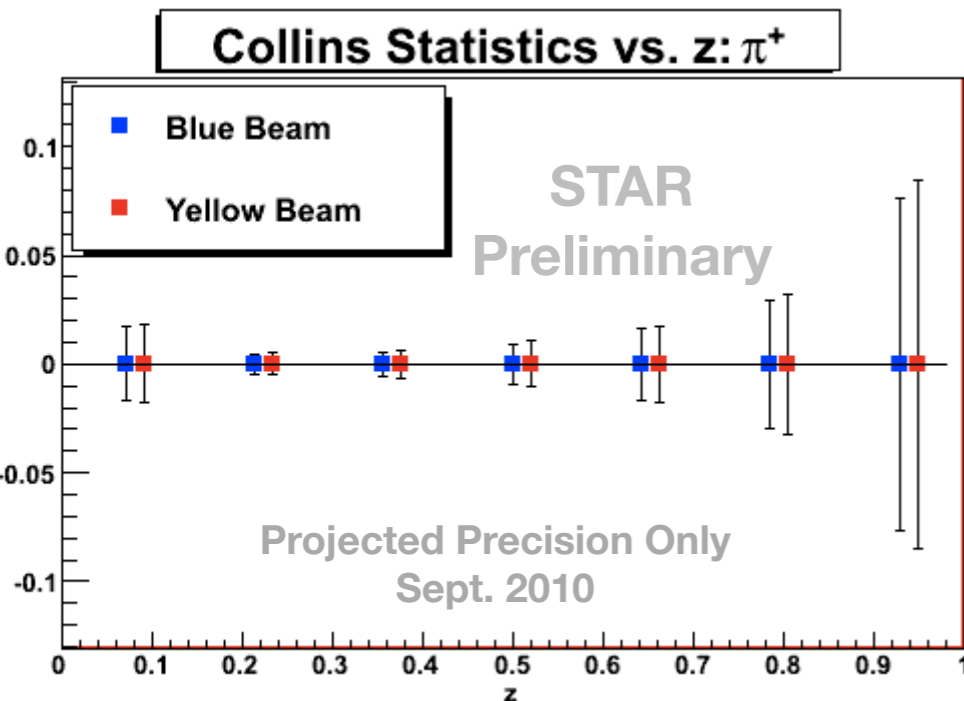


# Conclusion

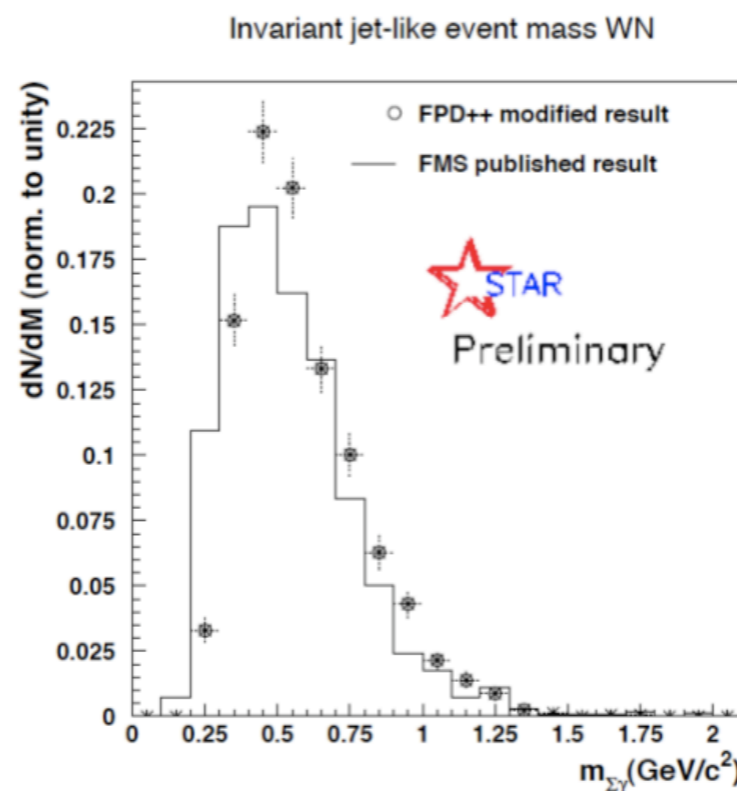
## Review of Abstract

Valence quark transverse spin distributions ( $\delta u(x, Q^2)$  and  $\delta d(x, Q^2)$ ) in the proton are not well-constrained by experimental data due to the limited amount of transverse data available to separate Collins and Sivers effects. Data from the expanded Forward Pion Detector (FPD++) and the Forward Meson Spectrometer (FMS) at high pseudorapidity ( $2.0 < |\eta| < 4.0$ ), in the Solenoidal Tracker at RHIC (STAR), enable reconstruction of “jet-like events” and  $\pi^0$  mesons in polarized  $p \uparrow p \rightarrow \text{jet}(\pi^0) + X$  reactions.

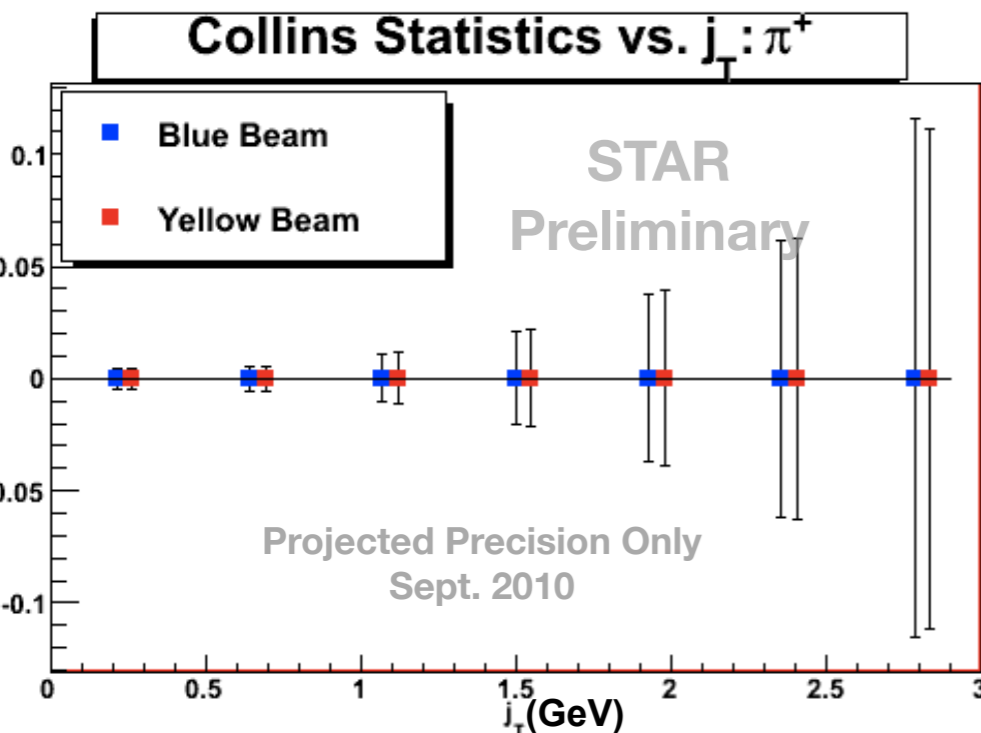
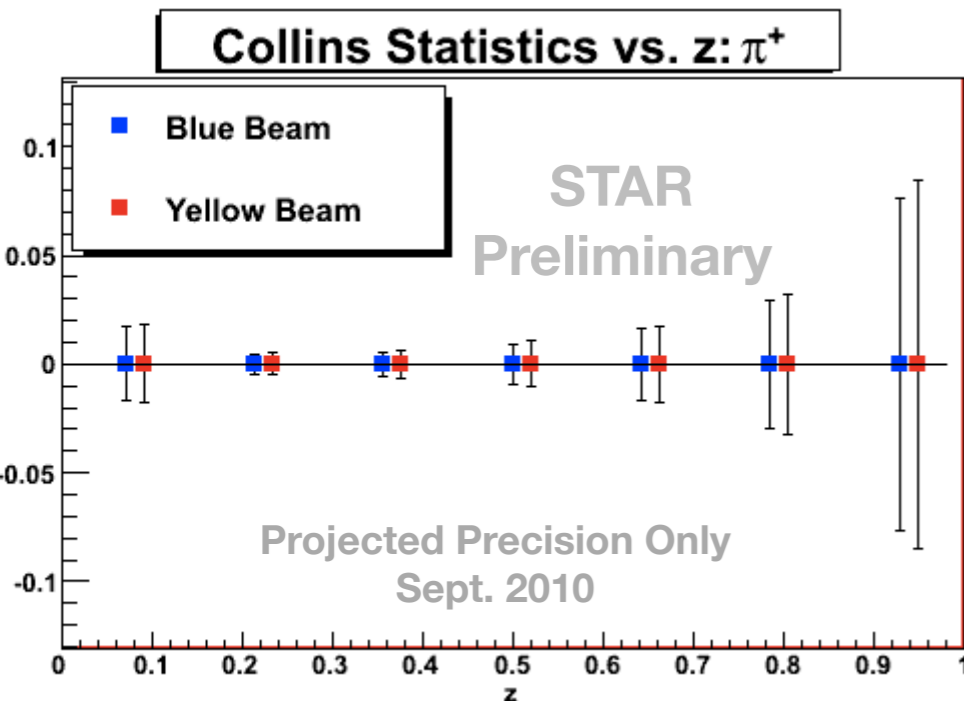
Measurement of the azimuthal distribution of  $\pi^0$  mesons in left-right scattering asymmetries allows separation of the Collins contribution from the analyzing power  $A_N$ . Extension of this concept to midrapidity ( $|\eta| < 1.0$ ) jets in STAR allows measurement of the Collins effect for  $\pi^\pm$ , as well. Progress toward the extraction of these azimuthally asymmetric distributions with respect to the jet momentum axis for  $\langle x \rangle \sim 0.2$  will be shown.



**Similar statistics available for  $\pi^-$**



# Conclusion

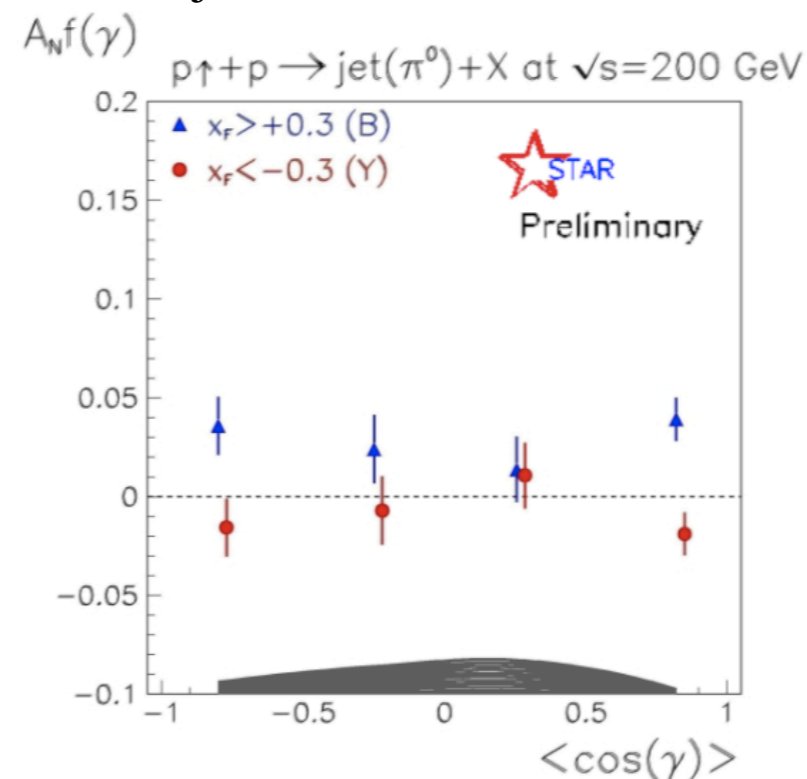


**Similar statistics available for  $\pi^-$**

## Review of Abstract

Valence quark transverse spin distributions ( $\delta u(x, Q^2)$  and  $\delta d(x, Q^2)$ ) in the proton are not well-constrained by experimental data due to the limited amount of transverse data available to separate Collins and Sivers effects. Data from the expanded Forward Pion Detector (FPD++) and the Forward Meson Spectrometer (FMS) at high pseudorapidity ( $2.0 < |\eta| < 4.0$ ), in the Solenoidal Tracker at RHIC (STAR), enable reconstruction of “jet-like events” and  $\pi^0$  mesons in polarized  $p \uparrow p \rightarrow \text{jet}(\pi^0) + X$  reactions.

Measurement of the azimuthal distribution of  $\pi^0$  mesons in left-right scattering asymmetries allows separation of the Collins contribution from the analyzing power  $A_N$ . Extension of this concept to midrapidity ( $|\eta| < 1.0$ ) jets in STAR allows measurement of the Collins effect for  $\pi^\pm$ , as well. Progress toward the extraction of these azimuthally asymmetric distributions with respect to the jet momentum axis for  $\langle x \rangle \sim 0.2$  will be shown.

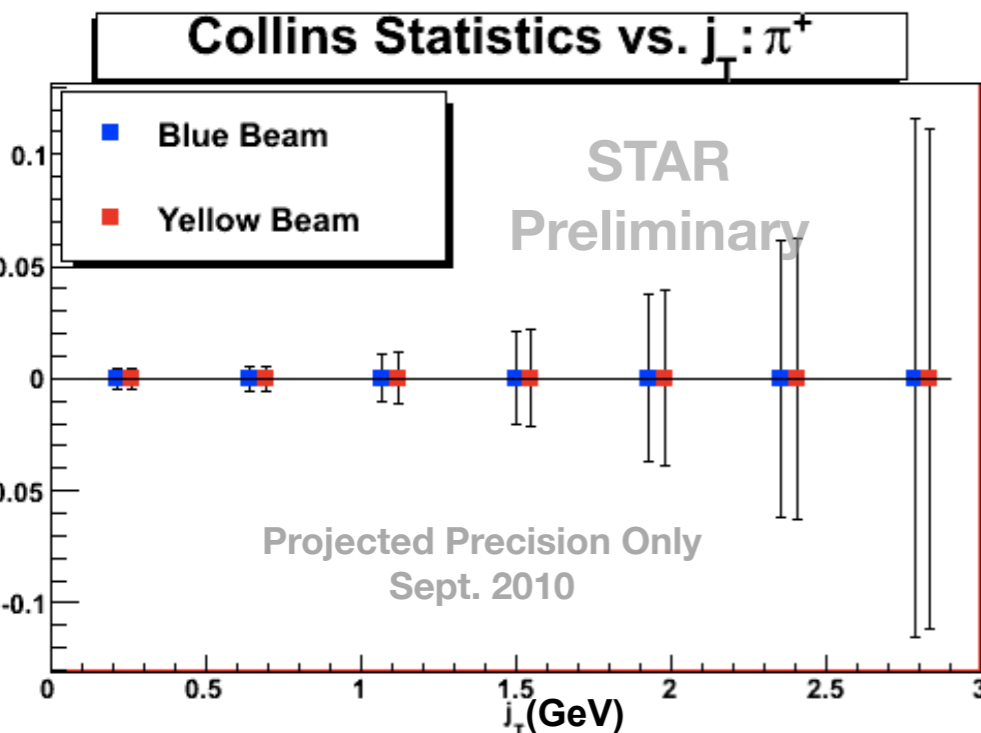
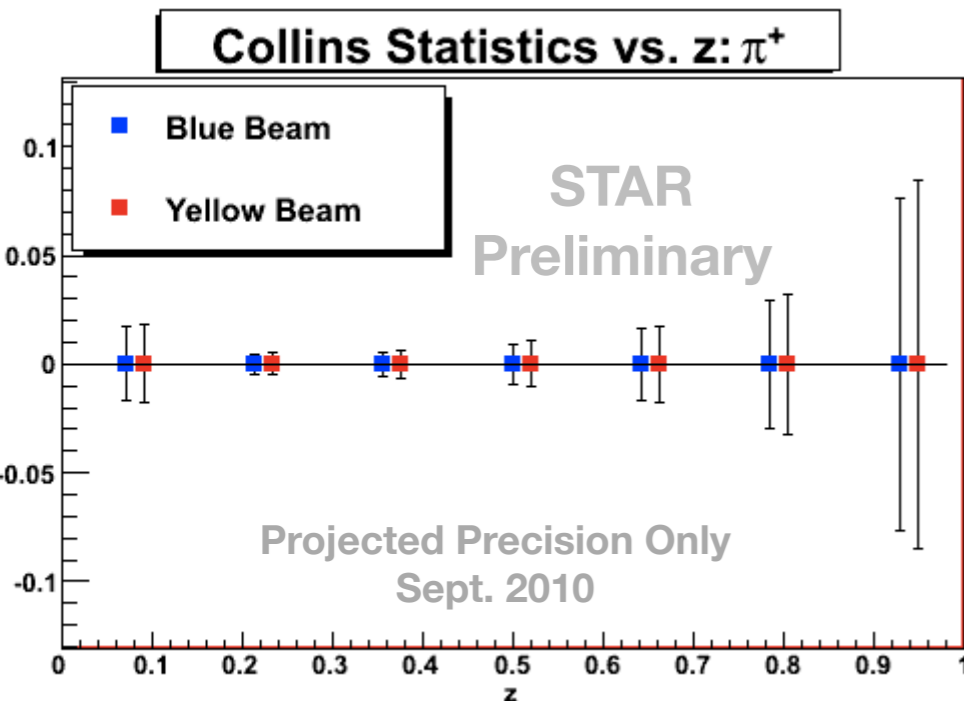


Special Thanks to Nikola Poljak for the  $\pi^0$  results

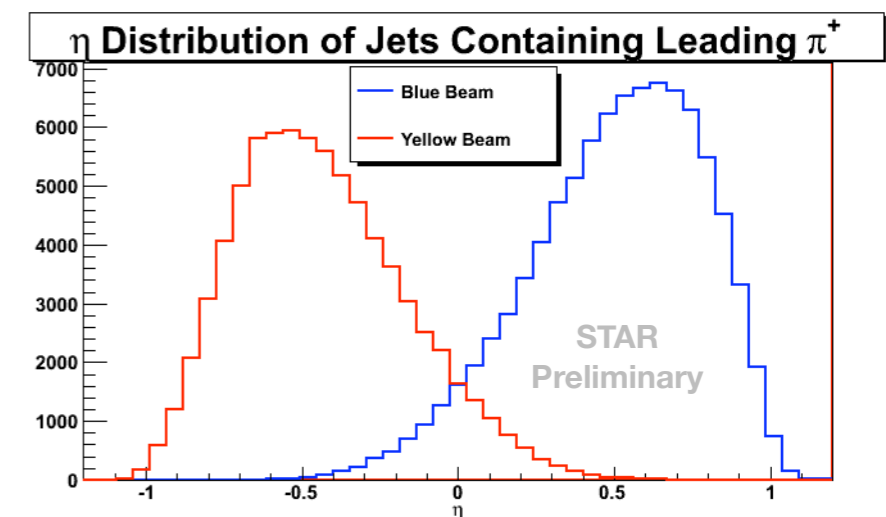
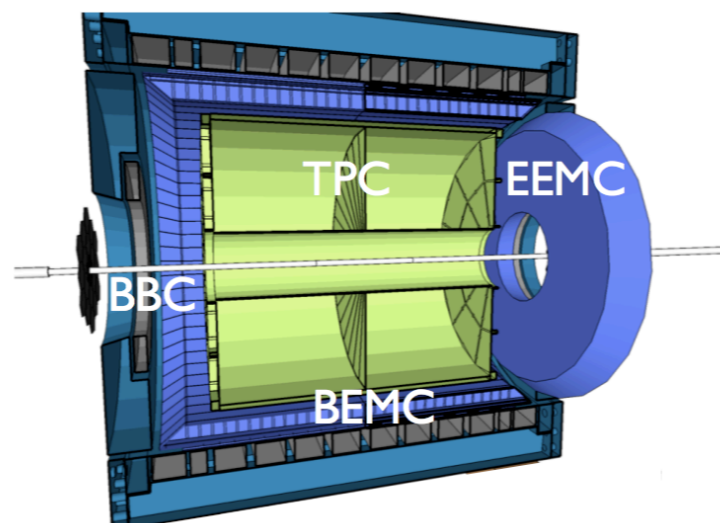
# Conclusion

## Review of Abstract

Valence quark transverse spin distributions ( $\delta u(x, Q^2)$  and  $\delta d(x, Q^2)$ ) in the proton are not well-constrained by experimental data due to the limited amount of transverse data available to separate Collins and Sivers effects. Data from the expanded Forward Pion Detector (FPD++) and the Forward Meson Spectrometer (FMS) at high pseudorapidity ( $2.0 < |\eta| < 4.0$ ), in the Solenoidal Tracker at RHIC (STAR), enable reconstruction of “jet-like events” and  $\pi^0$  mesons in polarized  $p \uparrow p \rightarrow \text{jet}(\pi^0) + X$  reactions. Measurement of the azimuthal distribution of  $\pi^0$  mesons in left-right scattering asymmetries allows separation of the Collins contribution from the analyzing power  $A_N$ . Extension of this concept to midrapidity ( $|\eta| < 1.0$ ) jets in STAR allows measurement of the Collins effect for  $\pi^\pm$ , as well. Progress toward the extraction of these azimuthally asymmetric distributions with respect to the jet momentum axis for  $\langle x \rangle \sim 0.2$  will be shown.



**Similar statistics available for  $\pi^-$**

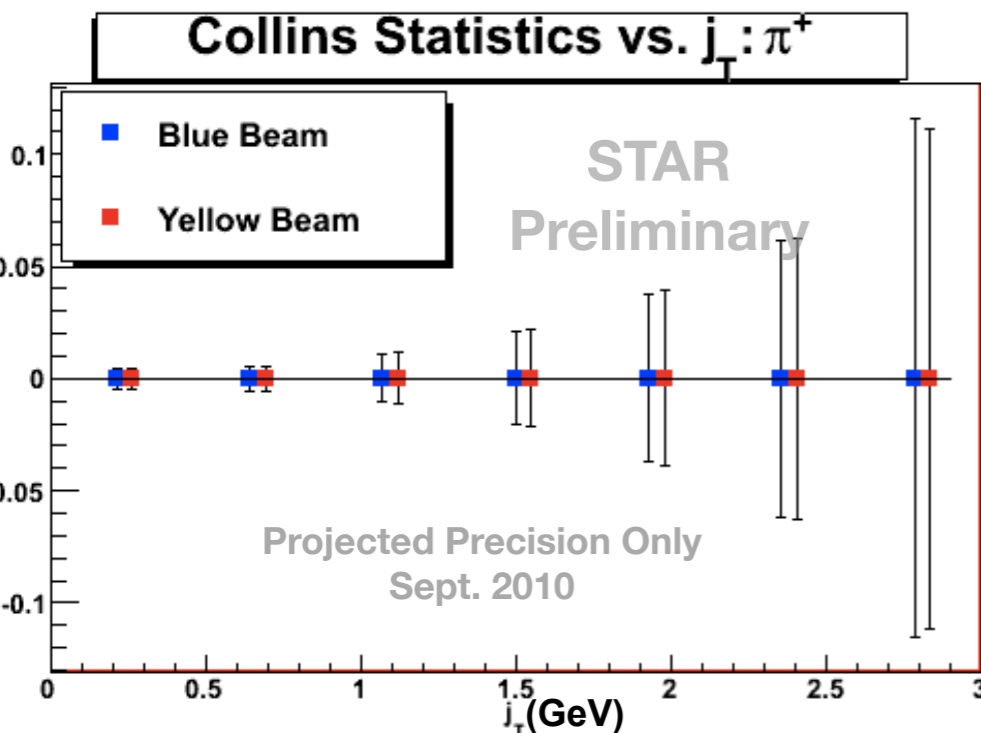
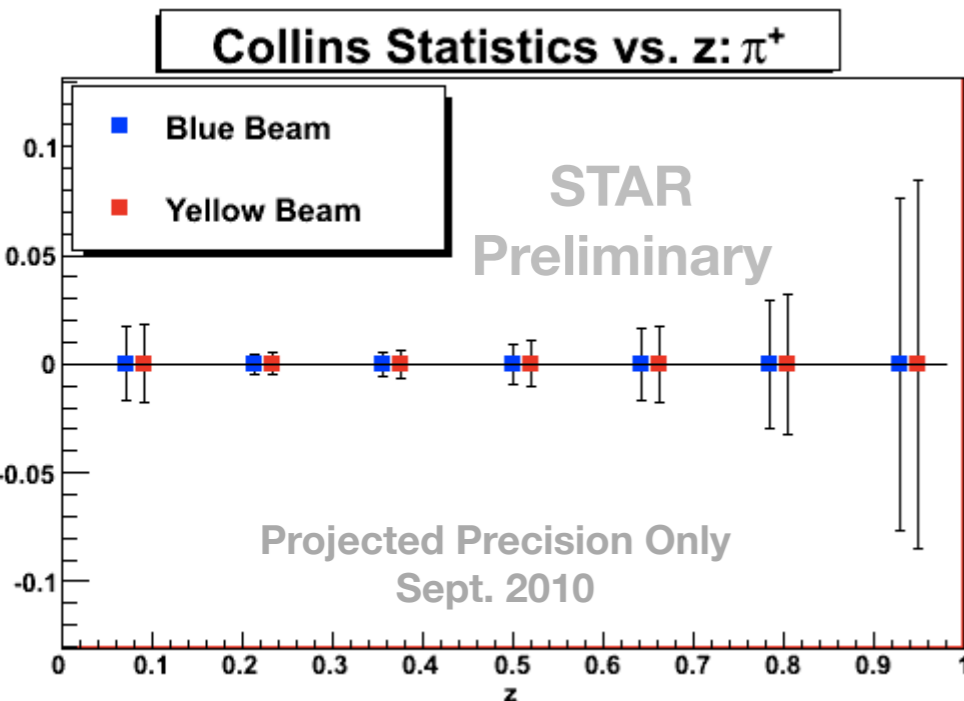


# Conclusion

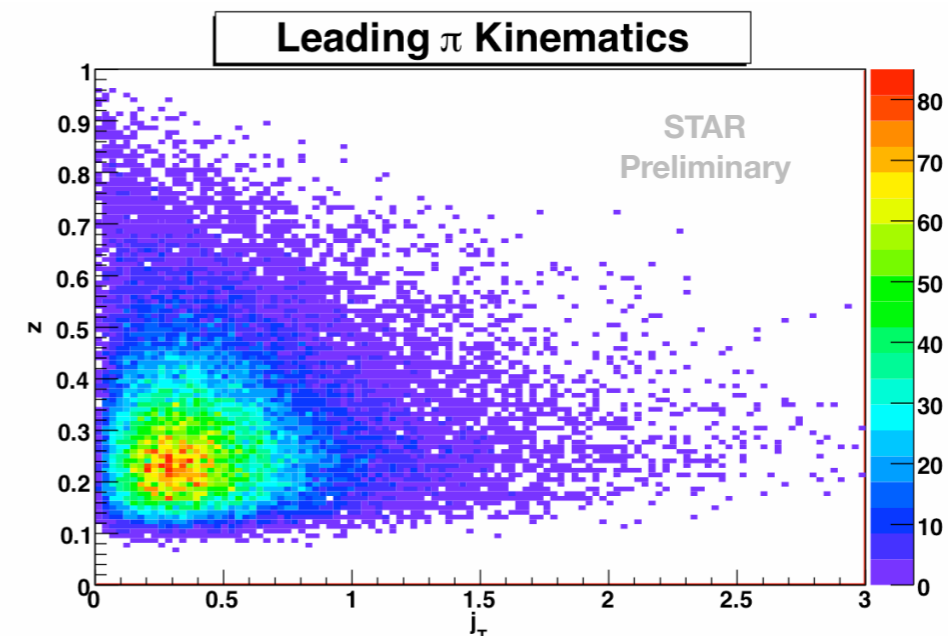
## Review of Abstract

Valence quark transverse spin distributions ( $\delta u(x, Q^2)$  and  $\delta d(x, Q^2)$ ) in the proton are not well-constrained by experimental data due to the limited amount of transverse data available to separate Collins and Sivers effects. Data from the expanded Forward Pion Detector (FPD++) and the Forward Meson Spectrometer (FMS) at high pseudorapidity ( $2.0 < |\eta| < 4.0$ ), in the Solenoidal Tracker at RHIC (STAR), enable reconstruction of “jet-like events” and  $\pi^0$  mesons in polarized  $p \uparrow p \rightarrow \text{jet}(\pi^0) + X$  reactions. Measurement of the azimuthal distribution of  $\pi^0$  mesons in left-right scattering asymmetries allows separation of the Collins contribution from the analyzing power  $A_N$ . Extension of this concept to midrapidity ( $|\eta| < 1.0$ ) jets in STAR allows measurement of the Collins effect for  $\pi^\pm$ , as well.

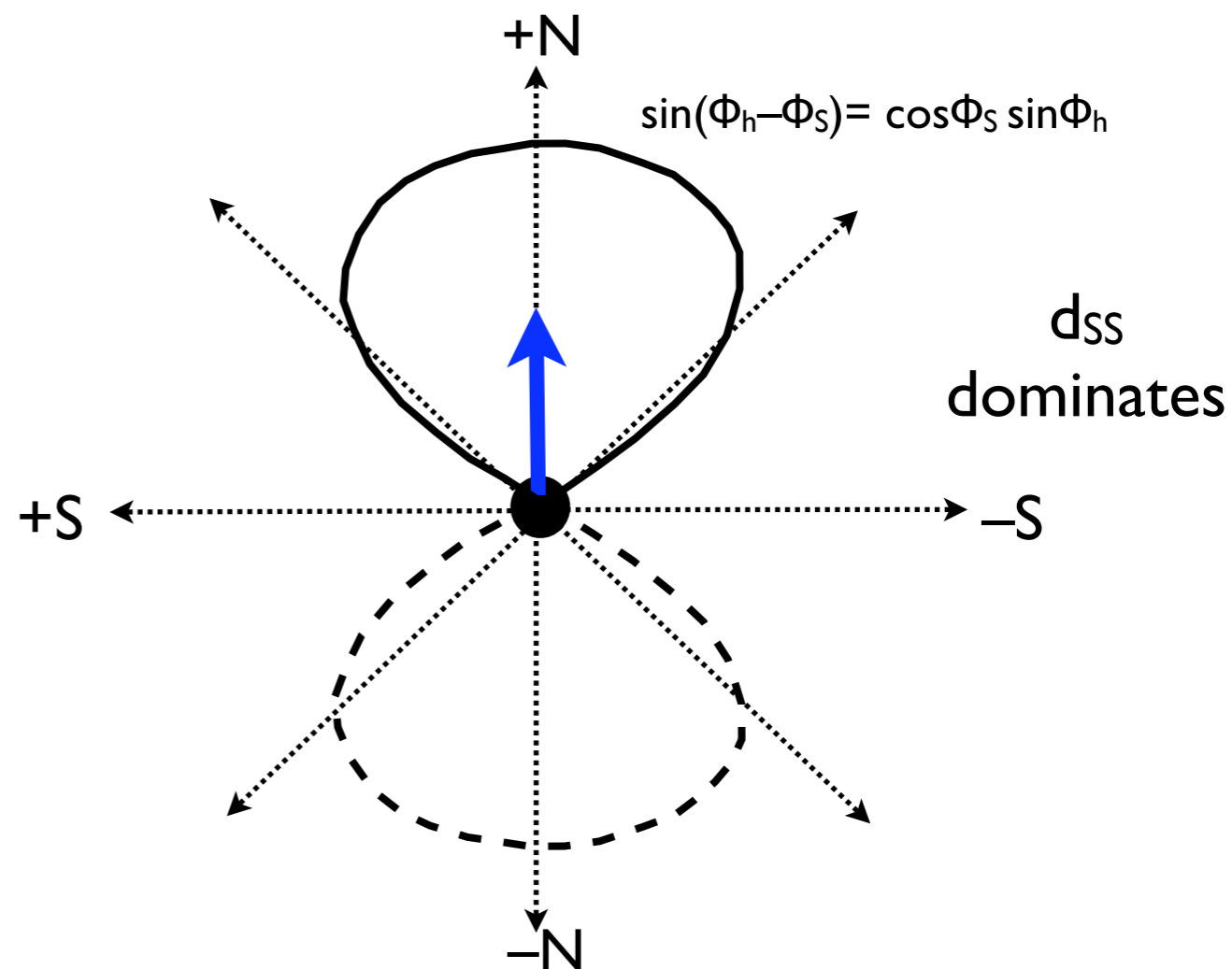
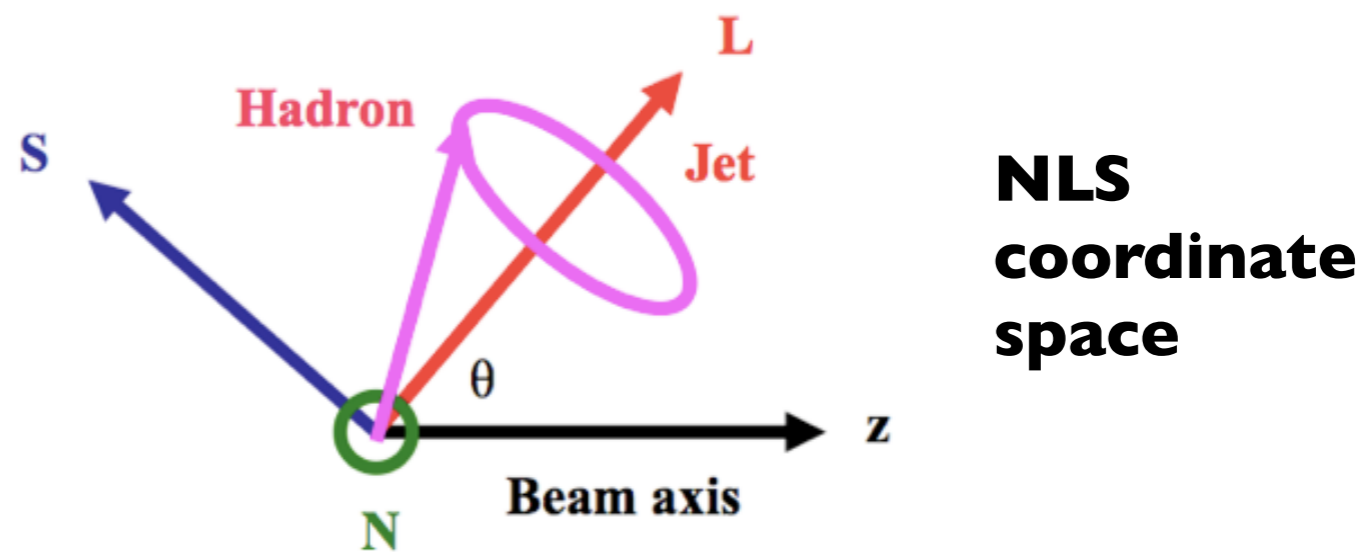
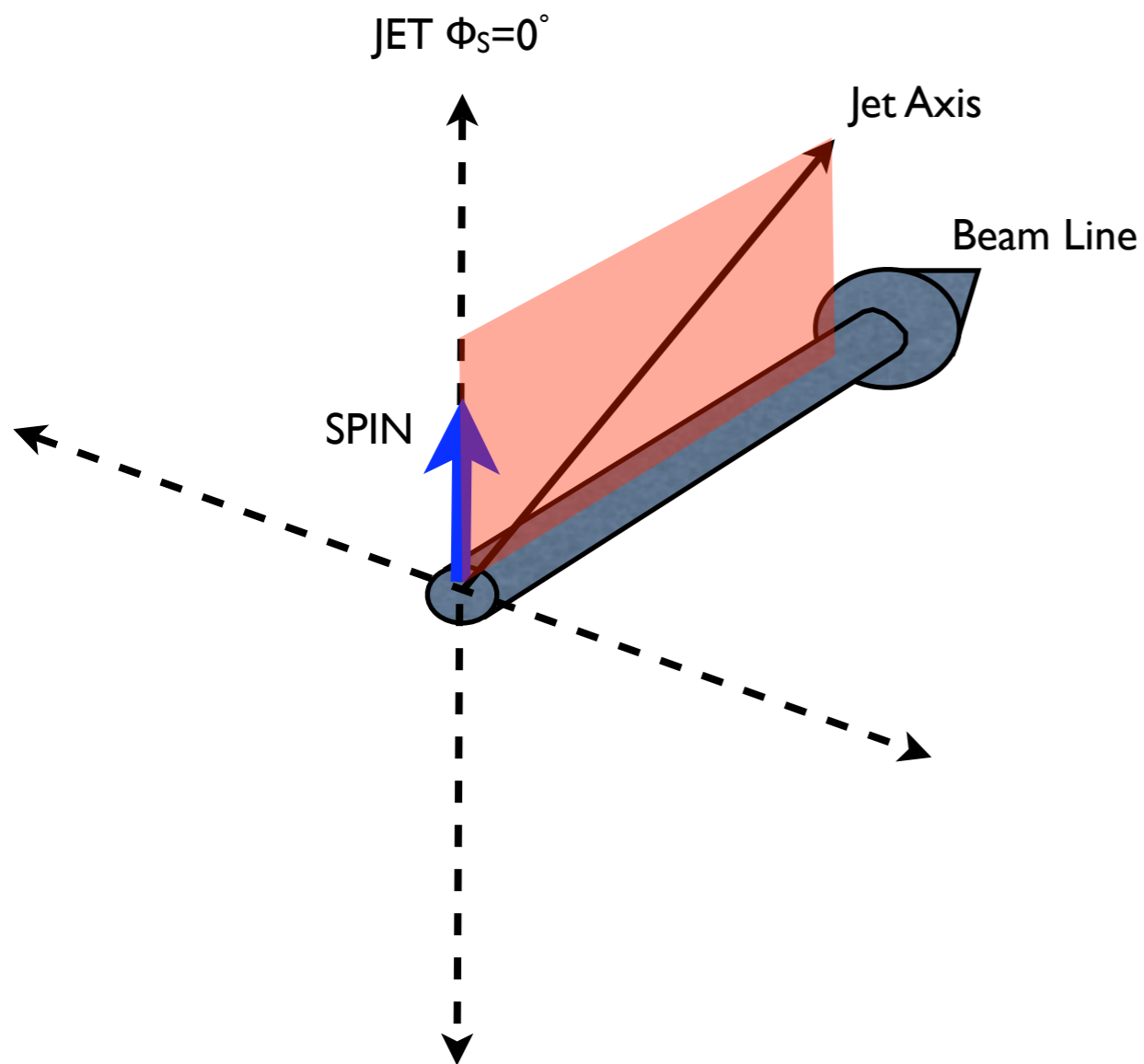
Progress toward the extraction of these azimuthally asymmetric distributions with respect to the jet momentum axis for  $\langle x \rangle \sim 0.2$  will be shown.



**Similar statistics available for  $\pi^-$**

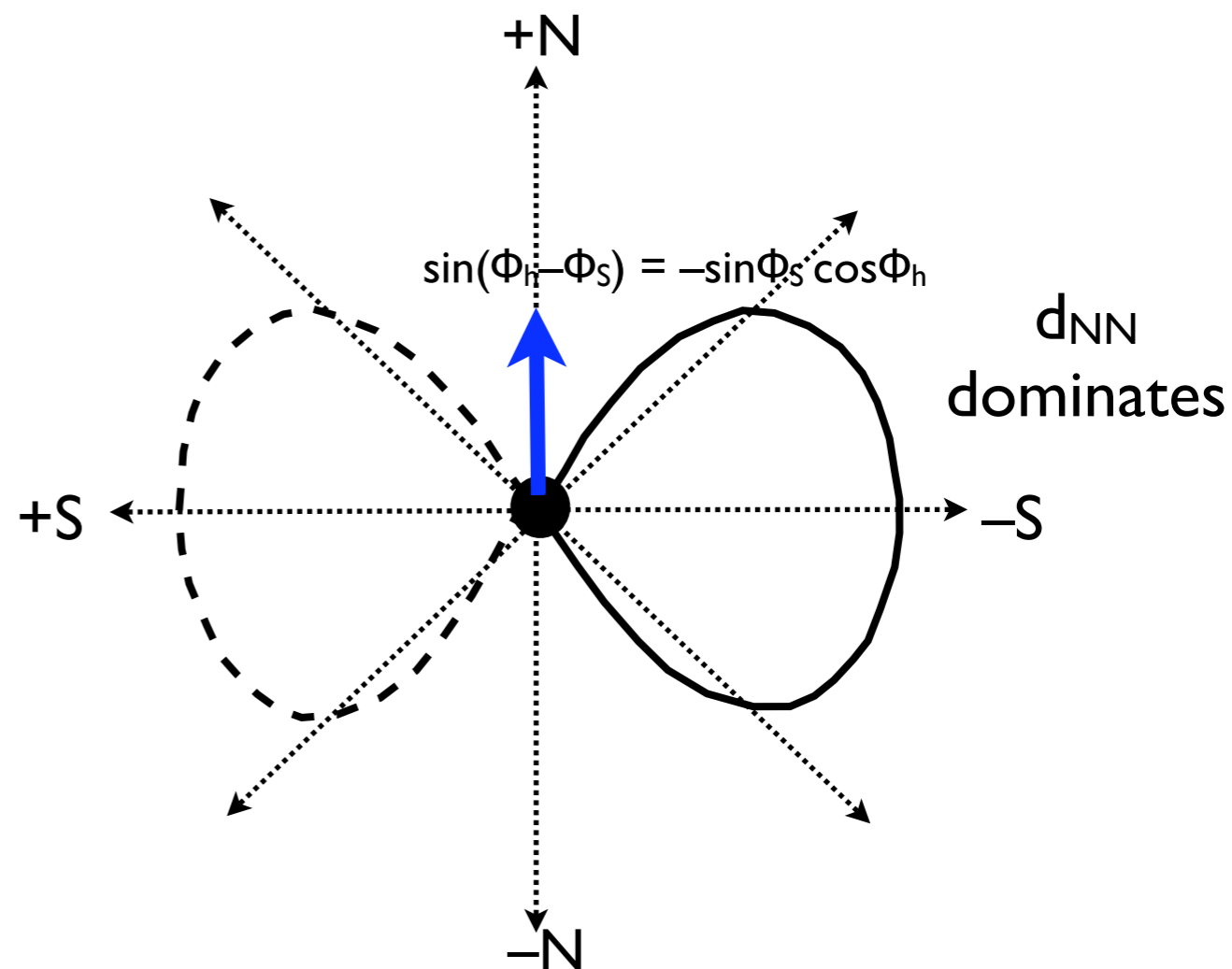
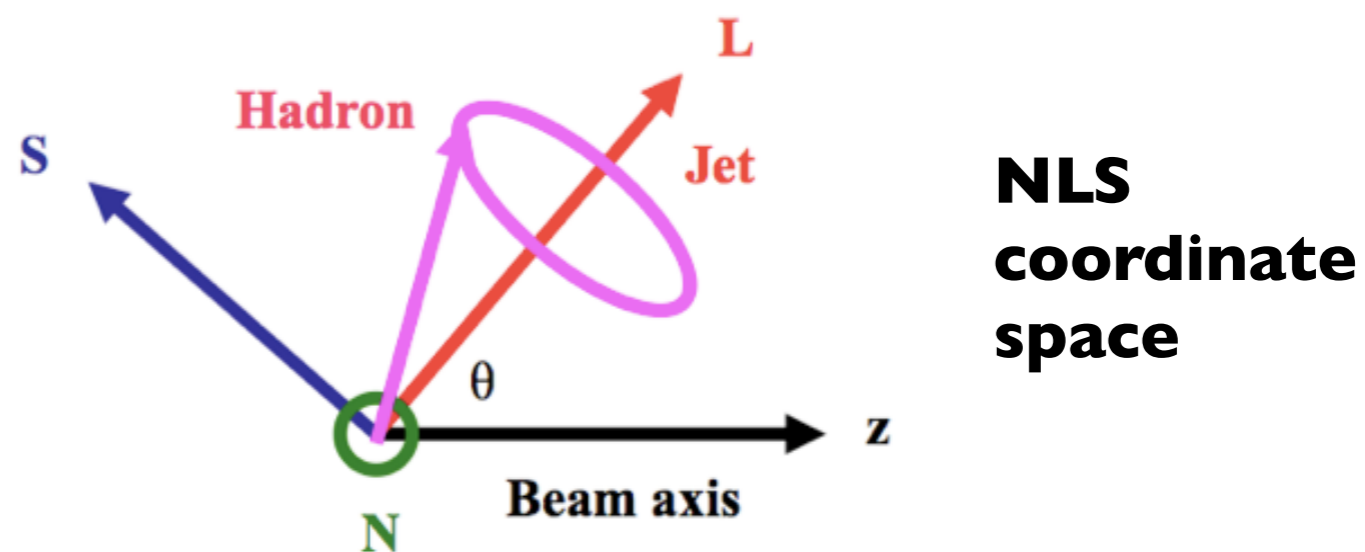
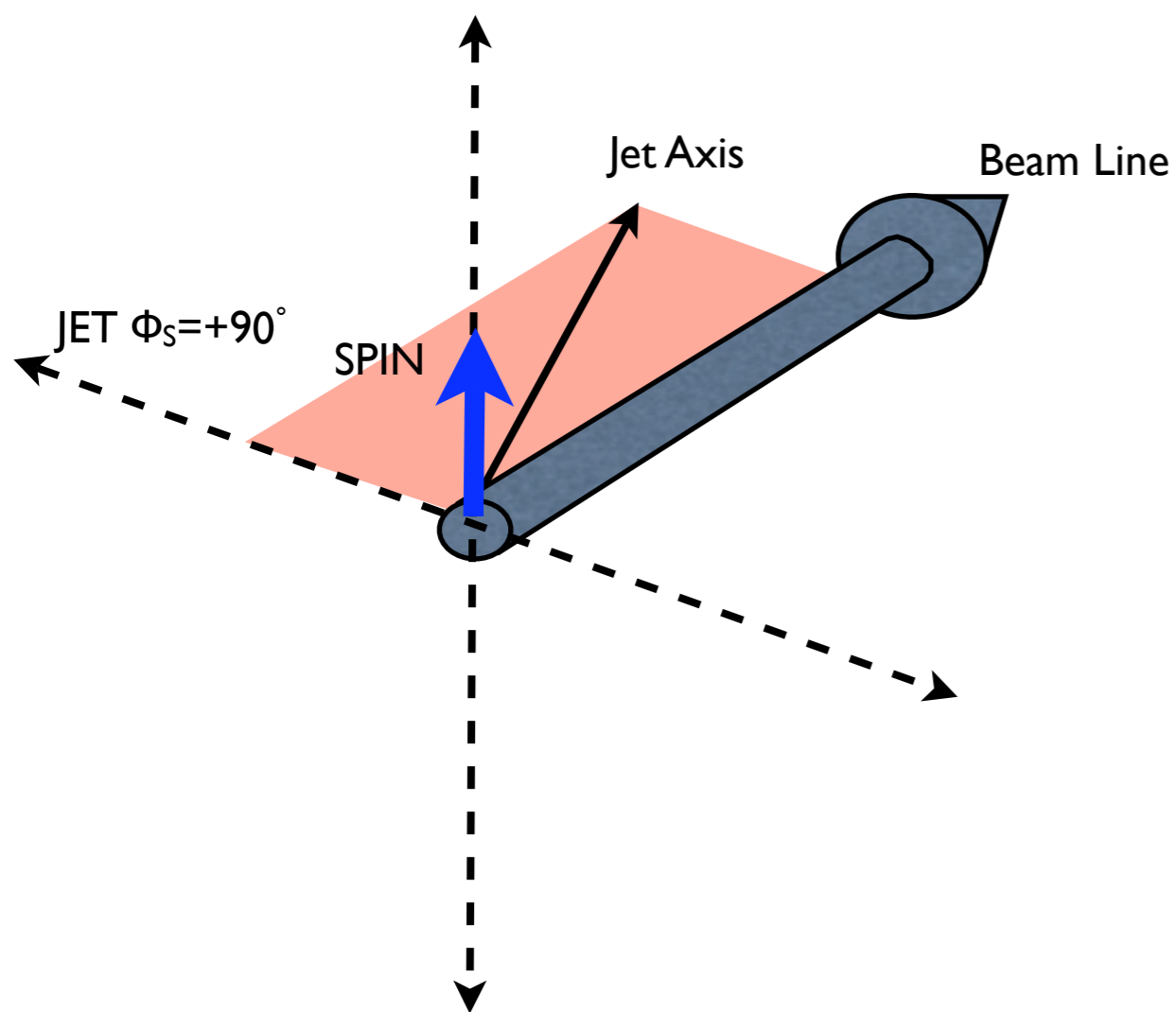


**EXTRA SLIDES:**  
**Demonstration of**  
**Asymmetry at different**  
**angles in the lab frame**

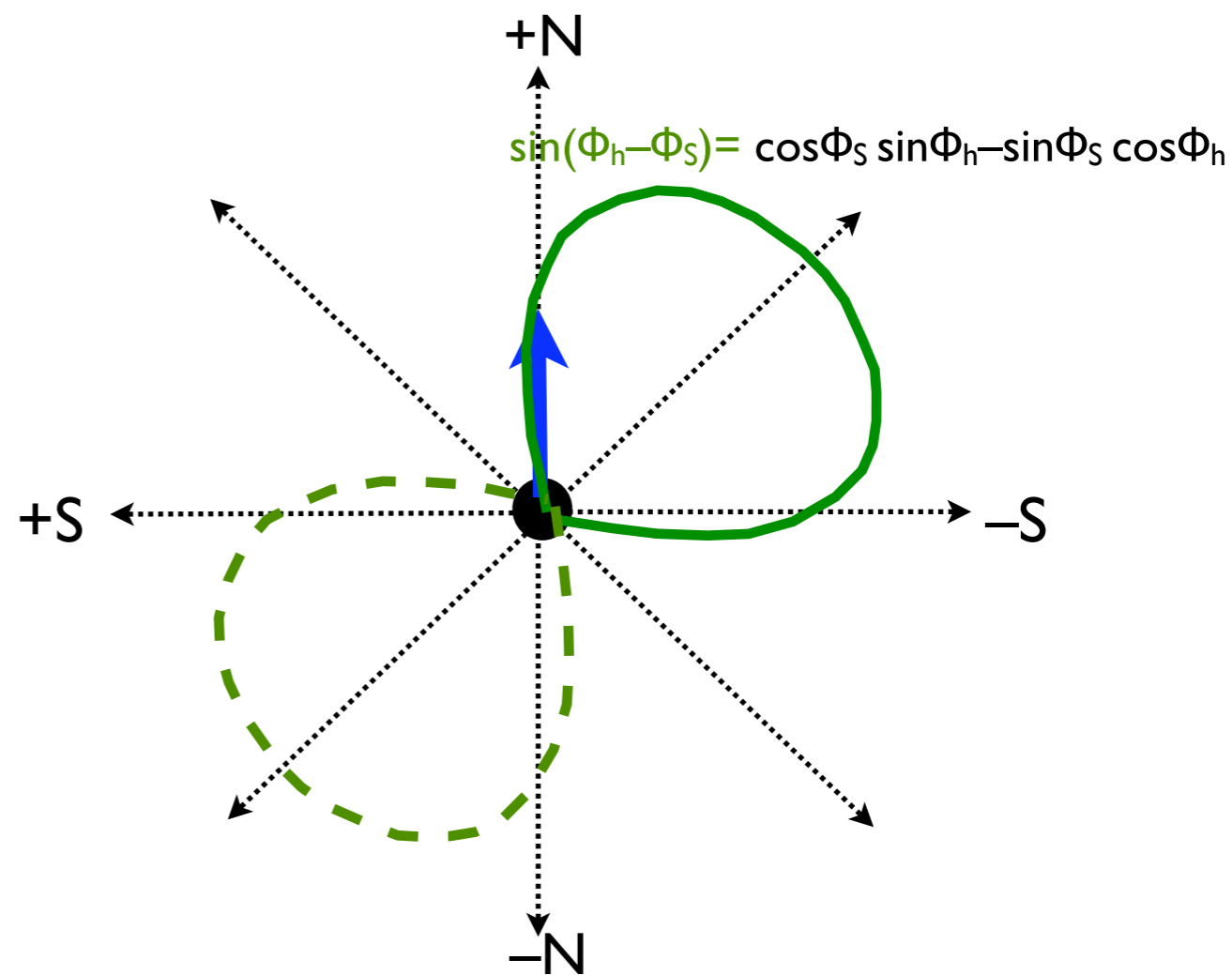
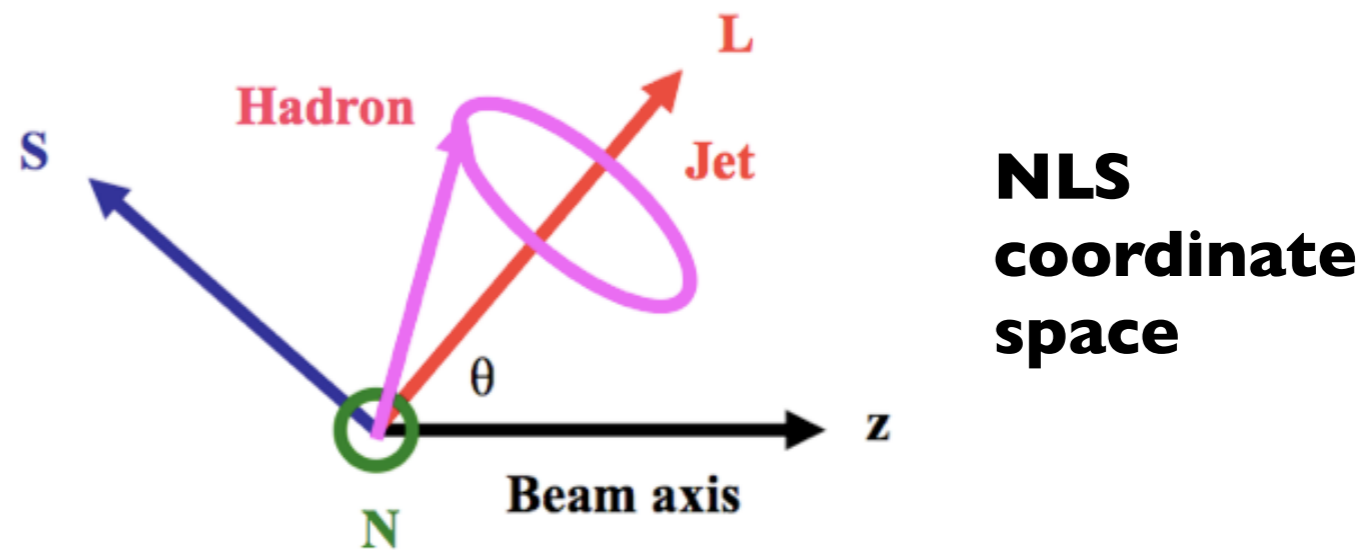
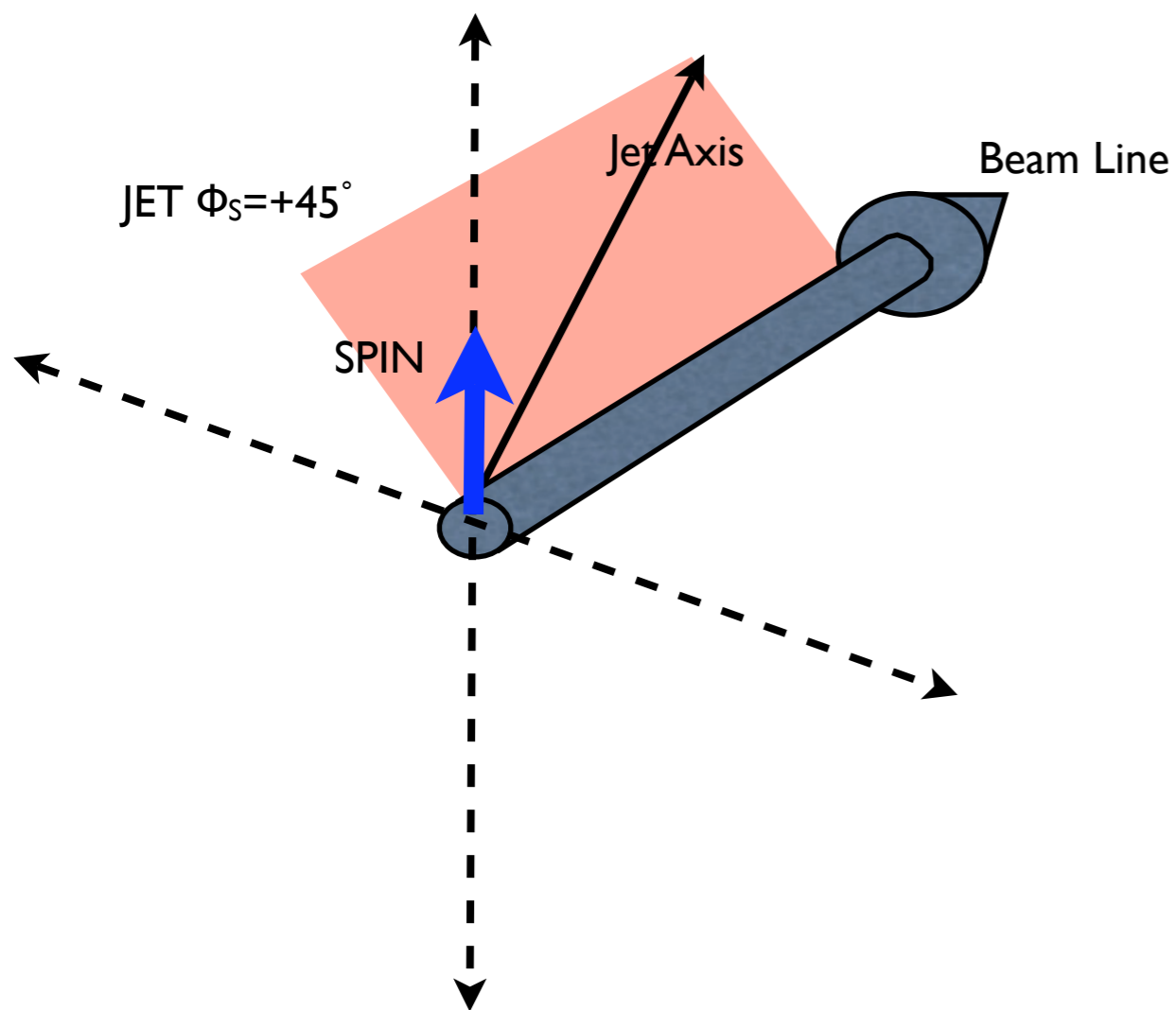


**View looking down jet axis from vertex**

———— = positive values of radial direction of  $\pi$  fragmentation  
 - - - - = negative values of radial direction of  $\pi$  fragmentation

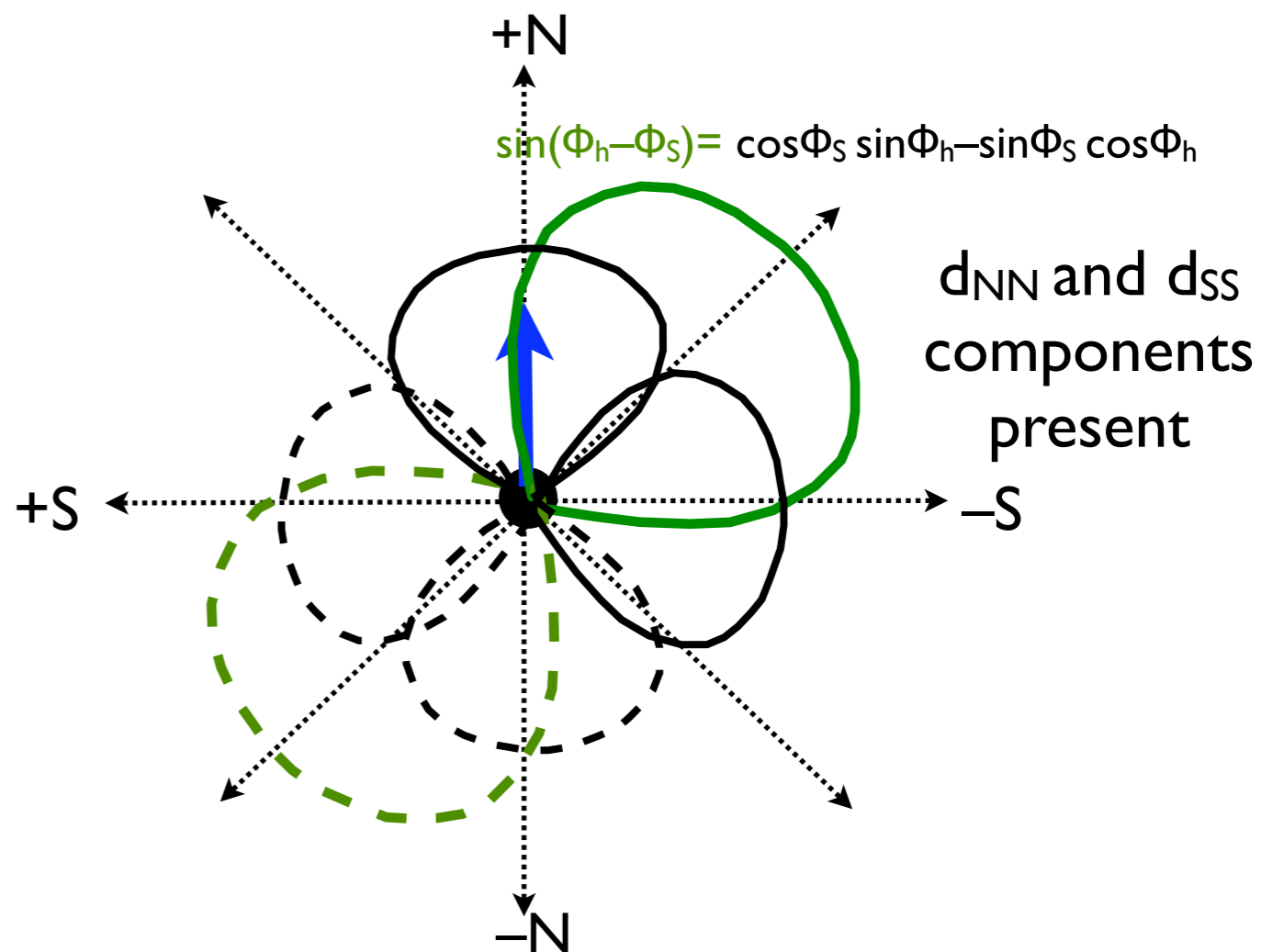
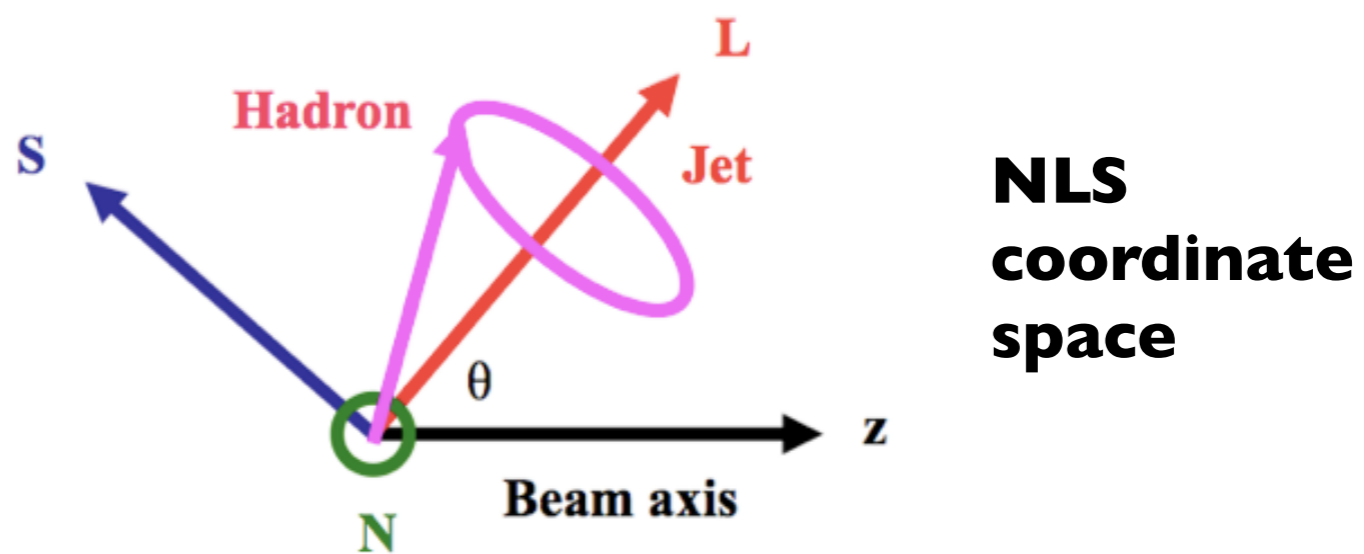
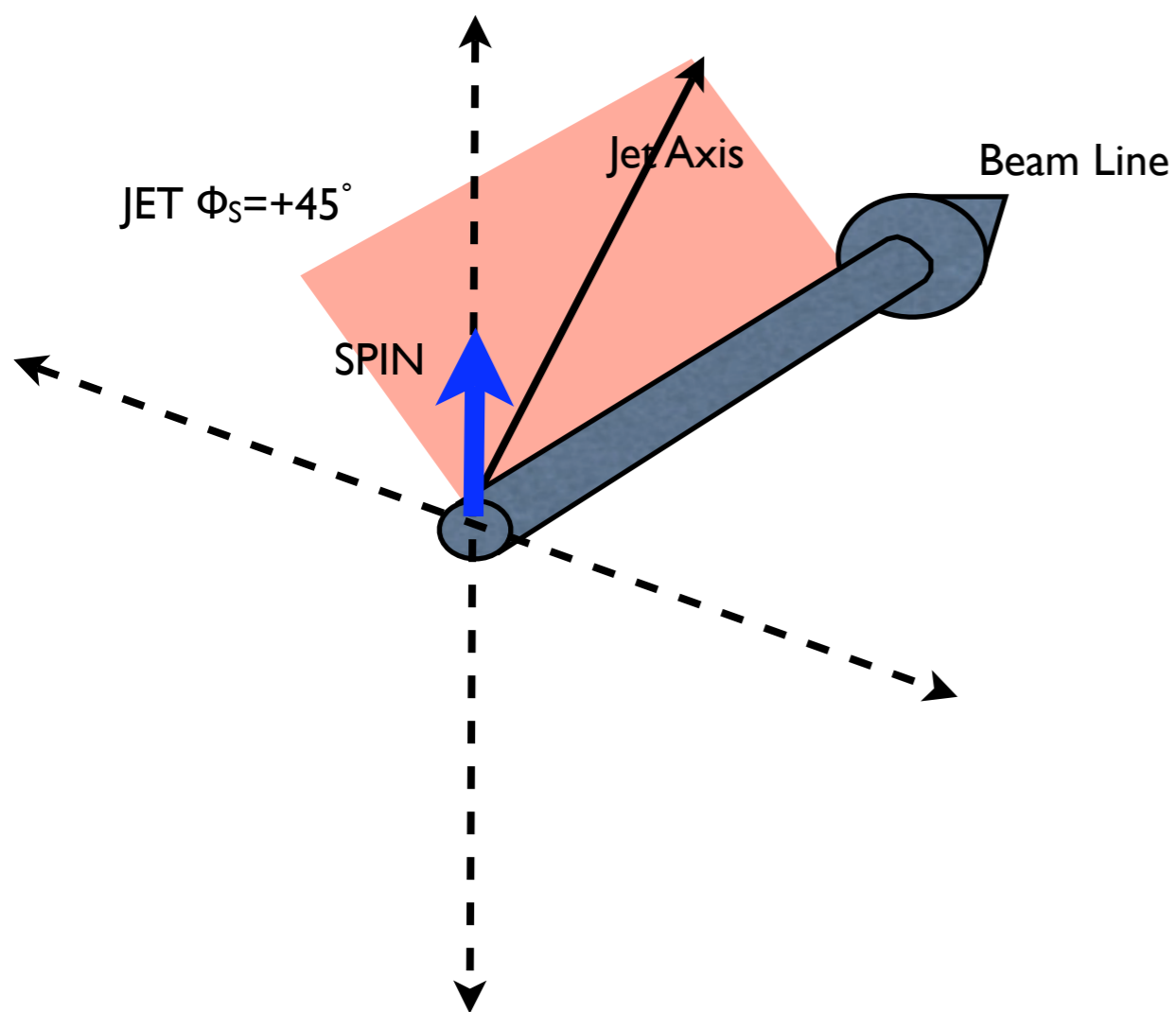


———— = positive values of radial direction of  $\pi$  fragmentation  
 - - - - - = negative values of radial direction of  $\pi$  fragmentation



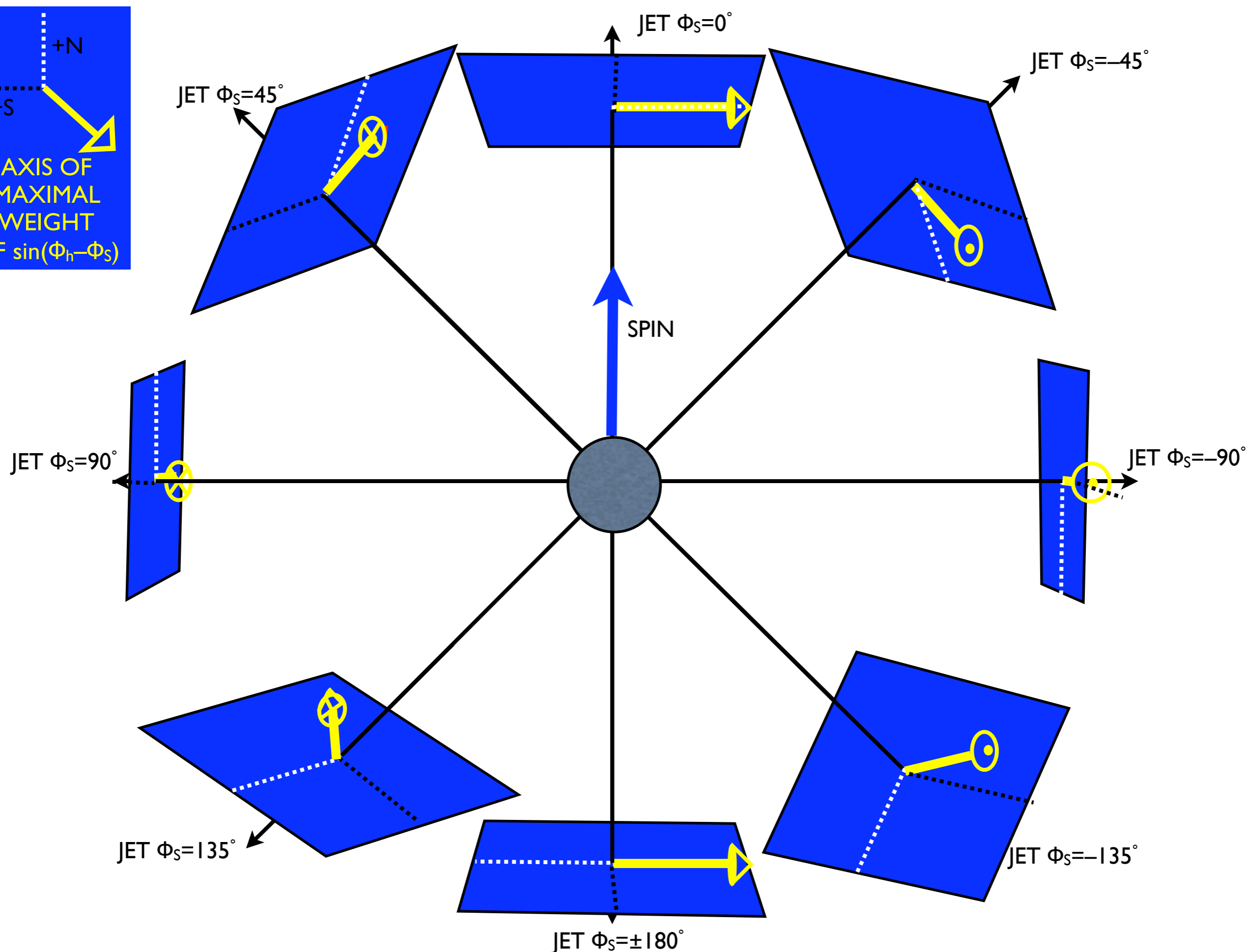
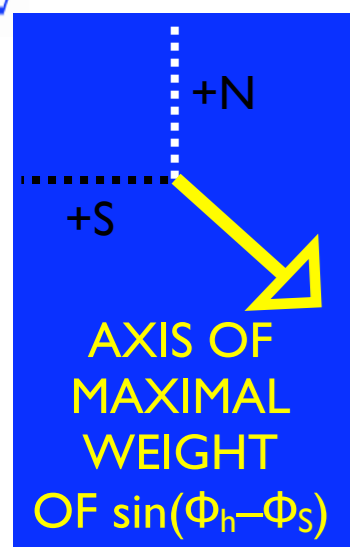
**View looking down jet axis from vertex**

———— = positive values of radial direction of  $\pi$  fragmentation  
 - - - - = negative values of radial direction of  $\pi$  fragmentation



**View looking down jet axis from vertex**

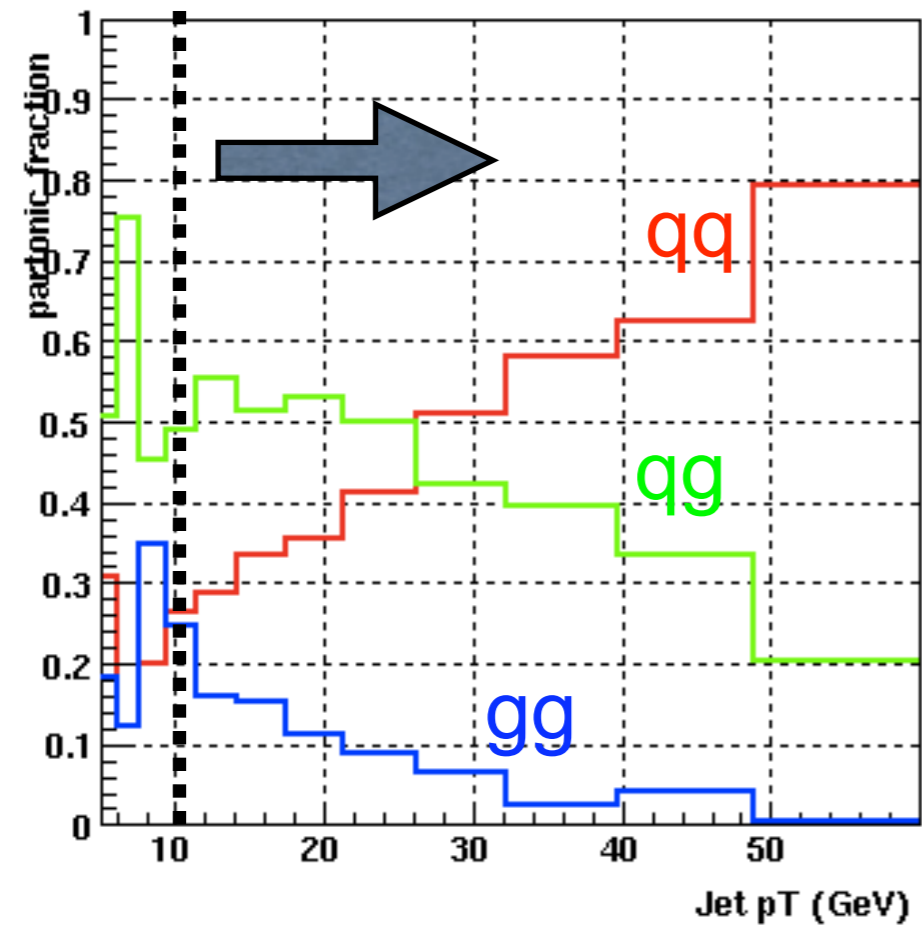
— = positive values of radial direction of  $\pi$  fragmentation  
 - - - - = negative values of radial direction of  $\pi$  fragmentation



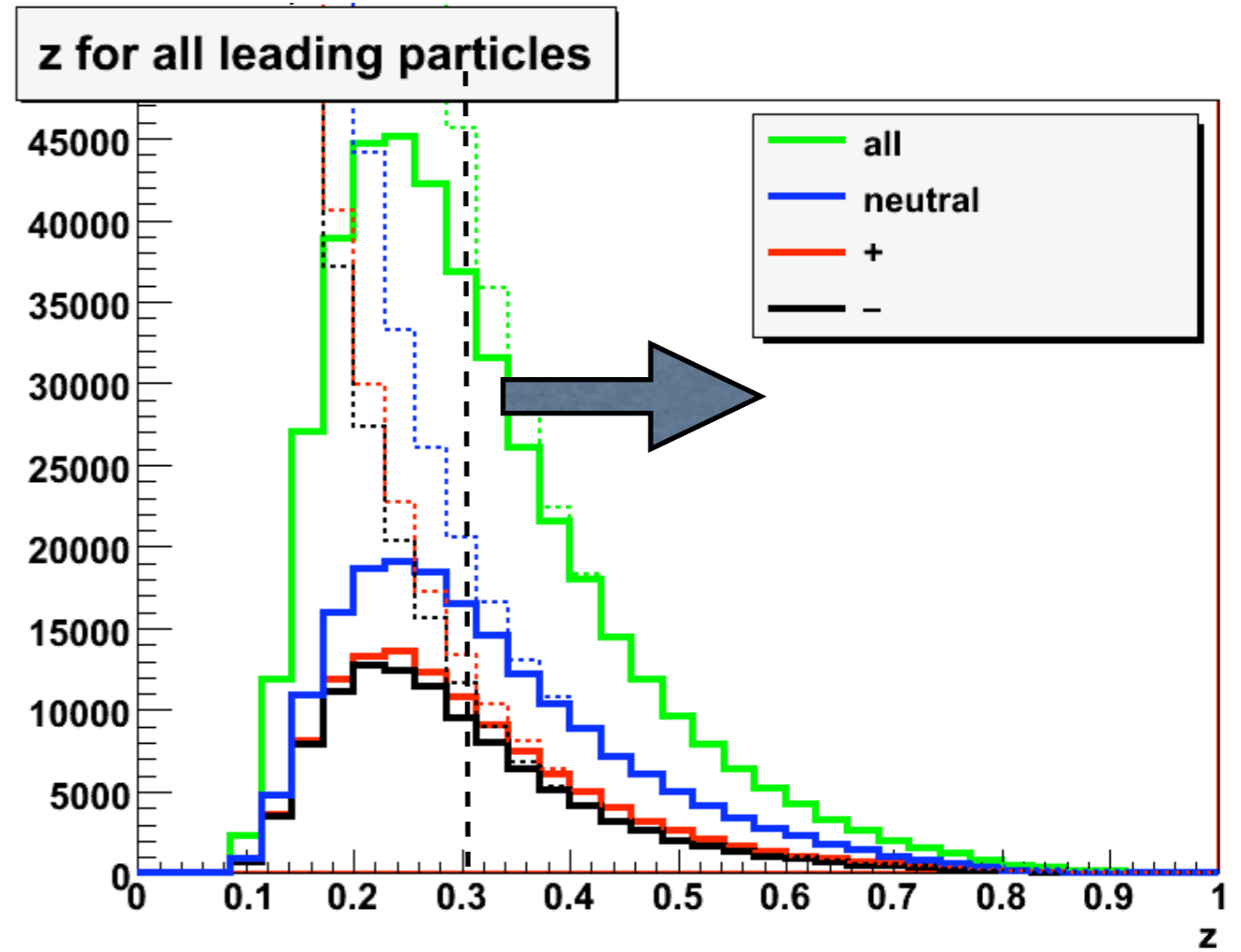
**View down proton beam line (polarized protons moving into page)**

STAR simulation at  $\sqrt{s} = 200$  GeV

BJP1 -127221

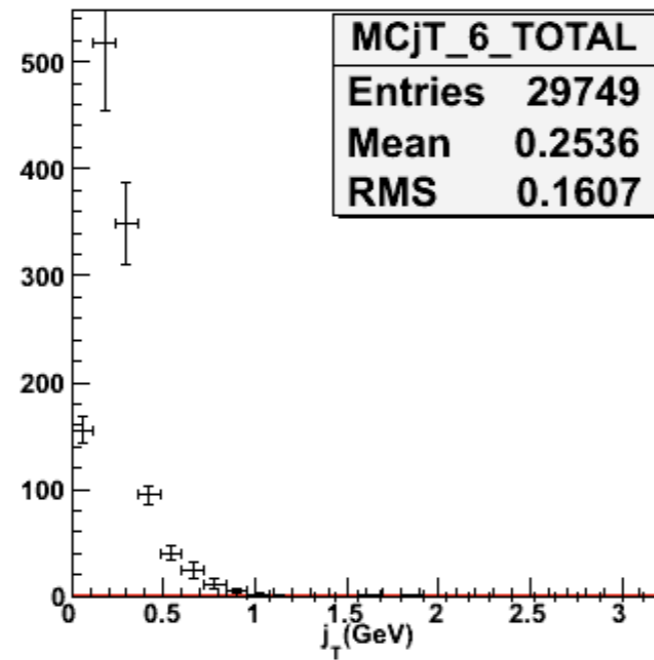


(Colored dotted lines are inclusive yields for comparison)

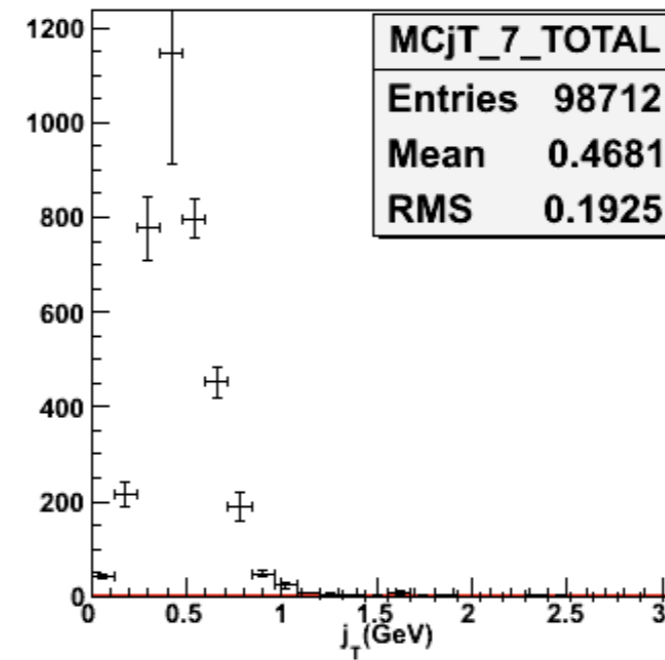


## (MonteCarlo) Particle $j_T$ in 2 Detector $j_T$ bins

$j_T$ [MC] ( $0.10 < j_T < 0.25$  GeV)

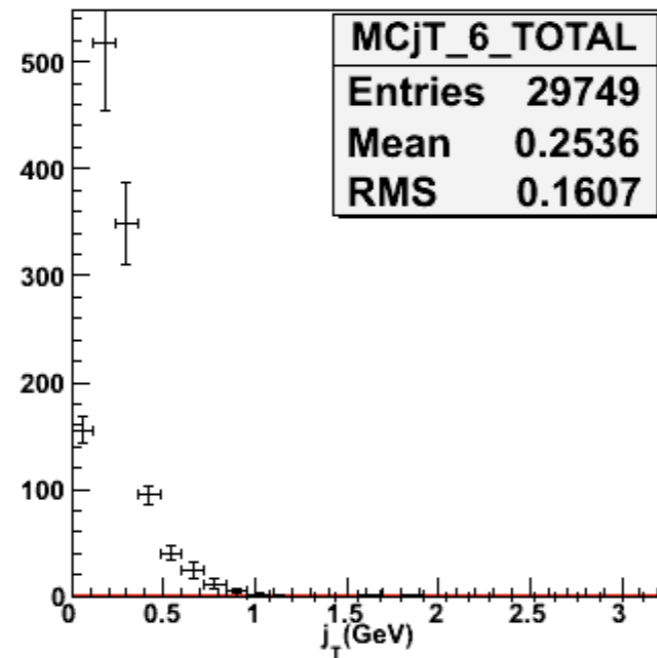


$j_T$ [MC] ( $0.25 < j_T < 0.63$  GeV)

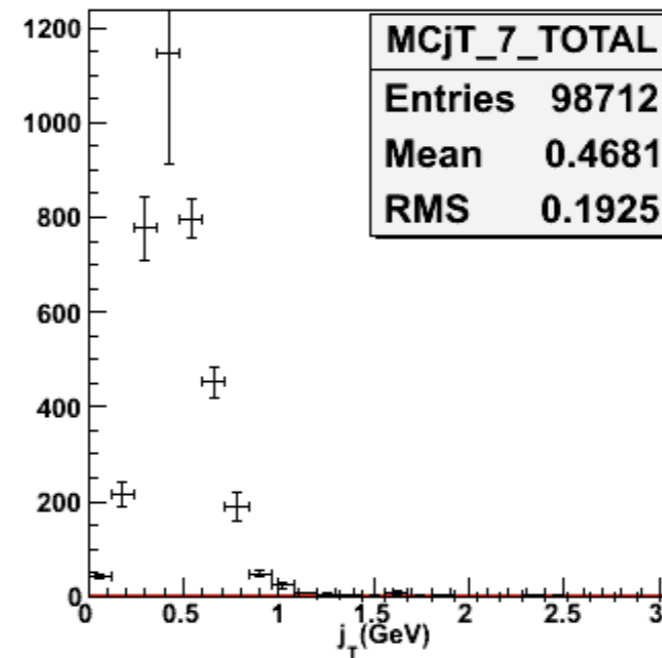


## (MonteCarlo) Particle $j_T$ in 2 Detector $j_T$ bins

$j_T$ [MC] ( $0.10 < j_T < 0.25$  GeV)

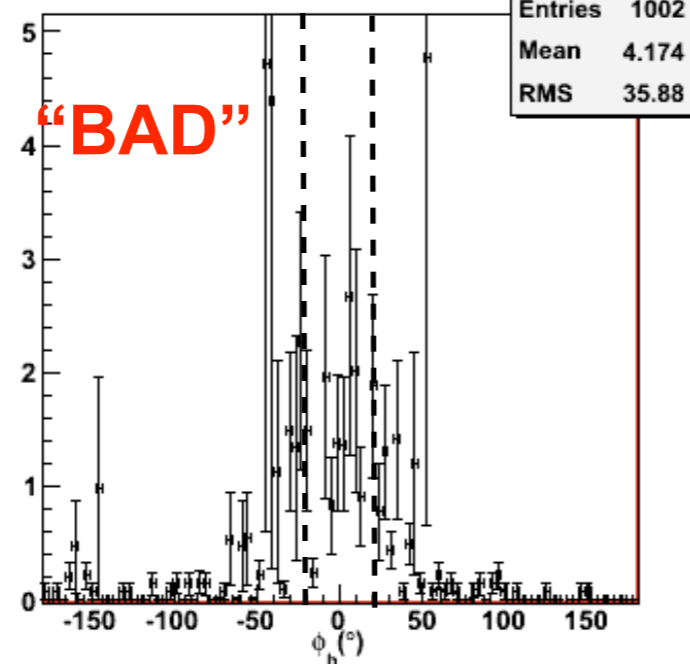


$j_T$ [MC] ( $0.25 < j_T < 0.63$  GeV)



## (MonteCarlo) $\phi_h$ in 2 Detector $j_T$ bins for a $40^\circ$ cut in Detector $\phi_h$

$\phi_h$ [MC] ( $0.10 < j_T < 0.25$  GeV)



$\phi_h$ [MC] ( $0.25 < j_T < 0.63$  GeV)

